United States
Environmental Protection
Agency

Office of Research and
Development
Washington DC 20460

EPA/600/R-94/197
November 1994

EPA

# An Experimental Evaluation of Two Sharp Front Models for Vadose Zone Non-Aqueous Phase Liquid Transport

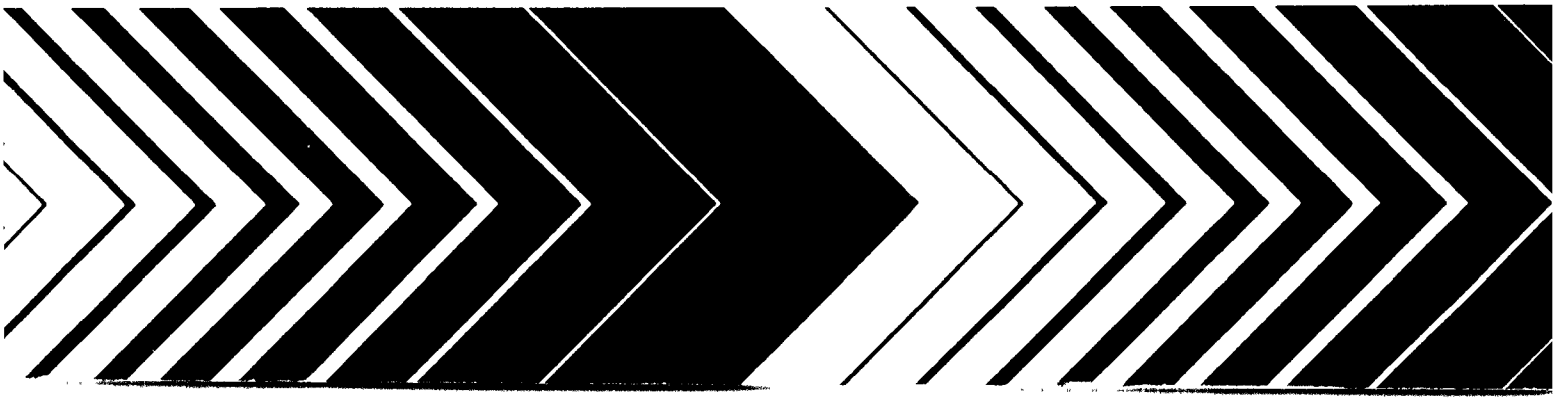

EPA/600/R-94/197
November 1994

# AN EXPERIMENTAL EVALUATION OF TWO SHARP FRONT MODELS FOR VADOSE ZONE NON-AQUEOUS PHASE LIQUID TRANSPORT

by

Tissa Illangasekare, Dobroslav Znidarčić, Gabriele Walser
Department of Civil, Environmental and Architectural Engineering
University of Colorado
Boulder, Colorado 80309

and

James Weaver
Robert S. Kerr Environmental Research Laboratory
United States Environmental Protection Agency
Ada, Oklahoma 74820

CR-816807

Project Officer

James Weaver
Processes and Systems Research Division
Robert S. Kerr Environmental Research Laboratory
Ada, Oklahoma 74820



ROBERT S. KERR ENVIRONMENTAL RESEARCH LABORATORY
OFFICE OF RESEARCH AND DEVELOPMENT
UNITED STATES ENVIRONMENTAL PROTECTION AGENCY
ADA, OKLAHOMA 74820

# DISCLAIMER

The information in this document has been funded in part by the United States Environmental Protection Agency under CR-816807 to the University of Colorado at Boulder. The authors also acknowledge funding from the EPA Great Plains-Rocky Mountains Hazardous Substance Research Center and equipment support from the National Science Foundation. It has been subjected to the Agency's peer and administrative review, and it has been approved for publication as an EPA document. Mention of trade names or commercial products does not constitute endorsement or recommendation for use.

All research projects funded by the U.S. Environmental Protection Agency that make conclusions or recommendations based on environmentally related measurements are required to participate in the Agency Quality Assurance Program. This project was conducted under an approved Quality Assurance Project Plan and the procedures therein specified were used. Information on the plan and documentation of the quality assurance activities are available from the Principal Investigator.

# FOREWORD

EPA is charged by Congress to protect the Nation's land, air and water systems. Under a mandate of national environmental laws focused on air and water quality, solid waste management and the control of toxic substances, pesticides, noise and radiation, the Agency strives to formulate and implement actions which lead to a compatible balance between human activities and the ability of natural systems to support and nurture life.

The Robert S. Kerr Environmental Research Laboratory is the Agency's center of expertise for investigation of the soil and subsurface environment. Personnel at the Laboratory are responsible for management of research programs to: (a) determine the fate, transport and transformation rates of pollutants in the soil, the unsaturated and the saturated zones of the subsurface environment; (b) define the processes to be used in characterizing the soil and subsurface environments as a receptor of pollutants; (c) develop techniques for predicting the effect of pollutants on ground water, soil, and indigenous organisms; and (d) define and demonstrate the applicability of using natural processes, indigenous to the soil and subsurface environment, for the protection of this resource.

Light nonaqueous phase liquids (LNAPLs) are one of the most common, yet complex, subsurface contaminants. Although the LNAPL itself remains distinct from the subsurface water, chemical constituents of the LNAPL can cause serious ground water contamination. Because of the number of parameters which determine the flow and transport of LNAPL contaminants, models are needed to assess the impacts of this kind of contaminant. Models are derived from a certain conceptualization of the flow and from theoretical principles. Before model results can be accepted, there needs to be testing of the models with experimental data. This report describes a set of experiments that were designed to test two models for LNAPL flow in the vadose zone, and the comparison of the models against the data. As a result of the study, there is a clearer understanding of the abilities and limitations of these models.



Clinton W. Hall

Clinton W. Hall, Director
Robert S. Kerr Environmental
Research Laboratory

# ABSTRACT

Recent research efforts on the transport of immiscible organic wastes in subsurface systems have focused on the development of numerical models of various levels of sophistication. However, in real field applications, the site characterization data needed to obtain the model parameters are either difficult to obtain or are not easily available. As an alternative, a number of simple sharp front models which require relatively less data have been developed. Less rigorous data requirements and simplicity of use allows these types of models to be used as screening tools in risk assessment and remediation design. Laboratory experiments have been conducted to test two such models developed by the authors. Fundamental transport parameters for the media were determined using a flow-pump system. One-dimensional spill simulations of a non-aqueous phase liquid were conducted in vertical soil columns. Ponding depth and front location were tracked visually. A dual-source gamma system was tested and then used to obtain saturation profiles of the water and oil phases. The profiles indicate the existence of a sharp front at the leading edge of the infiltrating oil phase. At the trailing end of the infiltrating oil, a gradual decline in saturation was observed. One of the models, which is similar in concept to the Green-Ampt type infiltration models, assumes sharp leading and trailing fronts. It deviates from the experimental results for long modeling times. The second model based on kinematic wave formulation and the method of characteristics approximates the gradual decline in saturation behind the front and simulates the spill behavior well. Based on these experimental evaluations, the suitability and limitations of these simple models are determined. Simulated rainfall experiments have been conducted to observe extent of mobilization of the organic phase through water application. Water pushes the organic phase as a slug in front of the water phase (piston displacement). However, the water mobilizes nearly none of the organic phase below a phase content of 0.1. Two-dimensional experiments were conducted in a tank to test the applicability of the one-dimensional models to a two-dimensional situation. The saturation profiles were again determined using the dual-gamma system. The vertical movement of the organic phase in the tank experiments differed little from the movement in the column experiments, indicating the applicability of one-dimensional models to the vertical infiltration of immiscible fluids in the unsaturated zone of a homogeneous soil.

This report was submitted in fulfillment of CR-816807 by the University of Colorado at Boulder under the partial sponsorship of the U.S. Environmental Protection Agency. This report covers a period from July 1990 to August 1992 and work was completed as of August 1992.

# CONTENTS

FIGURES

TABLES

# SECTION 1
# INTRODUCTION

There are approximately 180,000 confirmed releases of petroleum products and other chemicals from underground storage tanks. The magnitude of this problem has led to the creation of a number of regulatory programs at both the state and federal level. Managers of these programs are required to make decisions concerning underground storage tank sites, but must do so with limited resources. These managers recognize that in making technically defensible decisions, models play a role in some circumstances. An example is the siting of storage tank facilities. In some states, monitoring frequency must be based on the estimated arrival time of a leaked petroleum hydrocarbon at the water table. Arrival time estimates can best be made from flow model results.

Leaking underground storage tanks and accidental spills result in contaminant releases in the unsaturated zone. The organic liquid then travels downward until it reaches the water table. Typically, organic and other chemical wastes are only marginally soluble in water, and therefore persist as a separate liquid phase for some distance and time from the initial spill location. The separate phase material may exist either as continuous bulk phase or as discontinuous pockets of "residual" material. Although direct human exposure to non-aqueous phase liquid (NAPL) is generally minimal, the persistence of the NAPL hinders cleanup efforts and provides a long-term source of contamination into the ground water through leaching of more soluble components. The presence of NAPLs has been identified by the United States Environmental Protection Agency (1992) as a major problem at superfund sites and a major reason for the failure of pump and treat remediation schemes to meet their cleanup goals in a reasonable amount of time.

Transport and entrapment behavior of NAPLs in soils depends on the distribution and interaction of three fluid phases, namely water, NAPL and air. The effective control of groundwater contamination requires assessment and remediation of these multiple fluid phases occurring in soils. Guiding any assessment and remediation efforts are field data and models for the interpretation of that data. Unfortunately, neither are widely available for separate phase contaminants. Several models have been reported in literature, for example those of Faust (1985), Baehr and Corapcioglu (1984), Abriola and Pinder (1985), Osborne and Sykes (1986), Kuppusamy et al. (1987), Kaluarachchi and Parker (1989), Faust et al. (1989) and Kueper and Frind (1991). These models are based on concepts currently used to describe petroleum reservoir behavior (e.g. Muskat et al., 1937; Peaceman, 1977) despite the different goals and needs for modeling near-surface, localized contaminant movement. Despite a number of simplifying assumptions, these models remain complex; and have proven useful in situations where extensive site and contamination characterization have been justified.

Complex models, such as those listed above, however, may not always be the most desirable tool for a given field problem. Accurate simulations using such models may require large computing resources, and there may be a significant investment in training users to set up the model, run it properly and interpret the output. A large amount of field data and transport parameter values are required to run such a model. In addition to the parameters for aqueous phase solute transport (such as hydraulic conductivity, dispersivity, sorption parameters),

multiphase transport parameters are needed (interphase partition coefficients, capillary pressures and relative permeabilities) for each different zone or material present in the field. The latter properties are not well understood and are difficult to obtain for field problems. Site data is usually incomplete because of monetary, safety and regulatory limitations. Historical records of pollutant releases are normally nonexistent, although such knowledge should be precisely defined in a model. Sampling limitations often result in situations where the spatial distribution and the total mass of contaminants cannot be defined. These limitations may require many approximations when running a model.

"Sharp front" models, which are computationally efficient and simple to apply, may prove useful for certain applications. Although they contain a number of simplifying assumptions, such models are based on qualitative understanding of the physical behavior of NAPLs in soils. A model (the Three Parameter Sharp Front Model) has been developed based on laboratory experiments of transport and entrapment behavior of organics in the saturated and unsaturated zone (Illangasekare et al., 1987a, 1987b; Illangasekare and Reible, 1987a, 1987b; Reible and Illangasekare, 1989). This model assumes sharp fronts at the advancing and drainage fronts of the NAPL and utilizes three parameters which characterize the soil and the fluid. These parameters consist of a capillary drive term at each front and the effective conductivity of the NAPL. From a parallel development, similar models were developed from kinematic wave theory. These are the Kinematic Oily Pollutant Transport (KOPT) (Weaver et al. 1994a) and Kinematic Rainfall and Oily Pollutant Transport (KROPT) Models (Charbeneau et al. 1989). Both of these implementations were for one-dimensional downward transport in uniform soils. KROPT includes the effect of individual rainfall events on the NAPL. Here the kinematic wave theory predicts the displacement of the NAPL into "NAPL banks," which move ahead of infiltrating water (Charbeneau et al., 1989). The intensity of rainfall, soil properties and/or NAPL properties may cause the kinematic theory not to apply to some or part of the simulation. Currently, improved dynamic approximations are being developed at RSKERL (Weaver, 1989, 1991). These have been shown to be general models which include the kinematic model as a special case (Weaver, 1991). Theoretical results so far suggest that there are two flow regimes for the dynamic model. One is characterized by incomplete displacement of the NAPL into a NAPL bank and the other by complete by-passing of the NAPL by the water phase (Weaver, 1991).

Although NAPL flow through the vadose zone is significant for certain problems, as discussed in the introduction, interactions with the water table and dissolution of chemical constituents of the NAPL are an obvious problem. For NAPLs lighter than water, KOPT has been linked with an approximate model for oil lens development at the water table, dissolution of the chemical contaminant of interest, and subsequent transport to a receptor well (Weaver et al., 1994b). Thus the simple models have applicability to the vadose zone itself and as a means of approximating contaminant loadings to lenses at the water table and ground water contamination.

## 1.1 OBJECTIVES

The primary intent of this study was to generate accurate data sets that describe the flow of a NAPL in the vadose zone. These data can be used to obtain an understanding of the transport behavior of NAPLs in the vadose zone and to test simulation models.

The specific objectives of this research were:

1) To develop laboratory techniques and instrumentation necessary for the estimation of soil and fluid parameters critical to porous media flow.
2) To perform parameter estimation for selected sands and fluids.
3) To develop experimental techniques to simulate spills in unsaturated media with given boundary conditions.
4) To perform spill simulations in one- and two-dimensional systems and generate a data base on the vertical infiltration of NAPLs in the vadose zone.
5) To test two simple computer models (the Three Parameter Sharp Front Model and KOPT) against the experimental results.

The objectives were realized through the following steps: A flow pump system was used to obtain accurate values for the capillary suction-saturation relationship and hydraulic conductivity. A dual-gamma attenuation system was calibrated for correct phase content measurements in multiphase systems during spill experiments. The conductivity of a fine sand (#125) and a coarse sand (#70) to water and a lighter than water organic test fluid, Soltrol, were determined using a flow pump. The flow pump system and the gamma system were used independently to obtain the capillary pressure versus saturation relationships for the two sands. A column setup was developed to conduct spill experiments in homogeneously packed sand that was residually saturated with water. Spill experiments with Soltrol were conducted in the column and a two-dimensional tank. Saturation was measured continuously during the spills using the gamma system. Computer simulations with the CU-Three Parameter Sharp Front model and the KOPT model were conducted. The experimental results were used to evaluate the two models.

# SECTION 2

# CONCLUSIONS AND RECOMMENDATIONS

The objective of this project was to generate data for testing unsaturated zone NAPL flow models. Procedures were developed for measuring transient NAPL and water flow in the unsaturated zone using dual gamma attenuation. Methods were also developed for measuring necessary model parameters using the flow pump. The gamma attenuation system provides a convenient way for the non-destructive measurement of fluid phase contents in laboratory soil columns and two-dimensional soil tanks. Phase content of one- and two-phase systems can be measured during the experiment. However, great care has to be taken to obtain accurate measurements when using the gamma system. The suction-saturation curves measured with the gamma system agreed well with those measured with the flow pump setup. Hydraulic conductivity was measured with the flow pump setup.

A number of spill experiments were conducted in a one-dimensional column and in a two-dimensional tank. The sand was packed dry, completely saturated with water and then drained to residual saturation. Then a measured volume of NAPL was applied at the surface. These spill experiments conducted on residually water saturated soils showed that the Soltrol front moves, in some cases, quickly during infiltration, when there is Soltrol ponded at the soil surface. Once the ponding ends the rate of movement of the front decreases rapidly. The leading edge of the LNAPL body remained largely sharp, while the trailing edge became diffuse. Although the water content in the columns was reduced to residual before beginning the experiment, the Soltrol mobilized some of the residually entrapped water. Release of water was not unexpected because the Soltrol/water interfacial tension is less than half of the surface tension of water.

The simulated rainfall experiments demonstrated that incoming water has the ability to displace mobile NAPL into a bank moving ahead of the water front. Once the NAPL saturation in the bank is reduced below the maximum, the water bypasses the NAPL front. The simulated rainfalls, however, did not completely remove the NAPL, demonstrating that some NAPL remained trapped in the unsaturated zone even under the action of infiltrating rainwater. Infiltration of the NAPL, on the other hand, sometimes caused displacement of the residual pore water.

Simulations of the transient column experiments were performed using the three-parameter model of the University of Colorado and the KOPT model of RSKERL. These models, although apparently based on diverse assumptions, are related by the fact that they are both generalized method of characteristics solutions for a pulse release of NAPL at the ground surface. With appropriate choices of parameter values, both models can be made to reproduce the observed NAPL front position as a function of time. The three-parameter model requires a fitting procedure for determination of its input parameters, so that accurate application of the model to situations with no measured front locations is difficult. This model assumes that the NAPL saturation behind the front remains fixed during redistribution. This assumption caused the model to over predict the front position when parameters were used from the previous experiment to simulate a subsequent experiment. To apply this model without field calibration, it i necessary to develop methods to estimate the model parameters directly from the soil-water-NAPL characteristics. KOPT was seen to match the qualitative behavior of the NAPL front by using

measured parameter data. There appears to be a tendency in KOPT to under predict the infiltration rates. Quantitative agreement of KOPT simulations with the experimental results depends on the accuracy of the input parameters. KOPT allows the reduction of the NAPL saturations behind the NAPL front during redistribution. The resulting saturation profiles, however, are highly idealized in comparison to the measured profiles. In summary, prediction of NAPL infiltration and redistribution by the three-parameter model is limited by the need to fit the model to transient flow experimental data, which is not likely to be available for field problems. KOPT predictions are generally limited by the ability to measure the input parameters, primarily the hydraulic conductivity. Although the observed displacement of the residual water violated the assumptions of the models, at least in these cases, the models were still able to fit the experimental results reasonably well.

The following recommendations are derived from this work:

1. The University of Colorado, three-parameter model should be revised to include the effects of reduced NAPL saturation behind the wetting front. Kinematic or other appropriate theories should be used to accomplish this revision. The ability to predict flow experiment behavior with fitted parameter sets from previous experiments should then be reevaluated.

2. The assumptions in the RSKERL KOPT Green-Ampt infiltration model should be reevaluated, based on the apparent inability of KOPT to accurately predict the ponding time of the experiments. This work should focus on the assumptions underlying kinematic models in general and could be accomplished using kinematic models for water flow in the unsaturated zone. The use of kinematic models for water, rather than for NAPL, permits the use of relative permeability expressions (for water) that are more well-established than those for the NAPL; thus one source of uncertainty would be eliminated.

3. Simple models such as these should be included in screening methodologies for subsurface NAPL flow. The simple models are of sufficient accuracy to be acceptable for screening calculations. The primary factor which will limit accuracy of model predictions is the ability to determine the model parameter values. This statement is true for both simple and complex models. The complexity of the model used for a particular analysis should be appropriate for the availability of data, the level of detail of the analysis, and the ability to test model predictions.

4. Further experimental work should be performed on the effects of rainfalls on displacement of NAPLs in the unsaturated zone. The experiments presented in this report suggest that rainfalls can cause NAPL banks to form. This behavior was predicted by a model developed by Weaver (1991), but was not used in this work because it requires restrictive assumptions concerning the boundary and initial conditions. Some of the qualitative behavior predicted by the model, however, appears to be consistent with the experimental results.

# SECTION 3
# THEORETICAL BACKGROUND

The purpose of this section is to summarize some of the important principles and define the parameters that control the flow of immiscible fluids in porous media. The application of these to the infiltration and redistribution of liquids in the vadose zone is described. The basis of the KOPT and Three Parameter Sharp Front Model are then described.

## 3.1 FLOW OF IMMISCIBLE FLUIDS THROUGH POROUS MEDIA

### 3.1.1 Porous Media

In the most general sense, a porous medium is a solid body containing voids or pores. Bear (1972) describes it as a volume occupied by a multi-phase matter in which at least one phase is solid and at least one is non-solid. This definition includes solid material and gases or liquids which occupy the void space. The solid phase is called the solid matrix. The space within the porous medium domain that is not part of the solid matrix is referred to as pore space.

Pores in a porous medium may be either interconnected or isolated. The interconnected pore space is termed effective pore space. A fluid can only flow if at least part of the pore space is interconnected. Most natural porous materials have a random void structure. Pore size, shape and interconnectedness characterize the void space on the microscopic or pore scale. Macroscopically, effective porosity, n, is defined as the volume fraction of the medium that consists of interconnected pores which may conduct fluid.

### 3.1.2 Darcy's Law

Darcy's law provides a relationship between the specific discharge and the hydraulic gradient. Mathematically, Darcy's law may be expressed by the equation

$$q = -K\nabla h \qquad (1)$$

where q is the Darcy velocity or specific discharge, K the coefficient of proportionality or hydraulic conductivity and h is the hydraulic head. The Darcy velocity is a macroscopic flux defined over a representative element or bulk area. This area is taken to be normal to the direction in which the gradient of h is measured. Hydraulic conductivity for a fully saturated medium depends on fluid density and viscosity, as well as the size and distribution of the pores.

Darcy's equation can also be applied when the medium is partially saturated. In this case, the pressure difference will be determined by capillary forces in addition to gravitational forces. The conductivity of the medium for either phase depends on fluid phase content of the medium.

### 3.1.3 Fluid Saturation

The simultaneous flow of one or more immiscible liquids and a gas, e.g. air, is often described as unsaturated or partially saturated flow. Under unsaturated conditions the void space of a porous material may be partially filled with one or more of the liquids with gas filling the remaining pore space. The amount of the void space which is occupied by each fluid affects the flow through the porous medium.

The saturation at a point or reference volume, with respect to a particular fluid, is defined as the fraction of the void volume occupied by that particular fluid. Thus for water the saturation, $S_w$, is defined as

$$S_w = \frac{\textit{volume of water in the medium}}{\textit{total volume of voids in the medium}} \qquad (2)$$

The saturations of all the fluids occupying the void space must sum to 1.

Fluid phase content can also be expressed as volume fraction of the total volume of a porous medium in which it is contained. The latter is called the "volumetric water content" or "phase content," and in most literature is designated by $\theta$. The relationship between the fluid saturation, $S_f$, and volumetric content, $\theta_f$, of fluid f is expressed as:

$$\theta_f = S_f n \qquad (3)$$

where n is the effective porosity.

### 3.1.4 Capillary Pressure

Two fluids are mutually immiscible because the net attractive force between their molecules differs. For example, the net attractive force between molecules of a gas is generally lower than that between molecules of a liquid. Likewise the net attractive force between molecules of a nonpolar liquid is lower that that between molecules of a polar liquid, like water. Along the interface between the fluids, the differing forces of molecular attraction lead to an interfacial tension which causes the fluids to remain distinct, i.e., to be immiscible. When the fluids are in contact with a solid surface, similar interfacial forces exist between the solid and the fluids. Generally one fluid is more strongly attracted to the solid surface than the other. This fluid is called the wetting fluid and the other fluid is called the nonwetting fluid. The nature of the interaction (i.e., which fluid is wetting) depends on the fluid properties and the nature of the surface.

In a porous medium when two immiscible fluids are in contact, a discontinuity in pressure exists across the interface that separates them. The difference in pressure is called the capillary pressure, $P_c$, and is defined as the pressure difference between the nonwetting, $P_{nw}$, and wetting fluids, $P_w$:

$$P_c = P_{nw} - P_w \quad (4)$$

The magnitude of the pressure difference depends on the radius of curvature and the surface tension at the fluid-fluid interface. In a porous medium, the pore geometry and the fluid saturation determine the radius of the interface and thus the capillary pressure. Low values of the capillary pressure are associated with large pores, and on the contrary high values of capillary pressure are associated with small pores.

### 3.1.5 Capillary Pressure-Saturation Relationship

To obtain the relationship between saturation and capillary pressure, various test procedures have been developed by petroleum engineers and soil scientists. In general, the sample is de-saturated by increasing the capillary pressure in known increments. The sample is allowed to reach equilibrium after each pressure change. Measured values of the change in saturation and pressure are used to determine the so-called "capillary pressure-saturation curve." It is also common to plot the capillary pressure as a function of the volumetric water content, the curve is then referred to as "water retention curve" or "water characteristic curve." Example results are presented in Section 6. The measured capillary pressure curves depend on the pore geometry, the fluid-fluid interactions and the wettability. Thus the curve incorporates the underlying multiphase interactions in a form that is used in modeling.

The capillary pressure versus saturation relationship can be defined either when the sample is drained from full wetting-fluid saturated conditions or when the wetting phase is allowed to enter the sample and displace the nonwetting fluid. Usually these curves are measured on a drainage cycle. A minimum capillary pressure is required before the sample starts de-saturating from initially saturated conditions. At this point the non-wetting fluid, such as air, can enter the porous sample. This minimum pressure is called the "air-entry pressure," or if the non-wetting phase is not air, "threshold pressure." Experimental results show that the wetting fluid remains in the sample at high capillary pressures. The limiting value of saturation when capillary pressure increases no longer cause a release of the wetting fluid is commonly called the "residual saturation."

### 3.1.6 Permeability and Relative Permeability

Permeability is a function of the porous medium only, whereas hydraulic conductivity depends both on fluid and porous medium properties. The relationship between the hydraulic conductivity and the soil permeability and fluid properties is given by:

$$K = \frac{k \rho g}{\mu} \quad (5)$$

where K is the hydraulic conductivity, k is called the intrinsic permeability and is presumed to be a property of the media, $\rho$ is the fluid density, g is the acceleration due to gravity, and $\mu$ is the

dynamic viscosity.

The concept of relative permeability was first postulated by Muskat et al. (1937). Their work consisted of extending Darcy's law to two-phase systems. The term relative permeability is used to describe the effect of the degree of saturation on the hydraulic conductivity of a particular phase. It is also defined as the ratio of the permeability of a fluid at a specific saturation to the permeability under completely saturated conditions. Relative permeabilities, for wetting, $k_{rw}$ and non-wetting phases, $k_{rnw}$ are given by:

$$k_{rw} = \frac{K_w}{K} \qquad k_{rnw} = \frac{K_{nw}}{K} \tag{6}$$

The sum of the relative permeabilities for all phases is always less than one, because of interference between phases sharing the same flow channels. This interference is directly related to the wettability characteristics of the soil grains and the fluids (Honarpour et al., 1986).

### 3.1.7 Governing Equations of Multiphase Flow in Porous Media

The sharp front models presented below are based on a simplified version of the mass conservation law for multiphase flow system. (See, for example, Abriola and Pinder, 1985). Assuming that the porosity and density of each fluid are constants, and that the flow is one dimensional gives a phase conservation equation for fluid f

$$n \frac{\partial S_f}{\partial t} + \frac{\partial q_f}{\partial z} = 0 \tag{7}$$

where $q_f$ is the darcy flux of fluid f. In equation (7), effects of dissolution, volatilization and partitioning of the NAPL are ignored. Such phenomena can be incorporated into a simplified model by assuming that they do not alter the fluid properties of the NAPL and that the NAPL is not completely lost by these processes (Weaver et al., 1994a).

The flux, $q_f$, in equation (7) is given by a modified form of Darcy's law ((1)) that includes multiphase phenomena; that is, it includes the capillary pressure and relative permeability:

$$q_f = \frac{k k_{rf}}{\mu_f} \left( \rho_f g - \frac{\partial P_f}{\partial z} \right) \tag{8}$$

where $k_{rf}$ is the relative permeability of the matrix to fluid f, $P_f$ is pressure in phase f and z has been taken as positive downward. The capillary pressure is included implicitly in equation (8) as each fluid pressure $P_f$ is related to the other fluid pressures through capillary pressure relationships (equation (4)).

## 3.2 SHARP FRONT MODELS

In this section, the principles of infiltration are presented along with a discussion of the two computer models: the Kinematic Oily Pollutant Transport Model the Three-Phase Sharp Front Model.

### 3.2.1 Infiltration and Redistribution

Infiltration and redistribution of liquids in the unsaturated zone are driven by gravity and pressure gradients. The pressure gradient may be divided into component of applied pressure, such as that due to the weight of the liquid, and a component due to the capillary pressure in the soil or porous medium. The contribution to flow in the unsaturated zone of each of these driving forces is described below. Gravity acts throughout infiltration and redistribution and must always be included in the model. The magnitude of the gravity contribution is, at most, equal to the magnitude of the effective conductivity of the medium. Pressures may be imposed on the system during infiltration. For example, ponding of liquid at the surface provides a positive pressure, P, equal to

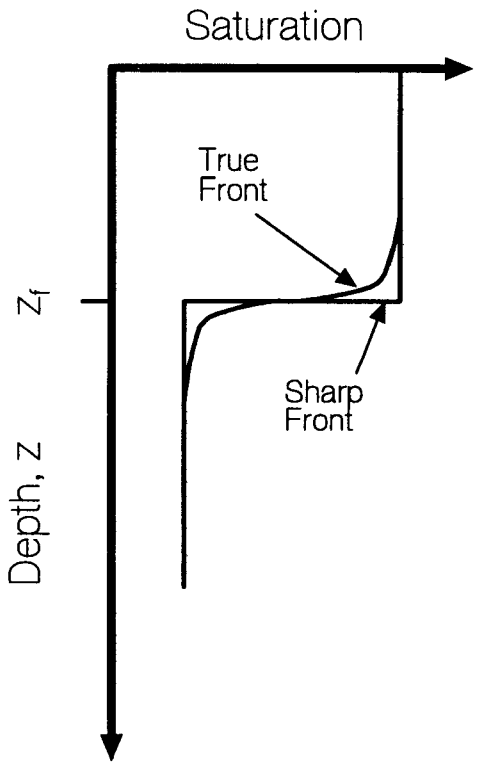


Figure 1. Schematic representation of the relationship between sharp fronts and true spreading fronts.

$$P = \rho g d \tag{9}$$

where $\rho$ is the liquid density, g is the acceleration due to gravity, and d is the depth of ponding. The ponding depth helps drive liquid into the unsaturated zone. The capillary pressure gradient at the soil surface has a number of important influences on unsaturated zone flow. During infiltration, one influence of the capillary pressure gradient is to provide an additional driving force, which is commonly called capillary suction. The magnitude of this force depends on the soil properties and the antecedent liquid content. For infiltration, the combined effects of gravity, the imposed pressure gradient, and the capillary pressure gradient must be included in a model in order to properly compute the mass of liquid drawn into the profile (Weaver and Charbeneau, 1992).

### 3.2.2 Kinematic Oily Pollutant Transport (KOPT) Model

In the Kinematic Oily Pollutant Transport (KOPT) Model, the kinematic and dynamic behavior is approximated in two parts: one for infiltration and one for redistribution (Weaver et al., 1994a). For infiltration, a version of the Green-Ampt (1911) model is used, which includes the effects of gravity, ponding at the surface, and capillary suction on the infiltrating liquid. This model accounts for the capillary suction of the media but does not include the effect of the capillary pressure gradient on the shape of the front. Thus the model assumes a sharp front at the leading edge of the infiltrating liquid. Behind the sharp front, a constant NAPL saturation is assumed to exist. Charbeneau (1984) presented a theoretical discussion which demonstrated that since sharp front models derive from mass conservation, the mean displacement of the true front matches that of the sharp front. Figure 1 shows the relationship which is maintained between the true and sharp fronts. The speed of the sharp front is given by:

$$\frac{dz_f}{dt} = \frac{q_2 - q_1}{n(S_2 - S_1)} \tag{10}$$

where $z_f$ is the position of the front, $q_1$ is the NAPL flux ahead of the front, $q_2$ is the NAPL flux behind the front, $S_1$ is the NAPL saturation ahead of the front, and $S_2$ is the NAPL saturation behind the front. $S_1$ and $q_1$ are zero when the NAPL invades a pristine medium as they represent the antecedent conditions. The flux, $q_2$, is given by the Green-Ampt model

$$q_2 = K_m \frac{H_s + z_f + \int_{\psi_2}^{\psi_1} \frac{K_s}{K_m} k_{ro}\, d\psi - \psi_1}{z_f} \tag{11}$$

where $K_s$ is the saturated conductivity to NAPL, $K_m$ is the maximum conductivity to NAPL during infiltration, $H_s$ is the NAPL ponding depth at the surface, $\psi$ is the NAPL head, the subscripts on

$\psi$ refer to points behind (1) and ahead of the front (2), and $z_f$ is the front position. The integral in Equation (11) is evaluated using a procedure developed by Neuman (1976), so that all parameters of the model are based upon the fundamental measured porous media properties. $K_m$ is generally taken as one-half the maximum effective conductivity to the NAPL based on field observation of water infiltration (Bouwer, 1966).

During redistribution, no more liquid is drawn into the profile. The imposed pressure can obviously be dropped from a model. The gradient of the capillary pressure is also dropped as it does not affect the mean displacement speed of the front. The sharp front approximation is retained in KOPT, but now flow is driven only by gravity. Thus the redistribution model is a kinematic model. The multiphase Darcy's Law, which is used in the previous jump equation 11, becomes

$$q_o = K_o(S_w, S_o) \tag{12}$$

where the subscripts "o" and "w" refer to NAPL and water respectively, and a fixed amount of water in the pore space is assumed. In three phase systems, as evident in equation (12), the effective conductivity to the NAPL phase depends, at least, on the water saturation. Neglecting hysteresis, the phase conservation equation (7) for the NAPL can be simplified and expanded to

$$\frac{\partial S_o}{\partial t} + \frac{1}{n}\frac{\partial K_o}{\partial S_o}\frac{\partial S_o}{\partial z} = 0 \tag{13}$$

Application of the method of characteristics gives

$$\frac{DS_o}{Dt} \equiv \frac{\partial S_o}{\partial t} + \frac{dz}{dt}\frac{\partial S_o}{\partial z} = 0 \tag{14}$$

along characteristics defined by

$$\frac{dz}{dt} = \frac{1}{n}\frac{\partial K_o}{\partial S_o} \tag{15}$$

The KOPT model equations (11 and (15)) are all in the form of ordinary differential equations, which are solved relatively easily by a Runge-Kutta technique (Weaver and Charbeneau, 1992). Figure 2 shows a schematic representation of KOPT model results. In the figure the NAPL application begins at time "A" and ends at time "B." The results show a sharp front at the leading edge of the infiltrating NAPL and a continuous wave after infiltration ends. The process which follows after the infiltration ends is known as redistribution. During redistribution, the continuous wave is defined by characteristic lines which each represent a constant value of NAPL saturation. The continuous wave defines the distribution of the NAPL during redistribution, as well as determining the rate of advance of the various NAPL saturations. In this figure, a constant infiltration rate is used so that, initially, the sharp front moves at a constant rate. Once the characteristics intersect the front, its speed slows since the saturation at the front decreases

(equation (10)).

Figure 3 shows a schematic of depth modeled by KOPT as a function of saturation. During infiltration the NAPL is assumed to fill a fixed portion of the pore space from the release point to the sharp front. During redistribution the NAPL saturation varies with depth as determined by the continuous wave of Figure 2. The sharp front remains at the leading edge of the NAPL body, but the NAPL saturations behind the front can be reduced.

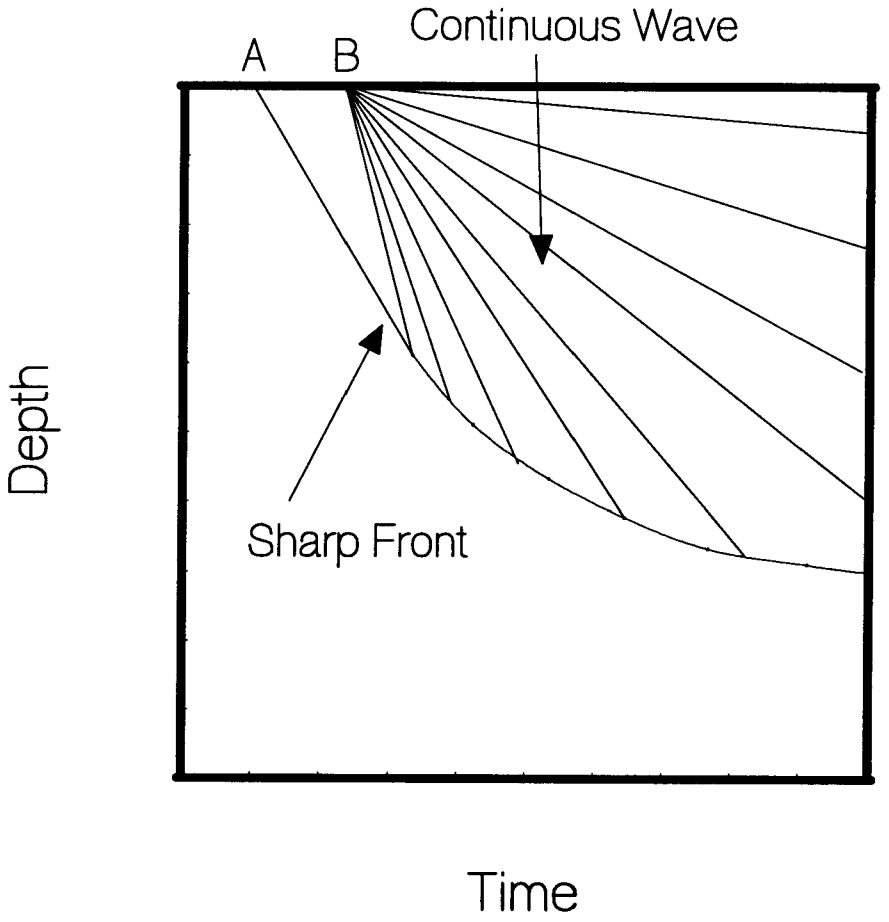


Figure 2. Base characteristic plane for the KOPT model showing the sharp front and continuous wave which comprise the solution.

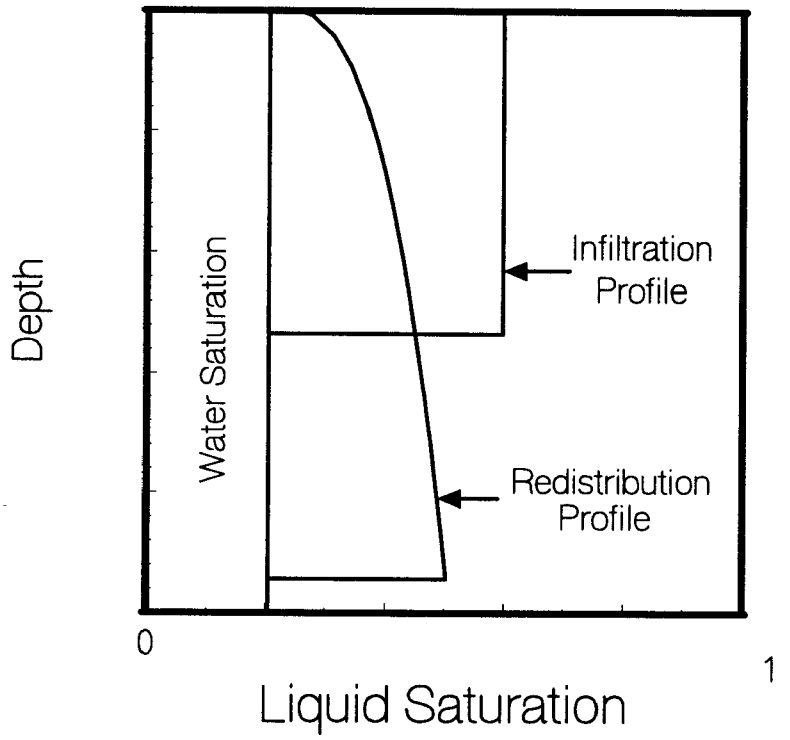


Figure 3 Schematic of a KOPT depth vs. saturation profile

### 3.2.3 Three-Parameter Sharp Front Model

The Three-Parameter Sharp Front Model is a lumped parameter model which adopts the Green-Ampt (Green and Ampt, 1911) formulation used in infiltration processes of water in unsaturated soils. The model assumes a piston front of the chemical completely displacing the air in the available pore space. The available pore space is the total pore space minus the pore space used by residual water, which is assumed to be immobile. The model also assumes a sharp drainage front during redistribution. Thus, the medium is completely saturated between the two fronts and at residual oil and water saturation behind the drainage front (Figure 4).

This idea is put into a mathematical form by combining Darcy's Law with the continuity equation (Illangasekare and Reible, 1987a; Reible et al., 1990):

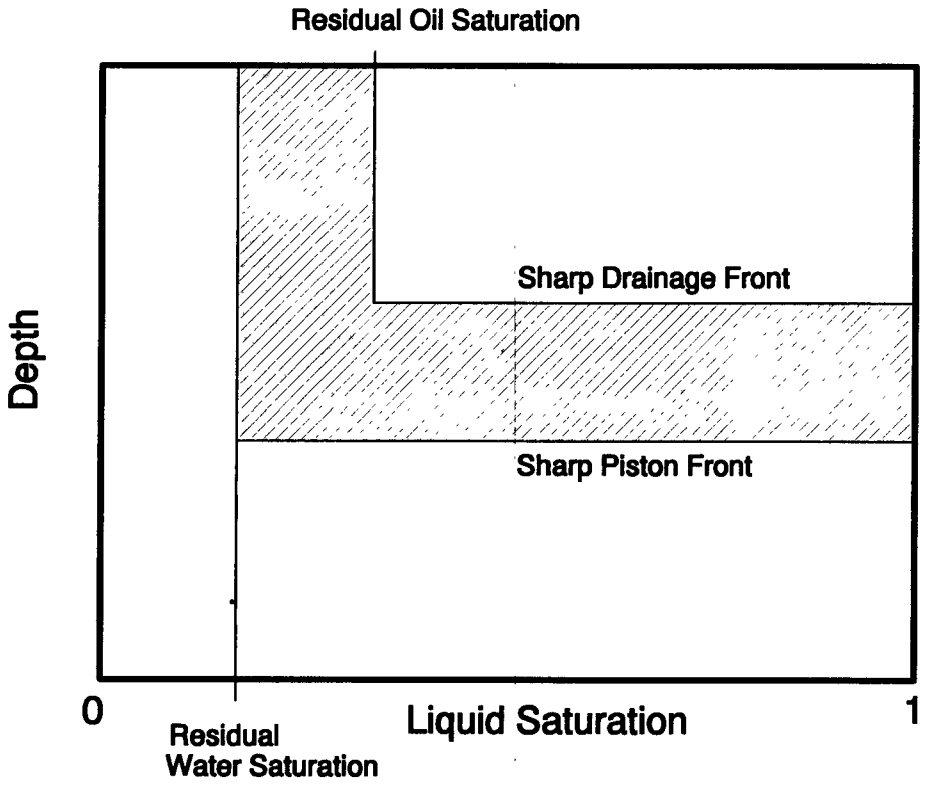


Figure 4. Assumed saturation profile for the Three-Parameter Sharp Front Model.

$$\frac{\partial \theta}{\partial t} + \frac{\rho g}{\mu} \frac{\partial}{\partial z} [K(\theta)\{1 - \frac{\partial \psi_p}{\partial z}\}] = 0 \qquad (16)$$

where $\theta$ is the volumetric content of organic phase [*], $K(\theta)$ is the permeability as a function of phase content [$L^2$], $\psi_p$ is the pressure head [L], z is the depth of infiltration [L].

It can be seen that the total head gradient during infiltration is constant, both under constant ponding and falling head conditions. The gradient can be determined from the head at two points, i.e. the head at the ground surface and the head at the front (Figure 1). The head gradient is:

$$\frac{\partial \psi}{\partial z} = \frac{1}{z_f} [h(z_f) - h(0)] \qquad (17)$$

Equations (16) and (17) :

$$\Theta_0 \frac{dz_f}{dt} = K_m \frac{z_f + H + h_f}{z_f} \quad (18)$$

where $\Theta_0$ is the volume fraction of organic phase behind front [*], $K_m$ is the effective organic phase conductivity behind front [L/T], $h_f$ is the effective capillary suction at sharp front [L], H is the ponding depth [L], and $z_f$ is the depth of infiltration [L]

Equation (18) is solved for three parts of the NAPL release. The first part is infiltration under constant ponding conditions, the second is infiltration under falling head conditions, and the third is redistribution after all of the NAPL has entered the medium and a drainage front is starting to develop. Since it is assumed that the zone between the two fronts is always at full saturation, the permeability is constant during each of these processes.

First, the equation is solved for constant head ponding of the infiltrating fluid. The ponded depth is designated by H. The differential equation can be solved with the initial conditions of $z_f = 0$ for $t = 0$ to give:

$$t = \frac{\theta_0}{K_m}[z_f - (H+h_f)\ln(\frac{z_f + H + h_f}{H + h_f})] \quad (19)$$

Secondly, equation ((18)) is solved for the period when the ponded depth is declining. During the falling head period, no material is added; thus the depth of the ponding organic phase at any time can be given by a simple mass balance:

$$H_0 = \theta_0 z_f + H \quad (20)$$

where $H_0$ = cumulative amount of liquid added [L]. Including this mass balance into the differential front movement equation and integrating from $z_f = z_{f1}$ at $t = t_1$ results in the following equation:

$$t = t_1 + \frac{\theta_0}{K_m(1-\theta_0)}[z_f - z_{f1} - H_2 \ln(\frac{z_f + H_2}{z_{f1} + H_2})] \quad (21)$$

$$\textit{where} \quad H_2 = \frac{h_f + H_0}{1 - \theta_0}$$

Thirdly, the differential equation is solved for the redistribution period after ponding has ended. For redistribution, the head gradient is redefined as the head gradient between the infiltrating front and the drainage front:

$$\frac{\partial h}{\partial z} = \frac{h(z_f) - h(z_d)}{z_f - z_d} \quad (22)$$

where $z_d$ = elevation of the drainage front [L]. A mass balance can be written as:

$$H_0 = \theta_0(z_f - z_d) + \theta_r z_d \quad (23)$$

where $\theta_r$ = residual organic phase content [*]. Integrating from $z_f = z_{f2}$ at $t = t_2$ gives:

$$t = t_2 + \frac{\theta_0}{K}\left[z_f - z_{f2} - \frac{(\theta_r - \theta_0)(h_f - h_d)}{\theta_r} \ln\left(\frac{z_f + H_3}{z_{f2} + H_3}\right)\right] \quad (24)$$

$$\text{where} \quad H_3 = \frac{-H_0 + (\theta_r - \theta_0)(h_f - h_d)}{\theta_r}$$

Equations (19), (21), and (24) in combination define the three-parameter model. The effective conductivity, $K_m$, and the capillary drive heads at the two fronts define the three model parameters.

### 3.2.4 Comparison of the Models

In form, the infiltration portion of the KOPT model is identical to the Three-Parameter Sharp Front model. However, in their basic formulation, the models differ in two ways. First a constant water saturation above residual is allowed in KOPT, but in the three parameter sharp front model the water saturation is at residual. The reason for this assumption in KOPT is that the effects of any recharge water flowing past trapped NAPL phases should be incorporated in field scale simulations. It is recognized that the effects of injection of a NAPL may be to displace water from the pore space (Weaver, 1991). Second, the parameters for KOPT are all determined from the basic multiphase flow parameters such as hydraulic conductivity, fluid densities and viscosities, and parameters of the capillary pressure curve. In the three parameter sharp front model, lumped parameters that are determined by experiment are used for the effective NAPL conductivity behind the front, $K_m$, the head at the front $h(z_f)$, and the head at the back front, $h(z_d)$.

During redistribution, KOPT uses a diffuse drainage wave for the saturation distribution, so that the assumed distribution shows a smooth variation with depth. The three parameter sharp front model uses a sharp front for redistribution as indicated in Figure 4. Thus the NAPL distribution during redistribution appears like a slug. The relationship between the assumptions for redistribution is discussed further in Section 6.

# SECTION 4
# MATERIALS AND METHODS

This section describes the sands and the NAPL that were used in the experiments. This discussion is followed by a detailed description of the apparatus and techniques used to perform the column and tank experiments.

## 4.1 SAND CHARACTERIZATION

Various sands, identified by characteristic mesh sizes from #8 to #125 ,have been used in experiments conducted at the University of Colorado. In this study, #70 sand and #125 sand have been selected as test media for vadose zone experiments. Both sands have been characterized based on their grain size distribution and on their lithology (Held, 1993).

The grain size distribution was obtained with two different methods:

- Standard Method for Sieve Analysis of Fine and Coarse Aggregates (ASTM C 136). Test samples are split representatively, dried at 110°C, weighed and dry sieved in a mechanical sieve shaker for 5 minutes. The analysis was conducted in the porous media laboratory of the Civil, Environmental, and Architectural Engineering Department.
- Settling Tube Analysis as employed in the sedimentology laboratory at INSTAAR, Boulder, Colorado. The procedure is automated, and data acquisition is handled by computer software from CIMAX Inc., Breckenridge, Colorado.

A microscopic investigation was performed and the results were compared visually to standard charts (Powers, 1953). The characterization for both sands is compiled in Table 1.

Figure 5 and Figure 6 give the grain size distribution for #70 and #125 sand, respectively. The filled squares show the grain size fraction as determined with the dry sieving method; the empty squares give the grain size fraction measured with the settling tube. It can be seen from the graphs that both sands are well sorted and fairly uniform.

Table 1. Characterization of #70 and #125 sands

| | #70 Sand | #125 Sand |
|---|---|---|
| a) Grain size | | |
| average particle size, $d_{50}$ (from dry sieving) | 0.185mm | 0.103mm |
| uniformity coefficient, $d_{60}/d_{10}$ | 1.86 | 1.45 |
| b) Grain form | very angular to sub-angular, spherical to sub-prismoidal | sub-angular to rounded, spherical |
| c) Sorting | very well to well sorted | very well sorted |
| d) Maturity | immature | mature |
| e) Modal components | | |
| Lithoclasts | 1% | - |
| Quartz, clear | 55% | 95% |
| Quartz, milky | 25% | - |
| Feldspar | 8% | 3% |
| Muscovite | 5% | - |
| Biotite | 5% | 1% |
| Accessories: Zircon, Hematite, Rutile, Garnet | about 1% | about 1% |
| f) Porosity for medium compaction | 0.45 | 0.39 |

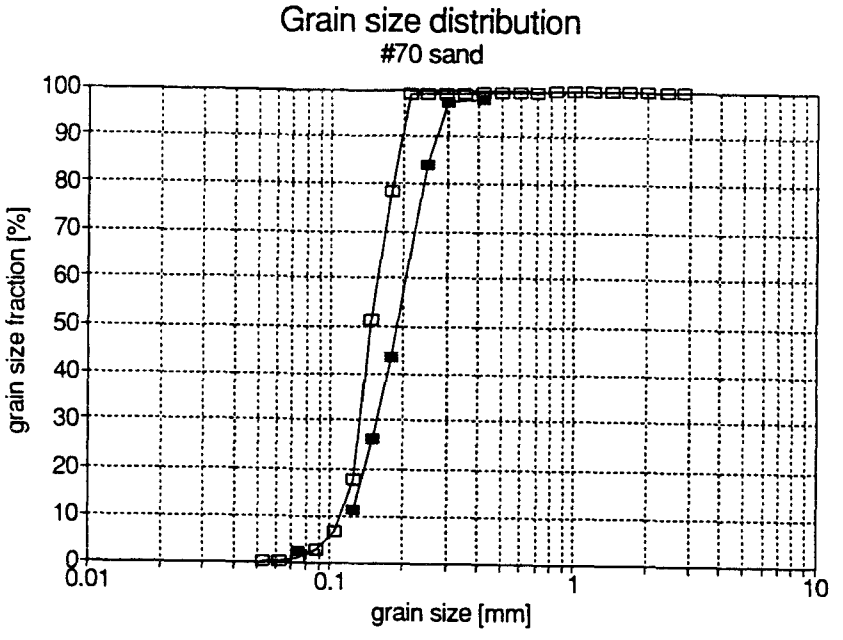


Figure 5. Grain size distribution for #70 sand. Measured with dry sieving method (filled squares) and settling tube method (empty squares).

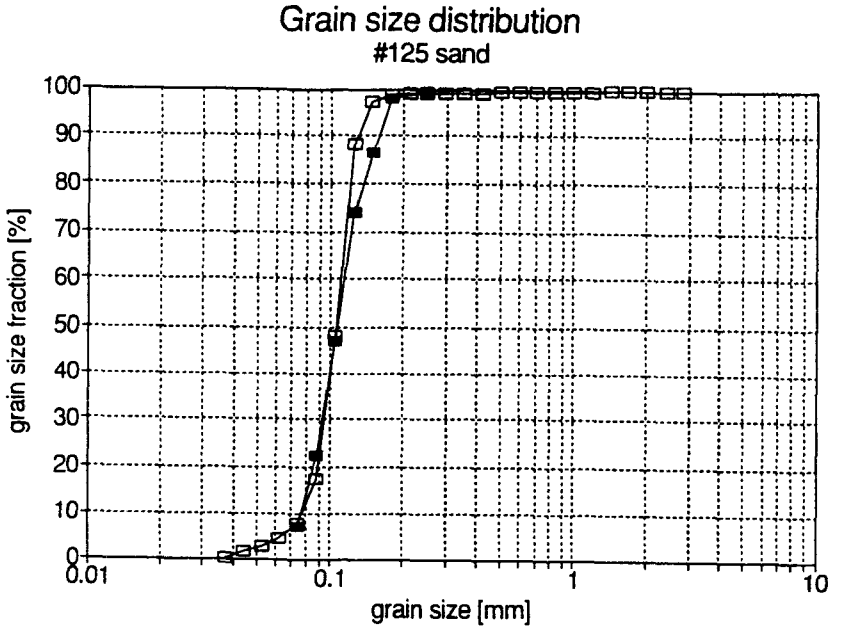


Figure 6. Grain size distribution for #125 sand. Measured with dry sieving method (filled squares) and settling tube method (empty squares).

## 4.2 CHARACTERIZATION OF THE TEST FLUID

A lighter-than-water liquid, Soltrol 220, was used as the test fluid in all the experiments. Soltrol 220 is an isoparaffinic solvent, manufactured by Phillips Petroleum Company. It is a colorless liquid mixture of C13 to C17 hydrocarbons, with a boiling point between 232°C and 288°C (Material Safety by Phillips Petroleum Data Sheet). Its solubility in water is negligible, which makes it ideal for experiments as a NAPL. The second reason to choose Soltrol for lab experiments is its low toxicity. Soltrol has a low vapor pressure of 0.004 psi, and its vapor is heavier than air. The specific gravity is 0.809 at 15°C. At 23°C, the density is 0.789 g $cm^{-3}$, kinematic viscosity as 6.12 centistokes, surface tension with water 42 dynes $cm^{-1}$, surface tension with air 27 dynes $cm^{-1}$ (Szlag and Illangasekare, 1992).

The gamma attenuation coefficient of Soltrol is very similar to that of water. Following the work of Lenhard and Parker (1987), 1-iodoheptane was mixed with Soltrol to increase the attenuation coefficient of Soltrol. A volume ratio of 1 to 9 of iodoheptane to Soltrol was used. The chemical formula of iodoheptane is $CH_3(CH_2)_6I$. Adding iodoheptane changes the kinematic viscosity of Soltrol to 4.8 centistokes at 23°C. The viscosities of Soltrol and the Soltrol-iodoheptane mixture are temperature dependent (Figure 7). The viscosity of the Soltrol (90%) and iodoheptane (10%) mixture was also determined by measurement at the US EPA Kerr Laboratory in Ada, Oklahoma. The procedure followed was ASTM D445, which used Cannon-Fenske viscometers suspended in a constant temperature water bath. At 25°C, the viscosity of the mixture was 3.78 cp and the density 0.85 g $cm^{-3}$. At Kerr Laboratory, the Soltrol surface tension was measured and found to be 24 dynes $cm^{-1}$.

Automate Red Dye (Morton International) was used to color the Soltrol. This water insoluble dye is soluble in petroleum products and insoluble in water. Very small amounts suffice to give the Soltrol a bright red color, but the dye does not change any of the physical properties affecting the flow of Soltrol. (Szlag and Illangasekare, 1992)

## 4.3 SAMPLE CELL AND COLUMN

Two columns were used in the experiments. The first was a small cell with a height of 4 cm. It was used for parameter determination experiments. The spill simulations were done in a 180 cm column. The columns consisted of a clear plexiglass tube with an inside diameter of 8.2 cm. Aluminum end covers were constructed to fit the top and bottom of the plexiglass tubes of both the cell and the column. The top and bottom fittings were designed to make an airtight seal to allow for evacuation of the fluids (air or water) from the sample. Valves were provided in both end fittings for the entry and exit of air and water. The bottom fitting contained a removable high-air-entry-value porous plate, through which the sample could be de-saturated.

O-rings were used to create an airtight seal around the plexiglass tube. The top fitting contained a porous metal plate which allowed for uniform air entry at the top of the soil surface (Figure 7). Two valves were connected to the porous metal plate. The bottom fitting consisted of two parts (Figure 8). The lower part held a porous ceramic plate, that was connected to the two valves. The porous ceramic plate had to fit tightly inside the aluminum end cover to prevent

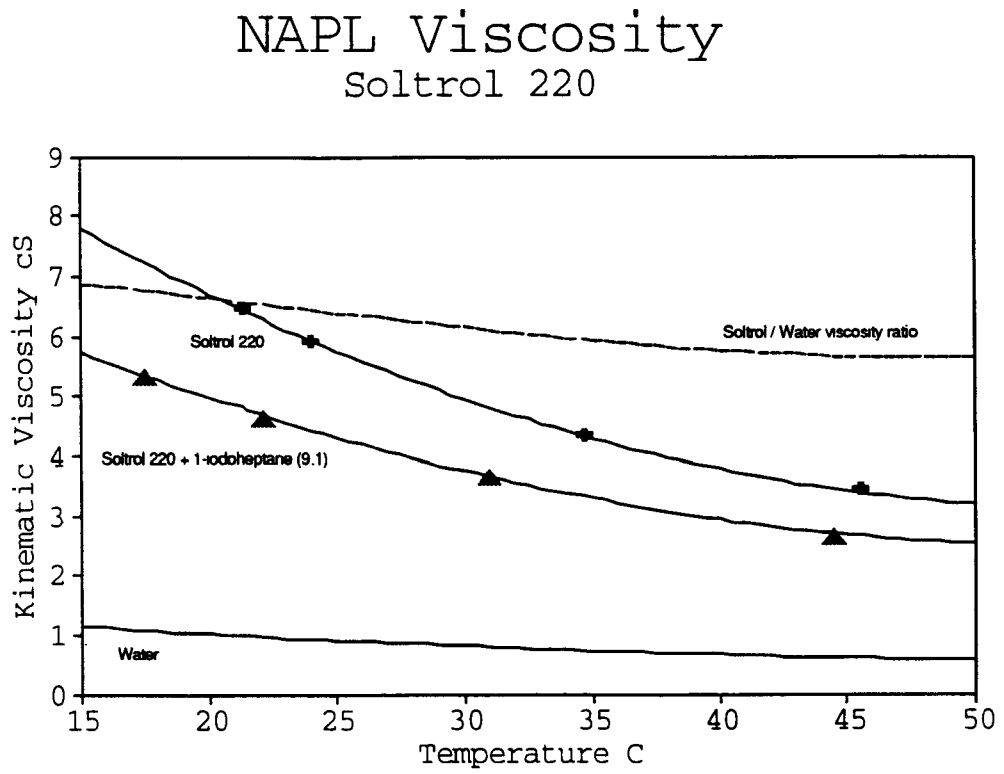


Figure 7. Kinematic viscosity of Soltrol, Soltrol + iodoheptane and water versus temperature. (Szlag and Illangasekare,1992)

air from leaking around it. An o-ring alone did not completely seal the system, so epoxy was used to glue the porous plate in place. The second part of the bottom connection was the fitting around the sample tube that closed off the bottom of the tube with a flexible mesh to prevent the sand from leaving the column when the porous plate was removed. The flexible mesh provided for full contact between the sand and the porous plate. An additional valve was placed in the side of the bottom fitting to allow for drainage or imbibition of water into the sample without flow through the porous plate. Permitting part of the flow to bypass the porous plate avoided two problems. First, a low flow rate, due to the low hydraulic conductivity of the plate, was avoided. Second, the ceramic porous plate had very fine pores, and fine particles suspended in the water were found to clog the pores. For these reasons, it was advantageous to drain only the minimum amount of water through the porous plate.

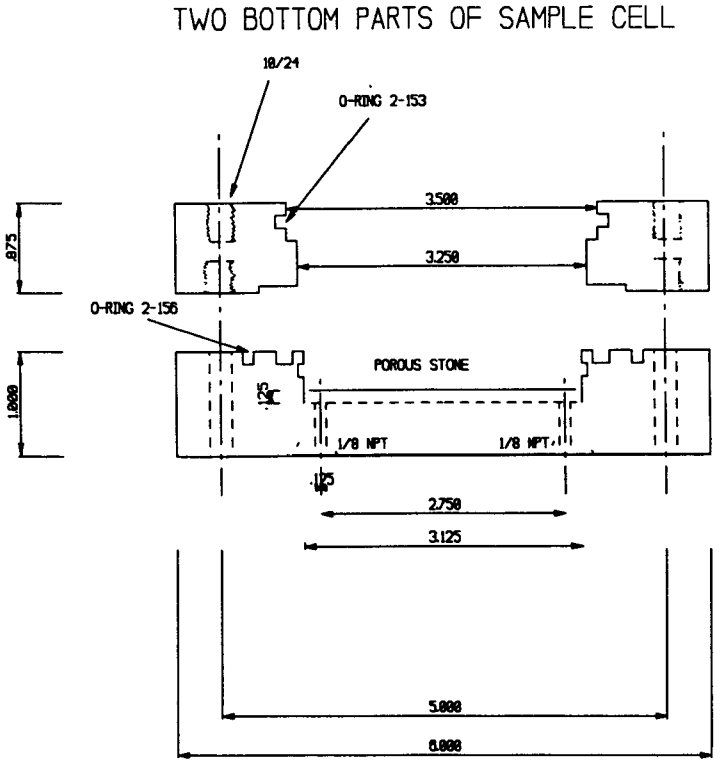


Figure 8. Aluminum fitting for bottom part of sample cell. Sizes are given in inches.

The top aluminum fitting of the sample cell was used to create controlled rainfall. A small cell was built that consisted of a 4 cm tall piece of the same kind of plexiglass tube that was used for the column. A bottom plate was glued to this plexiglass tube. Five holes were drilled in the bottom plate, and hypodermic needles were inserted into the holes. These needles served as rainfall ports. The rainfall cell was closed at the top with the top aluminum fitting, and filled with water supplied through the valves. Since the cell was closed on all sides, except for the small needle openings, water pressure built up inside the cell. The water pressure regulated the amount of water flowing through the needles and thus the simulated rainfall rate. The water pressure itself was regulated by the height of a supply reservoir placed above the cell. By fixing the elevation of the reservoir, a controlled rainfall rate was established. A calibration was performed before every experiment, during which the amount of water leaving the cell per unit time was measured for each elevation of the supply reservoir above the cell.

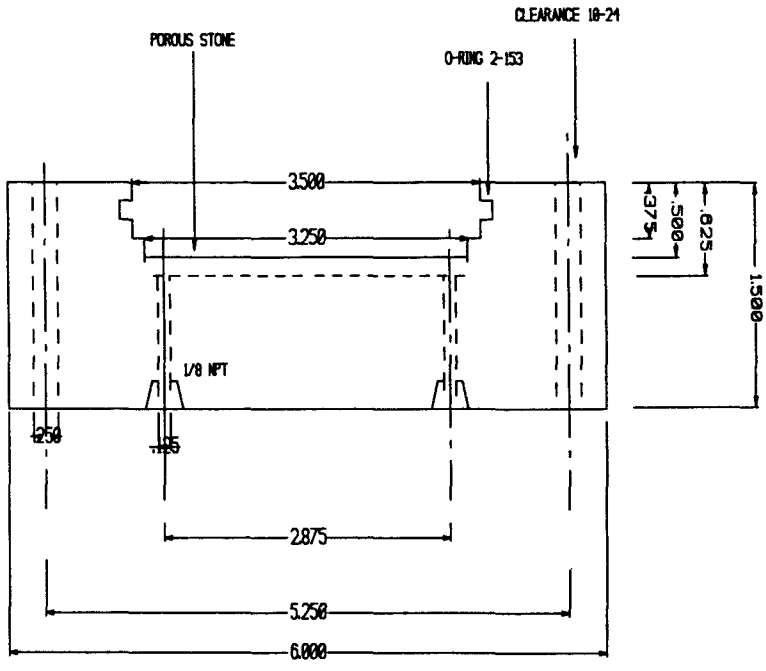


Figure 9. Aluminum fitting for top part of sample cell. Sizes are given in inches.

## 4.4 EXPERIMENTAL PROCEDURES FOR COLUMN EXPERIMENTS

In all experiments, it was necessary to pack the test cell or column as uniformly as possible with sand (Armbruster, 1990). To achieve a homogeneous filling, a long tube of smaller diameter was placed inside the long column, and the sand was poured into the inner tube. The sand was allowed to fall through eight holes in the tube (four sets each located approximately 30 cm and 60 cm above the column end) into the larger column. By slowly lifting the tube while the sand filled the column, the formation of sand layers was avoided. Pouring of the sand was stopped when the top of the sand was about 20 cm below the top of the column. The supply container holding the sand was weighed before and after filling the column to determine the amount of sand used in the packing. The volume of the sand pack was calculated from the height of the sample and was used with the known weight to estimate the porosity.

Next, the sand was completely saturated with the wetting phase (water or Soltrol, depending on the particular experiment). A vacuum was applied at the top of the column, or sample cell, to remove all air from the sand. After the air had been removed, the liquid was allowed to enter through the bottom of the column (Figure 10). The wetting phase was first pulled through the porous plate to ensure complete saturation of the plate. After the porous plate had been saturated, the saturation process was continued through the side port above the porous plate to permit a faster flow rate. This procedure ensured minimum air entrapment. The vacuum

level, as well as the flow rate of the liquid, could be adjusted with regulating valves. The column was filled until the fluid reached a level of about 10 cm above the sand.

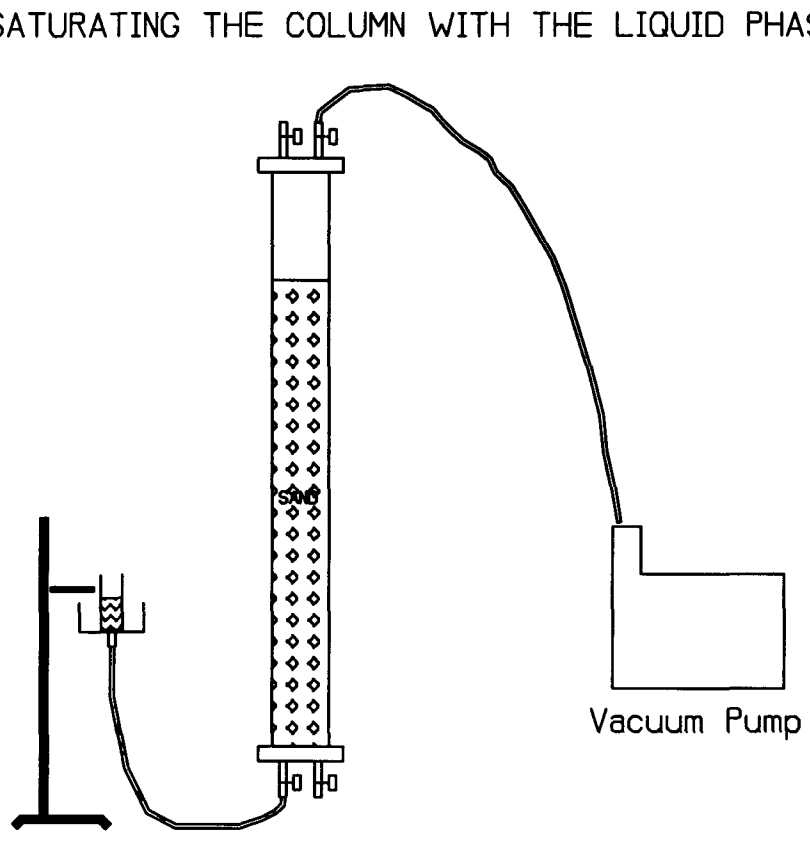


Figure 10. Saturating the sand filled column with wetting fluid.

The vacuum pump was disconnected and the fluid reservoir connected to the bottom of the column was lowered to create the desired level of suction. The column was allowed to drain for a minimum of 2 days. Residual saturation throughout the column was achieved by water draining through the porous plate. A suction head of 3 m of water was applied to the porous stone. The porous stone prevented air from channeling through the plate. As long as air was prevented from being pulled out of the sand, the full suction was applied to the water phase; and the sand was brought to residual saturation over the whole length of the column without the creation of a capillary fringe zone. The top of the column was covered with plastic wrapping, to avoid drying the top of the sand. The porous stone was removed from the bottom of the column after having obtained the uniformly residual saturated column. Air could now escape freely through the bottom of the column. Thus, the initial water saturation in the soil column was similar to the initial condition assumed in the computer models.

Gamma scans were taken after each of the above steps to obtain attenuation coefficients and the saturation distribution down the column. Gamma absorption was measured down the

length of the column at 1.0 cm intervals. In the first Gamma scan, taken before the introduction of water, the attenuation was measured along the 20 cm long empty portion of the column, as well as the sand-packed portion (Figure 11). In the second scan, taken after saturating the column, the attenuation was measured through the part of the empty column, the liquid filled portion, and the saturated sand pack (Figure 12). In the third scan, taken after draining the column, the attenuation was measured through the empty column, and the partly saturated sand (Figure 13).

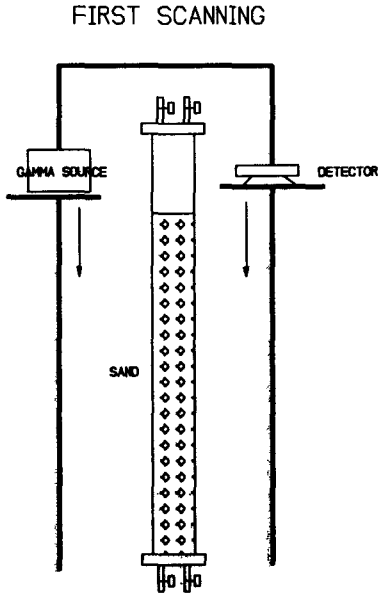


Figure 11. Setup for first scan through dry sand.

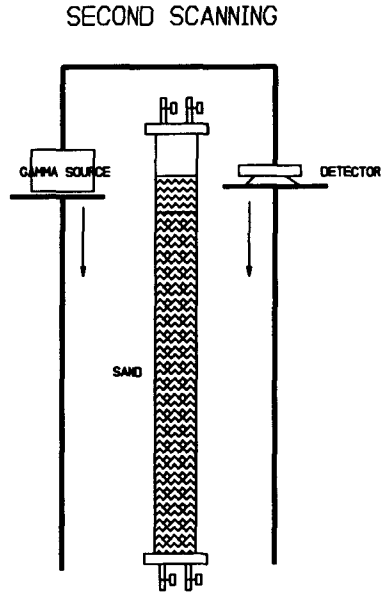


Figure 12. Setup for second scan through fully saturated sand. Water is ponding on top of sand.

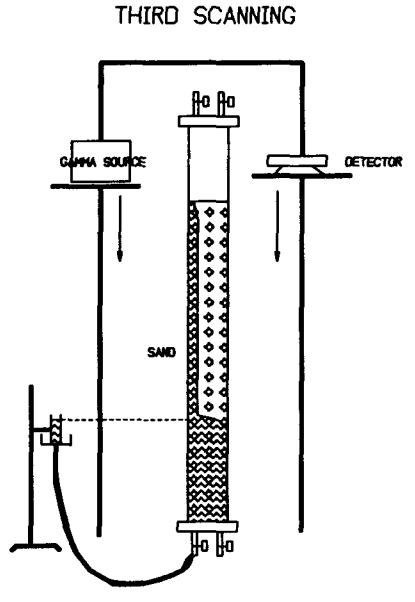


Figure 13. Setup for third measurement through partially saturated sand.

The phase content calculations were performed as follows. The equations defining the attenuation coefficients and illustrating their usage in the measurement of phase contents are given in Appendix 1. The variables and parameters used in the calculation are also defined in Appendix 1. In all three scans, that were described earlier, the gamma radiation $I_O$ was measured first through the empty column. These readings were used as a standard for correcting the count rate for detector sensitivity changes in subsequent measurements.

The first scan produced values of the initial radiation, $I_D$, through the dry sand. From the second scan, the lumped attenuation coefficient for the liquid phase was calculated. Scanning the empty column first, then the portion of the column filled with the liquid phase, allowed the calculation of the lumped attenuation coefficient (the attenuation coefficient density). The radiation measured through the fully saturated sand $I_{fl}$ was corrected using $I_S$ from the first and the second measurement. The phase content could then be calculated using the corrected $I_{fl}$, $I_D$ and the lumped attenuation coefficient.

After draining the column, the radiation through the partly saturated sand was measured. The phase content was calculated as above, with the attenuation coefficient calculated from the second scan.

In the spill experiments, a known volume of Soltrol was applied to the top of the column and allowed to infiltrate through the sand. The Soltrol was dyed with Automate Red, allowing visual observation of the front movement. At the same time, the gamma system was used to obtain phase content profiles along the length of the column. The scan through the residually saturated column was used to determine the initial count rate, $I_0$. The soil column was also scanned while the Soltrol was still ponded on top of the sand; the attenuation coefficient for Soltrol was calculated from this measurement. Soltrol content profiles during the spill were thus computed.

In the rainfall experiments, the rainmaker was placed on top of the column. Water was dyed green with food coloring so the water front could be observed. The food coloring did not change the viscosity or surface tension of the water (Szlag and Illangasekare, 1992).

The porosity of the sand pack must be known to calculate saturations from the volumetric phase contents that are determined with the gamma system. When calculating the error in the saturations, the error in the porosity has to be accounted for. Three techniques were used to calculate the porosity of the sand:

1. Gravimetric Procedure: The weight of the sand used to fill the column and the volume of the sample can be used directly to calculate the bulk density and porosity. The disadvantage of this approach is that mass of the sand cannot be determined exactly, because of spill losses during the filling of the column. Also, the use of total weight and volume gives only an average porosity for the whole sample. Assuming that not more than 400 g of sand are lost and the error in measuring the height of the sand is at most 1 cm, the maximum relative error in determining the average porosity for the whole column is ±3%.

2. Use of a single spectrum of the gamma system: From the first measurement through the empty column and the dry sand, a lumped attenuation coefficient for the sand can be calculated. Knowing the attenuation coefficient, the bulk density can be calculated. Problems with this approach are that the path length through the column cannot be determined very exactly (81 ±1 mm), which decreases the accuracy of the lumped attenuation coefficient. The lumped attenuation coefficient has a relative error of 1%. The mass attenuation coefficient as calculated in the error propagation calculations has a relative error of ±3%. Thus the total error in determining the porosity is ±4%. An advantage of this approach is that the bulk density can be calculated at any desired location along the column.

3. Use of two spectra of the gamma system: The Americium and Cesium spectra can be used to calculate bulk density and phase content simultaneously. However, the summation of the random errors of both spectra leads to high errors in the porosity measurements. The error in the calculation of porosity is about ±7%.

If experimental conditions allow for it, the bulk density should be determined gravimetrically and with a single spectrum measurement. Only if a measurement through dry sand is not possible, the two spectrum measurement to determine bulk density should be used.

## 4.5 TWO-DIMENSIONAL TANK EXPERIMENTS

Spill experiments were conducted in a two-dimensional vertical tank (180 *x* 120 cm *x* 5 cm) to investigate the two-dimensional movement of a NAPL in the unsaturated zone. The tank walls were made of glass-lined plexiglass walls. The glass lining protected the plexiglass walls from aggressive chemicals, while the 1.9 cm thick plexiglass provided the necessary wall strength to support the soil sample.

The tank was packed with sand using the following procedure. Approximately 5 cm thick layers of sand were placed in the tank through a funnel attached to a long tube. Every layer was then mixed by pulling a long rod through the soil before the next layer of sand was poured in. A nearly homogeneous packing was thus achieved. Two valves at the bottom of the steel end walls of the tank permitted saturating the sand with water from the bottom to minimize the entrapment of air. Unlike the one-dimensional column, the tank could not be completely air-evacuated. The water was drained from the bottom of the tank to create the unsaturated zone. The bottom of the tank had been filled with a layer of coarse gravel to prevent the valves from getting plugged with fines during desaturation. A capillary fringe formed at the bottom of the tank, because there was no provision for desaturation of the sand through a porous plate. All experiments were stopped when the spill front reached a point 15 cm above the saturated zone. Up to this depth, the assumption of uniform residual saturation held true for the experiments.

The spill experiments in the tank were conducted in a manner similar to the column experiments. The Soltrol was applied in a 30 cm wide slug, with a maximum ponding depth corresponding to the ponding depth in the column. PVC pipes with an outside diameter equal to the tank width were used to retain the infiltrating Soltrol within the source region. These barriers penetrated about 5 cm into the sand (Figure 14).

Simulated rainfall was applied across the total length of the tank from a 5 cm diameter PVC pipe with 86, 1 mm holes. The rainfall rate was regulated by controlling the number of holes through which water was allowed to flow. The rainfall rate was calibrated before every experiment. Green food coloring was applied to the rainwater to observe the water front in the soil. The observed outline of the fluid front was traced manually on the tank wall and later transferred to paper.

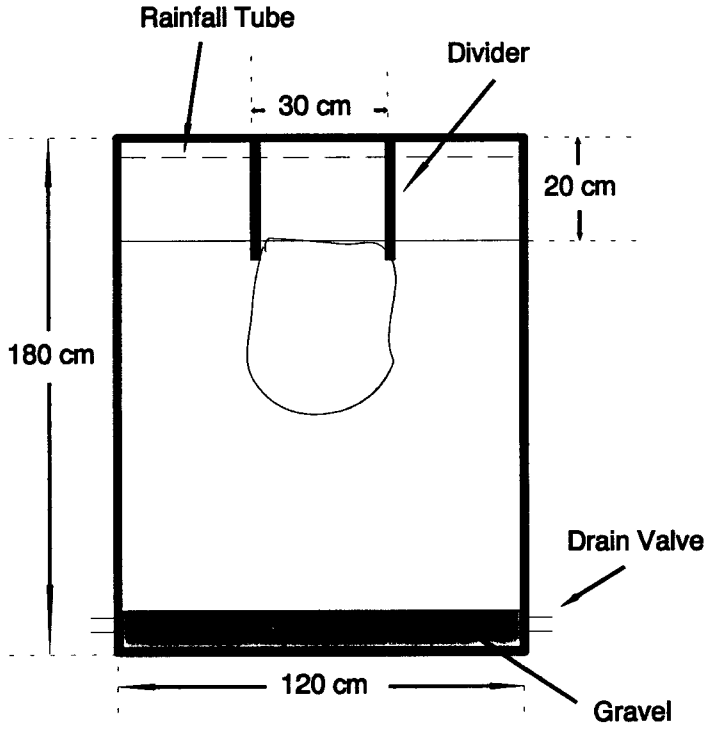


Figure 14. Schematic of a spill in the tank.

# SECTION 5
# RESULTS AND DISCUSSION

The experimental results and the model evaluation are presented and discussed in this section. Hydraulic conductivity and the capillary suction-saturation relationship for #70 and #125 sand for water and Soltrol were measured. These parameters were needed as input to the computer models. The model results were compared with the experimental results.

## 5.1 DETERMINATION OF MODEL INPUT PARAMETERS

Hydraulic conductivity is the single most sensitive input parameter for the KOPT and Three-Parameter-Sharp-Front models. The KOPT model also uses Brooks and Corey parameters for the capillary pressure versus saturation curve as input values in order to calculate permeability as a function of saturation. The Three-Parameter-Sharp-Front model assumes full saturation behind the front, thus capillary pressure versus saturation and permeability versus saturation are not used. Experiments with the flow pump, a small column at RSKERL, and the gamma system were used to obtain accurate values for hydraulic conductivity and capillary pressure versus saturation curves.

### 5.1.1 Hydraulic Conductivity

The value of the hydraulic conductivity used in the KOPT model simulations for the #125 sand was determined as follows. A meter long, 5.0 cm diameter, chromatography column was fitted with sampling ports spaced at 10 cm intervals along the length of the column. The sand was allowed to fall through a tube, which was gradually raised as the column was filled. Carbon dioxide was passed through the column to displace air before saturating the column with water. De-aired ground water was then used to saturate the column. Any entrapped carbon dioxide dissolved rapidly in the water, thus the column became fully saturated.

Manometers attached to the ports allowed measurement of the head drop along the length of the column. Steady state was established in the column and measurements were made after approximately 2 hours of flow. The variation of hydraulic conductivity along the column was determined by this procedure. Figure 15 illustrates variation of hydraulic conductivity along the length of the column. The average hydraulic conductivities from three experiments are shown in Table 2.

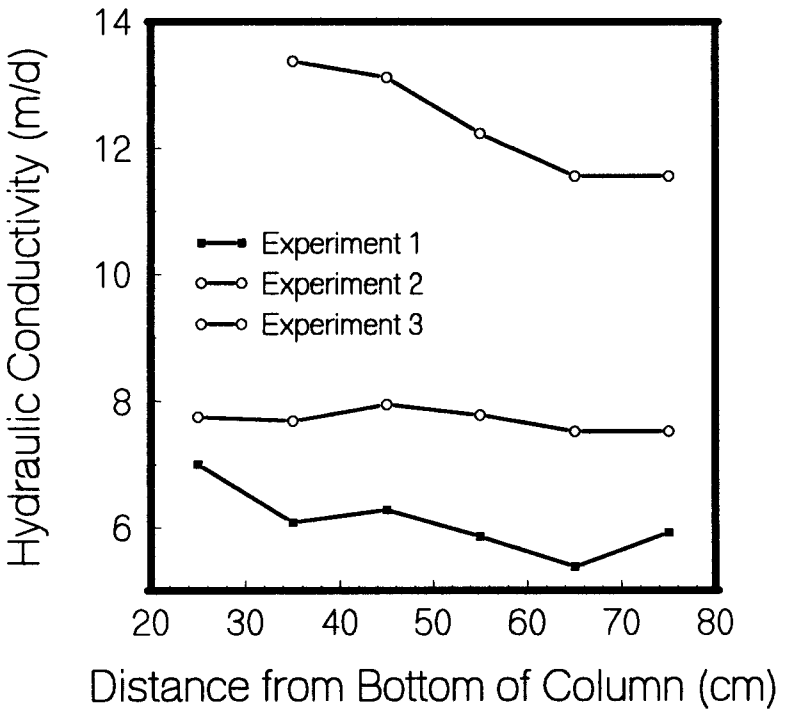


Figure 15 Variation in #125 sand hydraulic conductivity along the length of the chromatography columns.

Table 2. Hydraulic conductivity for #125 sand

| Hydraulic Conductivity | |
|---|---|
| Experiment | Average $K_s$ (m/d) |
| Long Column 1 | 7.70 |
| Long Column 2 | 6.09 |
| Long Column 3 | 12.36 |

Averaging the 17 individual measured conductivities gives a value of 8.50 m/d with a standard deviation of 2.71 m/d. The values were averaged to give a single measured $K_s$ value for use in KOPT. The standard deviation was used to show the variability associated with packing the sand in simulations presented later in this report (Figure 58).

For the #70 sand, long column experiments were not performed to determine the hydraulic conductivity. In this case, however, the hydraulic conductivity was adjusted until data from the 1000 ml spill was matched by the KOPT model. This value of 15.0 m/d was then used without further manipulation in the simulations of the 500 ml and 750 ml spills.

### 5.1.2 Suction-Saturation Measurements in the Small Cell

Steady state suction-saturation profiles for #125 sand for water were measured in the small cell. These measurements had the purpose of verifying the suction saturation profiles obtained with the flow pump. Suction was applied to the cell via the porous bottom plate. A water reservoir in direct connection with the sample through the porous plate was lowered in steps below the sample to achieve a number of defined suction heads. After gradual lowering of the water reservoir, one had two wait until the extra water was drained from the sample. The duration of this waiting period depended on the suction change and the starting saturation, but is usually the order of hours or days. Thus, a measurement of a large number of points was not feasible. Saturation was measured with the gamma system, using only the Americium source. The porosity was determined gravimetrically. The capillary suction head versus saturation for two experiments are graphed in Figure 16. Only a few points were obtained; however, it can be seen that the points can be connected to form the typical suction-saturation curve, but as can be expected these measurements are less precise than the flow pump data. In addition to the larger number of data points, the flow pump gives the suction-saturation relationship much quicker than the gamma system with the small cell.

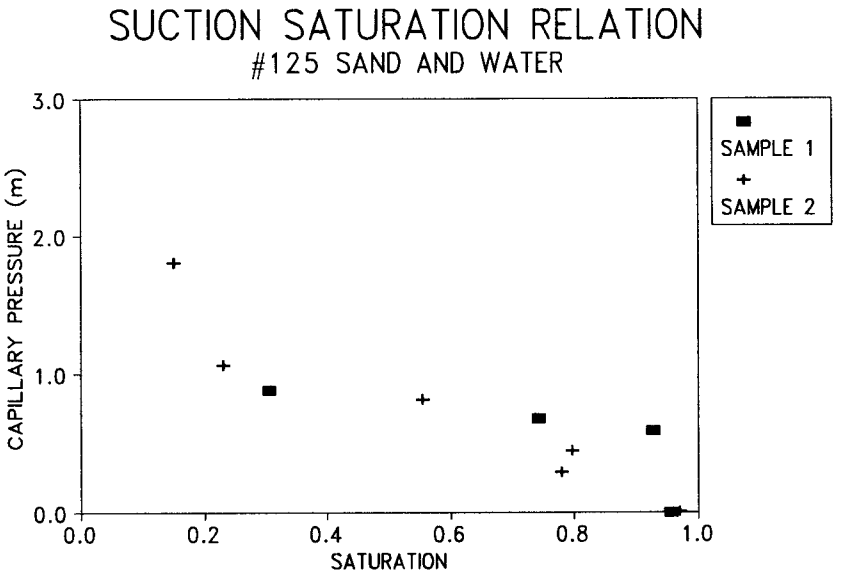


Figure 16. Suction-saturation curve measured in the small cell.

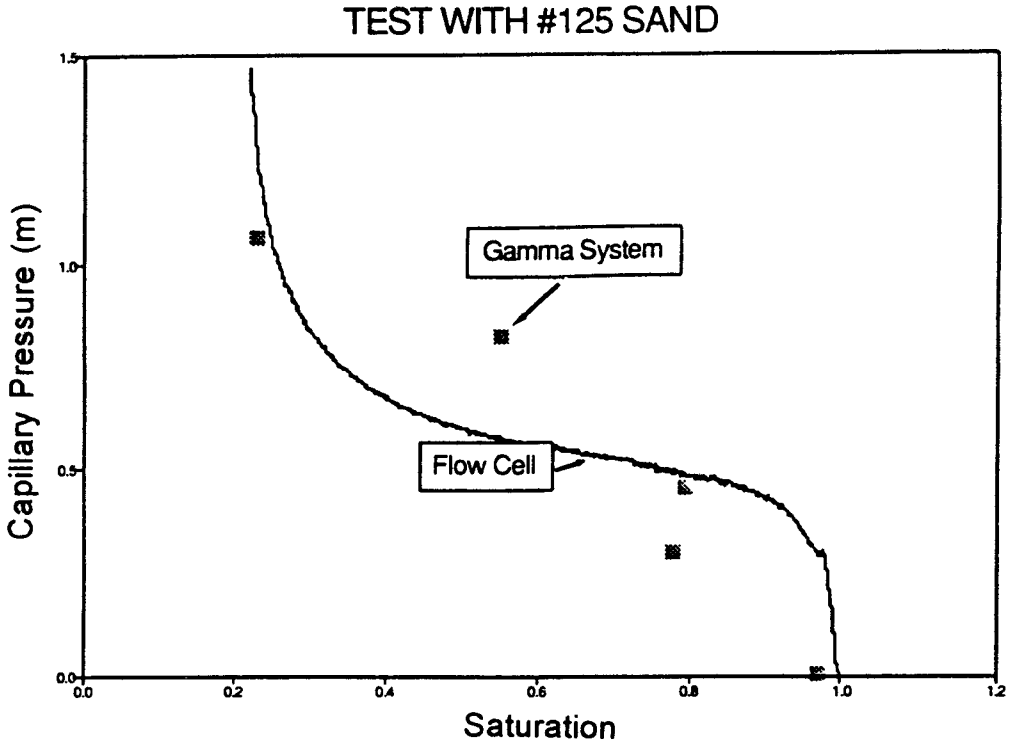


Figure 17. Suction-saturation curve for #125 sand. Comparison between flow pump and gamma system data for small cell.

### 5.1.3 Estimation of Brooks-Corey Parameters

The large amount of data obtained with the flow pump was reduced to van Genuchten model parameters. Since KOPT is designed to use Brooks and Corey model parameters, two approaches were used to estimate equivalent Brooks and Corey model parameters from the given van Genuchten model parameters. In the first approach, a water/air curve was generated using van Genuchten's model. The nonlinear fitting program RETC (van Genuchten et al., 1991) was then used to determine Brooks and Corey parameters for this "data" set.

The approximate conversion equations between Brooks and Corey model parameters and van Genuchten parameters developed by Lenhard et al. (1989) were used in the second approach. The Lenhard et al. (1989) equations are

$$\lambda = \frac{m}{1-m}\left(1 - 0.5^{\frac{1}{m}}\right) \tag{25}$$

$$h_{ce} = \frac{\bar{S}_e^{\left(\frac{1}{\lambda}\right)}}{\alpha}\left(\bar{S}_e^{\left(\frac{-1}{m}\right)} - 1\right)^{1-m} \tag{26}$$

where:

$$m = 1 - \frac{1}{n} \tag{27}$$

(where n is a parameter of the van Genuchten model) and $S_e$ is defined by Lenhard et al.'s (1989) empirical relation

$$\bar{S}_e = 0.72 - 0.35 \exp\left(-n^4\right) \tag{28}$$

The values of the van Genuchten parameters from the flow pump data were converted to equivalent Brooks and Corey model parameters using this set of equations. Plotted model curves for both approaches are shown in Figure 17.

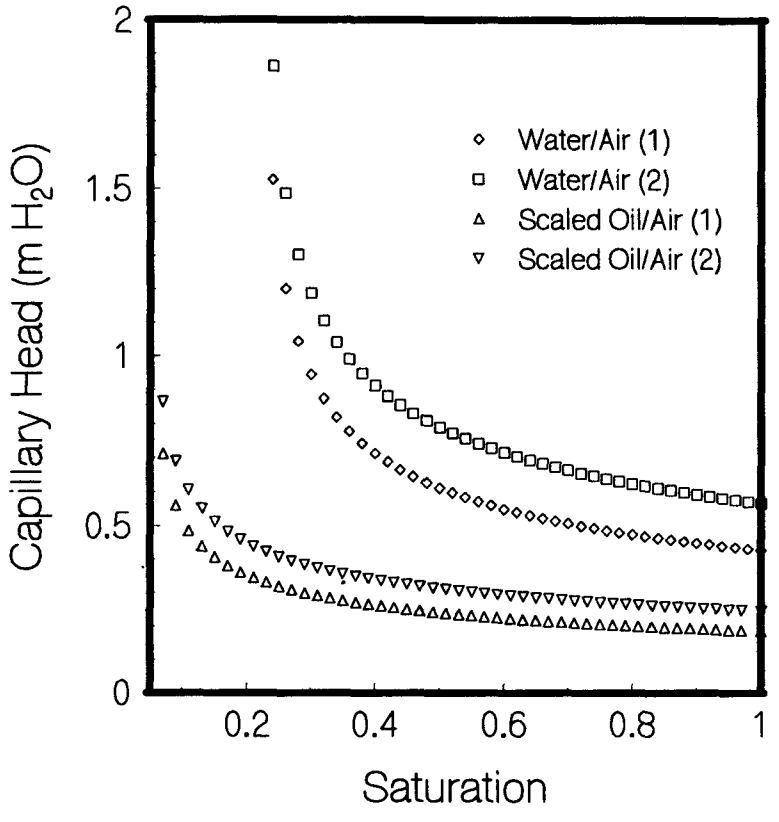


Figure 18. Water/air and scaled oil/air pressure curves for #125 sand using Brooks and Corey parameters.

Table 3 shows a comparison of the parameters obtained by each approach. With the first approach (nonlinear fitting with RETC), a range of values was obtained during the fitting; and the 95% confidence limits are shown in parenthesis for each parameter in the table. For each fitting, the residual water saturation was held to the value originally determined from the measured data.

Table 3. Equivalent Brooks and Corey parameters.

| Equivalent Brooks and Corey Parameters | | |
|---|---|---|
| | Approach 1 (nonlinear fitting with RETC) | Approach 2 (Lenhard et al. (1989) Conversion Equations) |
| *#125 Sand* | | |
| $h_{ce}$ (cm) | 42.8 (42.19,43.29) | 56.6 |
| $\lambda$ | 2.88 (2.70,3.06) | 3.76 |
| $S_{wr}$ | 0.22 | 0.22 |
| *#70 Sand* | | |
| $h_{ce}$ (cm) | 26.83 (26.39,27.25) | 37.05 |
| $\lambda$ | 2.44 (2.29,2.59) | 2.571 |
| $S_{wr}$ | 0.30 | 0.30 |

Although the air entry heads, $h_{ce}$, were consistently higher for approach 2, the scaled oil/air curves remained relatively close. Since KOPT is relatively insensitive to the capillary pressure curve parameters, at least during infiltration (Weaver et al., 1992), the model results were not greatly affected by these values. Figure 19 illustrates the effect of variation in the capillary pressure curve parameters used in KOPT for simulating the 1000 ml Soltrol spill in the #125 sand. The higher entry head had the effect of causing the front to be displaced downward. The result was due primarily to the increase in capillary suction during ponded infiltration. The effect of the procedure for determining the Brooks and Corey parameters was also examined for #70 sand (Figure 20) and found to be similar to that for the #125 sand.

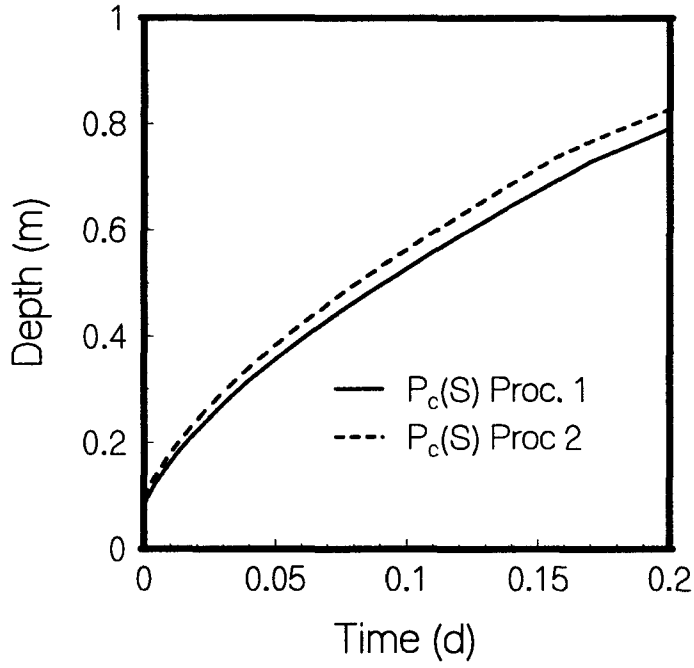


Figure 19. Comparison of front positions as simulated using KOPT in #125 sand for the capillary pressure curve parameters determined by approaches 1 and 2.

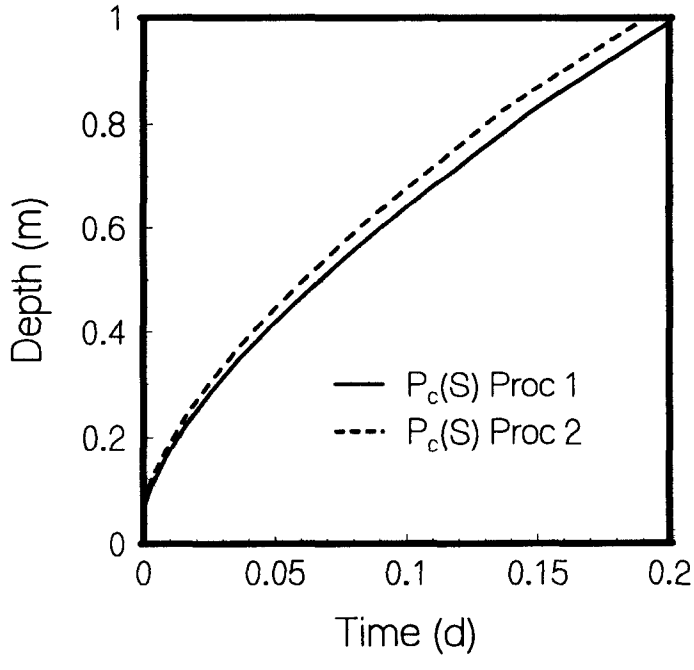


Figure 20. Comparison of front positions as simulated using KOPT in #70 sand for the capillary pressure curve parameters determined by approaches 1 and 2.

### 5.1.4 Comparison Between Suction-Saturation Curve Estimated from Flow-Pump Data and Gamma Measurements

The water/air and Soltrol/air suction-saturation curves were determined with the gamma system for the #125 and #70 sands. The column was first filled with sand, then completely saturated with the wetting fluid (water or Soltrol), and allowed to drain under gravity. The drainage water reservoir was held near the bottom of the column. The coordinate origin for the graphs was set at the elevation of the reservoir where the liquid phase pressure was atmospheric. All graphs of the suction-saturation curves show a fully saturated zone of sand at negative elevations, i.e. below the water (Soltrol) level, and a fully saturated capillary fringe above the water (Soltrol) level. Water (or Soltrol) at the top of the column is at residual saturation. The gamma data were compared with the suction saturation curves derived from the Brooks and Corey parameters, which in turn are obtained, as described before, by converting the van Genuchten parameters from the flow pump data with two different approaches. The gamma saturation was calculated from the phase content with the porosity calculated from the gamma scans. This resulted in full saturation values close to 1, and was thus found acceptable.

a) Water-air capillary pressure curve in sand #125 (Figure 21)

The scanning time for this experiment was 20 seconds at every point. Nine scans were repeated at every location. After nine scans, the gamma system moved 1.25 cm vertically down to the next scanning location.

The porosity of the sand as determined gravimetrically was 0.41. The average porosity calculated from the Americium scan was 0.39. The residual saturation was found to be approximately 0.2; the height of the capillary fringe was 0.5 m. The gamma data agree well with the Brooks and Corey suction-saturation curves derived from the flow pump data with approaches 1 and 2.

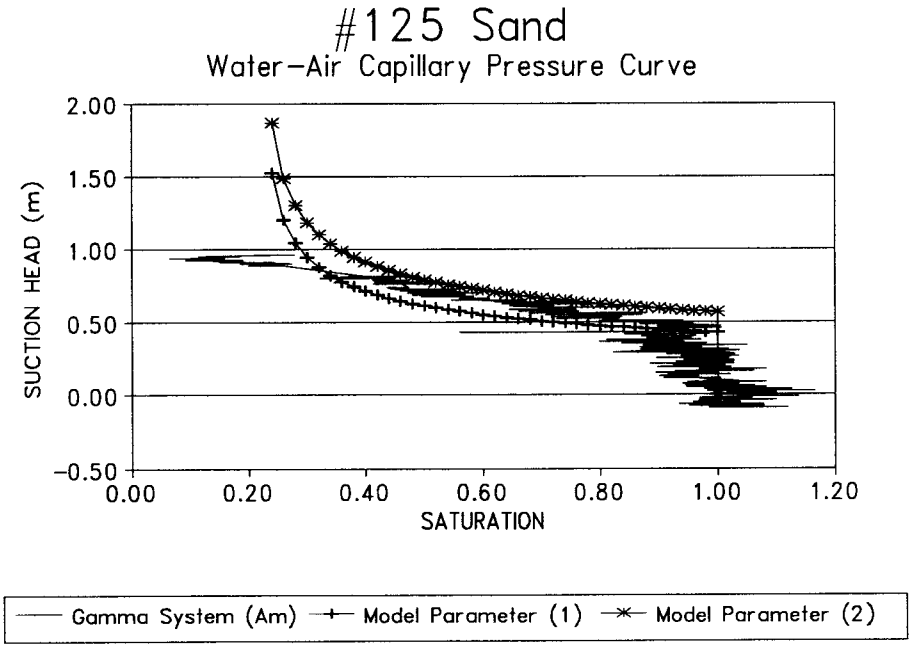


Figure 21. Suction-saturation profile for #125 sand and water-air.

b) Sand #70 and water (Figure 22).

As for the previous experiment, the same scanning time of 20 seconds was used. Two scans were repeated at every location. After 2 scans, the gamma system moved 1.25 cm vertically down to the next scanning location.

The porosity of the sand as determined gravimetrically was 0.48. The average porosity calculated from the Americium scan was 0.55. The residual saturation was found to be approximately 0.25, measured with Americium. The height of the capillary fringe was 0.2 m. The gamma data agree well with the Brooks and Corey suction-saturation curves derived from the flow pump data using approaches 1 and 2.

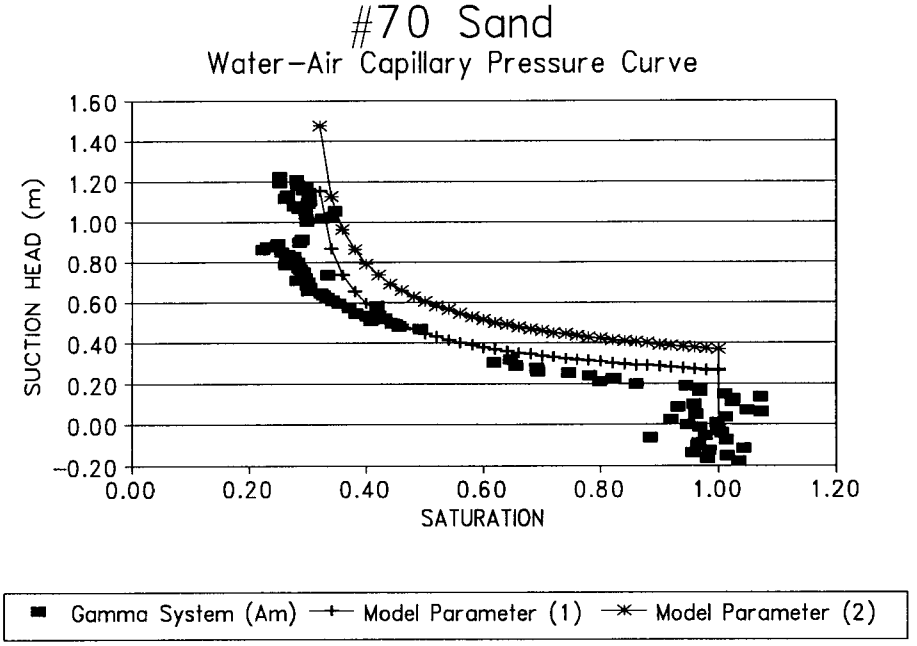


Figure 22. Suction-saturation profile for #70 sand and water-air.

c) Sand #125 and Soltrol (Figure 23).

The scanning time for this experiment was 20 seconds at every point. Two scans were repeated at every location. After 2 scans, the gamma system moved 1.25 cm vertically down to the next scanning location.

The porosity of the sand as determined gravimetrically was 0.37. The average porosity calculated from the Americium spectrum was 0.41. The residual saturation was found to be approximately zero, the height of the capillary fringe was 0.2 m. The gamma data agree well with the Brooks and Corey suction-saturation curves derived from the flow pump data using approaches 1 and 2.

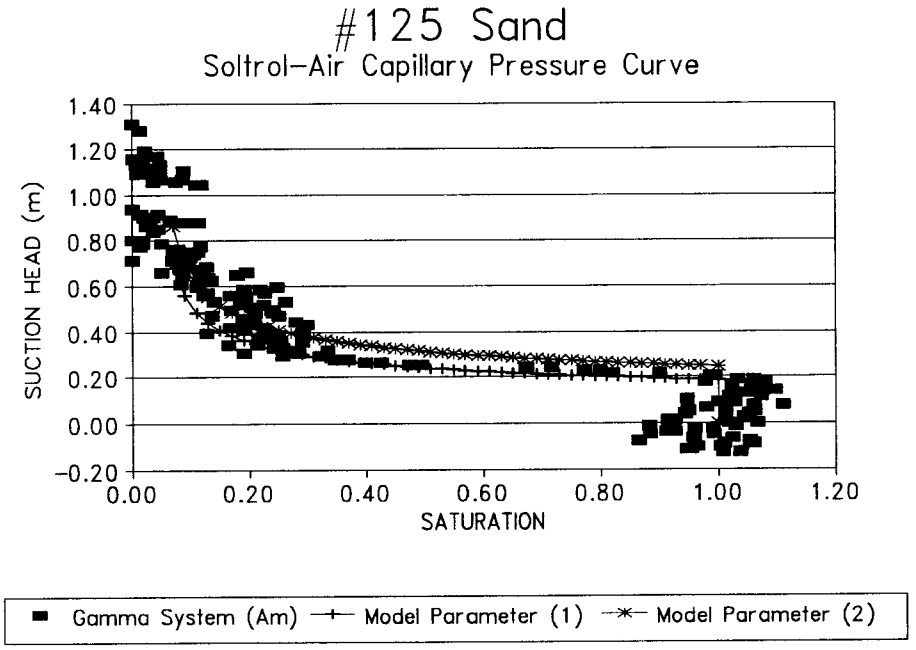


Figure 23. Suction-saturation profile for #125 sand and Soltrol-air.

d) Sand #70 and Soltrol (Figure 24)

The scanning time for this experiment was 20 seconds at every point. Two scans were repeated at every location. After 2 scans, the gamma system moved 1.25 cm vertically down to the next scanning location.

The porosity of the sand as determined gravimetrically was 0.49. The average porosity calculated from the Americium spectrum was 0.52. The residual saturation was found to be approximately 0.2; the height of the capillary fringe was 0.1 m. The gamma data show the same entry pressure as the Brooks and Corey suction-saturation curves derived from the flow pump data with approaches 1 and 2.

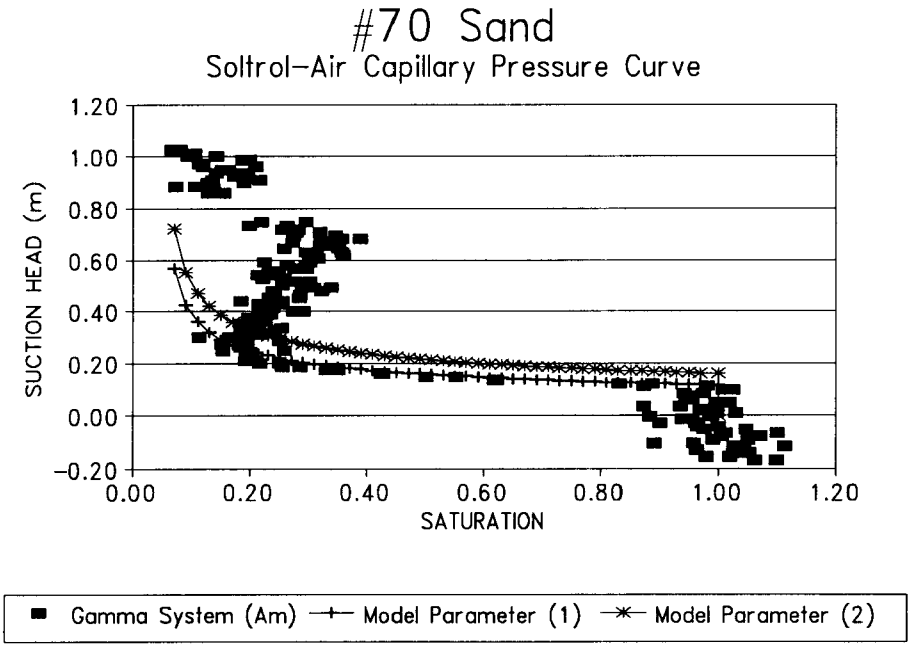


Figure 24. Suction-saturation profile for #70 sand and Soltrol-air.

The following steps were taken to calculate the saturation from the gamma count rate. The count rates were corrected for detector sensitivity by using measurements taken through a standard absorber. The count rate through the empty column was used as the standard count rate. However, this correction was usually very small compared to the random variation in the measurement. Measuring $I_0$ along the length of the column would allow the use of one $I_0$ for every point in the column. Even though all attempts were made to pack the column homogeneously, some small scale variations of porosity along the column are possible. The changes in $I_0$ over the length of the column due to the small variations of porosity were smaller than the random error in the measurement of $I_0$. Thus, $I_0$ was averaged over the whole column. The same was true for the porosity. The saturation was then computed from the phase content by using the porosity averaged from the gamma system measurements.

The suction-saturation curve for both sands with water that were measured with the gamma system have similar entry pressure and residual saturation as do the curves that were created from flow pump experiments. The suction-saturation curves for Soltrol showed a lower capillary fringe than for water due to the lower interfacial tension. The measurements with Americium show a large random variation, but the averaged values have a good accuracy. It was found that the attenuation coefficient is different for the #70 sand than for the #125 sand. The #70 sand was sieved from crushed sandstone, whereas the #125 came from naturally deposited material. The different composition of the two sands was responsible for the different attenuation coefficients.

The porosity as determined with the gamma system was generally higher than the porosity found gravimetrically. A possible explanation is an error in path length. A higher value of porosity (about 5%) was measured when the path length through the column was 3 mm shorter than that which was assumed for the calibration. If the gamma system does not shoot through the center of the column (along a diameter), but was off-centered by a maximum of 1.10 cm, the path length may change up to 3 mm (Figure 25).

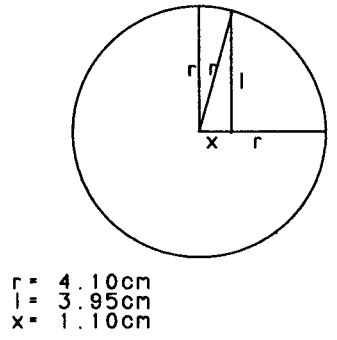


Figure 25. Schematic of the scanning path through the sample column. If the gamma detector moves 1.10 cm sideways from the center (x=1.1 cm), the actual path length measured is 3 mm less than assumed (2l=7.9 cm, while 2r=8.2 cm).

The suction-saturation relationship measurements in #70 and #125 sand for water and Soltrol were conducted with a large number of measurement points. This was expected to increase the accuracy of the suction-saturation curve. The suction-saturation curve for #125 sand and water was measured with the largest number of observations: 9 measurements over 20 seconds every 1.25 cm along the column length of 140 cm. This resulted in over 1000 measurements per column scan. One column scan took approximately 10 hours. Part of the reason for taking so long was the slow processing of data by computer integration at every scan point. The slow XT computer was subsequently replaced by a faster AT (286 PC) machine. The number of measurements per step was also reduced from nine to two for the next measurements. The suction-saturation curve for nine measurements per step produced results which are in good agreement with the flow pump measurements (Figure 26) and the curves parameterized from flow pump data.

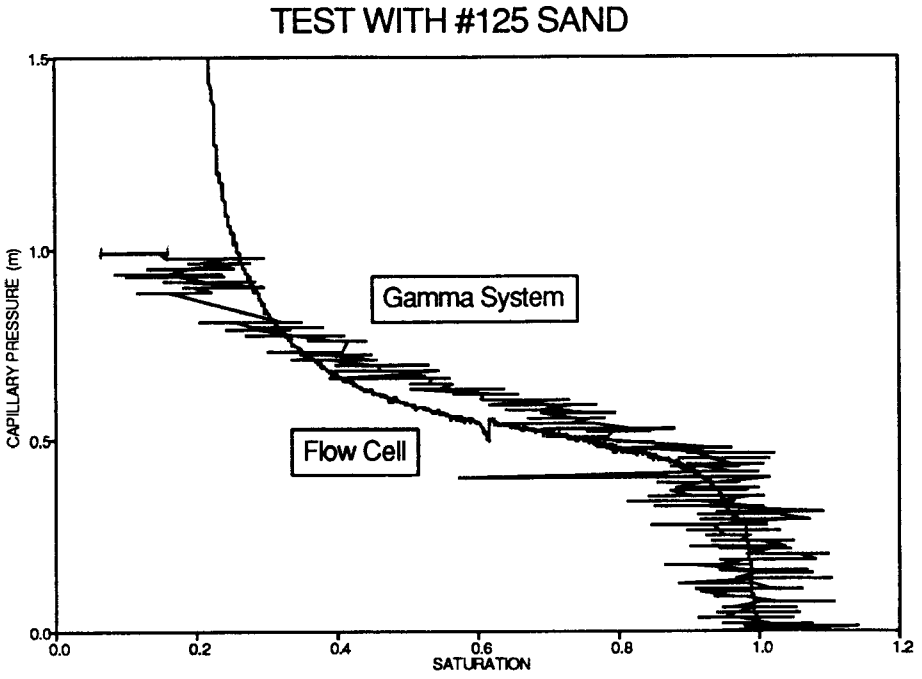


Figure 26. Comparison of suction-saturation profile as measured with Americium gamma scan and with flow pump.

## 5.2 SPILL EXPERIMENTS IN THE LONG COLUMN

After residual water saturation was established, Soltrol spills were performed in the long column. A slug of Soltrol was applied to the top of the column. The movement of the Soltrol was observed visually, and the front location and ponding depth were recorded. Simultaneously, gamma scans were performed to determine the phase content of Soltrol along the length of the column. Comparisons of the visually observed front location with the gamma data showed that the visually observed front coincided with the front detected by the gamma system.

Six different spill experiments were performed with spill volumes of 500 ml, 750 ml and 1000 ml Soltrol, respectively, on columns packed with #70 and #125 sand. The visually observed front elevations are shown in Figure 27 and Figure 28 for sand #70 and sand #125, respectively. The top of the sample was assumed to be at 120 cm for all experiments.

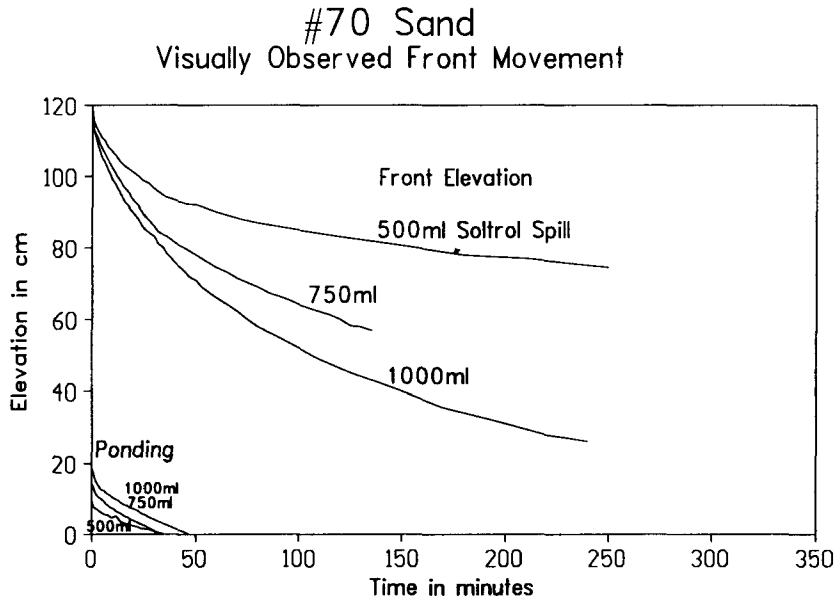


**Figure 27.** **Front elevation versus time for three spills, 500ml, 750ml and 1000ml Soltrol on #70 sand.**

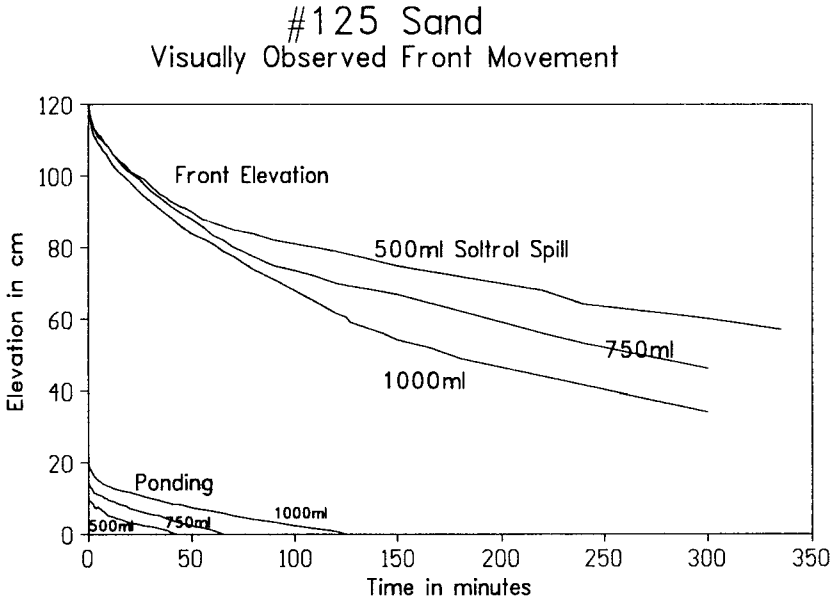


Figure 28. Front elevation versus time for three spills, 500ml, 750ml and 1000ml Soltrol in #125 sand.

As the Soltrol infiltrated downward, the rate of propagation of the front declined. It can be seen that the larger spill volumes of fluid penetrated faster into the sand due to the additional driving force from the greater ponding depths.

By comparing the profiles for #70 sand and #125 sand, it can be seen that in the beginning of the spills, the oil penetrated faster into the #70 sand than into #125 sand and ponding ended much faster for the coarser sand. This behavior was expected as the #70 sand has a higher hydraulic conductivity than the #125 sand (15 m/d vs. 8.5 m/d). However, the speed of movement decreased faster for #70 sand, and the oil movement in later stages of redistribution was slower than for #125 sand. The reason for this was the larger average pore size and porosity of the #70 sand. The larger the porosity, the faster was the decrease in the amount of free flowing liquid phase; and with a smaller amount of oil available for flow, the flow slowed down. It seems that the Soltrol movement depended mainly on the amount of Soltrol pushing behind the front. A highly oil saturated zone behind the front pushed the front faster than a lesser saturated zone. Since #70 sand has a larger porosity than #125 sand, the saturation dropped faster below full saturation. At that point in time the front slowed down markedly. Thus the front in the #70 sand slowed down faster than in #125 sand. This was specifically marked for the 500 ml Soltrol spill, where the front was slower in #70 sand soon after ponding ends.

The first experiment with 1000 ml Soltrol in #125 sand, was repeated twice. The experiments were named H and D and are so named in the Appendices. These experiments

gave slightly different results (Figure 29). This was not surprising as differences between nominally identical experiments were expected. Two possible explanations for the results are that there were differences in the packing of the columns, which led to variations in hydraulic conductivity; and that there were variations in the water saturation between the two experiments. However, the differences between the repeated experiments were small. Comparing two spills in #125 sand with 500 ml Soltrol shows that both fronts move almost simultaneously, until rainfall commenced in one of the experiments (Figure 42).

The gamma scans show the shape of the oil content profiles along the column. Three example profiles are shown here, while the complete set of profiles is shown later. The data are given in Appendix 3 in tabular form. Figure 30 shows an infiltration profile in #70 sand, while there was still ponding at the soil surface. Figure 31 and Figure 32 show the profile after redistribution of the Soltrol has begun. The times given in the figures are the exact times after the beginning of the spill at which the front was measured. The porosity of the #70 sand in this spill was 0.47; the residual water content approximately 0.1.

Figure 33 through Figure 39 show all of the Soltrol phase content profiles measured with the gamma system for infiltration of 1000 ml, 750 ml , 500 ml in the #70 and #125 sands. The earlier of the profiles show that the sample reached full saturation behind the front. However, after longer times, the saturation behind the front decreased until the Soltrol was near residual saturation throughout the column.

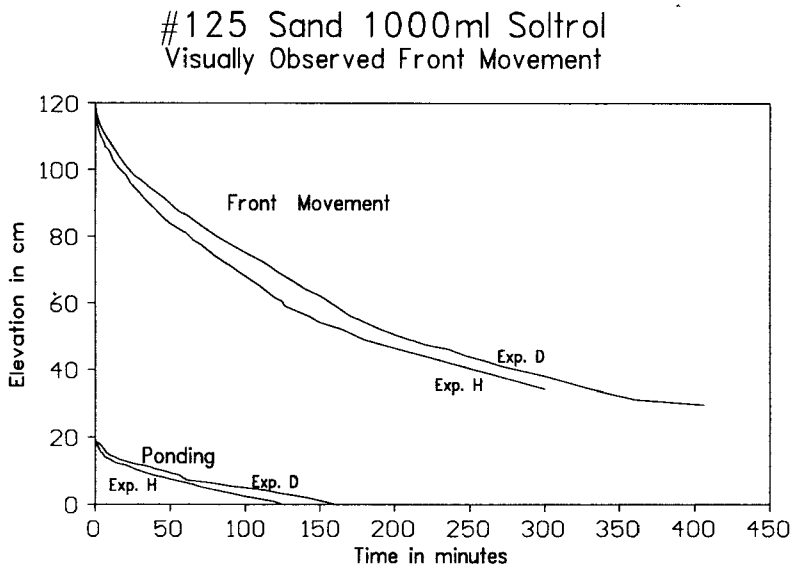


Figure 29. Comparison between two identical experiments with 1000ml Soltrol in #125 sand.

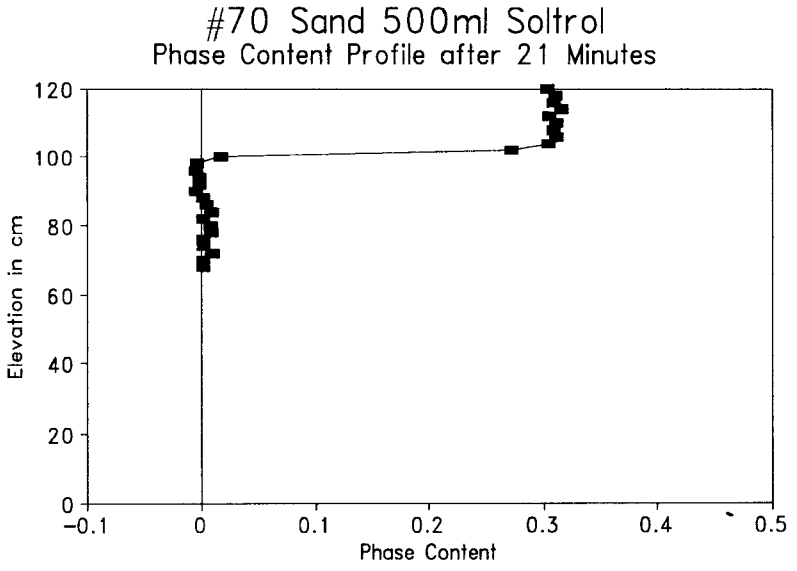


Figure 30. Phase content profile of 500ml Soltrol in #70 sand. Soltrol is still ponding on top of sand.

Integration of the Soltrol phase content for the 500 ml spill, #125 sand experiment shown in Figure 33 gives values close to the total spill volume of 500 ml. The profile taken at 357 min. gives a total Soltrol volume of 482 ml, 470 ml at 406 min., and 346 ml at 930 min. After 930 min., part of the Soltrol volume has already drained out of the columns. This integration shows that the gamma systems accounted for approximately the correct total volume of the spill.

Integration of the Soltrol phase content profiles in Figure 34, at 263 minutes and 410 minutes, gives total Soltrol volumes of 812 and 811 ml, respectively. The profiles were taken after the rainfall began at 45 minutes. The volume estimates were much higher than the actual spill volume of 500 ml. The reason for the large error is that both gamma spectra had to be used for the calculation of two unknown phase contents: water and Soltrol. This approach led to a larger error in the absolute values of phase content, as explained in Appendix 1. In the profiles after 263 min. and 410 min., the calculated water volume was negative, and the Soltrol content was too high. Thus the profiles give qualitative information about the shape of the Soltrol and water fronts, but do not give quantitative values for the phase contents. The phase content data for all profiles are given in Appendix 3.

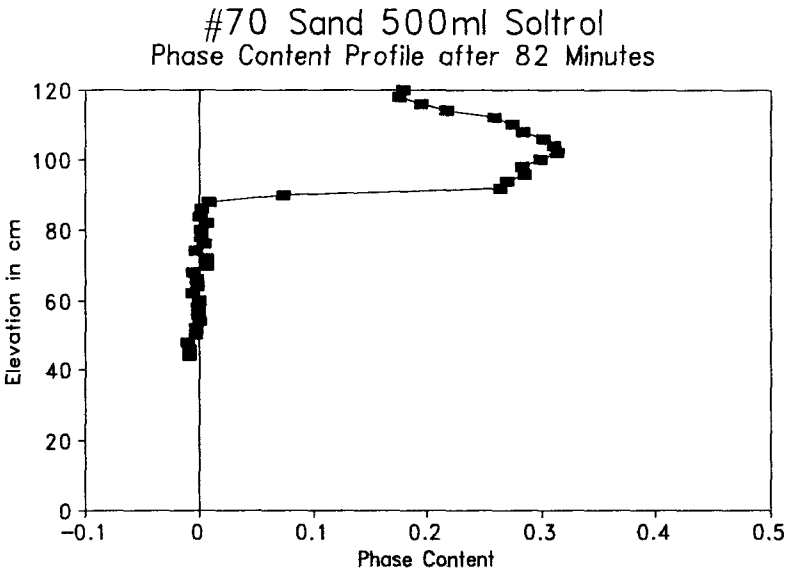


Figure 31. Phase content profile of 500ml Soltrol spill in #70 sand. A back front has started to develop.

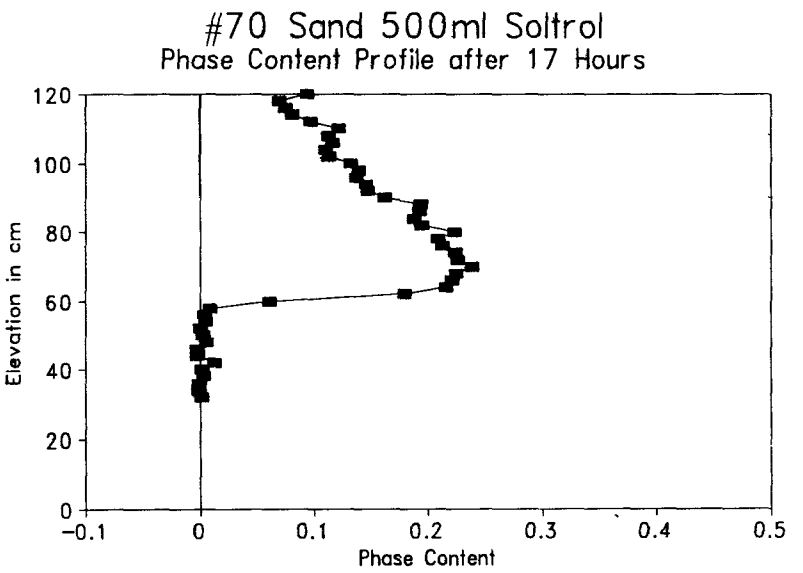


Figure 32. Phase content profile of 500ml Soltrol in #70 sand. A gradual decrease in phase content behind the front can be observed.

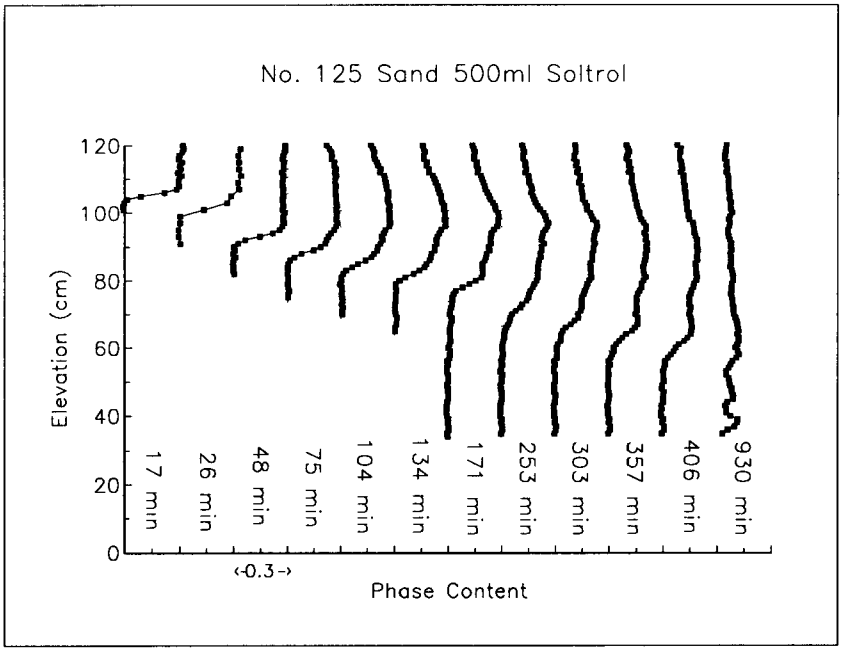


Figure 33. Set of phase content profiles for 500ml Soltrol spill in #125 sand.

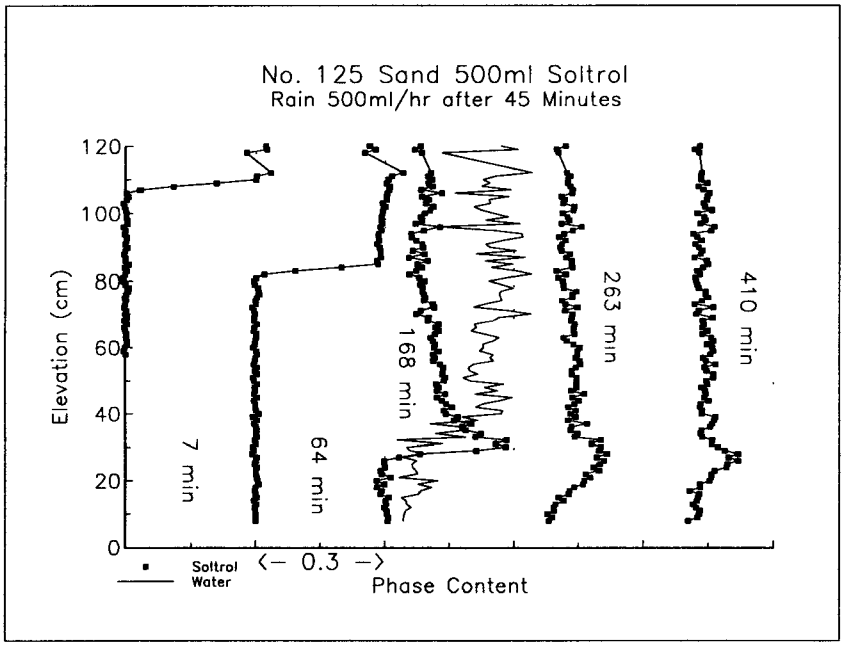


Figure 34. Set of phase content profiles for 500ml Soltrol spill in #125 sand. Rain started 45 minutes after spill.

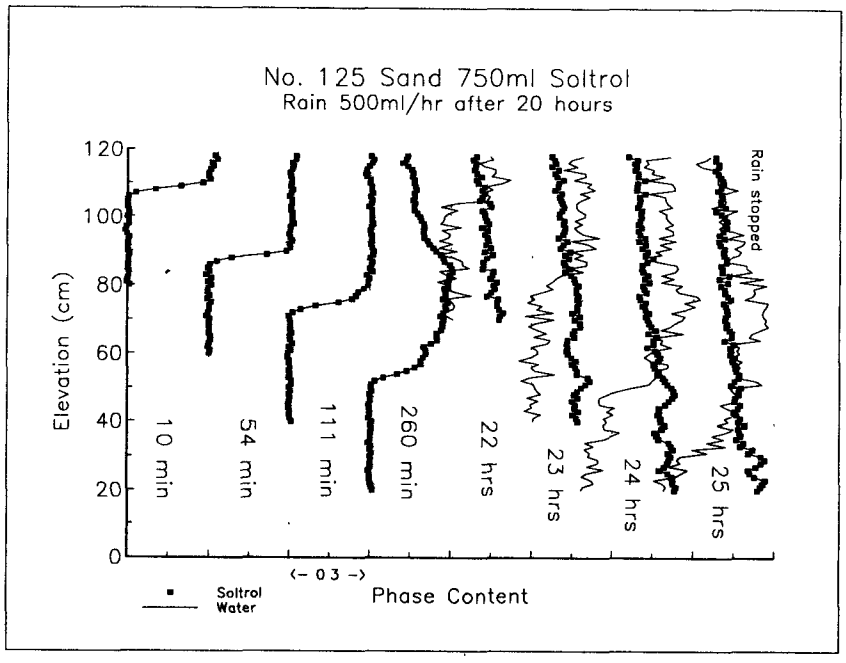


Figure 35. Set of phase content profiles for 750ml Soltrol spill in #125 sand. Rain started 20 hours after spill.

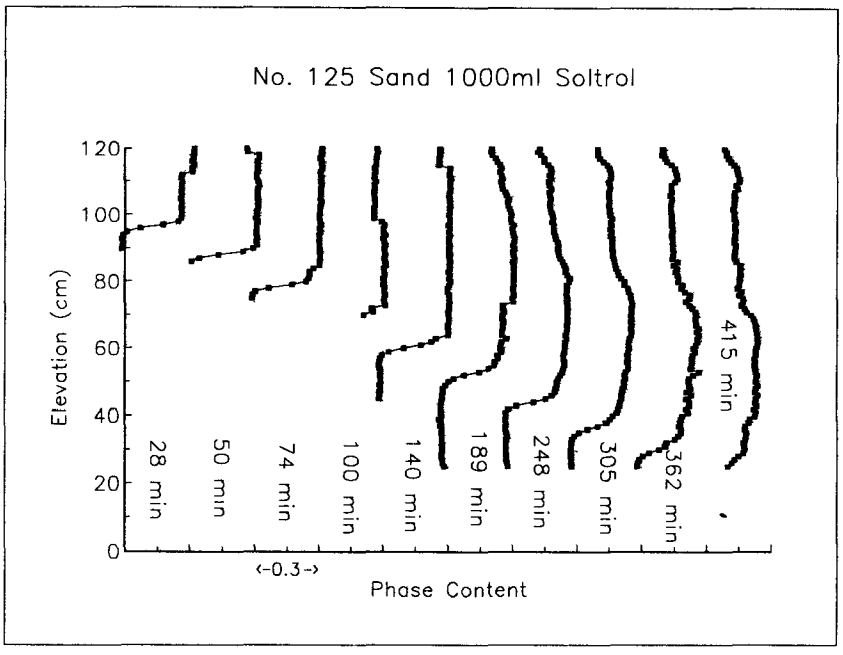


Figure 36. Set of phase content profiles for 1000ml Soltrol spill in #125 sand.

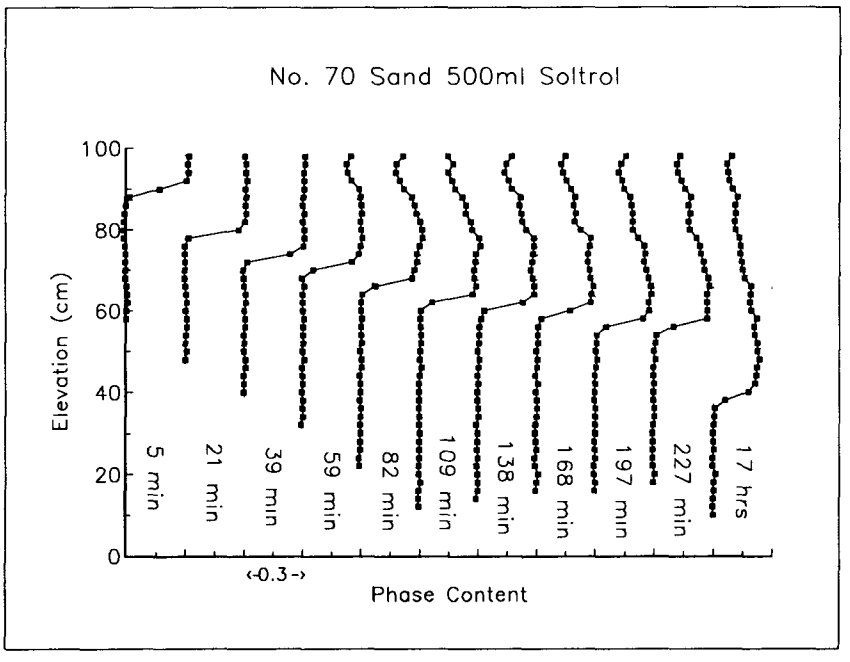


Figure 37. Set of phase content profiles for 500ml Soltrol spill in #70 sand.

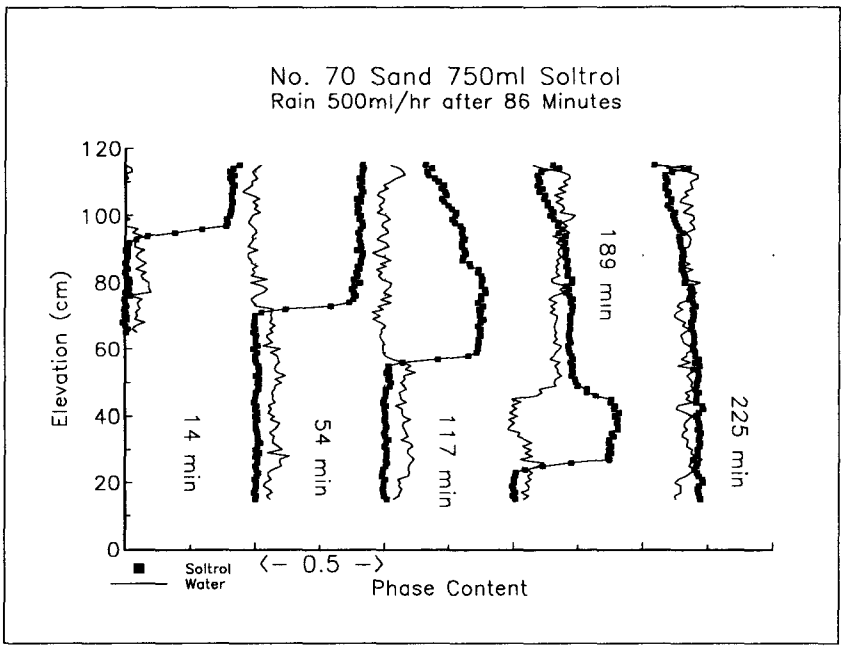


Figure 38. Set of phase content profiles for 750ml Soltrol spill in #70 sand.

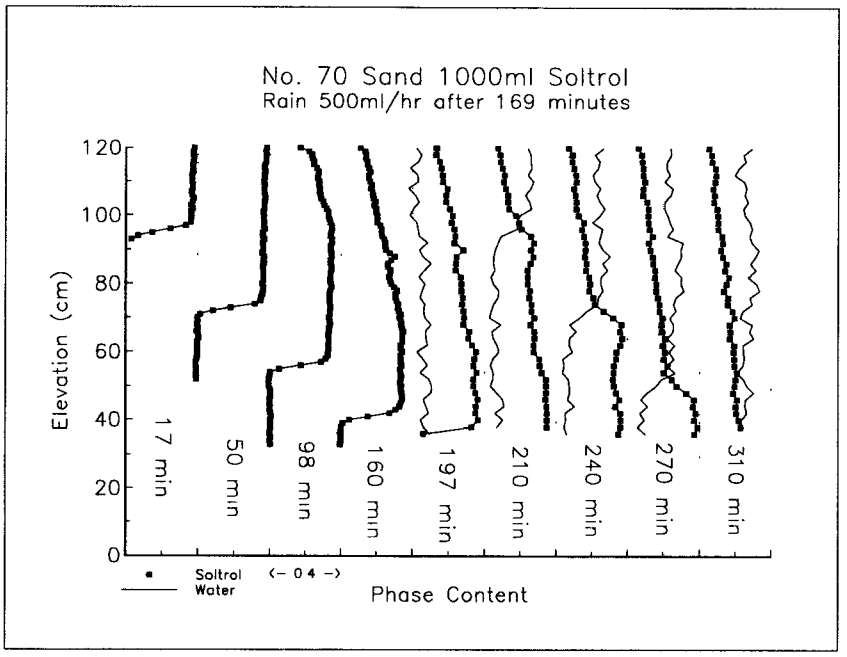


Figure 39. Set of phase content profiles for 1000ml Soltrol in #70 sand.

In general the gamma profiles taken during the spill show a sharp front at the leading edge of the Soltrol slug and a diffusive back front during the redistribution phase of the spill. During infiltration, the sand reached a maximum Soltrol saturation behind the front. When redistribution began, the maximum saturation Soltrol behind the front decreased. All of the simulations presented below were based on the assumption that the phase content of the residual water was constant and did not change during the spill. However, some experiments where Soltrol and water saturations were both determined indicate that Soltrol displaced some of the residual water (Figure 40). Actually, in well sorted sand like the ones that were used in these experiments, irreducible saturation is much lower (~5%) than the residual saturation we obtained (Personal communication, A.T. Corey, 1993). Release of water may also be due to the fact that the interfacial tension between Soltrol and water is about half of the surface tension of water.

The profiles were not taken at one point in time, because it takes about 40 minutes to complete the measurements from top of the column to the bottom. Figure 41 shows the front movement of a spill and the location of the gamma scan. The diagonal lines signify the downward moving gamma system. The time it takes to scan one profile is the horizontal distance between the beginning and the end of one diagonal scan line. It can be seen that the front moved before the complete profile was scanned. Hence, the same liquid mass might be measured twice leading to overestimation of the Soltrol volume.

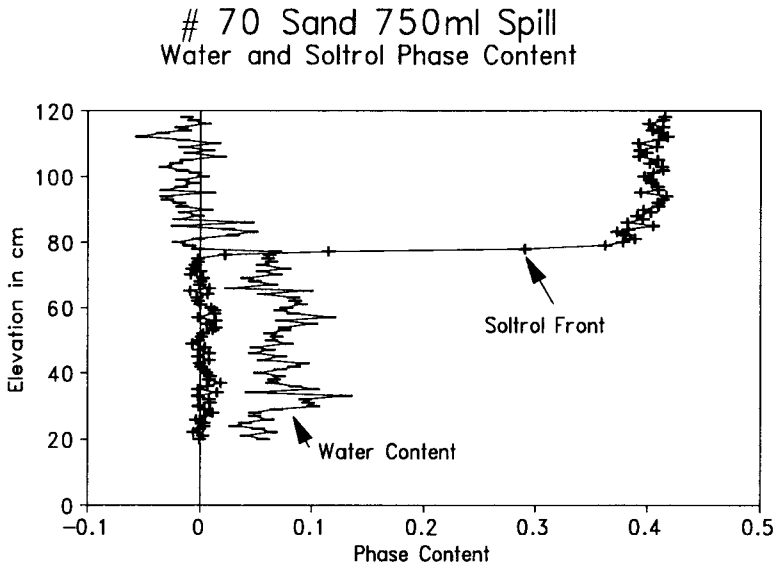


Figure 40. Water and oil content for 750ml Soltrol spill in #70 sand. Soltrol front seems to displace the residual water.

## 5.3 RAINFALL EXPERIMENTS IN THE LONG COLUMN

To observer and record the behavior of the spilled fluid during a rainfall event, simulations were conducted where water was applied at the soil surface after the Soltrol spill. A number of rainfall experiments were conducted where water and oil fronts were observed visually. The phase content profiles were recorded with the gamma system. A comparison between front movement of a 500 ml spill in #125 sand with and without simulated rainfall is shown in Figure 42. In one experiment a rainfall of 500 ml/hour (9.5 cm/hour) was started 45 minutes after the spill occurred. The water pushed the oil front downward compared to the front without rain.

The water for the rainfall simulation was dyed dark green with food coloring. This made it possible to observe the water front moving downward. However, in the sand that was reddened from residual Soltrol, the water front was hard to observe; and in some cases a water front could not be observed visually. In these cases, the water front position was determined from the gamma data. Such was the case for the spill shown in Figure 42. From the gamma scan, it was found that the water front was nearly at the same location as the Soltrol front (Figure 34). The water front caught up with the Soltrol front soon after the rain had started; then both fronts moved together. Figure 43 and Figure 44 show two spills conducted in the #70 sand: the first with 1000 ml Soltrol, the second with 750 ml Soltrol. In both cases, the rainfall was started more than 1 hour after the spill occurred. For both experiments, the water front could be observed. The water front moved with almost constant speed, as seen from the elevation versus distance curve being close to a straight line. This behavior was a result of the constant water flux applied to the

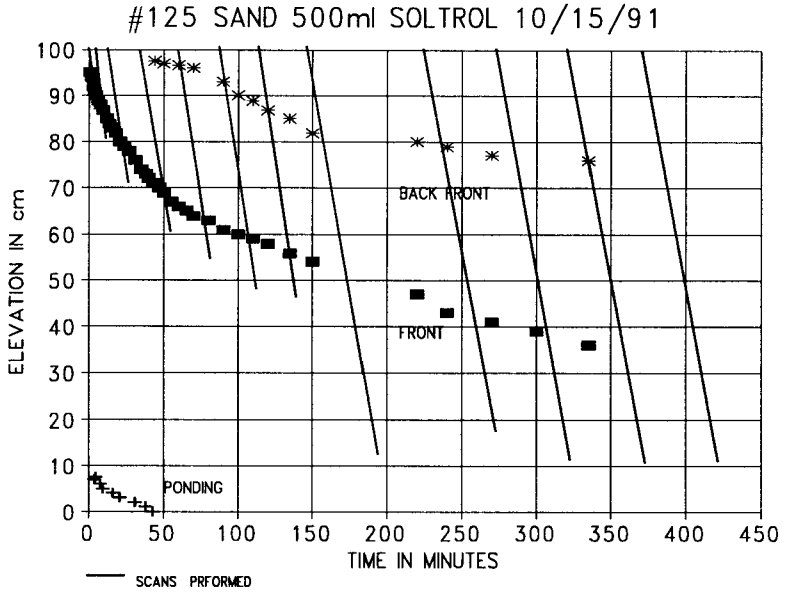


Figure 41. Front elevation versus time for 500ml Soltrol spill in #125 sand, included are gamma scanning time and location.

surface, which led to a constant water flux in the sand, and the observed movement of the water front. Even when the water enters the region where there was still large amounts of the slower moving Soltrol, the water phase did not slow down.

The graphs (Figure 43 and Figure 44) show a distinct bend in the Soltrol front where the water front began to push the Soltrol slug down. Later, however, the water front caught up with the Soltrol front. The point in time when the water front caught the Soltrol was determined by the amount of rainfall and the time when the rainfall started. The water front passed the Soltrol front when the phase content in the Soltrol slug decreased below the maximum saturation. The reduction in Soltrol content was attributable to the residual Soltrol content and the finite volume of the spill; as the front got deeper, more of the spilled volume of the Soltrol was trapped at the residual saturation. Eventually the phase content behind the front decreased because of continuity. This behavior can be best seen on the phase content profiles (Figure 38 and Figure 39).

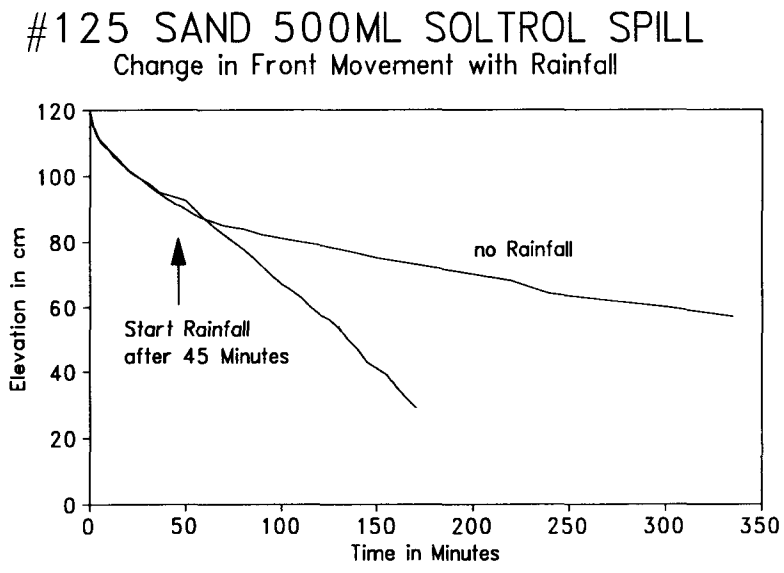


Figure 42. Comparison between rainfall application and no rain for 500ml Soltrol spill in #125 sand.

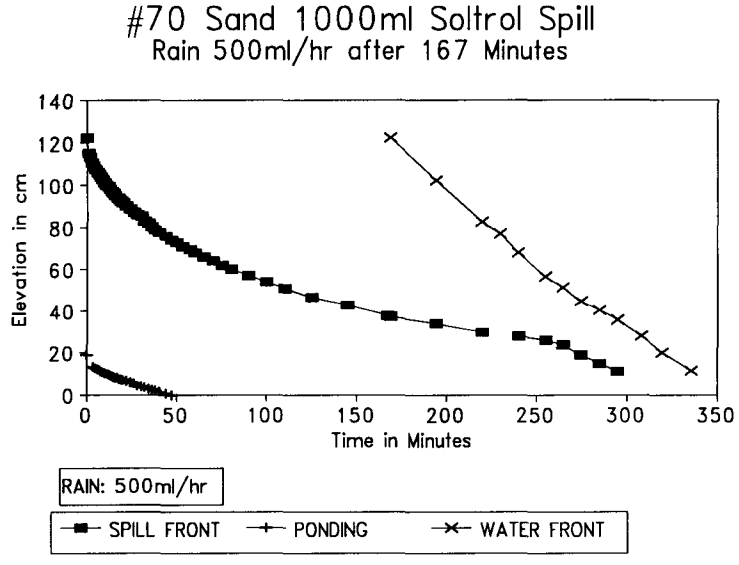


Figure 43. 1000ml Soltrol spill on #70 sand with rainfall application starting after 169 minutes. The rainfall rate was held constant at 9.5cm/hour.

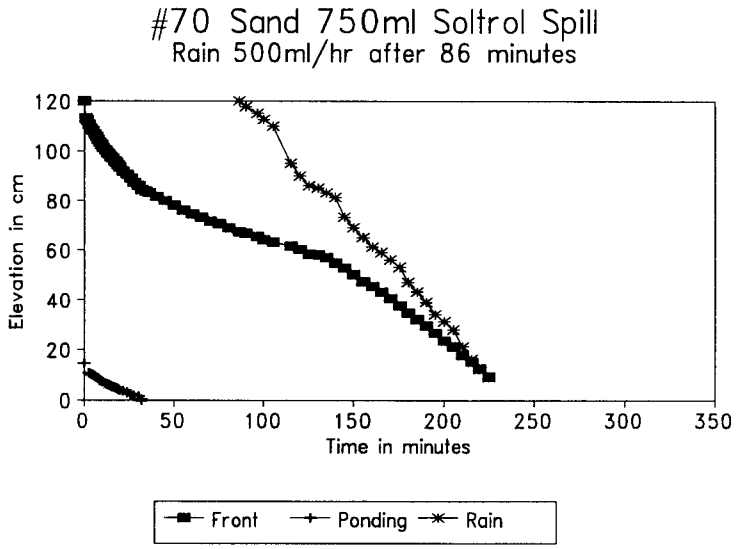


Figure 44. 750ml Soltrol spill on #70 sand with rainfall application starting after 86 minutes. The rainfall rate was held constant at 9.5 cm/hour.

Figure 45 and Figure 46 show profiles obtained with the gamma system. A profile taken 189 minutes after the spill started and 103 minutes after the rainfall started can be seen in Figure 45. The gamma scan confirmed that the water and the Soltrol back fronts are in the same location. This is a clear indicator that the water was pushing the Soltrol downward in a fully saturated NAPL "bank". Behind the Soltrol back front, the water and oil saturations added up to one. However, limitations of measurement accuracy of the gamma system prevented the measurement of small entrapped air saturations. It is important to note that the water did not seem to mobilize any of the entrapped Soltrol. Even at the top of the column where the most water had passed by, the Soltrol content is still 0.1. However, the Soltrol slug displaced some of the residual water, which was assumed to be irreducible in both models evaluated in this study.

No water front could be observed visually in the 500 ml spill in the #125 sand. However, the gamma scan in Figure 46 shows that a water front existed; but it was so close to the Soltrol front that it cannot be recognized visually. The Soltrol bank was very small, due to the small spill volume.

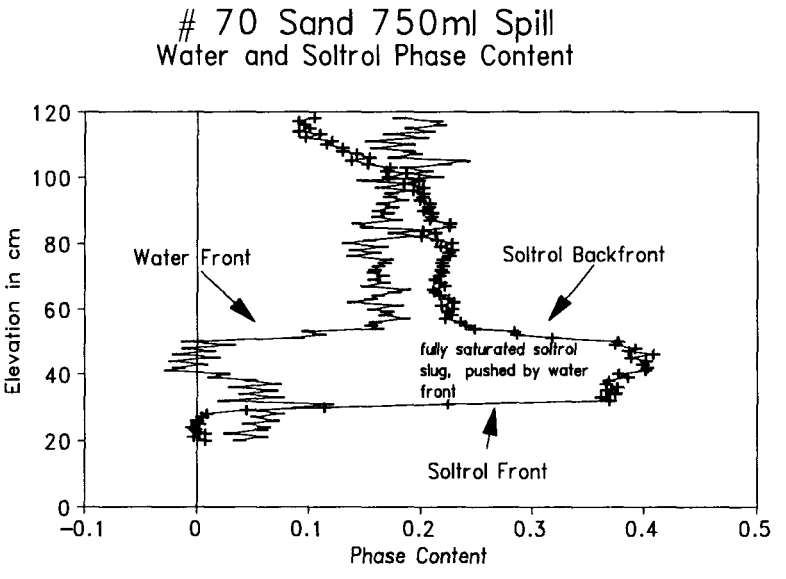


Figure 45. Water and Soltrol content profiles for 750ml spill in #70 sand. Gamma scans were taken 189 minutes after spill was started. A constant rainfall rate of 9.5cm/hour was applied 86 minutes after the spill was started.

One experiment was conducted to observe possible mobilization of the NAPL (Figure 35). One day after a 750 ml Soltrol spill in the #125 sand, a constant rainfall rate of 9.5 cm/hour was applied to the column. The column was at residual Soltrol saturation when the rainfall was started, except at the lower end of the column where a capillary fringe zone had built up. A two-hour rainfall did not change the amount of Soltrol in the upper part of the column; the only observed effect was that the water pushed the Soltrol out of the capillary fringe zone.

## 5.4 SPILL EXPERIMENTS IN THE TWO-DIMENSIONAL TANK

Tank experiments were conducted to observe two-dimensional behavior of NAPL spills in the vadose zone. These experiments were designed to be comparable to the column experiments. A 30 cm wide spill zone was created in a 120 cm wide tank that was packed with #70 sand. The volume of Soltrol applied to the tank resulted in a ponding depth of Soltrol above the sand of 9.5 cm, which corresponds to the 9.5 cm ponding depth for a 500 ml spill in the column. In Figure 47 the front movements of two tank experiments and one column experiment are compared. The front position for the tank experiment was taken as the front elevation directly below the center of the spill. The Soltrol plume had a U-shape, thus the front at the edges of the fluid body lagged behind the front at the center of the body; but by no more than 2 cm.

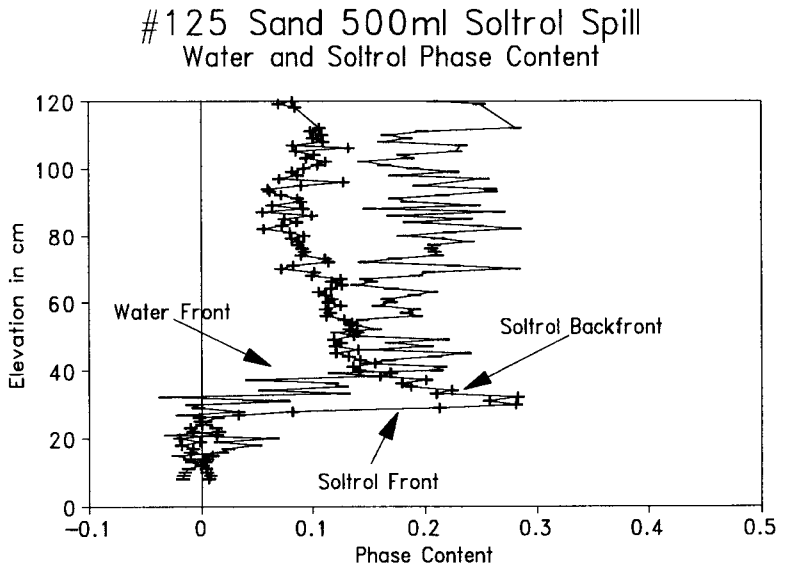


Figure 46. Water and Soltrol phase content for a 500ml soltrol spill in #125 sand. Gamma scans were taken 168 minutes after spill was started. A constant rainfall rate of 9.5cm/hour was applied 45 minutes after the spill was started.

It can be seen that there was no significant difference between the column and tank experiments. The difference between the two tank experiments seems larger than the difference between tank and column experiment. It can be concluded that the column experiments are a valid approximation of contaminant movement through the vadose zone in coarse homogeneous systems. The observed outline of the spill front in the tank also confirmed the validity of the one-dimensional assumption. The width of the spill area was 30 cm; maximum width of the plume was 40 cm. Thus, lateral spreading due to capillary forces on both sides was only 5 cm. The lateral spreading relative to the total width will be small for spills over a large area.

The gamma profiles for the tank experiment are shown in Figure 48. The profiles were taken along the vertical center line of the spill. The profiles exhibit a leading-edge sharp front and a slow decrease in phase content behind the front. No data could be collected at the elevation of 100 cm because a steel bar from the tank frame impaired the measurement. These profiles show the same characteristics as the profiles measured in the column.

A rainfall experiment was conducted in the tank with rainfall occurring over the whole length of the tank, not only in the spill zone. This completely prevented further lateral expansion of the Soltrol body. On the contrary, a narrowing of the downward moving body was observed. This was possibly due to the fact that a high rainfall rate of 21 cm $hour^{-1}$ was used. The visually tracked front movement is shown in Figure 49. This intense rainfall sped up the front movement.

The rainfall started 22 hours after the spill. At 23 hours the water front caught up with the Soltrol front, and pushed the Soltrol front downward. At 24 hours the water front passed the Soltrol front and started exiting the tank, while the Soltrol front was still above the bottom of the tank. The rainfall was stopped when the water reached the bottom of the tank. After the rainfall was stopped, the Soltrol front resumed it's pre-rainfall migration rate. The same can be observed from the phase content profiles (Figure 50).

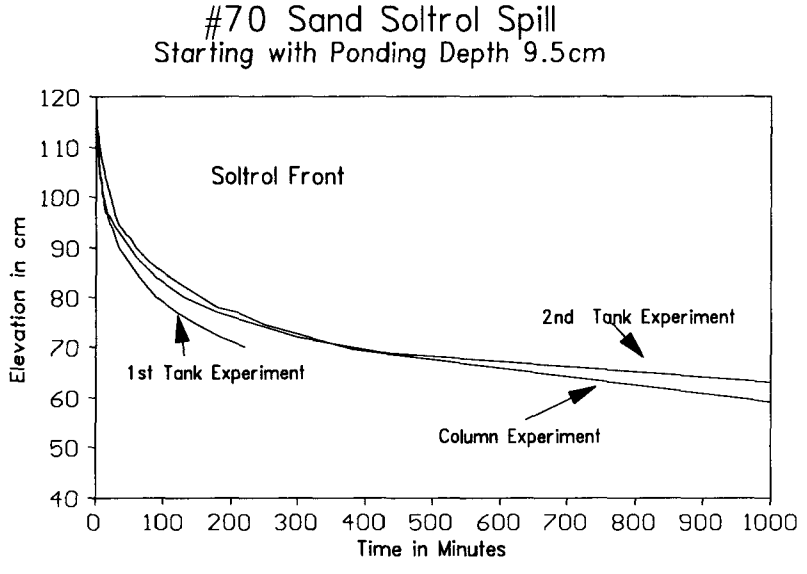


Figure 47. Comparison in front movement between tank and column experiment.

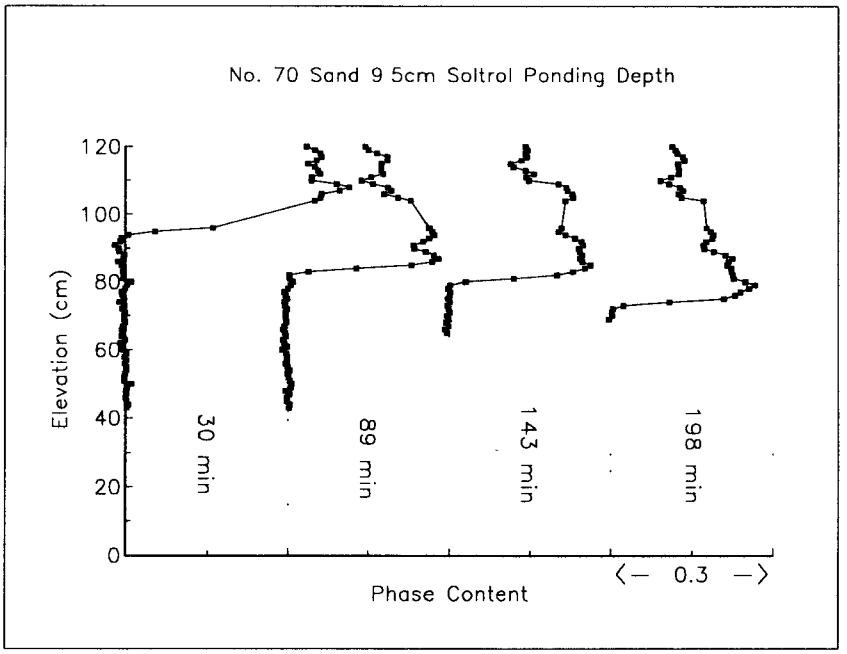


Figure 48. Set of phase content profiles for 9.5cm Soltrol spill in # 70 sand in the tank.

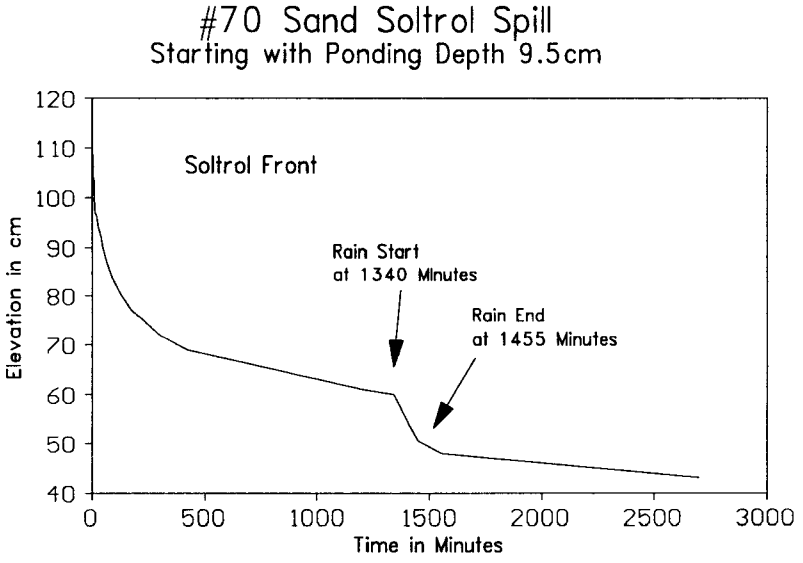


Figure 49. Soltrol spill front movement in tank with rainfall application.

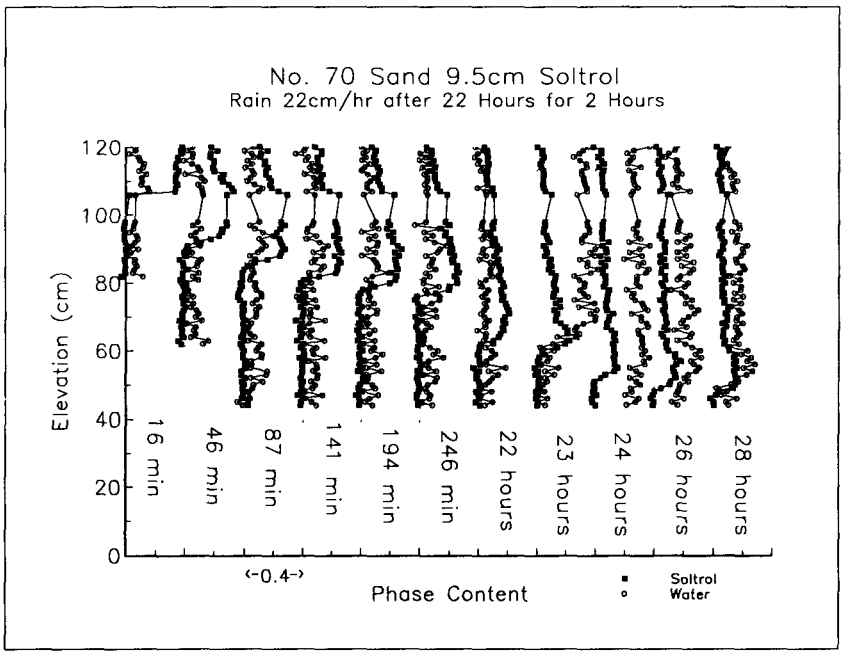


Figure 50. Set of phase content profiles for 9.5cm Soltrol spill in #70 sand in the tank with rainfall.

## 5.5 TESTING OF THE COMPUTER MODELS

Two computer models were used to simulate the NAPL spills in the column. The Three Parameter Sharp Front Model and the Kinematic Oily Pollutant Transport (KOPT) Model were compared and tested using the data from Soltrol spill experiment conducted in the long column.

The KOPT model was run with independently measured parameters for the #125 sand. The following input parameters were used: for Soltrol, a residual oil saturation of 0.05; for the sample, a porosity of 0.4 and a residual water saturation of 0.22. The complete set of parameters for the KOPT model is listed in Table 4. The three-parameter model was run with the same parameters; however, the capillary suction at the front and at the back-front are parameters which have to be fitted when running the model. The suction parameters cannot be estimated from independent experiments. The first spill with 500 ml Soltrol in #125 sand was used to calibrate the three-parameter model. The following values were found to give a good fit between model and experimental results: a front suction head of 0.3 cm and a back front suction head of 21 cm. For both models, the initial ponding depth was calculated by dividing the volume of NAPL spilled by the cross-sectional area of the column. The initial ponding depths were 18.9 cm, 14.2 cm and 9.45 cm for the 1000 ml, 750 ml, and 500 ml spills, respectively.

Table 4 KOPT parameter values for the #125 and #70 sands

| KOPT parameter values for the #125 and #70 sands | | |
|---|---|---|
| Parameter | #125 sand | #70 sand |
| Saturated Hydraulic Conductivity, $K_s$ | 8.5 m/d | 15 m/d |
| Brooks and Corey $\lambda$ | 2.88 | 2.44 |
| Porosity, $\eta$ | 0.41 | 0.41 |
| Residual Water Saturation | 0.22 | 0.30 |
| Water Saturation | 0.22 | 0.30 |
| Air entry head, $h_{ce}$ | 0.4280 m | 0.2683 m |
| Oil viscosity, $\mu_o$ | 3.78 cp | 3.78 cp |
| Oil density, $\rho_o$ | 0.85 g/cm$^3$ | 0.85 g/cm$^3$ |
| Residual oil saturation | 0.05 | 0.05 |
| Water surface tension | 65 dyne/cm | 65 dyne/cm |
| Oil surface tension | 24 dyne/cm | 24 dyne/cm |
| Initial Ponding depth, $H_s$<br>1000 ml spill<br>750 ml spill<br>500 ml spill | <br>0.1890 m<br>0.1420 m<br>0.0947 m | <br>0.1890 m<br>0.1420 m<br>0.0947 m |
| Radius | 0.025 m | 0.025 m |

The observed and calculated front position, back front position and ponding depths are graphed in Figure 51 along with the model results. Both models matched the experimental data reasonably well. In the each of the models, the NAPL is assumed to be instantaneously applied to the sand surface. In actuality, some small time was required for the ponding depth to reach its full extent as the NAPL was poured into the column. The capillary suction head for the front and the back-front were adjusted in the three-parameter model until the model fit the data. The fitted model then predicted the ponding time accurately. The KOPT model over-predicted the ponding time; however, it predicted the front accurately without the need to fit any parameters beyond considering the effect of variation in hydraulic conductivity. Three profiles were created with each model and compared with the profiles obtained from the gamma scans (Figure 51 through Figure 53).

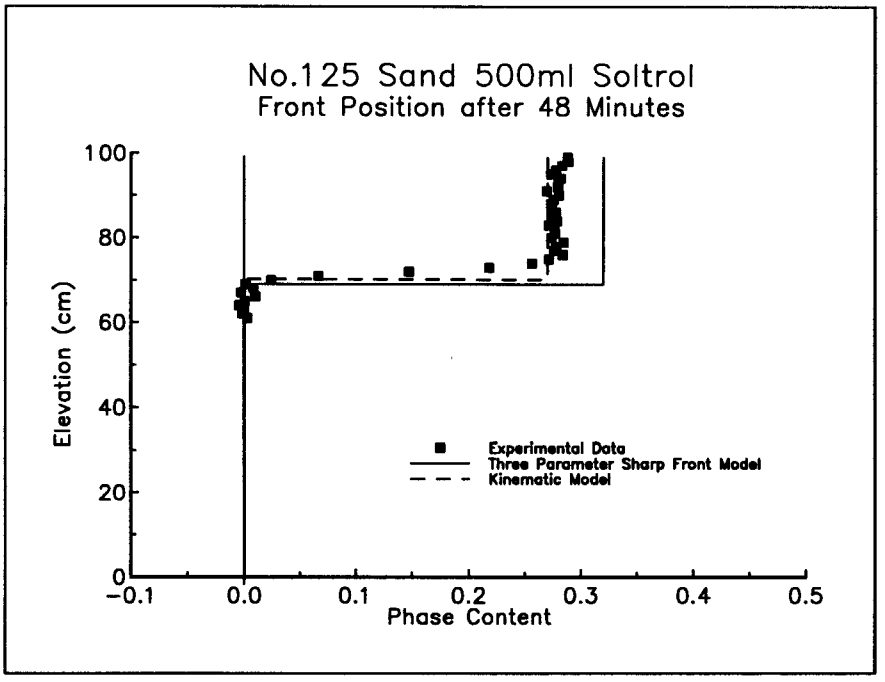


Figure 51. Phase content profile comparison between models and gamma scan. Soltrol is still ponding at the surface.

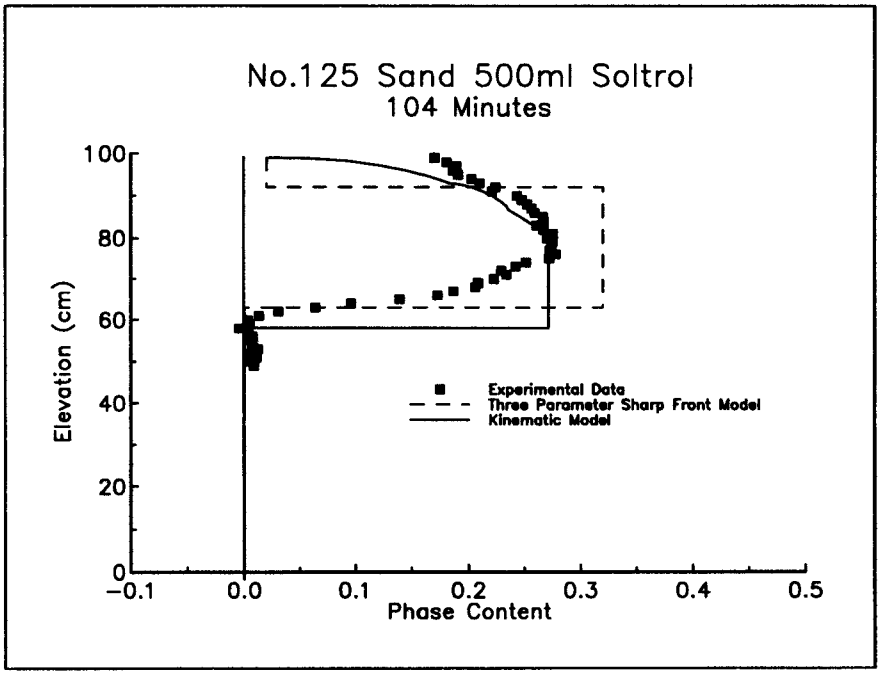


Figure 52. Phase content profile comparison between models and gamma scan.

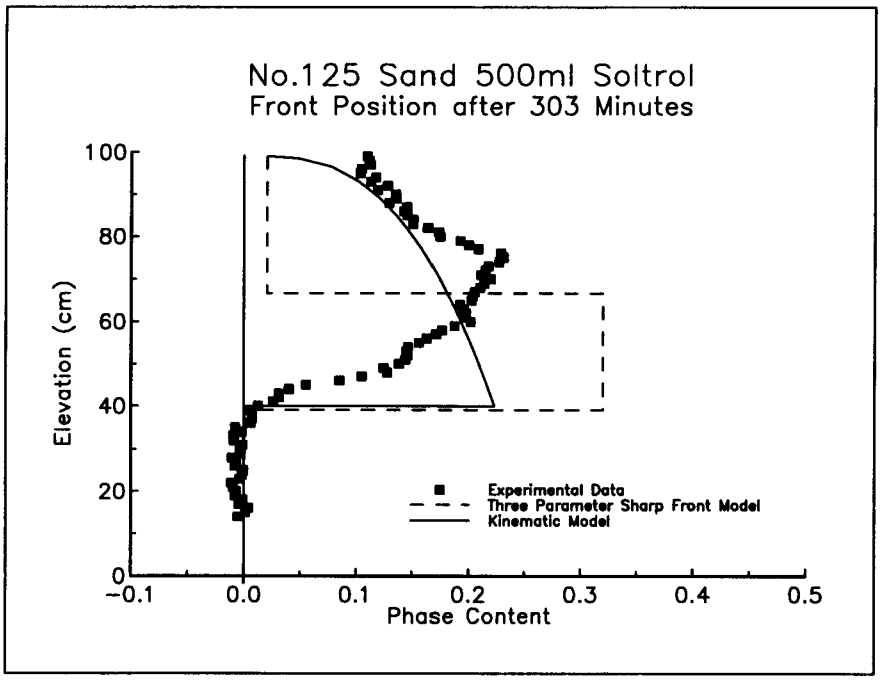


Figure 53. Phase content profiles comparison between models and experimental results.

Neither of the models represented the true shape of the profile exactly. Both models assume a sharp front at the leading edge of the NAPL. The experimental results, however, showed some degree of smearing of the front. The experimental data deviated from a sharp front mainly after the amount of moving Soltrol became very small. Thus the sharp front models tracked the experimental data with fair accuracy. Since the speed of the sharp front matches the speed of the spreading front (Equation (10)), the exact shape of the front is unimportant in determining its speed. This fact explains the ability of the sharp front models to match the experimental data to the degree that they do. The trailing edge (back front) exhibited a gradual decrease in phase content; it does not resemble the sharp front assumed by the three-parameter model nor the kinematic wave solution of KOPT exactly. The maximum phase content behind the front decreases as the Soltrol moves downward. The KOPT model allows reduction of the maximum NAPL phase content, while the three-parameter model assumes that the phase content behind the front is always at full saturation. Since the three-parameter model has been fitted to this data set, the front is tracked accurately despite the assumed NAPL saturation behind the front.

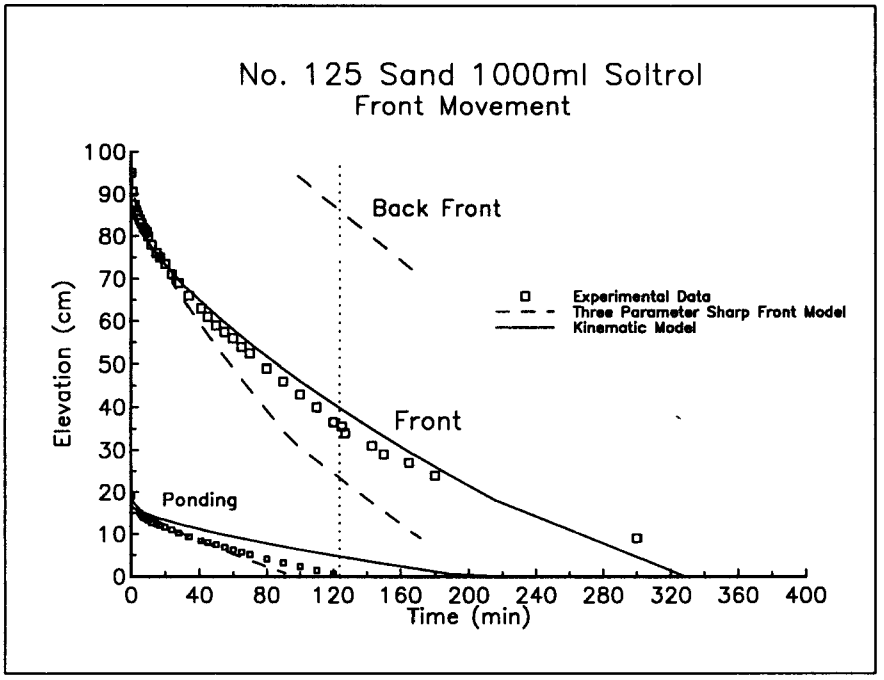


Figure 54. Front movement for 1000ml spill, comparison between model and experimental results.

Both models were tested on a spill of 1000 ml Soltrol (Figure 54). The same capillary suction head at front and back front were used as determined in the calibration for the 500 ml spill, since the suction heads are supposed to be material constants (fluid and soil). The KOPT model again approximates the front very closely; however, the three-parameter model deviates considerably from the experimental results. Use of the earlier calibrated suction heads did not yield an accurate prediction of the spill behavior with a different spill volume. This is a serious shortcoming of the three-parameter model. The profile comparisons (Figure 55 through Figure 57) show that the actual front is behind the three-parameter model front. This effect is due primarily to the assumption of full saturation behind the front, as evident in Figure 56, where the three-parameter model front is well ahead of the experimental data.

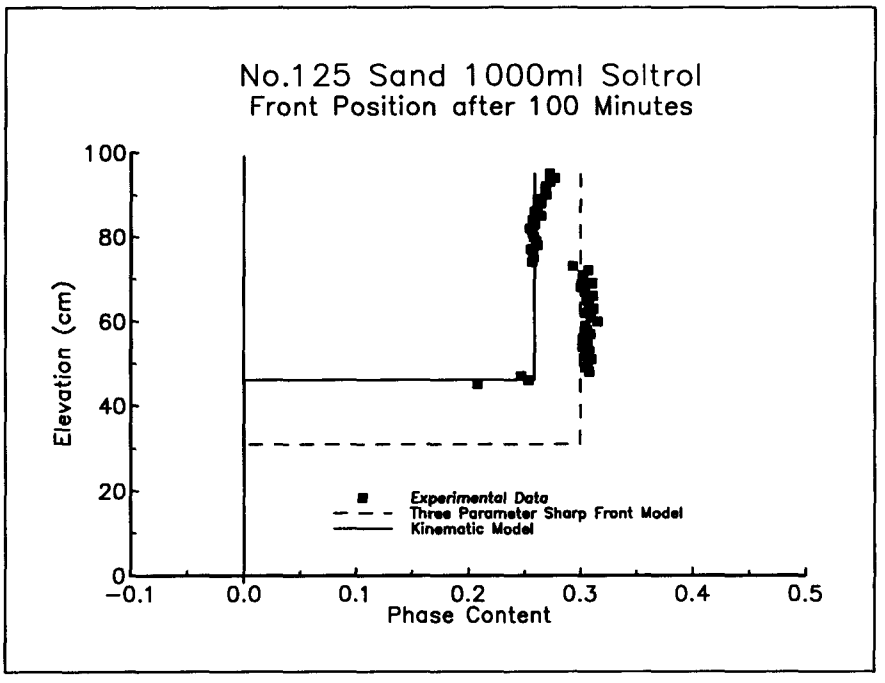


Figure 55. Phase content profile comparison between model and experimental results.

The influence of hydraulic conductivity on the KOPT model results was investigated. Previous uncertainty analysis with KOPT (Weaver et al., 1992) has demonstrated that the hydraulic conductivity is a dominant parameter of the model. In Figure 58, data from two 1000 ml spills in the #125 sand have been compared to the KOPT model predictions for three hydraulic conductivities (the average $K_s$ of 8.50 m/d and also +/- one standard deviation 5.79 m/d and 11.21 m/d). The conductivities were selected to represent the average hydraulic conductivity from the experimental determination, and the average plus and minus one standard deviation. It can be seen that both experiments fall within the predicted boundaries for one standard deviation of the hydraulic conductivity, and that accurate determination of hydraulic conductivity plays an important role in determining how closely the model can match the experimental results. As expected, the location of the front is highly dependent on the saturated hydraulic conductivity.

Comparisons of data from all the #70 sand experiments with the KOPT model are shown in Figure 59 through Figure 62. The hydraulic conductivity for the #70 sand was not measured as it was for the #125 sand. The hydraulic conductivity used in KOPT was selected so as to match the 1000 ml experimental result at approximately 250 minutes. This value was then used to simulate the 500 ml and 750 ml releases. In each case, KOPT over predicted the time of ponding. KOPT also somewhat under predicted the front speed during infiltration. These two features of the simulations suggest that the chosen hydraulic conductivity is too low for the 750 and 1000 ml experiments, as the long ponding time indicates a relatively low flux in the sand.

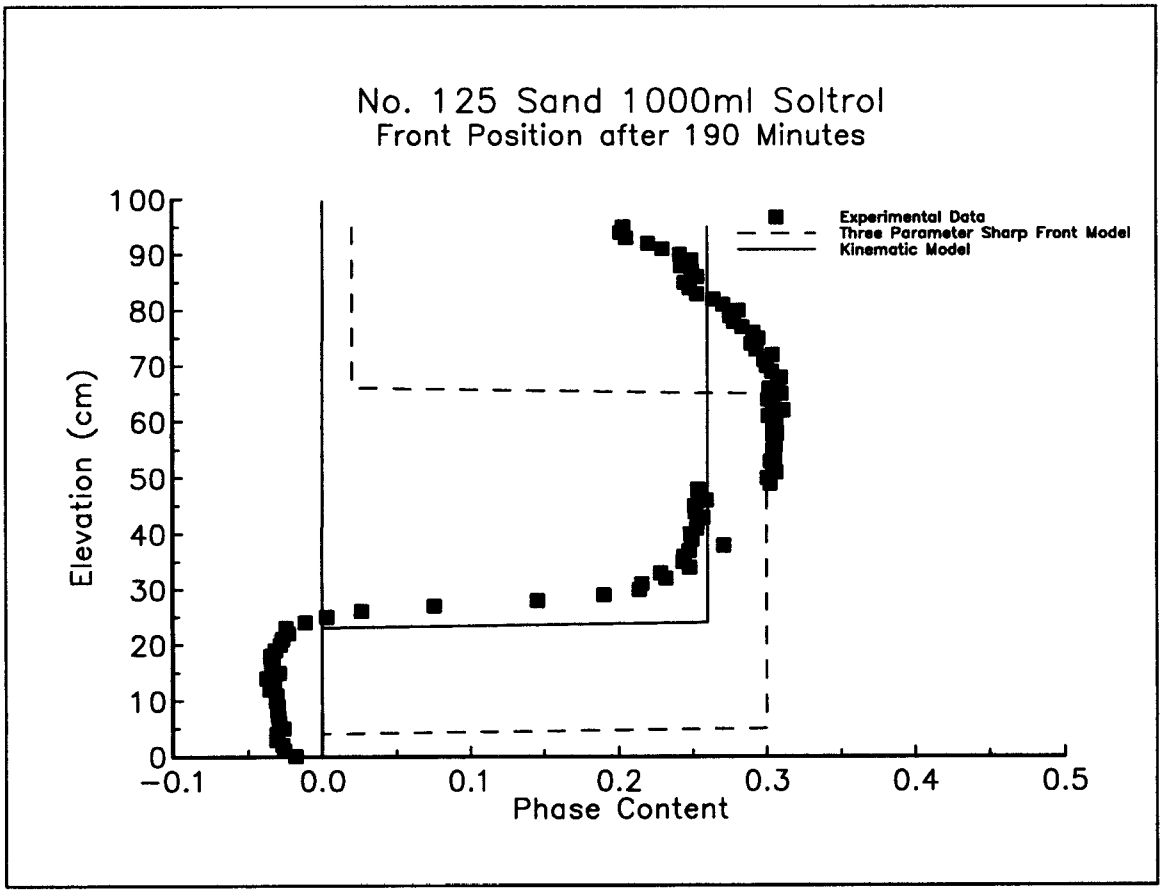


Figure 56. Phase content profile comparison between model and experimental results.

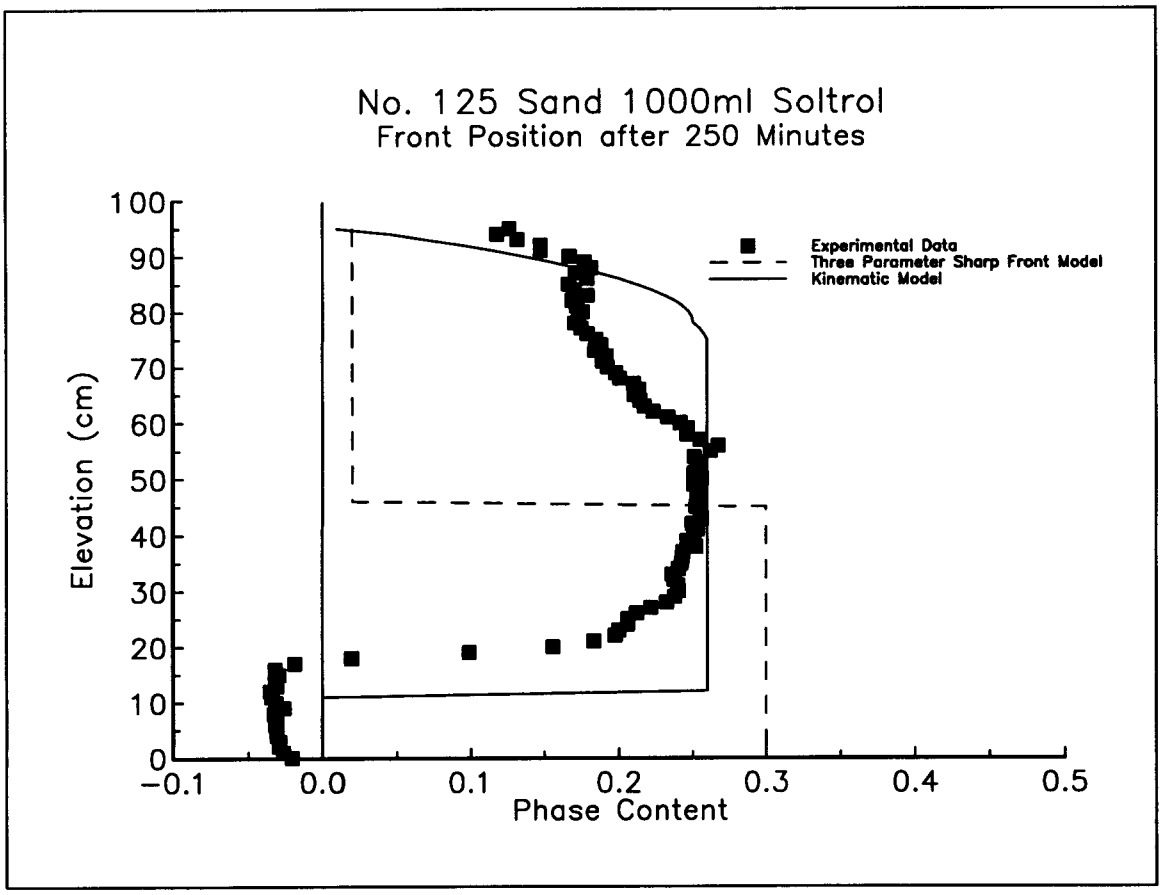


Figure 57. Phase content profile comparison between model and experimental results.

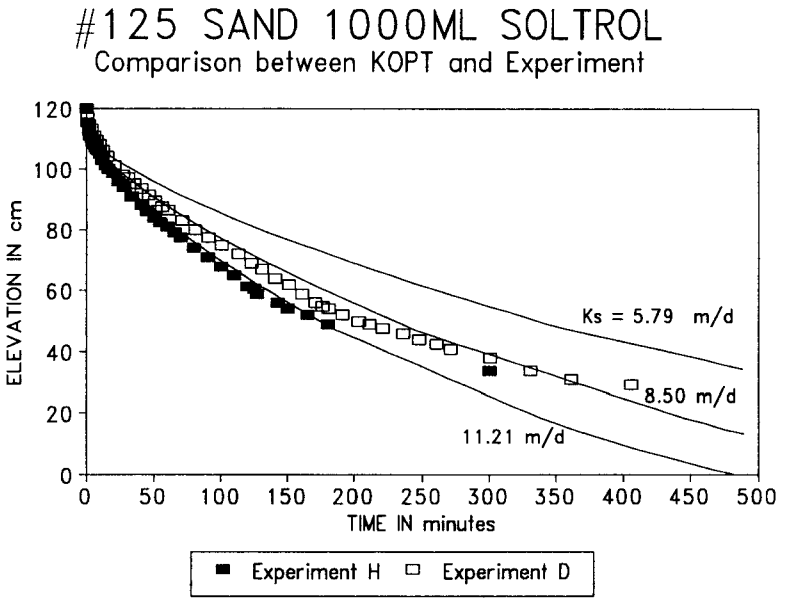


Figure 58. Front movement comparison between experiment and KOPT for different hydraulic conductivities.

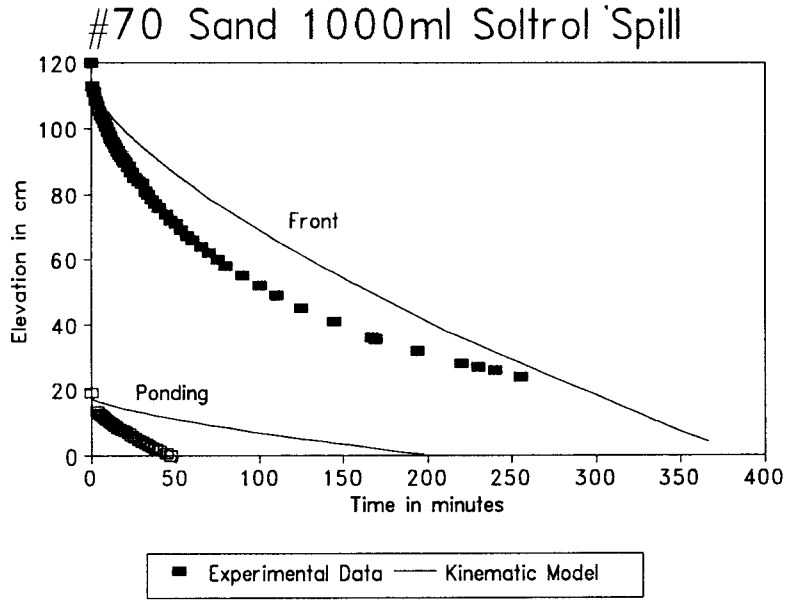


Figure 62. Front movement for 1000ml spill in #70 sand, comparison between KOPT and experimental results.

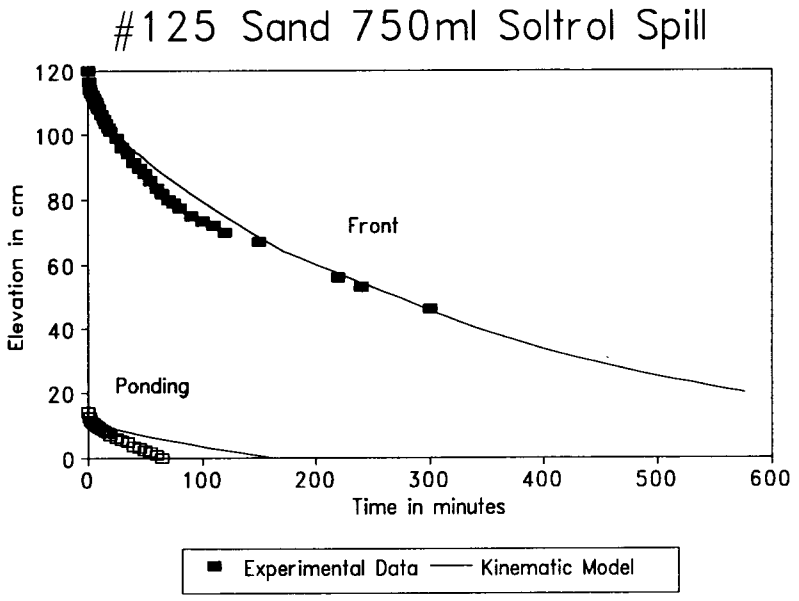


Figure 59. Front movement of 750ml spill in #125 sand, comparison between KOPT and experimental results.

By adjusting the parameters used in KOPT, the model may be forced to match the experimental results. The selection of the parameter values is not entirely arbitrary as each model parameter has a unique effect on the front position. For example, increasing the hydraulic conductivity generally increases the depth of the front as the liquid at all saturations tends to move faster. Increasing the air entry head, $h_{ce}$, increases the front depth during infiltration, as there is a greater contribution of capillary suction with increasing $h_{ce}$. Of course, if the front position is increased during infiltration, it will also be deeper during redistribution. The front speed during redistribution, however, is unaffected by changing $h_{ce}$ as $h_{ce}$ is not used in the kinematic wave solution for redistribution (Equation (15)) . Decreasing the Brooks and Corey $\lambda$ causes the curvature of the front-time plot to increase, because lower $\lambda$ values are associated with wider pore size distributions. In materials with wide pore size distributions, the effective conductivity $K_{ew}(S_w)$ drops off rapidly with decreasing saturation, here illustrated for the water phase by the Brooks and Corey (1964) relationship

$$K_{ew}(S_w) = K_w \left( \frac{S_w - S_{wr}}{1 - S_{wr}} \right)^{\varepsilon} \qquad \varepsilon = 3 + \frac{2}{\lambda} \qquad \textbf{(29)}$$

Since $\varepsilon$ is proportional to a constant plus $1/\lambda$, as $\lambda$ decreases, $\varepsilon$ increases. So for materials with wide pore size distributions (low $\lambda$), the effective conductivity to water decreases rapidly with

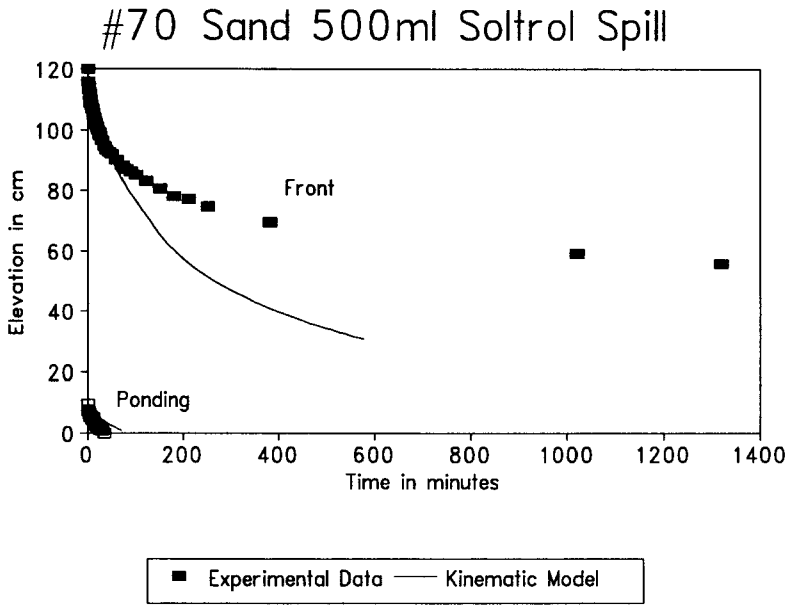


Figure 60. Front movement for 500ml spill in #70 sand, comparison between KOPT and experimental results.

decreasing saturation, $S_w$. This phenomena results in front vs. time plots where the front speed decreases sharply with time and has a large curvature. Table 5 summarizes parameter adjustments that were used to fit the experimental data for the #70 sand.

Table 5 Summary of KOPT Model Parameter Adjustments

| Parameter Adjustments | | |
|---|---|---|
| Parameter | Direction | Effect |
| Saturated Conductivity | increase | Increase depth of front at all times |
| Air entry head, $h_{ce}$ | increase | Increase depth of front especially during infiltration |
| Brooks and Corey $\lambda$ | decrease | Increase curvature of the front-time plot |

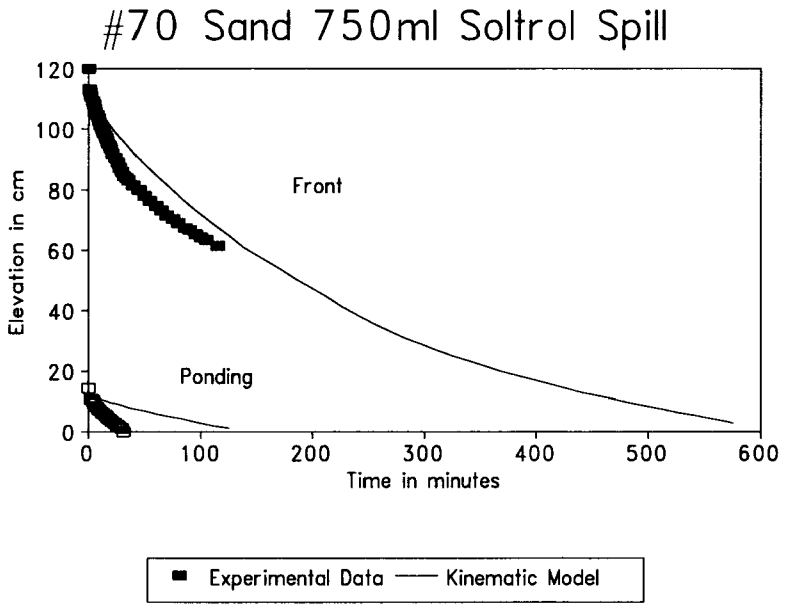


Figure 61. Front movement for 750ml spill in #70 sand, comparison between KOPT and experimental results.

The forced match of KOPT to each of the experiments in the #70 sand will be considered in turn. Generally, KOPT lags the experimental data for most of the duration of the 1000 ml spill and the curvature of the plot is too low. Thus the hydraulic conductivity and $\lambda$ were targeted for change. It turned out that in order to match the data, the entry head also had to be increased. Figure 63 shows the revised simulation of the experiment. Table 6 shows the adjusted parameter values for each of the experiments.

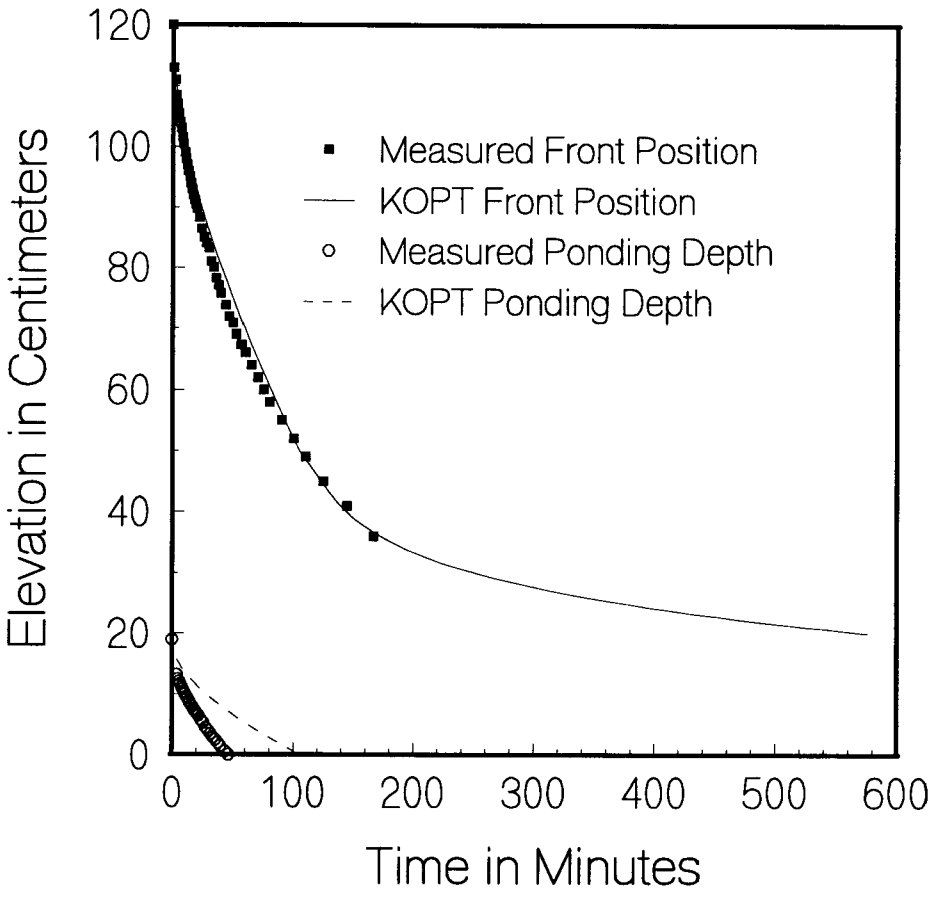


Figure 63 Adjusted KOPT simulation of the 1000 ml spill in the #70 sand

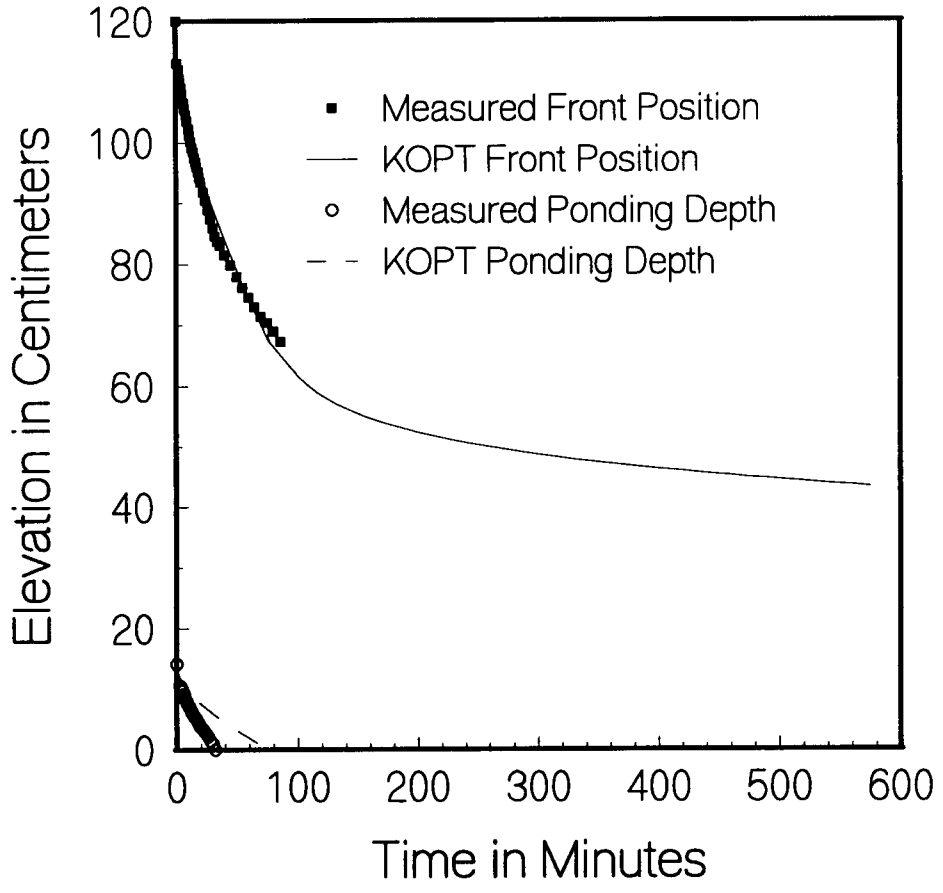


**Figure 64 Adjusted KOPT simulation of the 750 ml spill in the #70 sand**

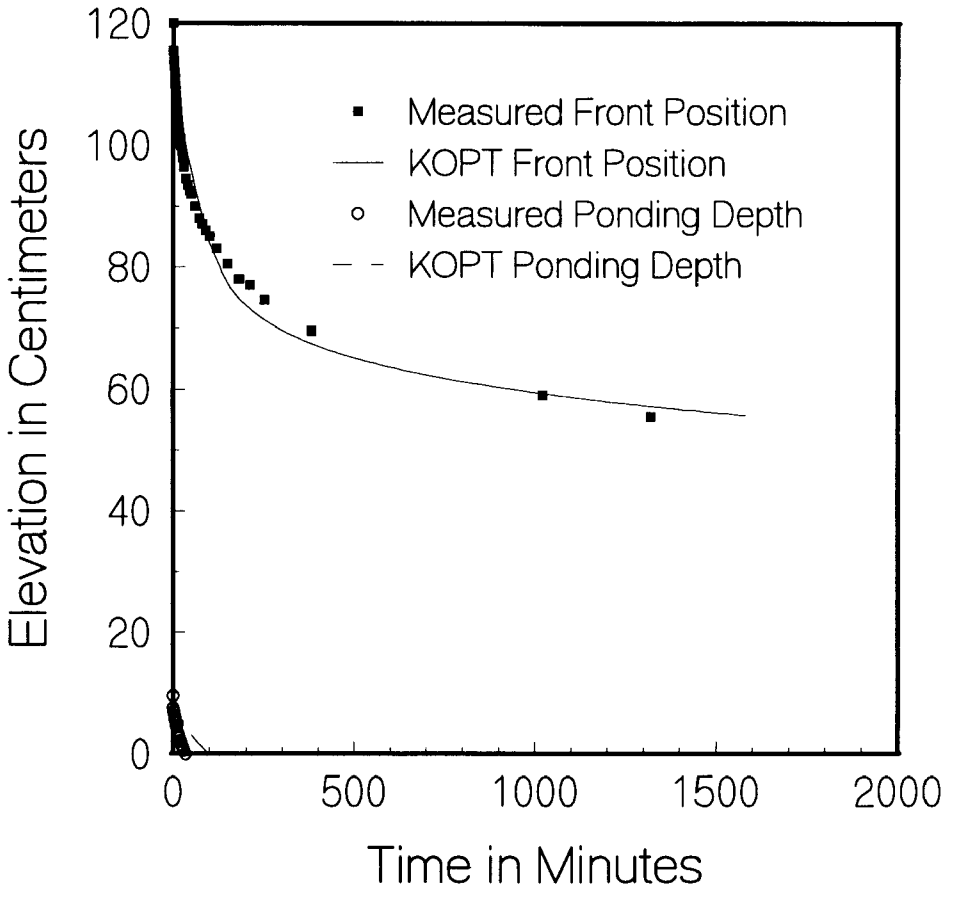


Figure 65 Adjusted KOPT simulation of the 500 ml spill in the #70 sand

Table 6 Adjusted KOPT parameter values for the #70 sand

| Adjusted KOPT parameter values for the #70 sand | | | |
|---|---|---|---|
| Parameter | 1000 ml spill | 750 ml spill | 500 ml spill |
| Saturated Hydraulic Conductivity, $K_s$ | 20 m/d | 18 m/d | 10 m/d |
| Brooks and Corey $\lambda$ | 0.25 | 0.25 | 0.4 |
| Porosity, n | 0.41 | 0.41 | 0.41 |
| Residual Water Saturation | 0.30 | 0.30 | 0.30 |
| Water Saturation | 0.30 | 0.30 | 0.30 |
| Air entry head, $h_{ce}$ | 0.4000 m | 0.4000 m | 0.2683 m |
| Oil viscosity, $\mu_o$ | 3.78 cp | 3.78 cp | 3.78 cp |
| Oil density, $\rho_o$ | 0.85 g/cm$^3$ | 0.85 g/cm$^3$ | 0.85 g/cm$^3$ |
| Residual oil saturation | 0.05 | 0.05 | 0.05 |
| Water surface tension | 65 dyne/cm | 65 dyne/cm | 65 dyne/cm |
| Oil surface tension | 24 dyne/cm | 24 dyne/cm | 24 dyne/cm |
| Ponding depth, $H_s$ | 0.1890 m | 0.1420 m | 0.0947 m |
| Radius | 0.025 m | 0.025 m | 0.025 m |

After obtaining a reasonable fit to the 1000 ml spill experiment, the same parameter set was used for the 750 ml spill. This approach was suggested by the similar match to the data that was found for the original parameter set (Figure 61 and Figure 62). Only a small reduction in hydraulic conductivity was necessary to force the model to fit the experimental results (Figure 64). It appears that both experiments are reasonably well fit by one parameter set and that the variation is similar to that due to the variation in hydraulic conductivity (Figure 58). For the 500 ml experiment, however, the original simulation had KOPT leading the data rather than following it, as it did for the 750 ml and 1000 ml experiments. Thus the hydraulic conductivity must be lowered in the 500 ml spill. As for the other fitted simulations, the Brooks and Corey $\lambda$ had to be decreased to fit the data. Figure 65 shows the revised simulation of the 500 ml spill experiment.

## 5.6 THE THEORETICAL RELATIONSHIP BETWEEN THE MODELS

The relationship between the three-parameter model and KOPT is discussed below. The basic conceptual framework for both models is essentially the same. A pulse of NAPL is applied at the surface of a homogeneous porous media, containing a uniform water saturation. The pulse begins and ends abruptly. Both models assume that the leading edge, or front, of the NAPL is sharp. As demonstrated by Smith (1983) and Charbeneau (1984), that all other things being equal, the sharp front models track the location of the true front.

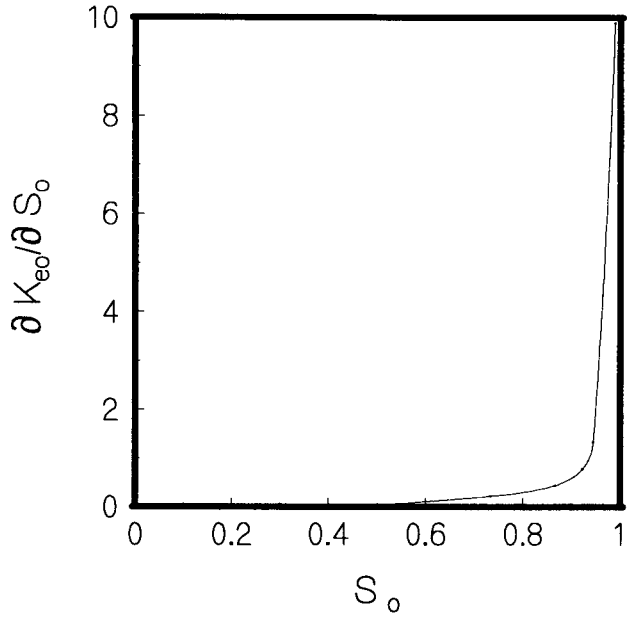


Figure 66. Schematic representation of the slope of the effective conductivity function.

Intuitively, one expects to treat the leading edge as a front. The nature of the function defining the wave speed is what determines if there is to be a discontinuity (sharp front) at the leading edge of the incoming liquid (Weaver, 1991). Figure 66 shows a monotonically increasing $\partial K_{ro}/\partial S_o$ function as would result from use of the Burdine (1953) and Brooks and Corey (1964) relative permeability model. When the NAPL release begins, the transition along the boundary is from some low saturation, $S_L$, to some high saturation, $S_H$. Because the characteristic speeds are determined by the $\partial K_o/\partial S_o$ and that function is monotonically increasing, the characteristic speeds increase from $S_L$ to $S_H$. The result is that the characteristics associated with the high saturation, $S_H$, move faster than those associated with the low saturation, $S_L$. These (and other characteristics between $S_L$ and $S_H$) must cross at some point in the domain (Figure 67, point A). Beyond that point, the classical method of characteristics solution does not hold, as it predicts the non-physical situation where multiple saturations are associated with points in the solution domain. For such situations, the solution is supplanted with the generalized solutions or jump conditions. When the boundary transition is abrupt, however, there is immediate generation of a front (Figure 68). Thus, based on the abrupt release scenario used for the two models, the

sharp front is expected for the leading edge of the infiltrating liquid.

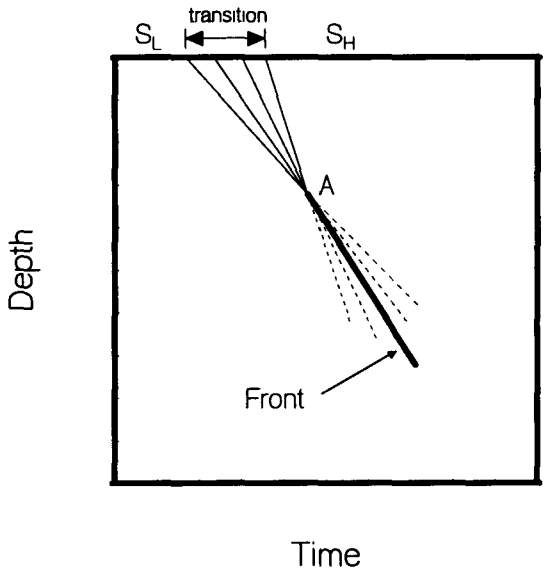


Figure 67. Continuous boundary transition from low to high saturation.

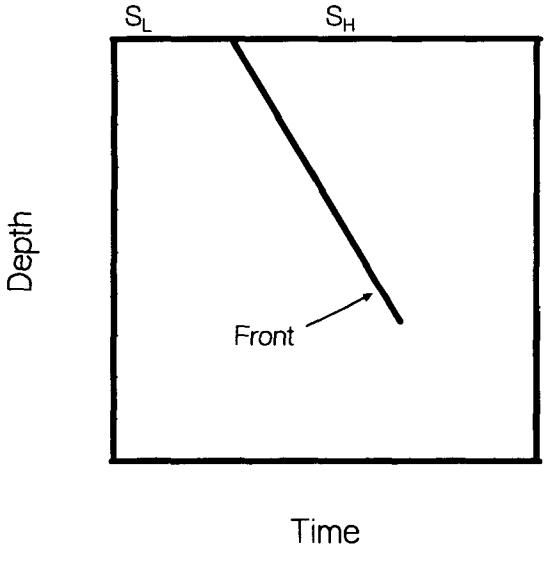


Figure 68. Abrupt boundary transition from low to high saturation which is immediately resolved into a discontinuity.

When the boundary transition is reversed (from $S_H$ to $S_L$), the characteristics do not cross and a fan-shaped wave is created. This situation occurs at the end of the NAPL release and is illustrated in Figure 69 and Figure 70. In Figure 69 the boundary transition from $S_H$ to $S_L$ is gradual, resulting in a continuous wave which originates from a zone along the surface. When the boundary transition is abrupt (Figure 70), the wave is said to be a centered simple wave. It is remarkable that in this case, discontinuous boundary data do not generate a discontinuity in the solution. In general the occurrence of a discontinuity in the solution depends both on the boundary data and the wave speed, which in this case is determined by the $\partial K_o/\partial S_o$ function.

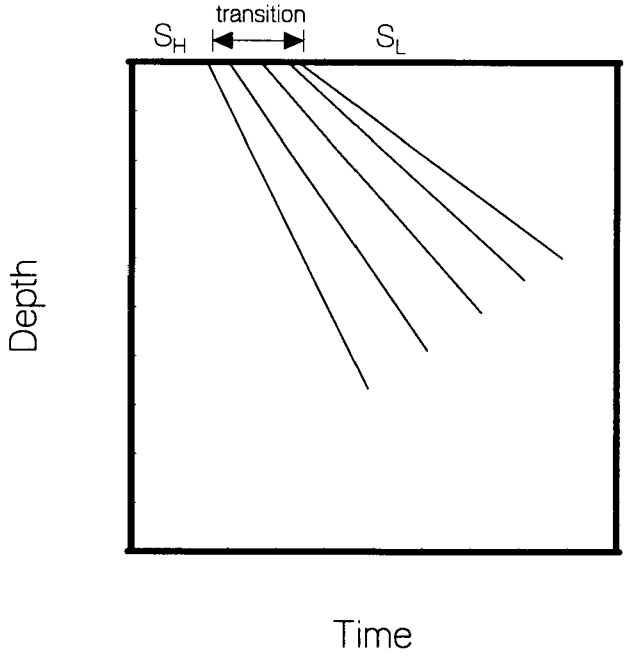


Figure 69. Continuous boundary transition from high to low saturation.

The KOPT model is based on this assumed scenario: an abrupt jump up in saturation followed by an abrupt jump down in saturation. The model results are seen to be a composite of the discontinuity of Figure 68 and the continuous wave of Figure 70. When profiles are constructed from the solution, they have low saturations near the surface since their characteristics move slowly. High saturations are found deeper in the profile as their characteristics move relatively fast. The profiles end at the sharp front which can be viewed as enforcing a mass balance condition.

If the profiles are perturbed, the sharp front tends to persist; because on the front, high saturations move faster than low saturations (Figure 71). The speed difference assures that the characteristics do not separate and spread the front. The neglected capillary pressure gradient term is balanced by the tendency of the front to persist. On the trailing edge, the saturations tend to separate because of the same speed difference. Thus the gravity term tends to create sharp fronts on the leading edge of the infiltrating liquid and also contributes to spreading of the wave on the trailing edge.

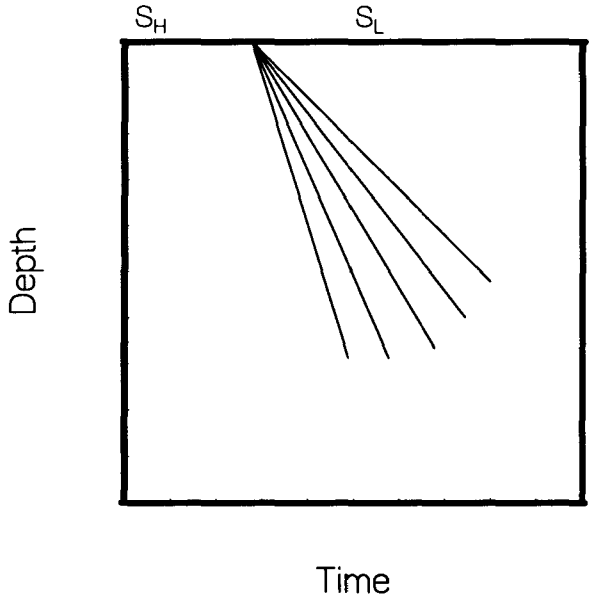


Figure 70. Abrupt boundary transition from high to low saturation, which generates a continuous wave.

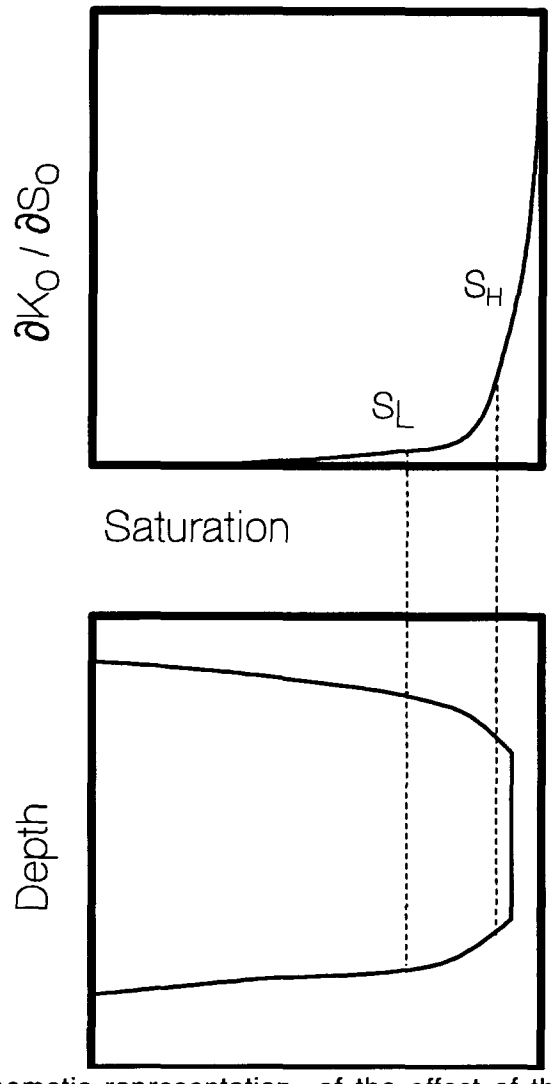


Figure 71. Schematic representation of the effect of the relative permeability derivative on the leading and trailing edges of the NAPL body.

In the three parameter model, a sharp front is assumed on the trailing edge of the liquid NAPL. There are at least two reasons for the occurrence of such a front. First, if the derivative of the relative permeability is not monotonically increasing as assumed in KOPT, then the boundary transition from high to low saturation can generate a sharp front. All that is required is that $\partial k_{ro}/\partial S_o$ is not a monotonically increasing function. Models developed by Mualem (1976) and Stone (1970) have non-monotonically increasing $\partial k_{ro}/\partial S_o$ functions. If the relative permeabilities are well described by these functions, then back fronts would be expected. The second reason for the existence of a back front is resistance due to air phase flow. Weaver (1991) shows that a back front is needed in method of characteristics models when unidirectional

air phase flow is included in the model. The back front, in that case, connects two continuous waves which are also a part of the boundary transition from high to low saturation. Even though they can be valid components of a method of characteristics solution, sharp back fronts are not likely to persist because of strong smoothing by gravity and capillary gradient forces.

# REFERENCES


Abriola, L.M., and G.F. Pinder, 1985. *"A Multiphase Approach to the Modeling of Porous Media Contamination by Organic Compounds, 1. Equation Development,"* Water Resources Research, Vol. 21, No. 1, pp 11-18.

Armbruster, E.J., 1990. *"Study of Transport and Distribution of Lighter than Water Organic Contaminants in Groundwater,"* Masters Thesis, University of Colorado, Boulder, Colorado.

Baehr, A., and M.Y. Corapcioglu, 1984. *"A Predictive Model for Pollution from Gasoline in Soils and Groundwater,"* Petroleum Hydrocarbons and Organic Chemicals in Ground Water, National Water Well Association, Washington, Ohio. No. 225, American Chemical Society.

Bazaraa, A.S., and H.J. Morel-Seytoux, 1979. *"Users Manual for a Gamma Attenuation System for the Determination of Water Content in Soils,"* Report HYDROWAR Program, Eng. Res. Cent., Colorado State Univ., Fort Collins, Colorado.

Bear, J., 1972. *"Dynamics of Fluids in Porous Media,"* Dover Publications Inc., New York, New York.

Bouwer, H., 1966. *"Rapid field measurements of air entry value and hydraulic conductivity of soil as significant parameter in flow system analysis"*, Water Resources Research, 2, 729-738.

Brooks, R.H., and A.T. Corey, 1966. *" Hydraulic Properties of Porous Media,"* Hydrology Papers, No. 3, Colorado State University, Fort Collins, Colorado.

Burdine, N.T., 1953. *"Relative Permeability Calculations from Pore-Size Distribution Data,"* Petr. Trans., Am. Inst. Mining Metal. Eng., Vol. 198, pp 71-77.

Campbell, J., 1992. *"Nonaqueous Phase Liquid (NAPL) Flow Through Heterogeneous Porous Media: Experimental Study and Conceptual Model Development,"* Masters Thesis, University of Colorado at Boulder.

Charbeneau, R.J., 1984, *"Kinematic models for soil moisture and solute transport,"* Water Resources Research, Vol. 29, pp 699-706.

Charbeneau, R.J., J.W. Weaver, and V.J. Smith, 1989. *"Kinematic Modeling of Multiphase Transport in the Vadose Zone,"* EPA /600/2-89/035.

Cathey, L., 1958. *"Fatigue in Photomultipliers,"* IRE Transactions on Nuclear Science, Vol. NS-5, pp 109-114.

Faust, C.R., 1985. *"Transport of Immiscible Fluids within and below the Unsaturated Zone: A Numerical Model,"* Water Resources Research, Vol. 21, No. 4, pp 587-596.

Faust, C.R., J.H. Guswaand, and J.W. Mercer, 1989. *"Simulation of Three-dimensional Flow of Immiscible Fluids Within and Below the Unsaturated Zone,"* Water Resources Research, Vol. 25, No. 12, pp 2449-2464.

Garder, W.H., and C. Calissendorf, 1967. *"Gamma Ray and Neutron Attenuation in Measurements of Soil Bulk Density and Water Content,"* Proceed. Symposium on Use of Isotopes and Radiation Techniques in Soil Physics and Irrigation Studies - International Atomic Energy Agency, Vienna, Austria.

Green, W.H., and G.A. Ampt, 1911. *"Studies on Soil Physics,"* Journal of Agricultural Science, Vol. 4, No. 5, p 1.

Held, R.J., 1993. *"Investigation of Fingering of Dense Non-Aqueous Phase Liquids in Saturated Porous Media"*, Masters Thesis, University of Colorado, Boulder, Colorado.

Honarpour, M.C., L. Koederitz, and A.H. Harvey, 1986. *"Relative Permeability of Petroleum Reservoirs,"* CRC Press Inc., Boca Raton, Florida.

Illangasekare, T.H., P. Brody, and D.D. Reible, 1987a. *"A Model for Two-Dimensional Transport of Concentrated Organics in Saturated and Unsaturated Soils,"* Proceedings of Seventh Annual American Geophysical Union Hydrology Days, Fort Collins, Colorado.

Illangasekare, T.H., P. Brody, and D.D. Reible, 1987b. *"A Model for Two-Dimensional Transport of Concentrated Organic Waste in the Unsaturated Zone,"* Proceedings of International Conference on Groundwater Contamination: Use of Models for Decision Making, Amsterdam, The Netherlands.

Illangasekare, T.H., and D.D. Reible, 1987a. *"A Simple Model for Transport of Free-Phase Organics in Unsaturated Zones of Aquifers,"* Proceedings NWWA Conference on Solving Groundwater Problems with Models, Denver, Colorado.

Illangasekare, T.H., and D.D. Reible, 1987b. *"A Study of Transport and Entrapment of Concentrated Organics in the Unsaturated Zone,"* Proceedings of International Conference on New Frontiers for Hazardous Waste Management, Pittsburgh, Pennsylvania.

Kaluarachchi, J.J., and J.C. Parker, 1989. *"An Efficient Finite Element Method for Modeling Multiphase Flow,"* Water Resources Research, Vol. 25, No. 1, pp 43-54.

Kueper, B.H., and E.O. Frind, 1991. *"Two-Phase Flow in Heterogeneous Porous Media; 1. Model Development,"* Water Resources Research, Vol. 27, No. 6, pp 1049-1057.

Kuppusamy, J.J., J. Sheng, J.C. Parker, and R.J. Lenhard, 1987. *"Finite Element Analysis of Multiphase Immiscible Flow Through Soils,"* Water Resources Research, Vol. 23, No. 4, pp 625-632.

Lenhard, R.J., J.C Parker, and S. Mishra, 1989. *"On the correspondence between Brooks-Corey and van Genuchten models,"* Journal of Irrigation and Drainage Engineering, Vol. 15, No. 4, pp 744-751.

Lenhard, R.J. and J.C. Parker, 1987. *"Measurement and Prediction of Saturation and Pressure Relationships in Three-Phase Porous Media Systems,"* J. Contam. Hydr., Vol. 1, pp 407-424.

McMaster, W.H., N. Kerr Del Grande, J.H. Mallet, J.H. Hubbell, 1969. *"Compilation of X-ray cross sections,"* Section II, Lawrence Radiation Laboratory, University of California, Livermore.

Manna, M., 1991, *Suction-Saturation Measurements in Soils Using the Flow Pump Technique*, Masters Thesis, University of Colorado, Boulder, Colorado.

Mualem, Y., 1976, *"A New Model for Predicting the Hydraulic Conductivity of Unsaturated Porous Media"*, Water Resources Research, Vol. 12, pp 513-522.

Muskat, M., R.D. Wykoff, H.G. Botset, and M.W. Meres, 1937. *"Flow of Gas-Liquid Mixtures Through Sands,"* Transactions, American Institute of Mining, Metallurgical and Petroleum Engineers, Vol. 123, pp 69-96.

Neuman, S. P., Wetting front pressure head in the infiltration model of Green and Ampt, Water Resources Research, 12, 564-566, 1976.

Nofziger, D.L., and D. Swartzendruber, 1974. *"Material Content of Binary Physical Mixtures as Measured with a Dual Energy Beam of X-Rays,"* J. Appl.Physics, Vol. 45, pp 5443-5449.

Oak, M.J., and R. Ehrlich, 1985. *A New X-Ray Absorption Method for Measurement of Three-Phase Relative Permeability,"* SPE 14420, Presented at the 60th Annual Conference of the Society of Petroleum Engineers, Las Vegas.

Osborne, M., and J. Sykes, 1986, *"Numerical Modeling of Immiscible Organic Transport at the Hyde Park Landfill,"* Water Resources Research, Vol. 22, No. 1, pp 25-33.

Peaceman, D., 1977. *"Fundamentals of Numerical Reservoir Simulation,"* Development in Petro. Science 6, Elsevier Publishing Co., pg 167.

Powers, M.C., 1953. *"A New Roundness Scale for Sedimentary Particles,"* Journal of Sedimentary Petrology, Vol. 23, No. 2, pp 117-119.

Reginato, R.J., 1974. *"Count Rate Instabilities in Gamma Ray Transmission Equipment,"* Soil Sci. Amer., Vol 38, pp 156-157.

Reible, D.D., and T.H. Illangasekare, 1989. *"Subsurface Processes of Non-Aqueous Phase Contaminants,"* Reviewed Book Chapter in Intermedia Pollutant Transport Modeling and Field Measurement, Editors D. Owen and I. Keplan, Plenum Press.

Reible, D.D., T.H. Illangasekare, D.V. Doshi, and M.E. Malhiet, 1990. *"Infiltration of Immiscible Contaminants in the Unsaturated Zone,"* Ground Water, Vol. 28, No. 5, pp 685-692.

Smith, R.E., 1983, *"Approximate Soil Water Movement by Kinematic Characteristics"*, Soil Science Society of America Journal, Vol. 47, pp 3-8.

Stillwater, R., and A. Klute, 1988. *"Improved Methodology for a Collinear Dual-Energy Gamma Radiation System,"* Water Resources Research, Vol. 24, No. 8, pp 1411-1422.

Szlag, D.C., and T.H. Illangasekare, 1992. *"Experimental Investigation in Modeling of Immiscible Liquid Entrapment n Porous Media,"* Proceedings of Conference on Hazardous Waste Research.

United States Environmental Protection Agency, 1992. *"Evaluation of Ground-Water Extraction Remedies: Phase II,"* Summary Report, USEPA, Office of Emergency and Remedial Response, Vol. 1, Washington, D.C. PB92-963346.

Weaver, J.W., 1989. *"Multiphase Flow Modeling by the Method of Characteristic Approximations,"* EPA/EPRI Environmental Research Conference, Groundwater Quality and Waste Disposal, Washington, D.C.

Weaver, J.W., 1991. *"Approximate Multiphase Flow Modeling by Characteristic Methods,"* US Environmental Protection Agency, EPA/600/2-91/015.

Weaver, J.W., R.J. Charbeneau, and B.K. Lien, 1994a, "*A Screening Model for Nonaqueous Phase Liquid Transport in the Vadose Zone Using Green-Ampt and Kinematic Wave Theory*", Water Resources Research, 30(1), 93-105.

Weaver, J.W., B.K. Lien, R.J. Charbeneau, J. Tauxe, J. Provost, 1994b. *"The Hydrocarbon Spill Screening Model (HSSM) Users Guide*", US Environmental Protection Agency, EPA/600/R-94/039a.

van Genuchten, M.T., 1980. *"A Close-for Equation for Predicting the Hydraulic Conductivity of Unsaturated Soils,"* Soil Science Society of America Journal, Vol. 44, pp 892-898.

# APPENDIX 1 DESCRIPTION AND TESTING OF THE DUAL-GAMMA SYSTEM

An automated gamma system was used for measurement of saturation and bulk density. Theory, configuration and testing of the gamma system are described in this appendix.

## 1.1 THEORY OF THE DUAL-GAMMA SYSTEM

Use of gamma spectroscopy for the measurement of bulk densities and fluid saturation of porous media is based on the exponential law for monoenergetic gamma radiation. This is a modified form of Lambert's law for light transmission through an absorbing medium. In gamma spectroscopy, the rate of energy transmission is described in terms of counts or counts per unit of elapsed time. A count refers to a recorded gamma emission. If the detected count rate can be compared with and without absorbing material present, it can be seen that the count rate is lower with absorbing material present. If the effective absorption rate of the material is known, then it is possible to predict the mass (or volume) of the material.

If $I_0$ represents the initial energy intensity emitted from a gamma source and entering an absorbing material, then the energy, $I$, emerging from the opposite side is given by:

$$I = I_0 e^{-\mu \rho x} \qquad (30)$$

where $\mu$ is the mass attenuation coefficient of the material, $\rho$ is the material density and $x$ is the path length through the material traversed by the gamma energy. The emerging intensity $I$ may be given in terms of either a count rate or as a total number of counts. For our application, $I$ is equal to the total number of counts recorded within a specified energy range or "region of interest."

Essential to the application of gamma theory is the knowledge of the energy absorbing characteristics of the materials present. Attenuation rates of gamma radiation differ widely between air, different fluids and soils. It is important to note that for our application the attenuation of gamma radiation by air is assumed to be negligible. This can be justified by noting that the attenuation coefficient of air is of the same order of magnitude as the attenuation coefficient for water (McMaster et al., 1969). However, air density is about three orders of magnitude smaller than the density of water; and thus, attenuation by air is about three orders of magnitude smaller than attenuation by water.

The mass attenuation coefficient, $\mu$, of a material describes the rate of gamma energy absorption. Units of measurement of the mass attenuation coefficient are in $cm^2/g$. This coefficient differs not only between materials but also for different energy levels of sources of gamma radiation (i.e. Americium and Cesium sources used in our dual-gamma system). Mass attenuation coefficients can be determined using Equation (30) and solving for $\mu$. The procedure which will be used to determine the attenuation coefficient will be described later.

In multi-phase systems, the attenuation due to each phase must be incorporated into Equation (30). For the case of sand and water, this equation takes the form,

$$I = I_D e^{-(\mu_s \rho_s x_s + \mu_w \rho_w x_w)} \quad (31)$$

where the subscripts s and w stand for sand and water, respectively. The initial count rate $I_D$ is defined as the count rate through the empty container, before it is filled with sand and water. Thus redefining the initial count rate eliminates the need to consider the absorption by the material of the column, or any container which is used to hold the sample. For further simplification, the new initial count rate, $I_D$, can be taken through dry sand. That is, attenuation due to the soil is implicit in $I_D$; and any further attenuation is only due to the presence of water. This leads back to Equation (30).

As the pores of the soil are partially saturated with water, the true path length through the water, $x_w$, cannot be measured. Only the path length through the total sample, x, is known. The following relation between $x_w$ and x is assumed to hold true:

$$x_w = nSx \quad (32)$$

where n is the porosity of the sample and S the water saturation.

A lumped calibration constant (Nofziger and Swartzendruber, 1974), $U$, can be defined for each material present and for each gamma energy:

$$\begin{aligned} U_{Aw} &= \mu_{Aw} \rho_o & U_{Ao} &= \mu_{Ao} \rho_o \\ U_{Cw} &= \mu_{Cw} \rho_w & U_{Co} &= \mu_{Co} \rho_o \end{aligned} \quad (33)$$

where A and C stand for Americium and Cesium sources, respectively.

Rewriting Equation (31):

$$I = I_D e^{-(U_s + nSU_w)x} \quad (34)$$

The lumped attenuation coefficient $U_s$ for the sand is always measured through porous sand, the porosity is therefore implicit in $U_s$ and does not need to be considered in the path length in the formulation given in Equation (34). When volumetric phase content $\theta$ needs to be introduced the relation $\theta = nS$ is used.

Saturation of two fluids can be determined with a dual gamma system by writing Equation (34) for each gamma source:

$$I_A = I_{AD} e^{-(\theta_W U_{AW} + \theta_O U_{AO})x} \quad (35)$$

$$I_C = I_{CD} e^{-(\theta_W U_{CW} + \theta_O U_{CO})x} \quad (36)$$

Equations (35) and (36) are solved simultaneously to yield volumetric phase content for water and oil:

$$\theta_W = \frac{U_{OA} \ln \frac{I_{CD}}{I_C} - U_{CO} \ln \frac{I_{AD}}{I_A}}{(U_{CW} U_{AO} - U_{AW} U_{CO})x} \quad (37)$$

$$\theta_O = \frac{U_{CW} \ln \frac{I_{AD}}{I_A} - U_{AW} \ln \frac{I_{CD}}{I_C}}{(U_{CW} U_{AO} - U_{AW} U_{CO})x} \quad (38)$$

In the above equations, $I_D$ is the count rate through the dry sand. $I_D$ can be expressed with the count rate through the empty box, using Equation (30):

$$I_D = I_o e^{-U_{SAIC} x} \quad (39)$$

The lumped calibration constant $U$ cannot be used when the bulk density of a sample is determined with the gamma system. Equation (34) can then be rewritten as:

$$I_A = I_{AD} e^{-(\mu_{AS} \rho_B + \theta_w U_{Aw})x} \quad (40)$$

$$I_C = I_{CD} e^{-(\mu_{CS} \rho_B + \theta_w U_{Cw})x} \quad (41)$$

These are two equations for Americium and Cesium with two unknowns, the bulk density and volumetric water content. It can be seen that the bulk density can only be calculated for

combinations of one solid phase and one liquid phase. With two liquid phases, three unknowns in only two equations would be present. Solving the two equations simultaneously yields solutions analogous to Equations (37) and (38).

$$\theta_W = \frac{\mu_{AS} \ln \frac{I_{CD}}{I_C} - \mu_{CS} \ln \frac{I_{AD}}{I_A}}{(U_{CW}\mu_{AS} - U_{AW}\mu_{CS})x} \quad (42)$$

$$\rho_B = \frac{U_{CW} \ln \frac{I_{AD}}{I_A} - U_{AW} \ln \frac{I_{CD}}{I_C}}{(U_{CW}\mu_{AS} - U_{AW}\mu_{CS})x} \quad (43)$$

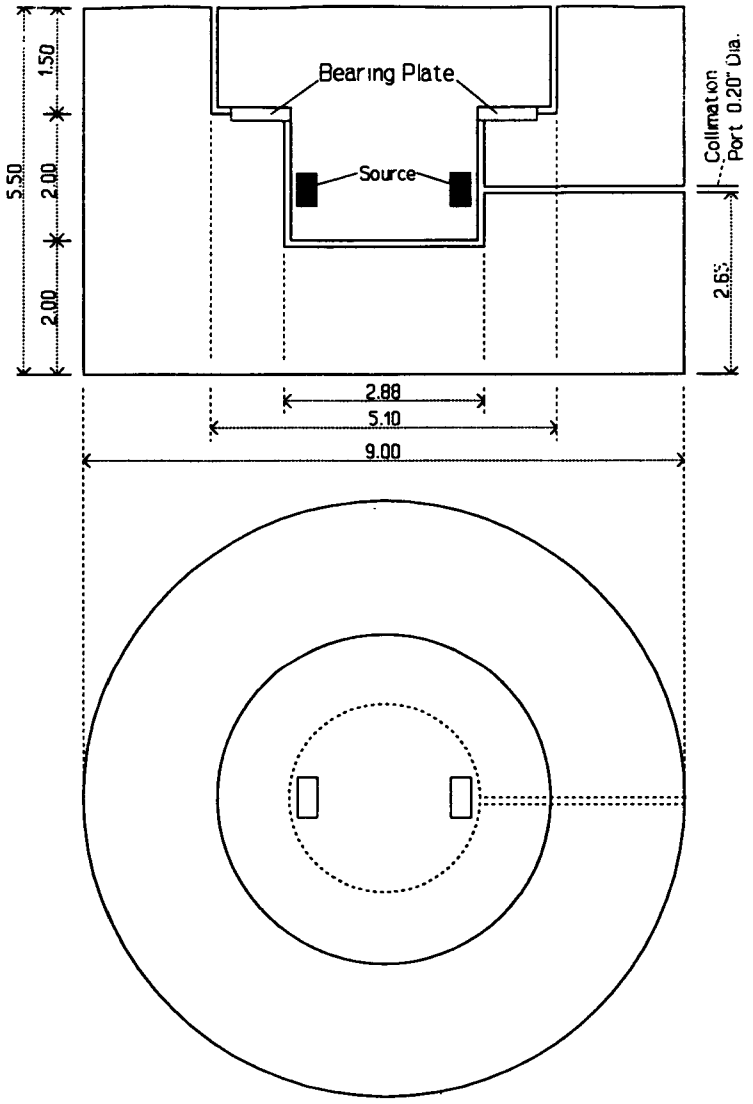


Figure 72. Radiation source housing (after Armbruster, 1990).

The bulk density of the solid phase and the volumetric saturation of one liquid phase can be calculated simultaneously.

Porosity and bulk density are interrelated in the following way:

$$n = 1 - \frac{\rho_b}{\rho_s} \quad (44)$$

where $\rho_B$ is the bulk density and $\rho_S$ is the density of the solid grain (for sand $\rho_S$ = 2.65 g/cm$^3$).

## 1.2 CONFIGURATION OF THE GAMMA SYSTEM

The physical setup of the gamma system is described in the following chapter.

### 1.2.1 Radiation Source

Various gamma emitting sources have been used by other investigators. Garder and Calissendorf (1967) found the isotopes Cesium 137 (Cs) and Americium 241 (Am) to be most convenient and useful for laboratory work in soil physics. Cesium 137 has a half-life of 30 years and an energy peak at 0.662 MeV and Americium 241 has a half-life of 458 years and a lower energy peak at 0.060 MeV. The half-lives are sufficiently long so that decay corrections are not required for laboratory measurements. The experimental setup described in this report contains a Cesium source with 50 mCi strength and an Americium source with a strength of 200 mCi. Using two different sources of gamma radiation gives the advantage of being able to solve for two unknowns, i.e. bulk density and saturation of a single fluid or for known bulk density saturation of two fluids, simultaneously. The two sources can be used by alternating the exposure from each source or arranging the sources in a collinear fashion. Collinear measurements have the advantage of saving time.

The sources are enclosed in a shielded lead housing (Figure 73). The two sources with the housing are mounted diametrically in a rotating inner cylinder mounted on a bearing. A second fixed lead cylinder encloses the inner cylinder. The outer cylinder has a 0.5 cm diameter collimation hole aligned with the detector. The inner cylinder with the radiation sources can be rotated in such a way that one of the sources is in front of the collimation hole. In this position, the second source gets located diametrically opposite to the first. During a measurement, the stronger Cesium source is rotated to the back, while the Americium source is in front. In this configuration, the radiation from both sources is detected simultaneously by the detector. All the tests which are reported here were conducted using this source configuration which produces two energy peaks in the spectrum. The distance between source collimation hole of the source and the detector is 34 cm.

### 1.2.2 *Solid Scintillation Counting System*

Radiation is detected using a thallium activated sodium iodide crystal and a photomultiplier tube. As the ionizing radiation interacts with the fluor crystal, a portion of its energy is transferred to the fluor molecules causing excitation of the orbital electrons. Electrons returning to their original energy level emit the absorbed energy as electromagnetic radiation in the visible or near ultraviolet region. The photomultiplier is employed in close proximity to the fluor crystal to convert the photons to photoelectrons which are greatly amplified by secondary electron emission through nine series of dynodes to a sizable electrical pulse. The detector used with this system is a 2 inch diameter and 2 inch thick NaI(Tl) scintillation photomultiplier tube (ORTEC 905-3). All other components of the counting system were manufactured by ORTEC, Oak Ridge, Tennessee. A preamplifier is used to shape the detector signal and to make the signal to cable noise ratio as high as possible. A second amplifier (ORTEC 575A) gives extra amplification and minimizes pulse overlap by shortening the time of duration of each amplifier pulse by clipping the pulse. The electronic system has a specific deadtime after every radiation pulse detected, in which no further impulses can be measured. The total deadtime during a measurement depends on the number of registered pulses and is shown by the software in percent. Positive pulse shaping was selected. This indicates the presence of only positive portions of the pulse.

A multi-channel analyzer (ORTEC 918A ADCAM) is used to select pulses of the desired energy. Pulses are counted using a timer-counter unit. EG&G Ortec ADCAM software is used to analyze the signals and present the results on a PC. A well regulated and highly stable voltage is required for the operation of the photomultiplier tube. The model used with this system is ORTEC 556.

A schematic diagram showing the different components of the gamma system is given in Figure 73.

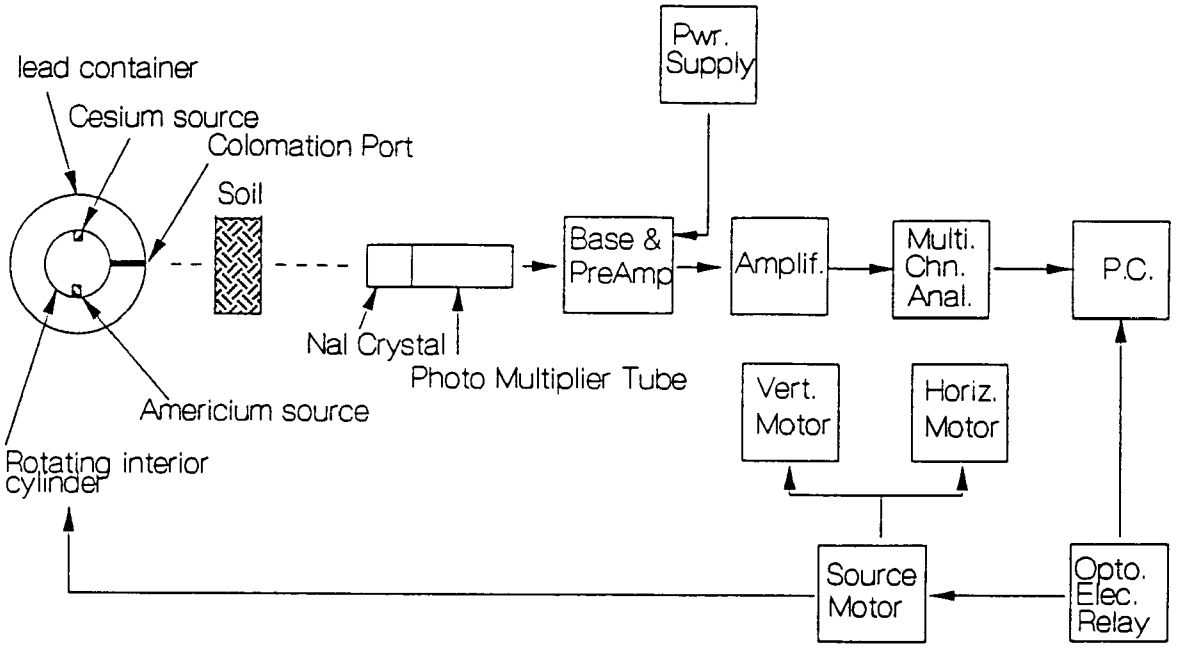


Figure 73. Schematic of computer controlled traversing gantry and gamma data acquisition system (after Armbruster, 1990).

### 1.2.3 Traversing Mechanism

The principle of the gamma attenuation necessitates, external to the soil sample, a radioactive source on one side of the test sample and a scintillation detector on the other side. The setup for these measurements consists of fixed and moving frames (Figure 74). The sample is attached to the fixed frame. The detector and source assembly are placed on the platforms of a moving frame. Horizontal and vertical movements are motor driven and can be controlled through software specifically designed for this purpose. The software automatically shuts off the motors while the measurement is taken, so there is no electronic interference between the detector and the motors.

### 1.2.4 Test Box

Following Bazaraa and Morel-Seytoux (1979), a multi-chambered plexiglass box was constructed for the testing of the Gamma system (Figure 75). The effective path length traversed by the gamma radiation may be precisely controlled by sequentially filling compartments with the material being tested. The path length was measured with mechanical tools to an accuracy of 1mm. An aluminum plate (10 mm) was used as a standard absorber.

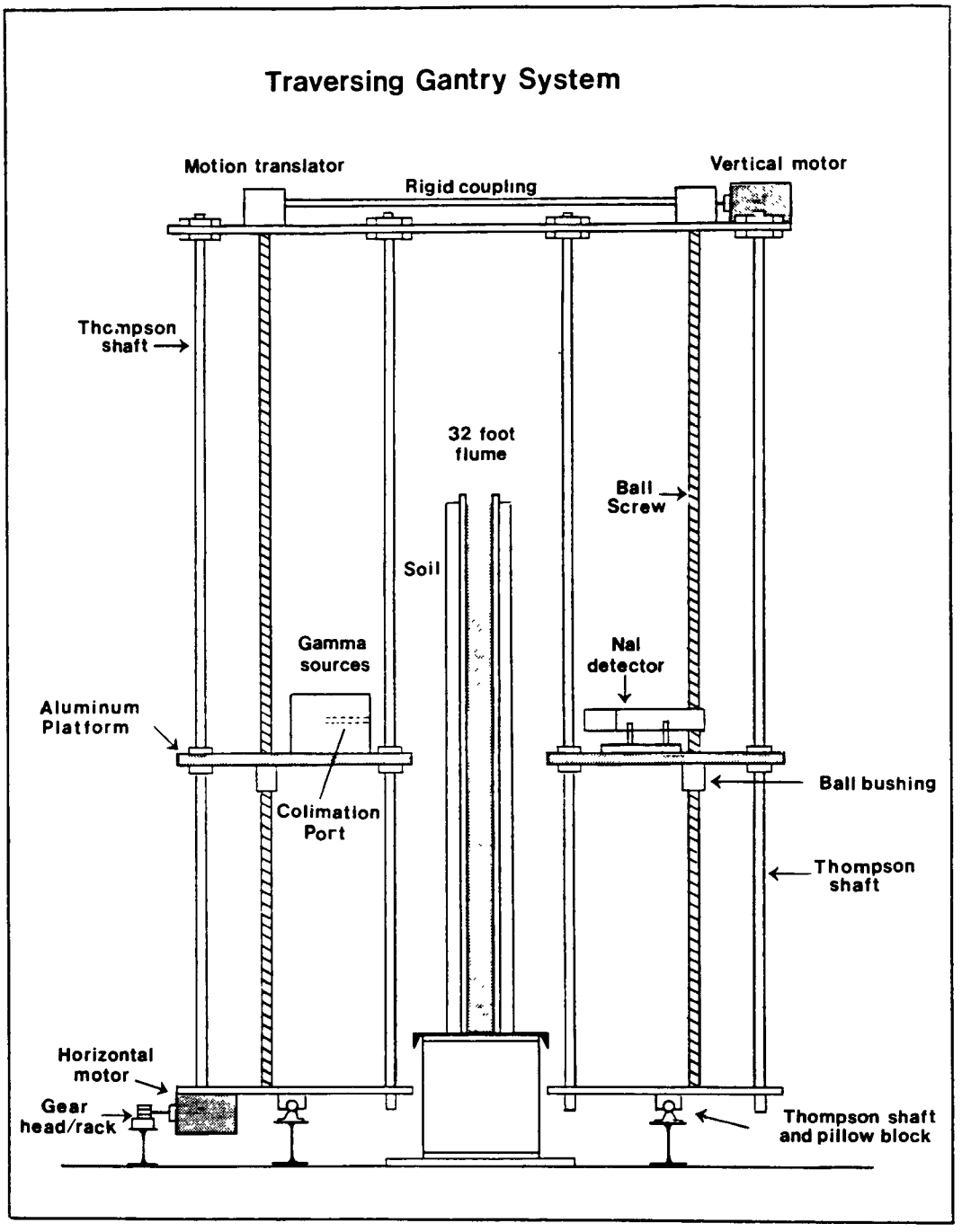


Figure 74. Computer automated traversing gantry system (after Armbruster, 1990).

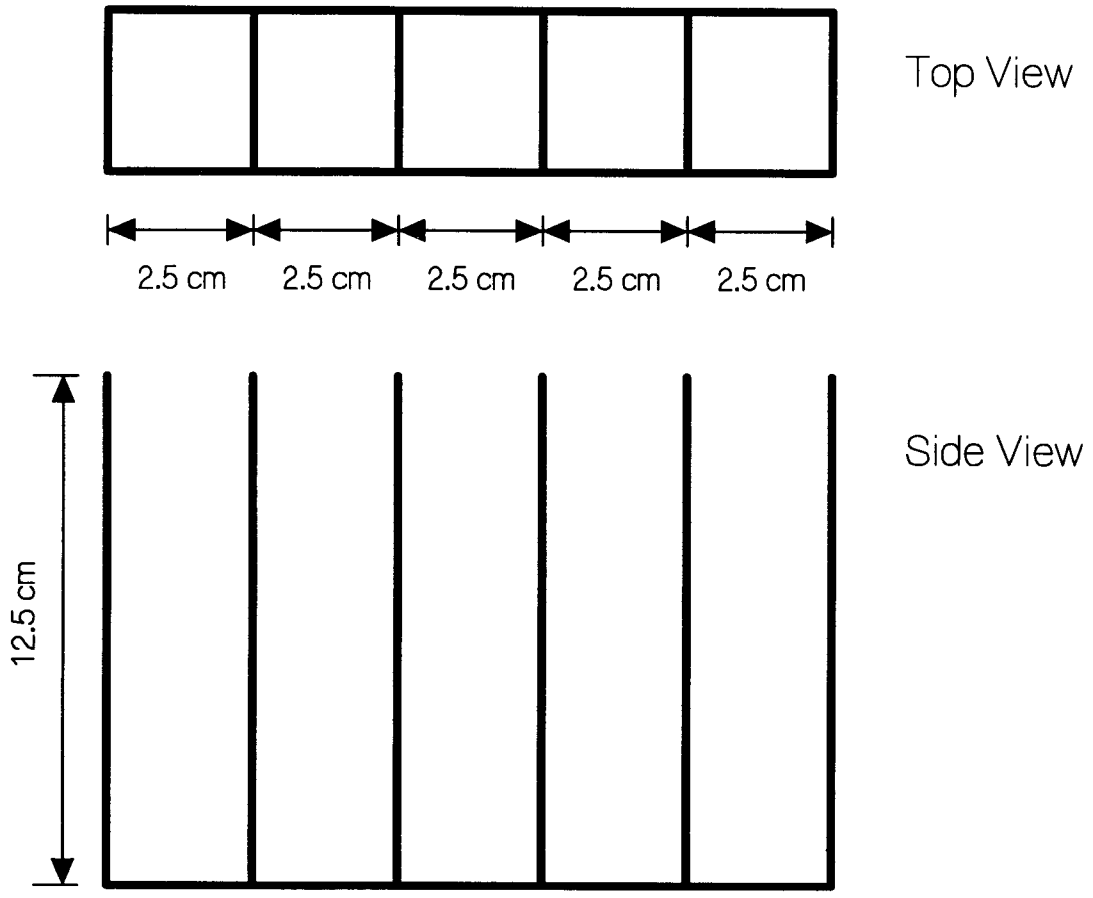


Figure 75. Multichambered plexiglass box for testing the gamma system

## 1.3 TESTING PROCEDURES FOR THE GAMMA SYSTEM

Since the gamma system was the primary instrument used in the collection of phase content data during spill experiments, it was tested extensively. The following chapter describes the testing of the gamma system.

### 1.3.1 Modifications of the Gamma System

Proper alignment of source and detector is an important prerequisite for good performance of the gamma system. In order to align the detector, elongated, oval-shaped slits were drilled into the bottom plate of the detector, thus allowing the detector to be moved in three directions to obtain the desired alignment. The detector can then be bolted down to the platform in the optimum position. By moving the detector in increments, the position was determined where the detector would read the maximum count rate. The detector was fastened down when proper alignment was indicated through the highest observed count rate. To maintain proper alignment of the signal, the source also needs to be secured to the platform. The gamma source is in danger of being moved slightly whenever the platform moves up or down. The gamma source was bolted tightly to the platform to prevent any movements during vertical motion of the source platform.

It is assumed that by securely fastening the source and detector to their platforms, the alignment will not change. However, the platforms on which the detector and the source are mounted move in relation to each other when moved up or down; thus the alignment between source and detector changes depending on the elevation at which the measurement is taken. However, initial calibration allows for correction of the count rate for the misalignment, assuming that the alignment is always the same for each vertical position.

Electronic shift in the detector moves the Americium and Cesium peak from their theoretical position on an energy scale. The software used (EG&G) integrates only over a set range of energy. If the peak shifts (partly) out of this region, the integration procedure does not capture the whole peak. There is also a limit to the width of the integration region. To eliminate this problem, a new integration scheme was developed (Campbell, 1992) to allow a wider region for the integration. This method tries to avoid problems with a shifting peak. However, most of the measurements for this research were conducted before the new software was finished. The calibration described in this report pertains to the original EG&G software. A comparison between the two integration schemes was performed; and no difference was found between them.

### 1.3.2 Determination of Warm-Up Time

It has to be assumed that the measurements with the gamma system are not accurate unless the detector is at steady state, which requires some warm-up time. Thus, the warm-up time for the gamma system was established, by using the following test. The system was completely shut off overnight, and a measurement was started right after the unit was turned on. The measured radiation intensity of Americium through a standard absorber changed for the first 20 minutes and stayed constant from then on (Figure 76a). The measured intensity of Cesium was constant from the start of the measurement (Figure 76b). It can be concluded that for this configuration of the gamma system, the warm-up time is 20 minutes until the readings for Americium stay constant.

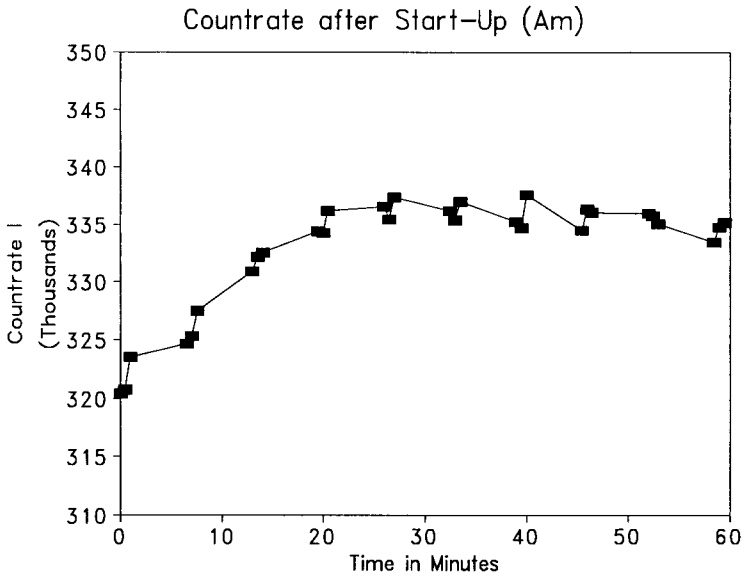


Figure 76. Delay in reading of constant count rate after start-up (Am).

### 1.3.3 Overloading of the Detector

The objective of this test was to determine whether exposure of the detector to the un-attenuated radiation will overload the detector. Reginato (1974) reported that the detector shows a hysteresis after being exposed to an overload of radiation, i.e. the detector stays saturated (up to about 30 minutes) even after the radiation beam is taken away from the detector. This would mean that after any prior exposure of the detector to the un-attenuated source, the detector may not measure accurately. This problem was investigated with the following procedure (similar to the one reported by Reginato, 1974). The detector was first exposed to the un-attenuated source for 5 minutes. Afterwards, the gamma intensity through a standard absorber was measured for 80 minutes. A constant intensity was found which did not decrease over time (Figure 77). It can be assumed that the radiation source in our experiment is weak enough so it does not cause any long lasting, over-saturation of the detector, even if there is no absorber between source and detector.

A second test was conducted to determine whether overloading of the detector led to fatigue in the detector during the measurement. High radiation causes fatigue in the detector which leads to unstable readings of the count rate. A high count rate per second (high dead time) has to be avoided. Repeated measurements were conducted through different absorbers over a 3-hour period. For an absorber which had little absorption (a thin aluminum sheet), the count rate for repeated 30 second counts varied widely over the 3-hour test period. The count rate through a highly absorbing aluminum block, however, stayed fairly constant. It was shown that for dead times below 10%, detector fatigue does not cause large variations in the Americium count rate. No such clear limit could be found for the Cesium count rate. It is possible that due to the higher energy of the Cesium radiation, there is always some degree of detector fatigue.

### 1.3.4 Random Variation

Fluctuations in the intensity of the gamma radiation are due to the random nature of the radioactive process. Repeated measurements give the statistical standard deviation of the process if the measurements are done right after each other, and it is assumed that the detector sensitivity does not change over a short period of time (Stillwater and Klute, 1988). Repeated measurements were conducted through different absorber thicknesses. For each absorber the measurement was repeated seven times. These seven measurements were averaged and the standard deviation calculated. As expected, the number of counts was found to decrease with increasing thickness of the absorber. The standard deviation of the measurements for the Americium source is roughly in the same order of magnitude as the square root of the number of counts (Table 7). For any natural process which follows a Poisson distribution, the standard deviation is the square root of the count number. Radioactive decay follows this distribution. By confirming this result with our measurements, it could be concluded that for measurements repeated in a short time period, only radioactive decay produces the random variability in the Americium count rate; and no other random factors influence the measurement. The Cesium count rate has a higher variability as explained above with detector fatigue due to the high energy gamma radiation.

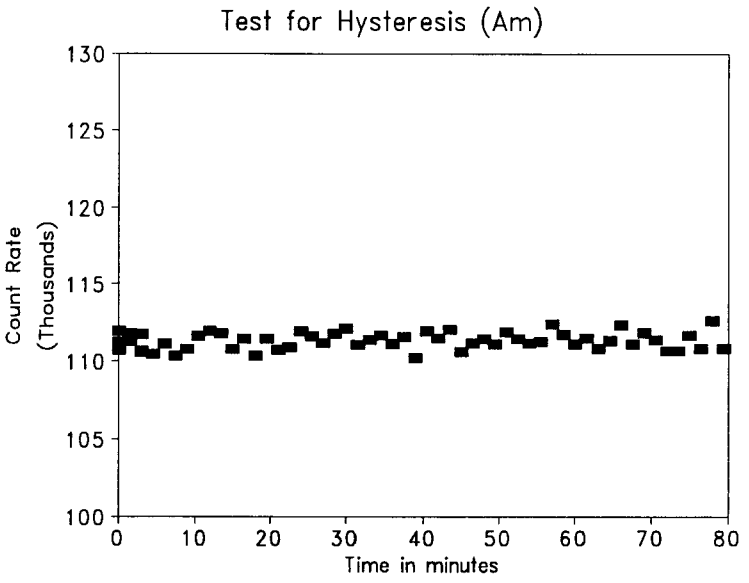


Figure 77. Test for hysteresis (Am).

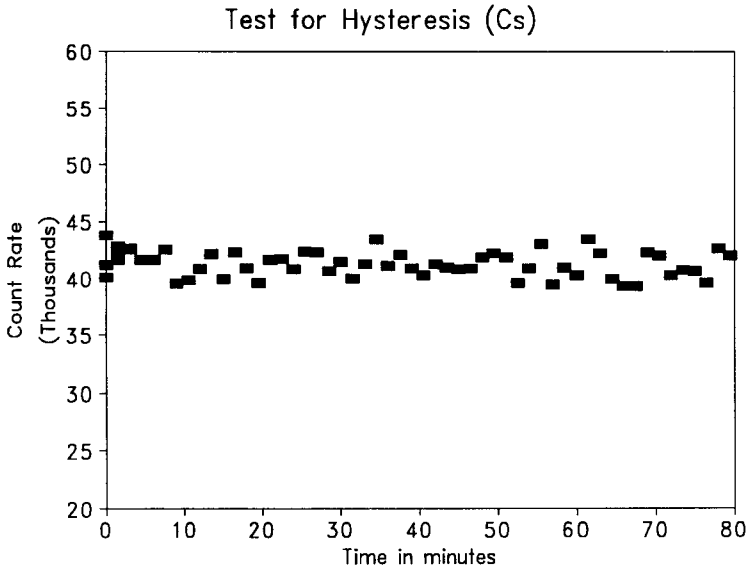


Figure 78. Test for hysteresis (Cs).

Table 7. Random variation comparison

| Absorber | Am | Cs | Am | | Cs | |
|---|---|---|---|---|---|---|
| 2.5 cm | 420746 | 215399 | | | | |
| | 422512 | 213736 | | | | |
| | 422794 | 215162 | Average | 422212 | Average | 215693 |
| | 421951 | 218724 | Standard Dev. | 726 | Std. Dev. | 1551 |
| | 422748 | 215636 | Square root | 650 | Square root | 464 |
| | 421769 | 214287 | | | | |
| | 422962 | 216905 | | | | |
| 5.0 cm | 253828 | 176889 | | | | |
| | 253825 | 174382 | | | | |
| | 253610 | 175343 | average | 253945 | average | 175679 |
| | 253592 | 175540 | std | 284 | std | 885 |
| | 254257 | 174949 | square root | 504 | square root | 419 |
| | 254178 | 175677 | | | | |
| | 254328 | 176973 | | | | |
| 7.5 cm | 153991 | 142146 | | | | |
| | 152582 | 141825 | | | | |
| | 153482 | 141351 | average | 153264 | average | 142260 |
| | 153650 | 140603 | std | 484 | std | 1139 |
| | 153393 | 144475 | square root | 391 | square root | 377 |
| | 153129 | 142727 | | | | |
| | 152618 | 142691 | | | | |
| 10.0 cm | 93437 | 116292 | | | | |
| | 94467 | 115674 | | | | |
| | 93861 | 114680 | average | 93862 | average | 115584 |
| | 93774 | 116150 | std | 382 | std | 692 |
| | 93286 | 116223 | square root | 306 | square root | 340 |
| | 94001 | 114444 | | | | |
| | 94206 | 115627 | | | | |
| 12.5 cm | 57010 | 93060 | | | | |
| | 57826 | 94342 | | | | |
| | 57807 | 95165 | average | 57414 | average | 93801 |
| | 57471 | 94940 | std | 363 | std | 1031 |
| | 57082 | 93348 | square root | 240 | square root | 306 |
| | 56956 | 92001 | | | | |

The count rate was measured through the standard absorber for five different times for both Americium (Am) and Cesium (Cs). For every length of time, seven measurements were done. The measurements are averaged and the standard deviation was calculated. The standard deviation was in the same order of magnitude as the square root of the average.

### 1.3.5 Detector Sensitivity

Detector sensitivity is defined as the amplification factor of an incoming signal (one detected gamma ray) to the output signal sent to the computer. Change in sensitivity means that the same amount of detected gamma rays does not necessarily yield the same output voltage. Observed count rates thus may change even if there is no change in actual count rate. The detector sensitivity depends on the temperature of the detector crystal, which in turn depends on room temperature and detector history (i.e. previous radiation on the detector, total run time of the detector) which cannot necessarily be quantified. It is therefore assumed that the detector adds another random element to the fluctuations in the count rate measurements. Count rates through a number of absorbers were measured on different days in order to evaluate fluctuations of the intensity measurements due to the source plus the detector variations. All measurements were conducted with the same standard absorber. Measurements through the absorber were taken on randomly selected days and times to find the maximum variability in the count rate. The standard deviation for these measurements was about one order of magnitude larger than the square root of the count rate (Tables 8a and 8b). If the whole measurement can be conducted within a short time period, problems due to changing detector sensitivity are minimized. Longer measurements would be influenced by changing detector sensitivity. For long measurements, the count rate through a standard absorber has to be taken before and after the measurement, and any changes have to be accounted for in the calculation of the absorbance. For short measurements where the incident radiation cannot be measured before the measurement (e.g., the column through which the incident radiation is measured, is already filled with sand and water), the incident radiation through a standard absorber is measured before every sample exposure. By knowing the change in count rates through the standard absorber, the incident count rate can be corrected.

Table 8a. Count statistics for Americium

| Absorber Thickness (Sand) | Am day 1 | Am day 2 | Am day 3 | Average | Std. Dev. | Square root |
|---|---|---|---|---|---|---|
| 2.5 cm | 646849 | 627394 | 636045 | 636763 | 7959 | 798 |
| 5.0 cm | 399178 | 393543 | 395933 | 396218 | 2309 | 629 |
| 7.5 cm | 245226 | 242473 | 245629 | 244443 | 1402 | 494 |
| 10.0 cm | 150340 | 148680 | 149441 | 149487 | 678 | 387 |
| 12.5 cm | 90161 | 81765 | 79555 | 83827 | 4569 | 290 |

Table 8b. Count statistics for Cesium

| Absorber Thickness (Sand) | Cs day 1 | Cs day 2 | Cs day 3 | Average | Std. Dev. | Square Root |
|---|---|---|---|---|---|---|
| 2.5 cm | 222672 | 232268 | 221602 | 225514 | 4796 | 475 |
| 5.0 cm | 194077 | 195370 | 188036 | 192494 | 3196 | 439 |
| 7.5 cm | 155698 | 162304 | 157686 | 158563 | 2767 | 398 |
| 10.0 cm | 129029 | 133198 | 128501 | 130243 | 2101 | 361 |
| 12.5 cm | 107162 | 108229 | 106172 | 107188 | 840 | 327 |

The count rate through different absorber for 60 seconds repeated on 3 different days for Americium and Cesium. The count rates are averaged over the 3 days and the standard deviation was calculated. The standard deviation was about one order of magnitude larger than the square root of the average.

### 1.3.6 Determination of the Attenuation Coefficients

The lumped attenuation coefficients, $U$, for different materials were determined using the following procedure. First the total counts, $I_0$, were recorded through the empty multi-chambered plexiglass box (Figure 75). Attenuation due to the box is thus included in the initial count. The five compartments of the box were then sequentially filled with the test material (sand, water or oil). The effective path length through the material traversed by the gamma radiation can thus be precisely determined by adding the widths of the compartments filled with the test material. From Equation (30) it can be seen that plotting the natural logarithm of the ratio ($I_0/I$) against path length results in a straight line. A linear regression is performed, and the resulting slope of the line is equal to the lumped attenuation coefficient of the test material. Potential error due to the random nature of gamma emission was reduced by averaging seven separate scans at each of five measured path lengths.

The measurement of the attenuation coefficient for water was repeated four times. The lumped attenuation coefficients, the standard deviation of the regression, and the standard deviation between the four measurements are given in Table 9. The mean value of $U$ for water was 0.195 $cm^{-1}$ for Americium and 0.076 $cm^{-1}$ for Cesium. The total standard deviation of $U$ for four measurements was 0.0024 $cm^{-1}$ for Americium and 0.0034 $cm^{-1}$ for Cesium. The graphed results of one lumped attenuation coefficient determination can be seen in Figure 79.

As also can be seen in Table 9, the standard deviation for a single determination of the U for water (from each seven measurements for five different path lengths) is smaller than the standard deviation between the four measurements conducted on different days. Changing detector sensitivity as described above might cause the larger variability between separate measurements. Also, changes in detector-sample-source configuration may lead to different results of the measurement. The distance of the sample to the source influences the absorption, even if the distance between source and detector is constant. It is therefore important that the

geometrical configuration of the system stays exactly the same between different measurements.

Table 9. Lumped attenuation coefficient of water

| Am | | Cs | |
|---|---|---|---|
| *U*(water) | standard deviation of the regression | *U*(water) | standard deviation of the regression |
| 0.194 | 3.690e-04 | 0.077 | 3.080e-04 |
| 0.191 | 8.550e-04 | 0.074 | 4.140e-04 |
| 0.195 | 1.220e-03 | 0.071 | 3.900e-03 |
| 0.198 | 4.800e-04 | 0.081 | 3.000e-04 |
| | | | |
| total standard deviation: | | total standard deviation: | |
| 0.0024 | | 0.0034 | |

The lumped attenuation coefficient was determined four times. The results and the standard deviation for each determination are listed. An overall standard deviation of the four experiments was calculated. The graphs below (Figure 79) show the data for one determination of the lumped attenuation coefficient for Americium and Cesium.

### 1.3.7 Dependence of Apparent Attenuation Coefficient on Beam Strength

Attenuation coefficients are material constants, which do not change. It was observed, however, that the measured or apparent, attenuation coefficients seemed to change for different measurements. This does not mean that the attenuation coefficient actually changes, but the poor measurement techniques lead to apparent changes. Variable detector sensitivity, poor collimation and poor spectral windowing can cause a change in apparent attenuation coefficients. Thus further experiments were conducted to investigate the stability of the measured attenuation coefficients.

A test was conducted to determine whether the apparent attenuation coefficient of water is dependent on the radiation strength. The radiation strength was changed by placing different absorbers in front of the radiation source. For Cesium, it was found that the attenuation coefficient was too low for either very high or very low incident radiation. For a small band of incident radiation, the attenuation coefficient was almost constant (Figure 79). However, the attenuation coefficient seems to decrease slightly when the incident radiation increases. For Americium, the attenuation coefficient is a function of the incident radiation (Figure 80). The attenuation coefficient was graphed versus the 30 second count rate. The dependence of the attenuation coefficient on count rate shows that the attenuation coefficients are not constant. The count rate is a measure of radiation strength. The radiation strength is a function of the radiation source, the shielding of the source, the attenuation of the sample container and the distance between source and sample, and sample and detector. It is important to note that the source-sample-detector geometry and the material and geometry of the sample container may influence the attenuation coefficients.

Improvements in collimation and spectral windowing were completed after these experiments. Source and detector were realigned and the integration software was rewritten to improve spectral windowing. However, the effects of these improvements on the stability of the attenuation constants was not tested. It is still good policy to assume changes in apparent attenuation coefficients may occur. If the system allows for it, the measurement of the attenuation coefficient should be conducted in the same sample container as the actual saturation measurements, thus the same apparent attenuation coefficient would be used throughout all measurements. This procedure was followed in all experiments.

### 1.3.8 Attenuation Coefficient of Test Fluid (Soltrol)

The attenuation coefficient of Soltrol was found to be close to the attenuation coefficient of water (Oak and Ehrlich, 1985). A different attenuation coefficient between the two fluids (water and oil) is required to determine the saturation of two fluids in a three-phase system (sand, water and oil). Therefore, Soltrol was mixed with iodoheptane, where the latter has a larger attenuation (Oak and Ehrlich, 1985) coefficient and is easily soluble in Soltrol. Following the work of Lenhard and Parker (1987), a ratio of 1:9 by volume of 1-iodoheptane to the mineral oil Soltrol 220 was used. The lumped attenuation coefficient for the doped Soltrol was found to be 0.632 $cm^{-1}$ for Americium and 0.056 $cm^{-1}$ for Cesium (Figure 81). The standard deviation of the regression was 0.00698 $cm^{-1}$ for Americium and 0.000691 $cm^{-1}$ for Cesium.

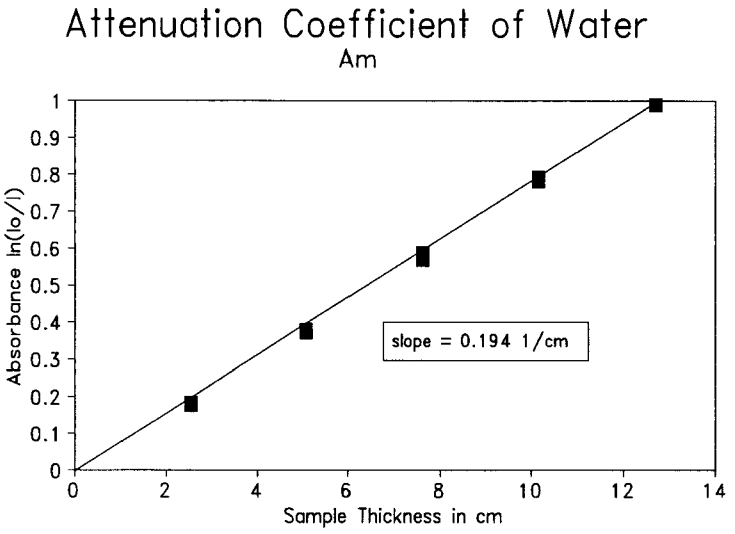


Figure 79. Attenuation coefficient of water (Am).

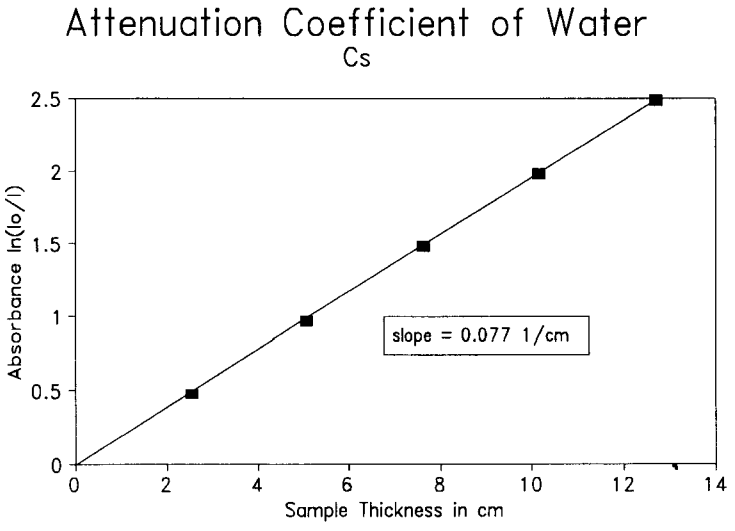


Figure 80. Attenuation coefficient of water (Cs).

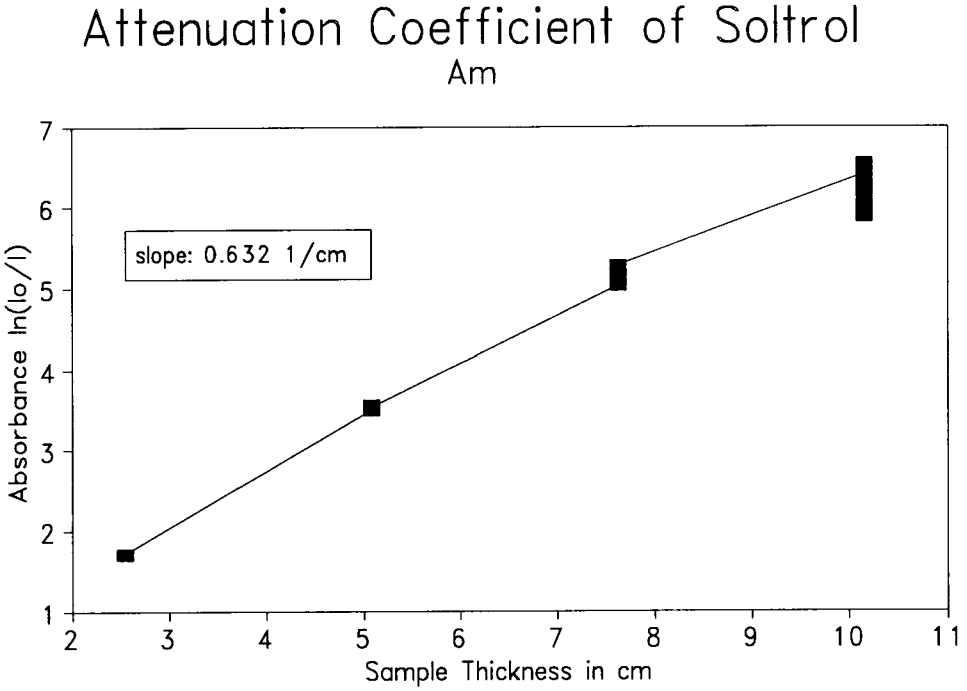


Figure 81. Attenuation coefficient of Soltrol and iodoheptane mixture (Am).

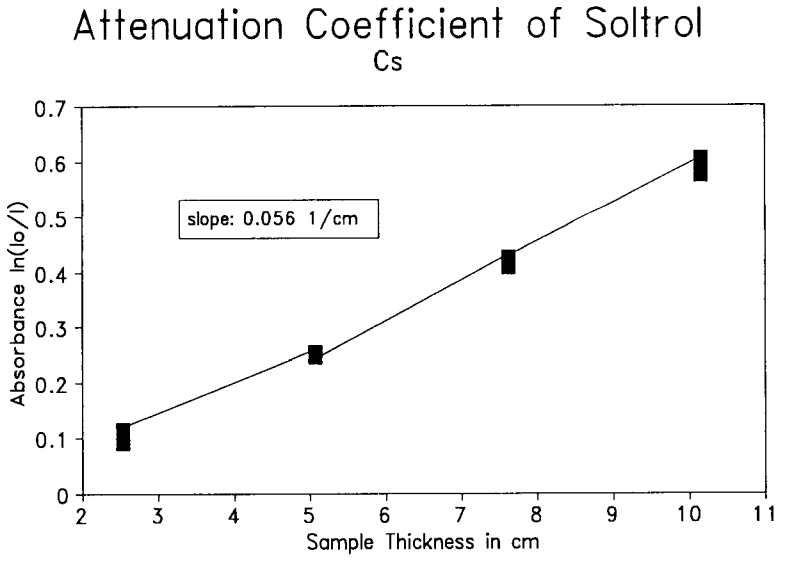


Figure 82. Attenuation coefficient of Soltrol and iodoheptane mixture (Cs).

### 1.3.9 Attenuation Coefficient of Sand

The lumped attenuation coefficient of sand depends on the bulk density which is related to porosity. The attenuation coefficient for one sand grain is a constant, but the void space between the grains differs depending on the packing of the sand. Thus, the lumped attenuation coefficient of the sandy material changes. It is not possible to measure the attenuation coefficient of one sand grain or to pack the sand in a way that no void spaces exist. However, by measuring the lumped attenuation coefficients for a known bulk density, a relation between attenuation coefficient and bulk density can be found; and the attenuation coefficient for sand independent of bulk density can be calculated. The following steps were taken to determine the relationship between bulk density and attenuation coefficient for sand. The sand was first weighed and loosely filled into the plexiglass compartment box. The volume of the sand was determined using measurements of the compartment size. From the sample weight and volume, the bulk density was determined. From the known mineral density, the porosity was calculated. Then the attenuation coefficient was determined with the gamma system. The procedure was repeated with different degrees of sand compaction, obtained by shaking the container a few times. The attenuation coefficient was determined for four values of bulk density. For graphing the results, it was assumed that for zero bulk density the attenuation coefficient is zero, since the absorbance of air is negligible (Figure 83). Using the four measured points and the point in the origin for a linear regression, the following relationships between bulk density, $\rho_B$, and lumped attenuation coefficient, $U$, were found:

$U = 0.236\ cm^3g^{-1}cm^{-1}\ \rho_B$ for Americium, with a standard error of the coefficient = 0.0015,

$U = 0.063\ cm^3g^{-1}cm^{-1}\ \rho_B$ for Cesium, with a standard error of the coefficient = 0.0006.

The lumped attenuation coefficients for sand without void spaces with a mineral density of 2.65 are then:

$U = 0.625\ cm^{-1}$ for Americium,

$U = 0.167\ cm^{-1}$ for Cesium.

### 1.3.10 Phase Saturation of Multi-Phase Systems

The multi-chambered plexiglass box was used to produce two-phase and three-phase mixtures of known phase content. Filling three compartments of the box with sand and one compartment with fluid gives a theoretical volumetric phase content of 33%; filling two compartments with fluid gives a volumetric phase content of 67% (Tables 10 through 12).

Every experiment included four different measurements: one measurement through the empty box ($I_0$), one through the box when three compartments are filled with sand ($I_{dry}$), and two measurements with three compartments filled with sand and one or two compartments filled with water ($I_1$ Water and $I_2$ Water, respectively). The volumetric phase content of the liquid phase was calculated in three ways: first, the volumetric phase content was calculated with the incident radiation through the dry sand (Equation (30)); second, with the incident radiation through the empty box (Equation (31)). Equation (29) assumes that the bulk density of the sand is constant

and included in the lumped attenuation coefficient. These calculations can be done for Cesium and Americium separately. However, since the bulk density of sand for this experiment was not previously determined, only an average value for the attenuation coefficient of the sand could be used. The third method of calculation used the Americium and Cesium counts simultaneously to calculate the phase content independent of the bulk density (Equation (42)).

Calculations with the incident radiation measured through sand produced the best results. It is important to note that measurements with Americium seem more reliable than measurements with Cesium. The attenuation of Cesium is very weak; the results from the Cesium spectrum are therefore more susceptible to small fluctuations. This can also be seen in the results where Cesium and Americium counts were used simultaneously for the calculations because the calculated phase contents are not as close to the theoretical values as those results calculated only from the Americium source. The calculations with the incident radiation through the empty box showed the largest deviation from the true value.

It seems ideal to measure the incident radiation through the dry sand and rely on the calculation of the phase content with the Americium data. However, this assumes bulk density is constant. Changes in bulk density when saturating the sand will cause some error. If large changes in bulk density occur, calculations of the phase content have to be done with Americium and Cesium spectra simultaneously. Then bulk density and phase content can be calculated independently of each other. No error from a change in bulk density will then affect the calculations, however, a larger error resulting from the Cesium spectrum has to be considered.

Three-phase mixtures do not allow for the measurement of the bulk density. The bulk density should be determined gravimetrically before the system is saturated. It has to be assumed that the bulk density does not change after saturation. A better assumption is that the bulk density does not change when an organic phase is introduced after the sand has already been saturated with water. In three-phase systems, the bulk density should be determined when the matrix is fully saturated.

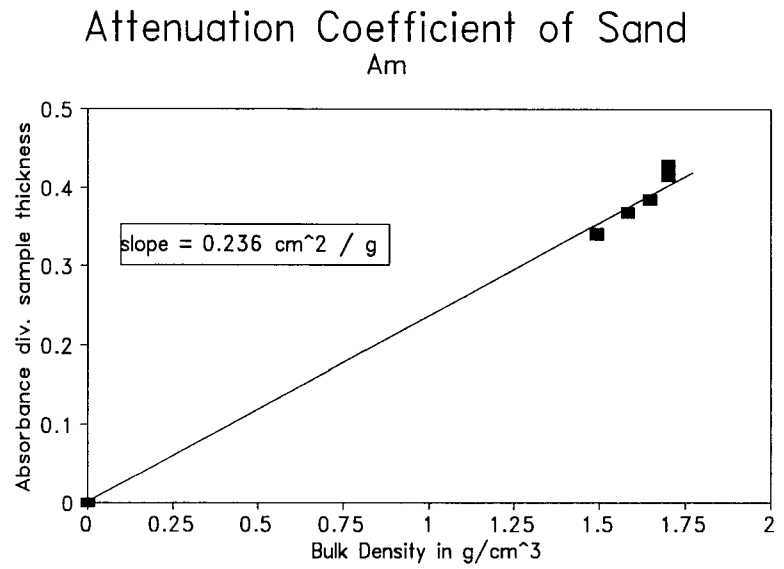


Figure 83. Attenuation coefficient versus bulk density for #125 sand (Am).

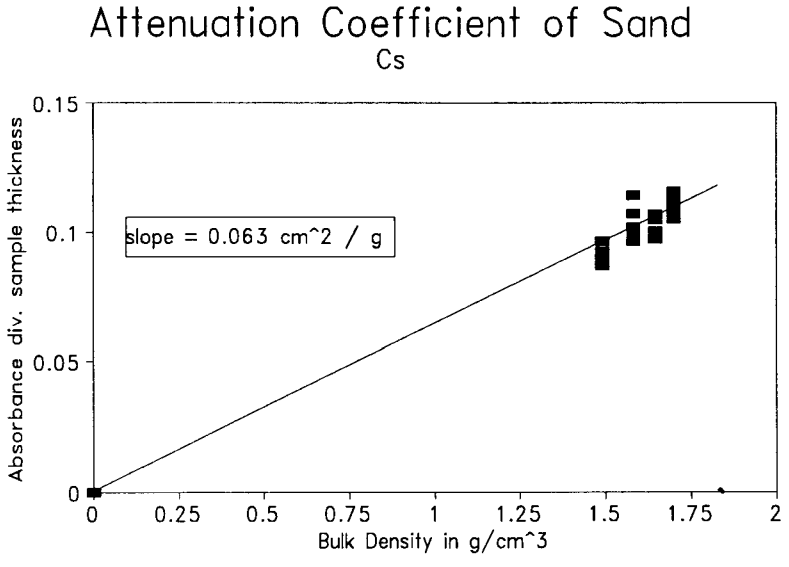


Figure 84. Attenuation coefficient versus bulk density for sand #125 (Cs).

Table 10. Volumetric water content in sand-water mixture

| Three compartments filled with sand, one or two filled with water | | | | | | | | | |
|---|---|---|---|---|---|---|---|---|---|
| Am | | | | | | | | | |
| $U$(water) = 0.197655 | | | | calc. with $I_{dry}$ | | calc. with $I_0$ | | calc. with Equation 37(42) | |
| $I_{dry}$ sand (1) | $I$ 1 comp. water (2) | $I$ 2 comp. water (3) | $I_0$ (4) | wa cont1 (5) | wa cont2 (6) | wa cont1 (7) | wa cont2 (8) | wa cont1 (9) | wa cont2 (10) |
| 45658 | 27709 | 16326 | 696423 | 0.332 | 0.683 | 0.286 | 0.637 | 0.161 | 0.445 |
| 46100 | 27348 | 16705 | 697342 | 0.347 | 0.674 | 0.295 | 0.623 | 0.101 | 0.635 |
| 45308 | 27287 | 17119 | 700459 | 0.337 | 0.646 | 0.300 | 0.609 | 0.188 | 0.661 |
| 45992 | 27562 | 16679 | 697945 | 0.340 | 0.673 | 0.291 | 0.624 | 0.185 | 0.720 |
| 46096 | 27415 | 16884 | 699347 | 0.345 | 0.667 | 0.296 | 0.617 | 0.160 | 0.411 |
| 45572 | 28352 | 16991 | 698219 | 0.315 | 0.655 | 0.272 | 0.612 | 0.251 | 0.576 |
| 45050 | 27856 | 16790 | 698018 | 0.319 | 0.655 | 0.284 | 0.620 | 0.240 | 0.501 |
| | | | avg | 0.333 | 0.665 | 0.289 | 0.620 | 0.161 | 0.493 |
| | | | std | 0.011 | 0.012 | 0.009 | 0.008 | 0.080 | 0.226 |
| Theoret. Water Content | | | | 0.333 | 0.667 | 0.333 | 0.667 | 0.333 | 0.667 |
| Theoret. Error% | | | | -0.04 | 0.278 | 13.31 | 6.955 | 51.73 | 26.1 |

| Cs | | | | | | | |
|---|---|---|---|---|---|---|---|
| $U$(water) = 0.08065 | | | | | | | |
| $I_{dry}$ | $I$1 water | $I$2 water | $I_0$ | wa cont1 | wa cont2 | wa cont1 | wa cont2 |
| 99474 | 81542 | 67097 | 197228 | 0.323 | 0.641 | 0.060 | 0.377 |
| 95478 | 81080 | 65925 | 199638 | 0.266 | 0.603 | 0.089 | 0.425 |
| 101295 | 82495 | 66073 | 202258 | 0.334 | 0.695 | 0.082 | 0.443 |
| 98706 | 81498 | 64582 | 199303 | 0.312 | 0.690 | 0.078 | 0.456 |
| 99865 | 81278 | 68830 | 200227 | 0.335 | 0.606 | 0.090 | 0.360 |
| 98483 | 80308 | 65946 | 198368 | 0.332 | 0.653 | 0.094 | 0.415 |
| | | | avg | 0.317 | 0.648 | 0.082 | 0.413 |
| | | | std | 0.024 | 0.036 | 0.011 | 0.034 |
| theoret. wa cont | | | | 0.333 | 0.667 | 0.333 | 0.667 |
| theoret. error | | | | 4.885 | 2.822 | 75.42 | 38.09 |

The test box was used to determine the volumetric water content in a defined sand-water mixture. The first four columns give the measured count rates through the box for three compartments filled with sand, three compartments filled with sand plus one compartment filled with water, three compartments filled with sand plus two compartments filled with water, and through the empty box, respectively. The fifth and sixth columns give the water content as calculated from Equation (30) with the initial count rate through the dry sand for one and two

compartments filled with water, respectively. The seventh and eighth columns give the water content, as calculated from Equation (31), with the initial count rate through the empty box. The last two columns (9 and 10) give the water content as calculated following Equation (42). The average and the standard deviation were calculated for the seven measurements. The average was compared with the theoretical water content and a theoretical error was calculated. The suite of calculations was performed for both Cesium and Americium.

Table 11a. Volumetric content of organic phase in sand

| Three compartments filled with sand, one or two filled with Soltrol | | | | | | | |
|---|---|---|---|---|---|---|---|
| Am | | | | calc with $I_{dry}$ | | calc with $I_0$ | |
| $I_{dry}$ (1) | $I_1$ Soltrol (2) | $I_2$ Soltrol (3) | $I_0$ (4) | So cont1 (5) | So cont2 (6) | So cont1 (7) | So cont2 (8) |
| 42372 | 6968 | 1125 | 711148 | 0.328 | 0.660 | 0.333 | 0.665 |
| 41197 | 7424 | 1631 | 714854 | 0.312 | 0.588 | 0.323 | 0.599 |
| 41608 | 7251 | 1401 | 715648 | 0.318 | 0.617 | 0.327 | 0.626 |
| 41250 | 6618 | 980 | 718232 | 0.333 | 0.681 | 0.344 | 0.692 |
| 41417 | 7286 | 1789 | 717223 | 0.316 | 0.572 | 0.327 | 0.582 |
| 41493 | 7206 | 1454 | 717690 | 0.319 | 0.610 | 0.329 | 0.620 |
| 40796 | 7281 | 1840 | 718012 | 0.314 | 0.564 | 0.327 | 0.577 |
| | | | avg | 0.320 | 0.613 | 0.330 | 0.623 |
| | | | std | 0.007 | 0.041 | 0.007 | 0.039 |
| | | | theoretical water cont | 0.333 | 0.667 | 0.333 | 0.667 |
| | | | theoretical error % | 4.015 | 8.047 | 0.983 | 6.531 |
| Cs | | | | calc with $I_{dry}$ | | calc with $I_0$ | |
| $I_{dry}$ (1) | $I_1$ Soltrol (2) | $I_2$ Soltrol (3) | $I_0$ (4) | So cont1 (5) | So cont2 (6) | So cont1 (7) | So cont2 (8) |
| 110399 | 89681 | 77091 | 244441 | 0.439 | 0.758 | 0.330 | 0.649 |
| 110187 | 91878 | 75849 | 247998 | 0.384 | 0.789 | 0.309 | 0.714 |
| 111275 | 91009 | 75121 | 252515 | 0.425 | 0.830 | 0.367 | 0.773 |
| 109966 | 90099 | 74006 | 246966 | 0.421 | 0.836 | 0.342 | 0.757 |
| 108925 | 91661 | 74816 | 248440 | 0.364 | 0.793 | 0.318 | 0.747 |
| 109528 | 89834 | 76908 | 248353 | 0.419 | 0.747 | 0.360 | 0.688 |
| 109500 | 90577 | 75271 | 242186 | 0.401 | 0.792 | 0.289 | 0.680 |
| | | | avg | 0.407 | 0.792 | 0.331 | 0.715 |
| | | | std | 0.024 | 0.031 | 0.026 | 0.042 |
| | | | theoretical water content | 0.333 | 0.667 | 0.333 | 0.667 |
| | | | theoretical error % | -22.218 | -18.814 | 0.765 | -7.322 |

The test box was used to determine the volumetric Soltrol content in a defined sand-Soltrol mixture. The first four columns give the measured count rates through the box for three compartments filled with sand, three compartments filled with sand plus one compartment filled with Soltrol, three compartments filled with sand plus two compartments filled with Soltrol and through the empty box respectively. The fifth and sixth columns give the Soltrol content as calculated from Equation (30), with the initial count rate through the dry sand for one and two compartments filled with Soltrol, respectively. The seventh and eighth give the Soltrol content, as calculated from Equation (31), with the initial count rate through the empty box. The average and the standard deviation were calculated for the seven measurements. The average was compared to the theoretical Soltrol content, and a theoretical error was calculated. The suite of calculations was performed for both Cesium and Americium.

Table 11b. Volumetric content of the organic phase calculated with Equation (42)

| Calculated with *l*-values from Table 5a. | So cont1 | So cont2 |
|---|---|---|
| | 0.271 | 0.661 |
| | 0.264 | 0.512 |
| | 0.24 | 0.528 |
| | 0.283 | 0.648 |
| | 0.266 | 0.467 |
| | 0.247 | 0.564 |
| | 0.283 | 0.494 |
| average | 0.265 | 0.554 |
| standard deviation | 0.015 | 0.07 |
| theoretical volume content | 0.333 | 0.666 |
| theoretical error % | 20.5 | 16.9 |

Table 12. Volumetric content of water and organic phase in sand-water-organic mixture

| Three compartments filled with sand, one filled with Soltrol and one with water. | | | | | |
|---|---|---|---|---|---|
| Am | | Cs | | water content | oil content |
| $I_{dry}$ | /1wa+1so | $I_{dry}$ | /1wa+1so | with $I_{dry}$ | with $I_{dry}$ |
| 37639 | 4359 | 105418 | 71739 | 0.349 | 0.280 |
| 38261 | 3917 | 105630 | 71722 | 0.333 | 0.307 |
| 37240 | 4282 | 106489 | 71927 | 0.361 | 0.277 |
| 37752 | 4303 | 105915 | 70418 | 0.388 | 0.270 |
| 37914 | 4260 | 105602 | 70463 | 0.379 | 0.276 |
| 36665 | 3970 | 105874 | 70816 | 0.369 | 0.285 |
| 37579 | 4179 | 105821 | 72186 | 0.338 | 0.290 |
| | | average | | 0.360 | 0.284 |
| | | std | | 0.019 | 0.011 |
| | | std % | | 5.366 | 3.982 |
| | | | theoretical phase content | 0.333 | 0.333 |
| | | | theoretical error | -7.892 | 14.910 |
| Denominator k = 0.046 | | | | | |

The volumetric content of water and organic phase were determined simultaneously. The first two columns give the count rate for Americium through the dry sand and through the sand-water-oil mixture, respectively. The third and forth columns give the count rates for Cesium. The fifth and sixth columns give the volumetric phase content for water and oil, calculated with Equations (37) and (38), respectively. The average and the standard deviation of seven measurements were calculated and compared to the theoretical phase content. It can be seen that calculations of two phases simultaneously may lead to error up to 15%.

## 1.4 ANALYSIS OF TEST RESULTS

The results showed that a number of rules have to be followed in order to obtain accurate results with the gamma system. It has been shown that random decay of the radioactive source leads to a randomness in the count rate. The standard deviation of the count rate is equal to the square root of the count rate. Thus, the count rate has to be sufficiently large to avoid a large percentage error. The count rate can be increased by increasing source strength or by increasing counting time. Increase in the source strength may lead to detector fatigue and should be avoided. The counting time can be increased only if the variable to be measured within the sample does not change rapidly and long measurement times are acceptable. A compromise between source strength and measurement time has to be found. In this research, measurements in spill and rainfall experiments needed to be conducted in short time intervals. A measurement time of 20 seconds was chosen for all of the spill experiments. The absorption of the column was small; thus, without using any absorbers, the observed dead time was above the threshold which was found to lead to detector fatigue (10% dead time). An aluminum (1.5

cm thickness) absorber was placed in front of the source to decrease the radiation.

Detector sensitivity was defined as the amplification factor of an incoming signal (one detected gamma ray) to the output signal sent to the computer. The detector sensitivity was shown to have a large influence on the measurements. Temperature changes the amplification gain of the photo multipliers inside the detector (Cathey, 1958). A constant temperature is necessary to achieve good measurements. However, the detector temperature depends not only on the environment temperature, but also on the time the detector has already been subjected to radiation and possibly even the amount of radiation.

As has been shown during the calibration experiments, the detector sensitivity did not change within "short" time periods; thus all measurements performed later were conducted within the same day, if possible. Every experimental measurement was preceded by a measurement through a standard absorber (which could be an aluminum block or the top part of the empty column). The count rate was then corrected according to the change in the count rate through the standard. A 5% change in the count rate through the standard meant that the count rate in the experiment was accordingly adjusted with a 5% increase (or decrease). Also, no measurements were performed earlier than one hour after the equipment had been turned on to insure maximum detector stability.

It was also seen that the attenuation coefficient is dependent on radiation strength. In the physical sense, the attenuation coefficient depends only on the material and the wave length, not on the radiation strength. The observed dependence on radiation strength results from the changing detector sensitivity. Radiation strength as seen by the detector depends not only on the actual strength of the source, but on the absorbance of absorbers, sample and sample holder. It is important to note that absorbance might also depend on the location of the sample between source and detector. A consistent source-sample-detector configuration was maintained during all experiments. Ideally the attenuation coefficients are measured in the same setting as the actual experiments are performed. This was done for all the column and tank experiments to insure the greatest accuracy for the measurements.

In general the results obtained from measurements with the Cesium source are not as reliable as results measured with Americium. The high energy radiation emitted by the Cesium source is subject to very small absorption. Thus, the change between incident radiation (dry sand) and sample radiation (saturated sand) is very little. Hence a change in count rate due to changing detector sensitivity may have a large effect. Ideally, the Cesium source would be replaced with another radioactive source emitting a lower energy gamma radiation. However sources with a lower energy and a long half-life are not generally used in industry or research and are extremely expensive. Most gamma systems are therefore equipped with an Americium and a Cesium source. A lower accuracy for the Cesium measurements has to be accepted. It was thus decided for the spill experiments to calculate the bulk density gravimetrically and use the Americium counts for calculations of phase content for single-phase systems. Cesium counts were only used for measurements involving two-phase systems (spill experiments with rainfall). Spill experiments in immobile, residually water saturated columns can be treated as single-phase experiments, if the residual saturated column is measured and this measurement is used as the incident radiation, which is assumed to be constant. In all experiments the results were calculated with Americium and Cesium; however, when not stated otherwise the results presented

here show only data collected with Americium. The Cesium results confirmed the Americium results in most cases qualitatively, in some cases exactly. In cases where both scans presented quantitatively good results, the calculation for the spills was performed as for a two-phase system. The incident radiation was taken through the dry sand, and water and oil phases were calculated separately.

# APPENDIX 2 EXPERIMENTAL FRONT MOVEMENT DATA

SPILL H #125 SAND 500 ML SOLTROL SPILL
VISUALLY OBSERVED FRONT MOVEMENT

| TIME | ELEVATION | PONDING DEPTH | BACK FRONT |
|---|---|---|---|
| MINUTES | CM | CM | CM |
| 0 | 120 | 9.5 | |
| 1 | 116 | | |
| 2 | 115 | | |
| 3 | 113 | | |
| 4 | 112 | 7 | |
| 5 | 111 | 7.5 | |
| 6 | 110 | | |
| 8 | 109 | 6 | |
| 10 | 108 | 5 | |
| 12 | 106 | | |
| 14 | 105 | | |
| 16 | 104 | 4 | |
| 18 | 103 | | |
| 21 | 101 | 3 | |
| 24 | 100 | | |
| 27 | 99 | | |
| 31 | 97 | 2 | |
| 35 | 95 | | |
| 38 | 94 | 1 | |
| 40 | 93 | | |
| 43 | 92 | 0 | |
| 44 | 91.5 | | 118.5 |
| 47 | 91 | | |
| 50 | 90 | | 118 |
| 55 | 88 | | |
| 60 | 87 | | 117.5 |
| 65 | 86 | | |
| 70 | 85 | | 117 |
| 80 | 84 | | |
| 90 | 82 | | 114 |
| 100 | 81 | | 111 |
| 110 | 80 | | 110 |
| 120 | 79 | | 108 |
| 135 | 77 | | 106 |
| 150 | 75 | | 103 |
| 220 | 68 | | 101 |
| 240 | 64 | | 100 |
| 270 | 62 | | 98 |
| 300 | 60 | | |
| 335 | 57 | | 97 |
| 900 | 21 | | |

SPILL O #125 SAND 500 ML SOLTROL SPILL
RAIN 500ML/HR AFTER 45 MINUTES

| TIME MINUTES | ELEVATION CM | PONDING DEPTH CM |
|---|---|---|
| 0 | 120 | 9.5 |
| 2 | 115 | 7 |
| 3 | 114 | 6.8 |
| 4 | 112.5 | 6.2 |
| 5 | 111.3 | 5.8 |
| 6 | 110.5 | 5.5 |
| 7 | 110 | 5.3 |
| 8 | 109.4 | 4.9 |
| 9 | 108.7 | 4.6 |
| 10 | 108 | 4.5 |
| 13 | 106.3 | 3.9 |
| 15 | 105 | 3.5 |
| 20 | 102 | 2.5 |
| 27 | 99 | 1.3 |
| 30 | 98 | 1 |
| 35 | 95.5 | 0.2 |
| 36 | 95 | 0 |
| 40 | 94.3 | |
| 45 | 93.5 | |
| 50 | 92.5 | |
| 53 | 90.7 | |
| 55 | 89.5 | |
| 58 | 88 | |
| 60 | 87 | |
| 65 | 84.5 | |
| 70 | 82 | |
| 80 | 77.5 | |
| 85 | 75 | |
| 90 | 72.5 | |
| 95 | 69.5 | |
| 100 | 67 | |
| 105 | 65 | |
| 110 | 63 | |
| 115 | 60 | |
| 120 | 57.5 | |
| 125 | 56 | |
| 132 | 52 | |
| 135 | 50 | |
| 140 | 47 | |
| 145 | 43 | |
| 150 | 41 | |
| 155 | 39 | |
| 160 | 35 | |
| 165 | 32 | |
| 170 | 29 | |

SPILL P #125 SAND 750 ML SOLTROL SPILL
RAIN 500 ML/HR AFTER 22 HOURS

| TIME | ELEVATION | PONDING DEPTH |
|---|---|---|
| MINUTES | CM | CM |
| 0 | 120 | 14.2 |
| 1 | 116.5 | 13 |
| 2 | 114 | 12.5 |
| 3 | 113 | 11.5 |
| 4 | 112.3 | 11.1 |
| 5 | 111.5 | 10.8 |
| 6 | 110.8 | 10.6 |
| 7 | 110 | 10.3 |
| 8 | 109 | 10 |
| 9 | 108.2 | 9.8 |
| 10 | 108 | 9.5 |
| 12 | 106 | 9 |
| 14 | 104.7 | 8.6 |
| 16 | 103.5 | 8.2 |
| 18 | 102 | 7.9 |
| 20 | 101 | 7 |
| 25 | 99 | 6.3 |
| 30 | 96 | 5.5 |
| 35 | 94 | 4.9 |
| 40 | 91.5 | 3.6 |
| 45 | 89.5 | 3 |
| 50 | 88 | 2.3 |
| 55 | 86 | 1.7 |
| 60 | 83.5 | 1 |
| 65 | 82 | 0 |
| 70 | 80 | |
| 75 | 79 | |
| 80 | 77.5 | |
| 90 | 75 | |
| 100 | 73.5 | |
| 110 | 72 | |
| 120 | 70 | |
| 150 | 67 | |
| 220 | 56 | |
| 240 | 53 | |
| 300 | 46 | |

SPILL D #125 SAND 1000 ML SOLTROL SPILL

| TIME | DISTANCE | PONDING DEPTH | BACK FRONT |
|---|---|---|---|
| MINUTES | CM | CM | CM |
| 0 | 120 | 19 | |
| 1 | 117 | | |
| 2.5 | 114.5 | | |
| 4 | 113 | 17.5 | |
| 6 | 111 | | |
| 8 | 109.5 | | |
| 10 | 108 | | |
| 13 | 106 | 14 | |
| 16 | 104 | | |

| TIME | DISTANCE | PONDING DEPTH | BACK FRONT |
|---|---|---|---|
| MINUTES | CM | CM | CM |
| | 21 | 101 | |
| 27 | 98 | 12 | |
| 31 | 97 | | |
| 36 | 95 | | |
| 41 | 93.5 | | |
| 46 | 91.5 | | |
| 51 | 89.5 | 9 | |
| 56 | 87.5 | | |
| 61 | 86.5 | | |
| 71 | 83 | | |
| 81 | 80 | 6 | |
| 91 | 77.5 | | |
| 101 | 75 | | |
| 113 | 72 | 4 | |
| 123 | 69 | | |
| 131 | 67 | | |
| 141 | 64 | 2 | |
| 151 | 62 | | |
| 161 | 59 | 0 | |
| 171 | 56 | | 117 |
| 176 | 55 | | 110 |
| 181 | 54 | | 107 |
| 191 | 52 | | 106 |
| 203 | 50 | | 105 |
| 211 | 49 | | 104 |
| 221 | 47.5 | | 101.5 |
| 236 | 46 | | 97 |
| 248 | 44 | | 91 |
| 261 | 42.5 | | |
| 271 | 41 | | 89 |
| 301 | 38 | | 86 |
| 331 | 34 | | 81 |
| 361 | 31 | | 74 |
| 406 | 29.5 | | 72 |

SPILL I #125 SAND 1000 ML SOLTROL
MANUALLY OBSERVED FRONT MOVEMENT

| TIME | ELEVATION | PONDING DEPTH |
|---|---|---|
| MINUTES | CM | CM |
| 0 | 120 | 19 |
| 1 | 115.5 | |
| 2 | 112.5 | |
| 3 | 111 | |
| 4 | 110 | |
| 5 | 109 | 15 |
| 6 | 108 | 14.5 |
| 7 | 107 | 14 |
| 8 | 106.5 | 13.8 |
| 9 | 106 | 13.6 |
| 10 | 105 | 13.3 |
| 12 | 103 | 12.7 |
| 15 | 101 | 12.3 |
| 17 | 100 | 12 |
| 20 | 98.5 | 11.6 |

| TIME | ELEVATION | PONDING DEPTH |
|---|---|---|
| MINUTES | CM | CM |
| 24 | 96 | 11 |
| 28 | 94 | 10.2 |
| 34 | 91 | 9.4 |
| 41 | 88 | 8.4 |
| 45 | 86 | 8 |
| 50 | 84 | 7.4 |
| 55 | 82.5 | 6.8 |
| 60 | 81 | 6.2 |
| 65 | 79 | 5.7 |
| 70 | 77.5 | 5.1 |
| 80 | 74 | 4.1 |
| 90 | 71 | 3.2 |
| 100 | 68 | 2.3 |
| 110 | 65 | 1.4 |
| 120 | 61.5 | 0.6 |
| 125 | 60.5 | 0 |
| 127 | 59 | |
| 143 | 56 | |
| 150 | 54 | |
| 165 | 52 | |
| 180 | 49 | |
| 300 | 34 | |

SPILL J #70 SAND 500 ML SOLTROL SPILL
VISUALLY OBSERVED FRONT MOVEMENT

| TIME | ELEVATION | PONDING DEPTH | BACK FRONT |
|---|---|---|---|
| MINUTES | CM | CM | CM |
| 0 | 120 | 9.5 | |
| 1 | 115.5 | 7.5 | |
| 2 | 114 | 7 | |
| 3 | 113 | 6.8 | |
| 4 | 112 | 6.3 | |
| 5 | 111 | 6 | |
| 6 | 110 | 5.6 | |
| 7 | 109 | 5.3 | |
| 8 | 108 | 5.2 | |
| 10 | 107 | 4.5 | |
| 12 | 105.5 | 5 | |
| 14 | 104 | 3.5 | |
| 16 | 103 | 3 | |
| 18 | 102 | 2.6 | |
| 20 | 101 | 2.2 | |
| 22 | 100 | 2 | |
| 24 | 99 | 1.5 | |
| 27 | 98 | 1.1 | |
| 30 | 96.5 | 0.6 | |
| 35 | 94.5 | 0 | |
| 40 | 93.5 | | 119 |
| 45 | 92.5 | | 117 |
| 50 | 92 | | 116 |
| 60 | 90 | | 114 |
| 72 | 88 | | 114 |
| 80 | 87 | | |
| 90 | 86 | | 108 |

| TIME | ELEVATION | PONDING DEPTH | BACK FRONT |
|---|---|---|---|
| MINUTES | CM | CM | CM |
| 100 | 85 | | |
| 120 | 83 | | 106 |
| 150 | 80.5 | | |
| 180 | 78 | | |
| 210 | 77 | | |
| 250 | 74.5 | | |
| 381 | 69.5 | | |
| 1020 | 59 | | |
| 1320 | 55.5 | | |

SPILL M #70 SAND 1000 ML SOLTROL SPILL
RAIN 500ML/HR AFTER 167 MINUTES

| TIME | ELEVATION | PONDING | BACK FRONT | WATER DEPTH |
|---|---|---|---|---|
| MINUTES | CM | CM | CM | CM |
| 0 | 120 | 19 | | |
| 1 | 113 | | | |
| 2 | 111 | | | |
| 3 | 108.5 | | | |
| 4 | 107 | 13.2 | | |
| 5 | 105.5 | 12.5 | | |
| 6 | 104 | 12.1 | | |
| 7 | 103 | 11.7 | | |
| 8 | 101.5 | 11.2 | | |
| 9 | 100.5 | 10.8 | | |
| 10 | 99 | 10.4 | | |
| 11 | 98 | 10 | | |
| 12 | 97 | 9.6 | | |
| 13 | 96 | 9.4 | | |
| 14 | 95 | 8.9 | | |
| 15 | 94 | 8.6 | | |
| 16 | 93 | 8.2 | | |
| 17 | 92 | 8 | | |
| 18 | 91.3 | 7.5 | | |
| 19 | 90.5 | 7.3 | | |
| 20 | 89.7 | 7 | | |
| 22 | 88.3 | 6.5 | | |
| 24 | 86.5 | 5.8 | | |
| 26 | 85 | 5.3 | | |
| 28 | 84 | 4.5 | | |
| 30 | 83.2 | 4 | | |
| 32 | 81 | 3.5 | | |
| 34 | 80 | 2.9 | | |
| 36 | 78.2 | 2.5 | | |
| 38 | 77 | 2 | | |
| 40 | 75.7 | 1.5 | | |
| 44 | 73.7 | 0.6 | | |
| 47 | 71.9 | 0 | | |
| 50 | 70.8 | | 119 | |
| 53 | 69 | | 114 | |
| 57 | 67.3 | | | |
| 60 | 66 | | | |
| 65 | 64 | | 108 | |
| 70 | 62 | | | |
| 75 | 60 | | 99 | |
| 80 | 58 | | 87 | |

| TIME MINUTES | ELEVATION PONDING CM | CM | BACK FRONT CM | WATER DEPTH CM |
|---|---|---|---|---|
| 90 | 55 | | | |
| 100 | 52 | | 81 | |
| 110 | 49 | | | |
| 125 | 45 | | | |
| 145 | 41 | | | |
| 167 | 36 | | | 120 |
| 169 | 35.5 | | | 100 |
| 194 | 32 | | | 80.5 |
| 220 | 28 | | | 75 |
| 230 | 120 | | | 66 |
| 240 | 26 | | | 54.5 |
| 255 | 24 | | | 49.5 |
| 265 | 22 | | | 43 |
| 275 | 17 | | | 38.5 |
| 285 | 13 | | | 34 |
| 295 | 9 | | | 26 |
| 308 | 3 | | | |

SPILL N #70 SAND 750 ML SOLTROL SPILL
RAIN 500 ML/HR AFTER 86 MINUTES

| TIME MINUTES | ELEVATION CM | PONDING CM | WATER FRONT CM |
|---|---|---|---|
| 0 | 120 | 14.2 | |
| 1 | 113 | | |
| 2 | 112 | | |
| 3 | 110.5 | 10.6 | |
| 4 | 109 | 10.2 | |
| 5 | 108 | 9.8 | |
| 6 | 106.5 | 9.2 | |
| 7 | 105.5 | 8.4 | |
| 8 | 104.5 | 8.1 | |
| 9 | 103.5 | 7.6 | |
| 10 | 102.3 | 7.2 | |
| 11 | 101.1 | 6.8 | |
| 12 | 100.1 | 6.4 | |
| 13 | 99.2 | 6 | |
| 14 | 98.5 | 5.7 | |
| 15 | 97.5 | 5.4 | |
| 16 | 96.8 | 5.1 | |
| 17 | 96 | 4.8 | |
| 18 | 95.2 | 4.4 | |
| 19 | 94.3 | 4.1 | |
| 20 | 93.5 | 3.7 | |
| 22 | 91.8 | 3.3 | |
| 24 | 90.4 | 2.7 | |
| 26 | 88.9 | 2.2 | |
| 28 | 87.3 | 1.5 | |
| 30 | 85.9 | 1 | |
| 32 | 84.5 | 0 | |
| 34 | 83.7 | | |
| 36 | 83 | | |
| 40 | 81.4 | | |
| 45 | 79.8 | | |
| 50 | 77.9 | | |
| 55 | 76.1 | | |
| 60 | 74.5 | | |
| 65 | 73 | | |
| 70 | 71.4 | | |
| 75 | 70.4 | | |
| 80 | 69 | | |
| 86 | 67.3 | | |
| 90 | 66.5 | | |
| 96 | 65.2 | | |
| 100 | 64.1 | | |
| 105 | 63.2 | | 110 |
| 115 | 61.3 | | 95 |
| 120 | 60.1 | | 90 |
| 125 | 58.3 | | 86 |
| 130 | 58 | | 85 |
| 135 | 56.8 | | 83 |
| 140 | 54.6 | | 81 |
| 145 | 52.8 | | 73 |
| 150 | 50.2 | | 69 |
| 155 | 47.4 | | 65 |
| 160 | 45.3 | | 61 |
| 165 | 43 | | 59 |
| 170 | 40.6 | | 56 |

| TIME | ELEVATION | PONDING DEPTH | WATER FRONT |
|---|---|---|---|
| MINUTES | CM | CM | CM |
| 175 | 37.5 | | 53 |
| 180 | 34.6 | | 47 |
| 185 | 32 | | 43 |
| 190 | 29.5 | | 39 |
| 195 | 26.5 | | 34 |
| 200 | 23.5 | | 31 |
| 205 | 21 | | 28 |
| 210 | 17.5 | | 21 |
| 215 | 15 | | 16 |
| 220 | 12 | | 12 |
| 225 | 9 | | 9 |
| 230 | 6 | | 6 |
| 235 | 4.5 | | 4.5 |
| 240 | 4 | | 4 |
| 245 | 3.5 | | 3.5 |

TANK A
#70 SAND - SOLTROL PONDING DEPTH 9.5 CM
TANK EXPERIMENT
VISUALLY OBSERVED FRONT MOVEMENT

| TIME MINUTES | ELEVATION CM |
|---|---|
| 0 | 120 |
| 2 | 110.7 |
| 3 | 109.8 |
| 4 | 107 |
| 5 | 105.5 |
| 6 | 104 |
| 7 | 103.5 |
| 8 | 102.5 |
| 9 | 101.5 |
| 10 | 100.3 |
| 12 | 99.5 |
| 15 | 98.5 |
| 20 | 95 |
| 25 | 93.5 |
| 30 | 92 |
| 35 | 90 |
| 60 | 85 |
| 90 | 80 |
| 120 | 77 |
| 150 | 74.5 |
| 185 | 72 |
| 220 | 70 |

TANK B
#70 SAND - SOLTROL PONDING DEPTH 9.5 CM
RAIN 12000 ML/H AFTER 22 HOURS
RAIN END AFTER 24 HOURS
RESIDUAL WATER CONTENT ASSUMED CONSTANT AT 0.06.

| TIME MINUTES | ELEVATION CM | PONDING DEPTH CM |
|---|---|---|
| 0 | 120 | 9.5 |
| 1 | 113 | 5.8 |
| 2 | 111 | 4.5 |
| 3 | 109.5 | 4 |
| 4 | 108 | 2.8 |
| 5 | 107 | 2.5 |
| 6 | 105 | 1.9 |
| 7 | 104 | 1.2 |
| 8 | 103.5 | 0.7 |
| 9 | 102 | 0 |
| 15 | 97 | |
| 20 | 96.5 | |
| 30 | 94 | |
| 40 | 92 | |
| 50 | 90 | |
| 60 | 88 | |
| 90 | 84 | |
| 130 | 80 | |
| 180 | 77 | |
| 300 | 72 | |
| 420 | 69 | |
| 1200 | 61 | |
| 1342 | 60 | |
| 1414 | 53.5 | |
| 1450 | 50.5 | |
| 1556 | 48 | |
| 2700 | 43 | |

# APPENDIX 3 EXPERIMENTAL PHASE CONTENT PROFILES

Spill H
#125 Sand 500 ml Soltrol Spill

Gamma Scan Data

Bulk Density grav.: 1.53g $cm^{-3}$
Porosity: 0.42
Temperature Soltrol: 23°C
Residual Water Content: 0.06

| Elevation cm | Time min | Soltrol Content | Time min | Soltrol Content | Time min | Soltrol Content |
|---|---|---|---|---|---|---|
| 120.00 | 3.00 | 0.32 | 9.00 | 0.32 | | |
| 119.00 | 4.00 | 0.31 | 9.00 | 0.32 | 21.00 | 0.34 |
| 118.00 | 4.00 | 0.31 | 10.00 | 0.32 | | |
| 117.00 | 5.00 | 0.30 | 10.00 | 0.30 | 21.00 | 0.33 |
| 116.00 | 5.00 | 0.29 | 11.00 | 0.29 | | |
| 115.00 | 6.00 | 0.31 | 11.00 | 0.31 | 22.00 | 0.33 |
| 114.00 | 6.00 | 0.30 | 12.00 | 0.30 | | |
| 113.00 | 7.00 | 0.30 | 13.00 | 0.31 | 22.00 | 0.33 |
| 112.00 | 8.00 | 0.29 | 13.00 | 0.29 | | |
| 111.00 | | | 14.00 | 0.31 | 23.00 | 0.34 |
| 110.00 | | | 14.00 | 0.30 | | |
| 109.00 | | | 15.00 | 0.29 | 23.00 | 0.32 |
| 108.00 | | | 15.00 | 0.30 | | |
| 107.00 | | | 16.00 | 0.28 | 24.00 | 0.33 |
| 106.00 | | | 16.00 | 0.22 | | |
| 105.00 | | | 17.00 | 0.09 | 24.00 | 0.28 |
| 104.00 | | | 17.00 | 0.01 | | |
| 103.00 | | | 18.00 | -0.01 | 25.00 | 0.26 |
| 102.00 | | | 18.00 | -0.01 | | |
| 101.00 | | | 19.00 | -0.01 | 26.00 | 0.13 |
| 100.00 | | | | | | |
| 99.00 | | | | | 26.00 | 0.00 |
| 98.00 | | | | | | |
| 97.00 | | | | | 27.00 | 0.00 |
| 96.00 | | | | | | |
| 95.00 | | | | | 27.00 | -0.01 |
| 94.00 | | | | | | |
| 93.00 | | | | | 28.00 | -0.01 |
| 92.00 | | | | | | |
| 91.00 | | | | | 28.00 | 0.00 |
| 120.00 | 34.00 | 0.29 | 58.00 | 0.22 | 86.00 | 0.17 |
| 119.00 | 34.00 | 0.29 | 58.00 | 0.24 | 86.00 | 0.18 |
| 118.00 | 35.00 | 0.28 | 59.00 | 0.25 | 87.00 | 0.19 |
| 117.00 | 35.00 | 0.28 | 59.00 | 0.25 | 87.00 | 0.19 |
| 116.00 | 36.00 | 0.27 | 60.00 | 0.25 | 88.00 | 0.19 |
| 115.00 | 37.00 | 0.28 | 60.00 | 0.26 | 88.00 | 0.20 |
| 114.00 | 37.00 | 0.28 | 61.00 | 0.26 | 89.00 | 0.21 |
| 113.00 | 38.00 | 0.28 | 62.00 | 0.27 | 89.00 | 0.22 |
| 112.00 | 38.00 | 0.27 | 62.00 | 0.27 | 90.00 | 0.22 |
| 111.00 | 39.00 | 0.28 | 63.00 | 0.28 | 90.00 | 0.24 |
| 110.00 | 39.00 | 0.28 | 63.00 | 0.27 | 91.00 | 0.25 |
| 109.00 | 40.00 | 0.27 | 64.00 | 0.27 | 91.00 | 0.25 |
| 108.00 | 40.00 | 0.27 | 64.00 | 0.27 | 92.00 | 0.26 |
| 107.00 | 41.00 | 0.28 | 65.00 | 0.27 | 92.00 | 0.26 |
| 106.00 | 41.00 | 0.27 | 65.00 | 0.27 | 93.00 | 0.27 |
| 105.00 | 42.00 | 0.28 | 66.00 | 0.27 | 93.00 | 0.27 |
| 104.00 | 42.00 | 0.27 | 66.00 | 0.27 | 94.00 | 0.26 |
| 103.00 | 43.00 | 0.28 | 67.00 | 0.28 | 95.00 | 0.27 |
| 102.00 | 43.00 | 0.28 | 67.00 | 0.28 | 95.00 | 0.28 |

| Elevation cm | Time min | Soltrol Content | Time min | Soltrol Content | Time min | Soltrol Content |
|---|---|---|---|---|---|---|
| 101.00 | 44.00 | 0.27 | 68.00 | 0.27 | 96.00 | 0.27 |
| 100.00 | 44.00 | 0.28 | 68.00 | 0.28 | 96.00 | 0.28 |
| 99.00 | 45.00 | 0.28 | 69.00 | 0.28 | 97.00 | 0.27 |
| 98.00 | 46.00 | 0.28 | 69.00 | 0.27 | 97.00 | 0.27 |
| 97.00 | 46.00 | 0.28 | 70.00 | 0.28 | 98.00 | 0.28 |
| 96.00 | 47.00 | 0.27 | 71.00 | 0.27 | 98.00 | 0.27 |
| 95.00 | 47.00 | 0.26 | 71.00 | 0.26 | 99.00 | 0.25 |
| 94.00 | 48.00 | 0.22 | 72.00 | 0.24 | 99.00 | 0.24 |
| 93.00 | 48.00 | 0.15 | 72.00 | 0.23 | 100.00 | 0.23 |
| 92.00 | 49.00 | 0.07 | 73.00 | 0.22 | 100.00 | 0.23 |
| 91.00 | 49.00 | 0.02 | 73.00 | 0.21 | 101.00 | 0.22 |
| 90.00 | 50.00 | 0.00 | 74.00 | 0.19 | 101.00 | 0.21 |
| 89.00 | 50.00 | 0.01 | 74.00 | 0.15 | 102.00 | 0.21 |
| 88.00 | 51.00 | 0.00 | 75.00 | 0.08 | 103.00 | 0.19 |
| 87.00 | 51.00 | 0.01 | 75.00 | 0.04 | 103.00 | 0.17 |
| 86.00 | 52.00 | 0.00 | 76.00 | 0.02 | 104.00 | 0.14 |
| 85.00 | 53.00 | 0.00 | 76.00 | 0.00 | 104.00 | 0.10 |
| 84.00 | 53.00 | 0.00 | 77.00 | 0.00 | 105.00 | 0.06 |
| 83.00 | 54.00 | 0.00 | 78.00 | 0.00 | 105.00 | 0.03 |
| 82.00 | 54.00 | 0.00 | 78.00 | 0.00 | 106.00 | 0.01 |
| 81.00 | | | 79.00 | 0.01 | 106.00 | 0.00 |
| 80.00 | | | 79.00 | 0.00 | 107.00 | 0.00 |
| 79.00 | | | 80.00 | 0.00 | 107.00 | 0.00 |
| 78.00 | | | 80.00 | 0.00 | 108.00 | 0.00 |
| 77.00 | | | 81.00 | 0.01 | 108.00 | 0.01 |
| 76.00 | | | 81.00 | 0.01 | 109.00 | 0.01 |
| 75.00 | | | 82.00 | 0.01 | 110.00 | 0.01 |
| 74.00 | | | | | 110.00 | 0.01 |
| 73.00 | | | | | 111.00 | 0.01 |
| 72.00 | | | | | 111.00 | 0.01 |
| 71.00 | | | | | 112.00 | 0.01 |
| 70.00 | | | | | 112.00 | 0.01 |
| | | | | | | |
| 120.00 | 114.00 | 0.16 | 150.00 | 0.13 | 228.00 | 0.11 |
| 119.00 | 115.00 | 0.16 | 150.00 | 0.14 | 228.00 | 0.12 |
| 118.00 | 115.00 | 0.17 | 151.00 | 0.15 | 229.00 | 0.13 |
| 117.00 | 116.00 | 0.16 | 151.00 | 0.14 | 229.00 | 0.12 |
| 116.00 | 116.00 | 0.16 | 152.00 | 0.14 | 230.00 | 0.12 |
| 115.00 | 117.00 | 0.18 | 153.00 | 0.16 | 230.00 | 0.13 |
| 114.00 | 117.00 | 0.18 | 153.00 | 0.16 | 231.00 | 0.13 |
| 113.00 | 118.00 | 0.19 | 154.00 | 0.16 | 231.00 | 0.14 |
| 112.00 | 118.00 | 0.19 | 154.00 | 0.16 | 232.00 | 0.13 |
| 111.00 | 119.00 | 0.21 | 155.00 | 0.18 | 232.00 | 0.15 |
| 110.00 | 119.00 | 0.22 | 155.00 | 0.19 | 233.00 | 0.15 |
| 109.00 | 120.00 | 0.23 | 156.00 | 0.19 | 233.00 | 0.15 |
| 108.00 | 120.00 | 0.24 | 156.00 | 0.20 | 234.00 | 0.16 |
| 107.00 | 121.00 | 0.24 | 157.00 | 0.21 | 234.00 | 0.17 |
| 106.00 | 122.00 | 0.25 | 157.00 | 0.22 | 235.00 | 0.16 |
| 105.00 | 122.00 | 0.26 | 158.00 | 0.23 | 235.00 | 0.17 |
| 104.00 | 123.00 | 0.26 | 158.00 | 0.23 | 236.00 | 0.18 |
| 103.00 | 123.00 | 0.27 | 159.00 | 0.25 | 237.00 | 0.19 |
| 102.00 | 124.00 | 0.28 | 159.00 | 0.26 | 237.00 | 0.20 |
| 101.00 | 124.00 | 0.27 | 160.00 | 0.27 | 238.00 | 0.21 |
| 100.00 | 125.00 | 0.28 | 161.00 | 0.28 | 238.00 | 0.23 |
| 99.00 | 125.00 | 0.28 | 161.00 | 0.28 | 239.00 | 0.24 |
| 98.00 | 126.00 | 0.28 | 162.00 | 0.28 | 239.00 | 0.25 |
| 97.00 | 126.00 | 0.28 | 162.00 | 0.28 | 240.00 | 0.26 |
| 96.00 | 127.00 | 0.28 | 163.00 | 0.27 | 240.00 | 0.25 |

| Elevation cm | Time min | Soltrol Content | Time min | Soltrol Content | Time min | Soltrol Content |
|---|---|---|---|---|---|---|
| 95.00 | 127.00 | 0.26 | 163.00 | 0.25 | 241.00 | 0.24 |
| 94.00 | 128.00 | 0.25 | 164.00 | 0.24 | 241.00 | 0.23 |
| 93.00 | 128.00 | 0.24 | 164.00 | 0.24 | 242.00 | 0.22 |
| 92.00 | 129.00 | 0.23 | 165.00 | 0.23 | 242.00 | 0.22 |
| 91.00 | 129.00 | 0.24 | 165.00 | 0.24 | 243.00 | 0.23 |
| 90.00 | 130.00 | 0.22 | 166.00 | 0.22 | 243.00 | 0.22 |
| 89.00 | 131.00 | 0.22 | 166.00 | 0.23 | 244.00 | 0.22 |
| 88.00 | 131.00 | 0.20 | 167.00 | 0.22 | 245.00 | 0.21 |
| 87.00 | 132.00 | 0.20 | 167.00 | 0.21 | 245.00 | 0.22 |
| 86.00 | 132.00 | 0.20 | 168.00 | 0.20 | 246.00 | 0.21 |
| 85.00 | 133.00 | 0.18 | 169.00 | 0.19 | 246.00 | 0.20 |
| 84.00 | 133.00 | 0.17 | 169.00 | 0.19 | 247.00 | 0.20 |
| 83.00 | 134.00 | 0.14 | 170.00 | 0.19 | 247.00 | 0.20 |
| 82.00 | 134.00 | 0.11 | 170.00 | 0.19 | 248.00 | 0.20 |
| 81.00 | 135.00 | 0.06 | 171.00 | 0.19 | 248.00 | 0.20 |
| 80.00 | 135.00 | 0.03 | 171.00 | 0.15 | 249.00 | 0.19 |
| 79.00 | 136.00 | 0.01 | 172.00 | 0.12 | 249.00 | 0.18 |
| 78.00 | 136.00 | 0.01 | 172.00 | 0.08 | 250.00 | 0.17 |
| 77.00 | 137.00 | 0.01 | 173.00 | 0.04 | 250.00 | 0.16 |
| 76.00 | 138.00 | 0.01 | 173.00 | 0.03 | 251.00 | 0.15 |
| 75.00 | 138.00 | 0.01 | 174.00 | 0.02 | 251.00 | 0.15 |
| 74.00 | 139.00 | 0.01 | 174.00 | 0.02 | 252.00 | 0.14 |
| 73.00 | 139.00 | 0.01 | 175.00 | 0.02 | 253.00 | 0.11 |
| 72.00 | 140.00 | 0.00 | 175.00 | 0.02 | 253.00 | 0.10 |
| 71.00 | 140.00 | 0.00 | 176.00 | 0.01 | 254.00 | 0.08 |
| 70.00 | 141.00 | 0.01 | 177.00 | 0.01 | 254.00 | 0.06 |
| 69.00 | 141.00 | 0.02 | 177.00 | 0.02 | 255.00 | 0.05 |
| 68.00 | 142.00 | 0.01 | 178.00 | 0.02 | 255.00 | 0.04 |
| 67.00 | 142.00 | 0.01 | 178.00 | 0.01 | 256.00 | 0.03 |
| 66.00 | 143.00 | 0.01 | 179.00 | 0.01 | 256.00 | 0.02 |
| 65.00 | 143.00 | 0.01 | 179.00 | 0.01 | 257.00 | 0.02 |
| 64.00 | | | 180.00 | 0.01 | 257.00 | 0.01 |
| 63.00 | | | 180.00 | 0.01 | 258.00 | 0.01 |
| 62.00 | | | 181.00 | 0.01 | 258.00 | 0.01 |
| 61.00 | | | 181.00 | 0.01 | 259.00 | 0.01 |
| 60.00 | | | 182.00 | 0.00 | 260.00 | 0.00 |
| 59 00 | | | 182.00 | 0.01 | 260.00 | 0.00 |
| 58.00 | | | 183.00 | 0.01 | 261.00 | 0.01 |
| 57.00 | | | 184.00 | 0.01 | 261.00 | 0.00 |
| 56.00 | | | 184.00 | -0.01 | 262.00 | 0.00 |
| 55.00 | | | 185.00 | 0.00 | 262.00 | 0.00 |
| 54.00 | | | 185.00 | -0.01 | 263.00 | 0.00 |
| 53.00 | | | 186.00 | -0.01 | 263.00 | -0.01 |
| 52.00 | | | 186.00 | 0.00 | 264.00 | 0.00 |
| 51.00 | | | 187.00 | 0.00 | 264.00 | 0.00 |
| 50.00 | | | 187.00 | 0.00 | 265.00 | 0.00 |
| 49.00 | | | 188.00 | -0 01 | 265.00 | -0.01 |
| 48 00 | | | 188.00 | 0.00 | 266 00 | -0.01 |
| 47.00 | | | 189.00 | 0.00 | 267.00 | 0.00 |
| 46.00 | | | 189.00 | 0.00 | 267.00 | 0.00 |
| 45.00 | | | 190.00 | 0.00 | 268.00 | 0.00 |
| 44.00 | | | 191.00 | -0.01 | 268.00 | 0.00 |
| 43.00 | | | 191.00 | -0.01 | 269.00 | -0.01 |
| 42.00 | | | 192.00 | -0.01 | 269.00 | -0.01 |
| 41 00 | | | 192.00 | -0.01 | 270.00 | -0.01 |
| 40.00 | | | 193.00 | -0.01 | 270.00 | -0.01 |
| 39.00 | | | 193.00 | 0.00 | 271.00 | 0.00 |
| 38.00 | | | 194.00 | 0 00 | 271.00 | 0.00 |
| 37.00 | | | 194.00 | 0 00 | 272.00 | 0.00 |

| Elevation cm | Time min | Soltrol Content | Time min | Soltrol Content | Time min | Soltrol Content |
|---|---|---|---|---|---|---|
| 36.00 | | | 195.00 | 0.00 | 273.00 | 0.00 |
| 35.00 | | | 195.00 | -0.01 | 273.00 | 0.00 |
| 34.00 | | | 196.00 | 0.00 | | |

| Elevation cm | Time min | Soltrol Content | Time min | Soltrol Content | Time min | Soltrol Content |
|---|---|---|---|---|---|---|
| 120.00 | 276.00 | 0.11 | 327.00 | 0.09 | 375.00 | 0.08 |
| 119.00 | 276.00 | 0.11 | 327.00 | 0.10 | 375.00 | 0.10 |
| 118.00 | 277.00 | 0.11 | 328.00 | 0.11 | 376.00 | 0.10 |
| 117.00 | 277.00 | 0.10 | 328.00 | 0.10 | 377.00 | 0.09 |
| 116.00 | 278.00 | 0.10 | 329.00 | 0.10 | 377.00 | 0.09 |
| 115.00 | 278.00 | 0.12 | 329.00 | 0.11 | 378.00 | 0.10 |
| 114.00 | 279.00 | 0.11 | 330.00 | 0.11 | 378.00 | 0.10 |
| 113.00 | 280.00 | 0.13 | 330.00 | 0.12 | 379.00 | 0.11 |
| 112.00 | 280.00 | 0.12 | 331.00 | 0.11 | 379.00 | 0.10 |
| 111.00 | 281.00 | 0.14 | 331.00 | 0.13 | 380.00 | 0.11 |
| 110.00 | 281.00 | 0.14 | 332.00 | 0.13 | 380.00 | 0.11 |
| 109.00 | 282.00 | 0.13 | 333.00 | 0.12 | 381.00 | 0.11 |
| 108.00 | 282.00 | 0.15 | 333.00 | 0.13 | 381.00 | 0.12 |
| 107.00 | 283.00 | 0.14 | 334.00 | 0.13 | 382.00 | 0.12 |
| 106.00 | 283.00 | 0.15 | 334.00 | 0.14 | 382.00 | 0.12 |
| 105.00 | 284.00 | 0.15 | 335.00 | 0.14 | 383.00 | 0.13 |
| 104.00 | 284.00 | 0.15 | 335.00 | 0.14 | 384.00 | 0.13 |
| 103.00 | 285.00 | 0.16 | 336.00 | 0.15 | 384.00 | 0.13 |
| 102.00 | 285.00 | 0.17 | 336.00 | 0.15 | 385.00 | 0.13 |
| 101.00 | 286.00 | 0.17 | 337.00 | 0.16 | 385.00 | 0.13 |
| 100.00 | 286.00 | 0.19 | 337.00 | 0.17 | 386.00 | 0.14 |
| 99.00 | 287.00 | 0.20 | 338.00 | 0.17 | 386.00 | 0.14 |
| 98.00 | 288.00 | 0.21 | 338.00 | 0.18 | 387.00 | 0.15 |
| 97.00 | 288.00 | 0.23 | 339.00 | 0.19 | 387.00 | 0.17 |
| 96.00 | 289.00 | 0.23 | 339.00 | 0.20 | 388.00 | 0.17 |
| 95.00 | 289.00 | 0.23 | 340.00 | 0.20 | 388.00 | 0.17 |
| 94.00 | 290.00 | 0.22 | 341.00 | 0.19 | 389.00 | 0.17 |
| 93.00 | 290.00 | 0.22 | 341.00 | 0.20 | 389.00 | 0.18 |
| 92.00 | 291.00 | 0.21 | 342.00 | 0.20 | 390 00 | 0.19 |
| 91.00 | 291.00 | 0.22 | 342.00 | 0.21 | 390.00 | 0.19 |
| 90.00 | 292.00 | 0.21 | 343.00 | 0.20 | 391.00 | 0.19 |
| 89.00 | 292.00 | 0.21 | 343.00 | 0.21 | 392.00 | 0.19 |
| 88.00 | 293.00 | 0.21 | 344.00 | 0.20 | 392.00 | 0.19 |
| 87.00 | 293.00 | 0.20 | 344.00 | 0.20 | 393.00 | 0.19 |
| 86.00 | 294.00 | 0.20 | 345.00 | 0.20 | 393.00 | 0.19 |
| 85.00 | 294.00 | 0.19 | 345.00 | 0.19 | 394.00 | 0.18 |
| 84.00 | 295.00 | 0.20 | 346.00 | 0.19 | 394.00 | 0.18 |
| 83.00 | 296.00 | 0.20 | 346.00 | 0.19 | 395.00 | 0.18 |
| 82.00 | 296.00 | 0.20 | 347.00 | 0.19 | 395.00 | 0.18 |
| 81.00 | 297.00 | 0.20 | 347.00 | 0.20 | 396.00 | 0.19 |
| 80.00 | 297.00 | 0.19 | 348.00 | 0.19 | 396.00 | 0.18 |
| 79.00 | 298.00 | 0.18 | 349.00 | 0.18 | 397.00 | 0.17 |
| 78.00 | 298.00 | 0.17 | 349.00 | 0.18 | 397 00 | 0.17 |
| 77.00 | 299.00 | 0.16 | 350.00 | 0.17 | 398.00 | 0.16 |
| 76.00 | 299.00 | 0.16 | 350.00 | 0.16 | 398.00 | 0.15 |
| 75.00 | 300.00 | 0.15 | 351.00 | 0.15 | 399.00 | 0.15 |
| 74.00 | 300.00 | 0.15 | 351.00 | 0.15 | 400.00 | 0.15 |
| 73.00 | 301.00 | 0.15 | 352.00 | 0.15 | 400.00 | 0.15 |
| 72.00 | 301.00 | 0.14 | 352.00 | 0.15 | 401.00 | 0.15 |
| 71.00 | 302.00 | 0.14 | 353.00 | 0.15 | 401.00 | 0.15 |
| 70.00 | 303.00 | 0.12 | 353.00 | 0.14 | 402.00 | 0.15 |
| 69.00 | 303.00 | 0.13 | 354.00 | 0.16 | 402.00 | 0.15 |
| 68.00 | 304.00 | 0.11 | 354.00 | 0.16 | 403.00 | 0.16 |
| 67.00 | 304.00 | 0.09 | 355.00 | 0.15 | 403.00 | 0.16 |
| 66.00 | 305.00 | 0.06 | 356.00 | 0.14 | 404.00 | 0.16 |
| 65.00 | 305.00 | 0.04 | 356.00 | 0.13 | 404.00 | 0.16 |
| 64.00 | 306.00 | 0.03 | 357.00 | 0.09 | 405.00 | 0.15 |
| 63.00 | 306.00 | 0.03 | 357.00 | 0.07 | 405.00 | 0.14 |
| 62.00 | 307.00 | 0.03 | 358.00 | 0.06 | 406.00 | 0.12 |

| Elevation cm | Time min | Soltrol Content | Time min | Soltrol Content | Time min | Soltrol Content |
|---|---|---|---|---|---|---|
| 61.00 | 307.00 | 0.01 | 358.00 | 0.04 | 406.00 | 0.09 |
| 60.00 | 308.00 | 0.00 | 359.00 | 0.02 | 407.00 | 0.07 |
| 59.00 | 308.00 | 0.01 | 359.00 | 0.03 | 408.00 | 0.06 |
| 58.00 | 309.00 | 0 01 | 360.00 | 0.02 | 408.00 | 0.04 |
| 57.00 | 310.00 | 0.01 | 360.00 | 0.01 | 409.00 | 0.03 |
| 56.00 | 310.00 | -0.01 | 361.00 | 0.00 | 409.00 | 0.01 |
| 55.00 | 311.00 | 0.00 | 361.00 | 0.01 | 410.00 | 0.01 |
| 54.00 | 311.00 | -0.01 | 362.00 | 0.00 | 410.00 | 0.01 |
| 53.00 | 312.00 | -0.01 | 363.00 | 0.00 | 411.00 | 0.00 |
| 52.00 | 312.00 | 0.00 | 363.00 | 0.00 | 411.00 | 0.00 |
| 51.00 | 313.00 | 0.00 | 364.00 | 0.00 | 412.00 | 0.00 |
| 50.00 | 313.00 | 0.00 | 364.00 | 0.00 | 412.00 | 0.01 |
| 49.00 | 314.00 | -0.01 | 365.00 | -0.01 | 413.00 | 0.00 |
| 48.00 | 314.00 | -0.01 | 365.00 | 0.00 | 413.00 | -0.01 |
| 47.00 | 315.00 | -0.01 | 366.00 | 0.00 | 414.00 | 0.00 |
| 46.00 | 315.00 | 0.00 | 366.00 | 0.00 | 415.00 | 0.00 |
| 45.00 | 316.00 | 0.00 | 367.00 | 0.00 | 415.00 | 0.00 |
| 44.00 | 317.00 | 0.00 | 367.00 | 0.00 | 416.00 | 0.00 |
| 43.00 | 317.00 | -0.01 | 368.00 | -0.01 | 416.00 | -0.01 |
| 42.00 | 318.00 | -0.01 | 368.00 | -0.01 | 417.00 | -0.01 |
| 41.00 | 318.00 | -0.01 | 369.00 | -0.01 | 417.00 | -0.01 |
| 40.00 | 319.00 | -0.01 | 370.00 | -0.01 | 418.00 | -0.01 |
| 39.00 | 319.00 | 0.00 | 370.00 | 0.00 | 418.00 | 0.00 |
| 38.00 | 320.00 | 0.00 | 371.00 | 0.00 | 419.00 | 0.00 |
| 37.00 | 320.00 | 0.00 | 371.00 | 0.01 | 419.00 | 0.01 |
| 36.00 | 321.00 | 0.00 | 372.00 | 0.01 | 420.00 | 0.01 |
| 35.00 | 321.00 | -0.01 | 372.00 | -0.01 | 421.00 | -0.01 |

| Elevation cm | Time min | Soltrol Content |
|---|---|---|
| 120.00 | 899.00 | 0.05 |
| 119.00 | 899.00 | 0.05 |
| 118.00 | 900.00 | 0.05 |
| 117.00 | 900.00 | 0.04 |
| 116.00 | 901.00 | 0.04 |
| 115.00 | 902.00 | 0.05 |
| 114.00 | 902.00 | 0.05 |
| 113 00 | 903.00 | 0.06 |
| 112.00 | 903.00 | 0.05 |
| 111.00 | 904.00 | 0.06 |
| 110.00 | 904.00 | 0.06 |
| 109.00 | 905.00 | 0.06 |
| 108.00 | 905.00 | 0.06 |
| 107.00 | 906.00 | 0.06 |
| 106.00 | 906.00 | 0.07 |
| 105.00 | 907.00 | 0.07 |
| 104.00 | 907.00 | 0.07 |
| 103.00 | 908.00 | 0.08 |
| 102.00 | 909.00 | 0.07 |
| 101.00 | 909.00 | 0.08 |
| 100.00 | 910.00 | 0.08 |
| 99.00 | 910.00 | 0.07 |
| 98.00 | 911.00 | 0.06 |
| 97.00 | 911.00 | 0.07 |
| 96.00 | 912.00 | 0.07 |
| 95.00 | 912.00 | 0.06 |
| 94.00 | 913.00 | 0.06 |
| 93.00 | 913.00 | 0.06 |
| 92.00 | 914.00 | 0.07 |
| 91.00 | 914.00 | 0.08 |
| 90.00 | 915.00 | 0.07 |
| 89.00 | 915.00 | 0.08 |
| 88.00 | 916.00 | 0.07 |
| 87.00 | 917.00 | 0.08 |
| 86.00 | 917.00 | 0.08 |
| 85.00 | 918.00 | 0.08 |
| 84.00 | 918.00 | 0.07 |
| 83.00 | 919.00 | 0.08 |
| 82.00 | 919.00 | 0.09 |
| 81.00 | 920.00 | 0.09 |
| 80.00 | 920.00 | 0.09 |
| 79.00 | 921.00 | 0.08 |
| 78.00 | 921.00 | 0.08 |
| 77.00 | 922.00 | 0.08 |
| 76 00 | 922.00 | 0.08 |
| 75.00 | 923.00 | 0.08 |
| 74 00 | 924.00 | 0.09 |
| 73.00 | 924.00 | 0.09 |
| 72.00 | 925.00 | 0.09 |
| 71.00 | 925.00 | 0.09 |
| 70.00 | 926.00 | 0.09 |
| 69.00 | 926.00 | 0.10 |
| 68.00 | 927.00 | 0.11 |
| 67.00 | 927.00 | 0.11 |
| 66.00 | 928.00 | 0.12 |
| 65.00 | 928.00 | 0.12 |
| 64.00 | 929.00 | 0.11 |
| 63.00 | 929.00 | 0.12 |
| 62.00 | 930.00 | 0.12 |

| Elevation cm | Time min | Soltrol Content |
|---|---|---|
| 61.00 | 931.00 | 0.11 |
| 60.00 | 931.00 | 0.10 |
| 59.00 | 932.00 | 0.11 |
| 58.00 | 932.00 | 0.12 |
| 57.00 | 933.00 | 0.11 |
| 56.00 | 933.00 | 0.08 |
| 55.00 | 934.00 | 0.07 |
| 54.00 | 934.00 | 0.06 |
| 53.00 | 935.00 | 0.05 |
| 52.00 | 935.00 | 0.05 |
| 51.00 | 936.00 | 0.06 |
| 50.00 | 936.00 | 0.07 |
| 49.00 | 937.00 | 0.07 |
| 48.00 | 937.00 | 0.08 |
| 47.00 | 938.00 | 0.08 |
| 46.00 | 939.00 | 0.09 |
| 45.00 | 939.00 | 0.09 |
| 44.00 | 940.00 | 0.06 |
| 43.00 | 940.00 | 0.04 |
| 42.00 | 941.00 | 0.05 |
| 41.00 | 941.00 | 0.05 |
| 40.00 | 942.00 | 0.07 |
| 39.00 | 942.00 | 0.11 |
| 38.00 | 943.00 | 0.11 |
| 37.00 | 943.00 | 0.09 |
| 36.00 | 944.00 | 0.06 |
| 35.00 | 944.00 | 0.03 |

Spill O
#125 Sand 500 ml Soltrol Spill
Rain 500ml/hour after 45 minutes. Temperature Soltrol: 22°C
Gamma Scan Data Temperature Water: 25°C
Residual water content assumed constant at 0.06.

| Elevation cm | Time min | Soltrol Content | Time min | Soltrol Content | Time min | Water Content | Soltrol Content |
|---|---|---|---|---|---|---|---|
| 120.00 | 0.00 | 0.32 | 42.00 | 0.26 | 116.00 | 0.27 | 0.08 |
| 119.00 | 1.00 | 0.33 | 43.00 | 0.28 | 117.00 | 0.31 | 0.07 |
| 118.00 | 1.00 | 0.28 | 43.00 | 0.25 | 117.00 | 0.13 | 0.08 |
| 112.00 | 5.00 | 0.33 | 47.00 | 0.34 | 121.00 | 0.34 | 0.11 |
| 111.00 | 5.00 | 0.30 | 47.00 | 0.32 | 121.00 | 0.26 | 0.10 |
| 110.00 | 6.00 | 0.30 | 48.00 | 0.31 | 122.00 | 0.23 | 0.11 |
| 109.00 | 7.00 | 0.21 | 49.00 | 0.30 | 123.00 | 0.24 | 0.10 |
| 108.00 | 7.00 | 0.11 | 49.00 | 0.31 | 123.00 | 0.22 | 0.11 |
| 107.00 | 8.00 | 0.03 | 50.00 | 0.31 | 124.00 | 0.29 | 0.08 |
| 106.00 | 8.00 | 0.00 | 50.00 | 0.31 | 124.00 | 0.16 | 0.13 |
| 105.00 | 9.00 | 0.01 | 51.00 | 0.30 | 125.00 | 0.29 | 0.09 |
| 104.00 | 10.00 | 0.00 | 52.00 | 0.30 | 126.00 | 0.24 | 0.10 |
| 103.00 | 10.00 | -0.01 | 52.00 | 0.29 | 126.00 | 0.25 | 0.10 |
| 102.00 | 11.00 | 0.00 | 53.00 | 0.30 | 127.00 | 0.21 | 0.11 |
| 101.00 | 12.00 | 0.00 | 53.00 | 0.30 | 127.00 | 0.23 | 0.11 |
| 100.00 | 12.00 | 0.00 | 54.00 | 0.29 | 128.00 | 0.25 | 0.09 |
| 99.00 | 13.00 | 0.00 | 55.00 | 0.29 | 129.00 | 0.29 | 0.08 |
| 98.00 | 13.00 | 0.00 | 55.00 | 0.29 | 129.00 | 0.23 | 0.09 |
| 97.00 | 14.00 | 0.00 | 56.00 | 0.29 | 130.00 | 0.31 | 0.07 |
| 96.00 | 15.00 | -0.01 | 56.00 | 0.29 | 130.00 | 0.13 | 0.13 |
| 95.00 | 15.00 | 0.00 | 57.00 | 0.29 | 131.00 | 0.26 | 0.09 |
| 94.00 | 16.00 | 0.00 | 58.00 | 0.28 | 132.00 | 0.32 | 0.06 |
| 93.00 | 16.00 | 0.00 | 58.00 | 0.28 | 132.00 | 0.32 | 0.06 |
| 92.00 | 17.00 | 0.00 | 59.00 | 0 29 | 133.00 | 0.28 | 0.07 |
| 91.00 | 18.00 | 0.00 | 60.00 | 0.28 | 133.00 | 0.23 | 0.09 |
| 90.00 | 18.00 | 0.00 | 60.00 | 0.29 | 134.00 | 0.24 | 0.09 |
| 89.00 | 19.00 | 0.00 | 61.00 | 0.29 | 135.00 | 0.30 | 0.06 |
| 88.00 | 19.00 | 0.00 | 61.00 | 0.29 | 135.00 | 0.21 | 0.09 |
| 87.00 | 20.00 | 0.00 | 62.00 | 0.29 | 136.00 | 0.33 | 0.06 |
| 86.00 | 21.00 | 0.00 | 63.00 | 0.28 | 136.00 | 0.23 | 0.10 |
| 85.00 | 21.00 | 0.01 | 63.00 | 0.28 | 137.00 | 0.30 | 0.08 |
| 84.00 | 22.00 | 0.00 | 64.00 | 0.20 | 138.00 | 0.25 | 0.09 |
| 83.00 | 22.00 | 0.00 | 64.00 | 0.09 | 138.00 | 0.31 | 0.07 |
| 82.00 | 23.00 | 0.00 | 65.00 | 0.02 | 139.00 | 0.34 | 0.06 |
| 81.00 | 24.00 | -0.01 | 66.00 | 0.00 | 140.00 | 0.28 | 0.08 |
| 80.00 | 24.00 | -0.01 | 66.00 | 0.00 | 140.00 | 0.24 | 0.09 |
| 79.00 | 25.00 | 0.00 | 67.00 | 0.00 | 141.00 | 0.27 | 0.08 |
| 78.00 | 26.00 | 0.01 | 67.00 | 0.01 | 141.00 | 0 30 | 0.09 |
| 77.00 | 26.00 | 0.01 | 68.00 | 0.01 | 142.00 | 0.27 | 0.09 |
| 76.00 | 27.00 | 0.00 | 69.00 | 0.01 | 143.00 | 0.27 | 0.09 |
| 75.00 | 27.00 | 0.00 | 69.00 | 0.00 | 143.00 | 0.27 | 0.09 |
| 74.00 | 28.00 | 0.00 | 70.00 | 0.00 | 144.00 | 0.27 | 0.09 |
| 73.00 | 29.00 | 0.00 | 70.00 | 0.00 | 144.00 | 0.23 | 0.11 |
| 72.00 | 29.00 | 0.00 | 71.00 | -0.01 | 145.00 | 0 21 | 0.11 |
| 71.00 | 30.00 | 0.00 | 72.00 | 0.00 | 146.00 | 0.29 | 0.08 |
| 70.00 | 30.00 | 0.00 | 72.00 | 0.00 | 146.00 | 0.34 | 0.07 |
| 69.00 | 31.00 | 0 00 | 73.00 | 0.00 | 147.00 | 0.26 | 0.10 |
| 68.00 | 32.00 | 0.00 | 74.00 | 0.00 | 147.00 | 0.25 | 0.10 |
| 67.00 | 32.00 | 0.00 | 74.00 | 0.00 | 148.00 | 0.21 | 0.13 |
| 66.00 | 33.00 | 0.00 | 75.00 | 0.00 | 149.00 | 0.21 | 0.12 |
| 65.00 | 33.00 | 0.00 | 75.00 | 0.00 | 149.00 | 0 20 | 0.13 |
| 64.00 | 34.00 | 0.00 | 76.00 | 0.00 | 150.00 | 0.23 | 0.12 |
| 63.00 | 35.00 | 0.00 | 77.00 | 0.00 | 150.00 | 0.27 | 0.11 |

| Elevation cm | Time min | Soltrol Content | Time min | Soltrol Content | Time min | Water Content | Soltrol Content |
|---|---|---|---|---|---|---|---|
| 62.00 | 35.00 | 0.00 | 77.00 | 0.00 | 151.00 | 0.25 | 0.11 |
| 61.00 | 36.00 | 0.00 | 78.00 | 0.00 | 152.00 | 0.23 | 0.12 |
| 60.00 | 37.00 | 0.00 | 78.00 | -0.01 | 152.00 | 0.23 | 0.11 |
| 59.00 | 37.00 | 0.00 | 79.00 | 0.00 | 153.00 | 0.22 | 0.13 |
| 58.00 | 38.00 | 0.00 | 80.00 | 0.00 | 153.00 | 0.25 | 0.11 |
| 57.00 | | | 80.00 | 0.00 | 154.00 | 0.24 | 0.12 |
| 56.00 | | | 81.00 | 0.00 | 155.00 | 0.25 | 0.11 |
| 55.00 | | | 82.00 | 0.00 | 155.00 | 0.21 | 0.13 |
| 54.00 | | | 82.00 | 0.00 | 156.00 | 0.19 | 0.14 |
| 53.00 | | | 83.00 | 0.00 | 156.00 | 0.20 | 0.14 |
| 52.00 | | | 83.00 | 0.00 | 157.00 | 0.22 | 0.13 |
| 51.00 | | | 84.00 | -0.01 | 158.00 | 0.18 | 0.14 |
| 50.00 | | | 85.00 | 0.00 | 158.00 | 0.20 | 0.14 |
| 49.00 | | | 85.00 | 0.00 | 159.00 | 0.28 | 0.12 |
| 48.00 | | | 86.00 | 0.00 | 159.00 | 0.23 | 0.13 |
| 47.00 | | | 86.00 | 0.00 | 160.00 | 0.26 | 0.12 |
| 46.00 | | | 87.00 | 0.00 | 161.00 | 0.21 | 0.14 |
| 45.00 | | | 88.00 | 0.00 | 161.00 | 0.30 | 0.12 |
| 44.00 | | | 88.00 | 0.00 | 162.00 | 0.27 | 0.13 |
| 43.00 | | | 89.00 | 0.00 | 163.00 | 0.23 | 0.14 |
| 42.00 | | | 90.00 | 0.00 | 163.00 | 0.21 | 0.16 |
| 41.00 | | | 90.00 | 0.00 | 164.00 | 0.27 | 0.14 |
| 40.00 | | | 91.00 | 0.01 | 164.00 | 0.27 | 0.14 |
| 39.00 | | | 91.00 | -0.01 | 165.00 | 0.18 | 0.17 |
| 38.00 | | | 92.00 | 0.00 | 166.00 | 0.22 | 0.16 |
| 37.00 | | | 93.00 | 0.00 | 166.00 | 0.11 | 0.20 |
| 36.00 | | | 93.00 | 0.00 | 167.00 | 0.18 | 0.18 |
| 35.00 | | | 94.00 | 0.00 | 167.00 | 0.19 | 0.19 |
| 34.00 | | | 94.00 | 0.00 | 168.00 | 0.12 | 0.22 |
| 33.00 | | | 95.00 | 0.00 | 169.00 | 0.19 | 0.21 |
| 32.00 | | | 96.00 | 0.00 | 169.00 | 0.03 | 0.28 |
| 31.00 | | | 96.00 | 0.00 | 170.00 | 0.13 | 0.26 |
| 30.00 | | | 97.00 | -0.01 | 170.00 | 0.05 | 0.28 |
| 29.00 | | | 98.00 | 0.00 | 171.00 | 0.06 | 0.21 |
| 28.00 | | | 98.00 | -0.01 | 172.00 | 0.09 | 0.08 |
| 27.00 | | | 99.00 | 0.00 | 172.00 | 0.04 | 0.03 |
| 26.00 | | | 99.00 | 0.00 | 173.00 | 0.07 | 0.00 |
| 25.00 | | | 100.00 | 0.00 | 173.00 | 0.06 | 0.00 |
| 24.00 | | | 101.00 | 0.00 | 174.00 | 0.06 | 0.00 |
| 23.00 | | | 101.00 | 0.00 | 175.00 | 0.07 | -0.01 |
| 22.00 | | | 102.00 | 0.00 | 175.00 | 0.08 | -0.01 |
| 21.00 | | | 102.00 | 0.00 | 176.00 | 0.03 | 0.01 |
| 20.00 | | | 103.00 | 0.00 | 177.00 | 0.12 | -0.02 |
| 19.00 | | | 104.00 | 0.01 | 177.00 | 0.08 | 0.00 |
| 18.00 | | | 104.00 | 0.00 | 178.00 | 0.11 | -0.02 |
| 17.00 | | | 105.00 | 0.00 | 178.00 | 0.08 | -0.01 |
| 16.00 | | | 105.00 | 0.00 | 179.00 | 0.08 | -0.01 |
| 15.00 | | | 106.00 | 0.00 | 180.00 | 0.04 | 0.01 |
| 14.00 | | | 107.00 | 0.00 | 180.00 | 0.05 | 0.00 |
| 13.00 | | | 107.00 | 0.00 | 181.00 | 0.05 | 0.00 |
| 12.00 | | | 108.00 | 0.00 | 181.00 | 0.06 | 0.00 |
| 11.00 | | | 109.00 | 0.00 | 182.00 | 0.05 | 0.00 |
| 10.00 | | | 109.00 | 0.00 | 183.00 | 0.05 | 0.00 |
| 9.00 | | | 110.00 | 0.00 | 183.00 | 0.04 | 0.01 |
| 8.00 | | | 110.00 | 0.00 | 184.00 | 0.04 | 0.01 |

| Elevation cm | Time min | Soltrol Content | Time min | Soltrol Content |
|---|---|---|---|---|
| 120.00 | 263.00 | 0.12 | 410.00 | 0.13 |
| 119.00 | 263.00 | 0.10 | 411.00 | 0.12 |
| 118.00 | 264.00 | 0.10 | 411.00 | 0.13 |
| 112.00 | 268.00 | 0.12 | 415.00 | 0.14 |
| 111.00 | 268.00 | 0.13 | 415.00 | 0.13 |
| 110.00 | 269.00 | 0.13 | 416.00 | 0.13 |
| 109.00 | 269.00 | 0.13 | 417.00 | 0.15 |
| 108.00 | 270.00 | 0.13 | 417.00 | 0.13 |
| 107.00 | 271.00 | 0.14 | 418.00 | 0.14 |
| 106.00 | 271.00 | 0.14 | 419.00 | 0.15 |
| 105.00 | 272.00 | 0.11 | 419.00 | 0.15 |
| 104.00 | 272.00 | 0.12 | 420.00 | 0.15 |
| 103.00 | 273.00 | 0.11 | 420.00 | 0.14 |
| 102.00 | 274.00 | 0.14 | 421.00 | 0.14 |
| 101.00 | 274.00 | 0.14 | 422.00 | 0.16 |
| 100.00 | 275.00 | 0.11 | 422.00 | 0.12 |
| 99 00 | 276.00 | 0.12 | 423.00 | 0.14 |
| 98.00 | 276.00 | 0.13 | 424.00 | 0.14 |
| 97.00 | 277.00 | 0.11 | 424.00 | 0.13 |
| 96.00 | 277.00 | 0.16 | 425.00 | 0.16 |
| 95.00 | 278.00 | 0.14 | 426.00 | 0.16 |
| 94.00 | 279.00 | 0.12 | 426.00 | 0.12 |
| 93.00 | 279.00 | 0.11 | 427.00 | 0.12 |
| 92.00 | 280.00 | 0.12 | 427.00 | 0.13 |
| 91.00 | 280.00 | 0.11 | 428.00 | 0.12 |
| 90.00 | 281.00 | 0.11 | 429.00 | 0.13 |
| 89.00 | 282.00 | 0.11 | 429.00 | 0.14 |
| 88.00 | 282.00 | 0.13 | 430.00 | 0.13 |
| 87.00 | 283.00 | 0.12 | 431.00 | 0.12 |
| 86.00 | 283.00 | 0.13 | 431.00 | 0.15 |
| 85.00 | 284.00 | 0.14 | 432.00 | 0.15 |
| 84.00 | 285.00 | 0.14 | 433.00 | 0.14 |
| 83.00 | 285.00 | 0.10 | 433.00 | 0.12 |
| 82.00 | 286.00 | 0.12 | 434.00 | 0.13 |
| 81.00 | 286.00 | 0.10 | 435.00 | 0.12 |
| 80.00 | 287.00 | 0.11 | 435.00 | 0.12 |
| 79.00 | 288.00 | 0.12 | 436.00 | 0.12 |
| 78.00 | 288.00 | 0.12 | 436.00 | 0.13 |
| 77.00 | 289.00 | 0.15 | 437.00 | 0.14 |
| 76.00 | 290.00 | 0.14 | 438.00 | 0.14 |
| 75.00 | 290.00 | 0.14 | 438.00 | 0.15 |
| 74.00 | 291.00 | 0.11 | 439.00 | 0.14 |
| 73.00 | 291.00 | 0.12 | 440.00 | 0.12 |
| 72.00 | 292.00 | 0.15 | 440.00 | 0.16 |
| 71.00 | 293.00 | 0.12 | 441.00 | 0.13 |
| 70.00 | 293.00 | 0.14 | 442.00 | 0.12 |
| 69.00 | 294.00 | 0.14 | 442.00 | 0.16 |
| 68.00 | 294.00 | 0.13 | 443.00 | 0.14 |
| 67.00 | 295.00 | 0.14 | 444.00 | 0.14 |
| 66.00 | 296.00 | 0.14 | 444.00 | 0.14 |
| 65.00 | 296.00 | 0.14 | 445.00 | 0.15 |
| 64.00 | 297.00 | 0.14 | 445.00 | 0.14 |
| 63.00 | 297.00 | 0.12 | 446.00 | 0.16 |
| 62.00 | 298.00 | 0.12 | 447.00 | 0.16 |
| 61.00 | 299.00 | 0.14 | 447.00 | 0.15 |
| 60.00 | 299.00 | 0.15 | 448.00 | 0.16 |
| 59.00 | 300.00 | 0.15 | 449.00 | 0.16 |
| 58.00 | 300.00 | 0.15 | 449.00 | 0.15 |

| Elevation cm | Time min | Soltrol Content | Time min | Soltrol Content |
|---|---|---|---|---|
| 57.00 | 301.00 | 0.14 | 450.00 | 0.14 |
| 56.00 | 302.00 | 0.15 | 451.00 | 0.14 |
| 55.00 | 302.00 | 0.16 | 451.00 | 0.17 |
| 54.00 | 303.00 | 0.14 | 452.00 | 0.14 |
| 53.00 | 303.00 | 0.13 | 453.00 | 0.15 |
| 52.00 | 304.00 | 0.13 | 453.00 | 0.16 |
| 51.00 | 305.00 | 0.15 | 454.00 | 0.16 |
| 50.00 | 305.00 | 0.15 | 454.00 | 0.15 |
| 49.00 | 306.00 | 0.15 | 455.00 | 0.15 |
| 48.00 | 307.00 | 0.15 | 456.00 | 0.13 |
| 47.00 | 307.00 | 0.13 | 456.00 | 0.14 |
| 46.00 | 308.00 | 0.16 | 457.00 | 0.14 |
| 45.00 | 308.00 | 0.14 | 458.00 | 0.14 |
| 44.00 | 309.00 | 0.15 | 458.00 | 0.15 |
| 43.00 | 310.00 | 0.14 | 459.00 | 0.13 |
| 42.00 | 310.00 | 0.13 | 460.00 | 0.13 |
| 41.00 | 311.00 | 0.14 | 460.00 | 0.14 |
| 40.00 | 311.00 | 0.13 | 461.00 | 0.13 |
| 39.00 | 312.00 | 0.14 | 462.00 | 0.17 |
| 38.00 | 313.00 | 0.13 | 462.00 | 0.16 |
| 37.00 | 313.00 | 0.17 | 463.00 | 0.16 |
| 36.00 | 314.00 | 0.13 | 463.00 | 0.15 |
| 35.00 | 314.00 | 0.13 | 464.00 | 0.14 |
| 34.00 | 315.00 | 0.15 | 465.00 | 0.13 |
| 33.00 | 316.00 | 0.14 | 465.00 | 0.14 |
| 32.00 | 316.00 | 0.20 | 466.00 | 0.16 |
| 31.00 | 317.00 | 0.18 | 467.00 | 0.16 |
| 30.00 | 317.00 | 0.20 | 467.00 | 0.17 |
| 29.00 | 318.00 | 0.20 | 468.00 | 0.19 |
| 28.00 | 319.00 | 0.22 | 469.00 | 0.22 |
| 27.00 | 319.00 | 0.19 | 469.00 | 0.20 |
| 26.00 | 320.00 | 0.21 | 470.00 | 0.22 |
| 25.00 | 321.00 | 0.20 | 471.00 | 0.20 |
| 24.00 | 321.00 | 0.19 | 471.00 | 0.19 |
| 23.00 | 322.00 | 0.20 | 472.00 | 0.16 |
| 22.00 | 322.00 | 0.17 | 472.00 | 0.16 |
| 21.00 | 323.00 | 0.18 | 473.00 | 0.16 |
| 20.00 | 324.00 | 0.16 | 474.00 | 0.15 |
| 19.00 | 324.00 | 0.16 | 474.00 | 0.13 |
| 18.00 | 325.00 | 0.14 | 475.00 | 0.13 |
| 17.00 | 325.00 | 0.13 | 476.00 | 0.11 |
| 16.00 | 326.00 | 0.13 | 476.00 | 0.13 |
| 15.00 | 327.00 | 0.10 | 477.00 | 0.13 |
| 14.00 | 327.00 | 0.12 | 478.00 | 0.12 |
| 13.00 | 328.00 | 0.10 | 478.00 | 0.11 |
| 12.00 | 328.00 | 0.09 | 479.00 | 0.12 |
| 11.00 | 329.00 | 0.09 | 479.00 | 0.13 |
| 10.00 | 330.00 | 0.08 | 480.00 | 0.13 |
| 9.00 | 330.00 | 0.09 | 481.00 | 0.13 |
| 8.00 | 331.00 | 0.08 | 481.00 | 0.10 |

Spill P
#125 Sand 750 ml Soltrol Spill
Rain 500ml/hour after 22 hours.
Rain stopped after 24 hours.
Residual water content assumed constant at 0.06.

Bulk Density grav.: 1.58g $cm^{-3}$
Porosity: 0.40
Temperature Soltrol: 22°C
Temperature Water: 15°C

| Elevation cm | Time min | Soltrol Content | Time min | Soltrol Content | Time min | Soltrol Content |
|---|---|---|---|---|---|---|
| 118 | 4 | 0.321395 | 35 | 0.325105 | 84 | 0.304382 |
| 117 | 5 | 0.329321 | 36 | 0.323595 | 85 | 0.313989 |
| 116 | 5 | 0.309421 | 37 | 0.309167 | 86 | 0.307862 |
| 115 | 6 | 0.31455 | 37 | 0.312641 | 86 | 0.296759 |
| 114 | 7 | 0.305153 | 38 | 0.308274 | 87 | 0.286766 |
| 113 | 7 | 0.298672 | 38 | 0.300319 | 87 | 0.28335 |
| 112 | 8 | 0.297413 | 39 | 0.30346 | 88 | 0.28884 |
| 111 | 8 | 0.303576 | 40 | 0.3073 | 89 | 0.301457 |
| 110 | 9 | 0.277599 | 40 | 0.30692 | 89 | 0.300374 |
| 109 | 10 | 0.198615 | 41 | 0.302484 | 90 | 0.306737 |
| 108 | 10 | 0.102212 | 41 | 0.311327 | 90 | 0.305699 |
| 107 | 11 | 0.029248 | 42 | 0.306257 | 91 | 0.309914 |
| 106 | 12 | 0.002517 | 43 | 0.298406 | 92 | 0.300653 |
| 105 | 12 | -0.00058 | 43 | 0.308721 | 92 | 0.308305 |
| 104 | 13 | -0.00266 | 44 | 0.308584 | 93 | 0.305177 |
| 103 | 13 | -0.00066 | 45 | 0.304366 | 93 | 0.296264 |
| 102 | 14 | 0.002342 | 45 | 0.303474 | 94 | 0.307834 |
| 101 | 15 | 0.004893 | 46 | 0.310281 | 95 | 0.307007 |
| 100 | 15 | -0.00208 | 46 | 0.310277 | 95 | 0.308135 |
| 99 | 16 | 0.003454 | 47 | 0.310326 | 96 | 0.308367 |
| 98 | 16 | 0.003402 | 48 | 0.317247 | 96 | 0.312844 |
| 97 | 17 | -0.00502 | 48 | 0.303642 | 97 | 0.305466 |
| 96 | 18 | -0.00888 | 49 | 0.302242 | 98 | 0.301831 |
| 95 | 18 | -0.00261 | 49 | 0.298496 | 98 | 0.304773 |
| 94 | 19 | 0.00512 | 50 | 0.302162 | 99 | 0.308075 |
| 93 | 19 | 0.001176 | 51 | 0.310644 | 99 | 0.307153 |
| 92 | 20 | 0.001017 | 51 | 0.29687 | 100 | 0.302338 |
| 91 | 21 | -0.00238 | 52 | 0.301701 | 101 | 0.307091 |
| 90 | 21 | -0.00052 | 52 | 0.286235 | 101 | 0.312527 |
| 89 | 22 | 0.004406 | 53 | 0.213451 | 102 | 0.310579 |
| 88 | 23 | 0.00081 | 54 | 0.082764 | 102 | 0.298235 |
| 87 | 23 | 0.000389 | 54 | 0.027531 | 103 | 0.308088 |
| 86 | 24 | -0.00086 | 55 | 0.002169 | 104 | 0.305079 |
| 85 | 24 | -0.00259 | 55 | -0.00638 | 104 | 0.299197 |
| 84 | 25 | 0.002906 | 56 | 0.002443 | 105 | 0.308752 |
| 83 | 26 | 0.001231 | 57 | -0.01 | 105 | 0.288178 |
| 82 | 26 | -0.0014 | 57 | 0.007103 | 106 | 0.29696 |
| 81 | 27 | -0.0059 | 58 | -0.00598 | 107 | 0.293014 |
| 80 | 27 | 0.004867 | 58 | 0.007562 | 107 | 0.292916 |
| 79 | | | 59 | -0.00414 | 108 | 0.277381 |
| 78 | | | 60 | -0.00579 | 108 | 0.256315 |
| 77 | | | 60 | 0.002348 | 109 | 0.247997 |
| 76 | | | 61 | -0.00665 | 110 | 0.233654 |
| 75 | | | 62 | 0.008068 | 110 | 0.183608 |
| 74 | | | 62 | 0.00143 | 111 | 0.097119 |
| 73 | | | 63 | 0.001818 | 111 | 0.04173 |
| 72 | | | 63 | -0.00379 | 112 | 0.012097 |
| 71 | | | 64 | -0.00845 | 113 | -0.00341 |
| 70 | | | 65 | 0.002241 | 113 | 0.000023 |
| 69 | | | 65 | -0.00058 | 114 | 0.003362 |
| 68 | | | 66 | 0.000091 | 115 | 0.004117 |
| 67 | | | 66 | 0.001278 | 115 | 0.00383 |
| 66 | | | 67 | -0.00144 | 116 | 0.00905 |

| Elevation cm | Time min | Soltrol Content | Time min | Soltrol Content | Time min | Soltrol Content |
|---|---|---|---|---|---|---|
| 65 | | | 68 | 0.004448 | 116 | 0.000901 |
| 64 | | | 68 | 0.004911 | 117 | 0.004064 |
| 63 | | | 69 | -0.00001 | 118 | 0.011956 |
| 62 | | | 69 | -0.0039 | 118 | -0.00114 |
| 61 | | | 70 | 0.00382 | 119 | 0.005882 |
| 60 | | | 71 | 0.001178 | 119 | -0.0058 |
| 59 | | | | | 120 | -0.00698 |
| 58 | | | | | 121 | -0.00041 |
| 57 | | | | | 121 | -0.00096 |
| 56 | | | | | 122 | 0.000967 |
| 55 | | | | | 123 | -0.00416 |
| 54 | | | | | 123 | 0.001721 |
| 53 | | | | | 124 | -0.00465 |
| 52 | | | | | 124 | 0.005246 |
| 51 | | | | | 125 | 0.005169 |
| 50 | | | | | 126 | -0.00216 |
| 49 | | | | | 126 | 0.001984 |
| 48 | | | | | 127 | -0.00212 |
| 47 | | | | | 127 | -0.00054 |
| 46 | | | | | 128 | -0.00131 |
| 45 | | | | | 129 | -0.00525 |
| 44 | | | | | 129 | -0.00353 |
| 43 | | | | | 130 | 0.000072 |
| 42 | | | | | 130 | -0.00176 |
| 41 | | | | | 131 | 0.000754 |
| 40 | | | | | 132 | 0.006763 |

| Elevation cm | Time min | Soltrol Content | Time min | Water Content | Soltrol Content |
|---|---|---|---|---|---|
| 118 | 222 | 0.139204 | 1338 | 0.144979 | 0.091675 |
| 117 | 222 | 0.133433 | 1338 | 0.153465 | 0.081596 |
| 116 | 223 | 0.120415 | 1339 | 0.103516 | 0.091364 |
| 115 | 223 | 0.139868 | 1340 | 0.128181 | 0.088822 |
| 114 | 224 | 0.154603 | 1340 | 0.164198 | 0.084104 |
| 113 | 225 | 0.159364 | 1341 | 0.162028 | 0.094409 |
| 112 | 225 | 0.157828 | 1341 | 0.150073 | 0.113314 |
| 111 | 226 | 0.166068 | 1342 | 0.218776 | 0.092202 |
| 110 | 226 | 0.163941 | 1343 | 0.192452 | 0.101028 |
| 109 | 227 | 0.168992 | 1343 | 0.130889 | 0.12352 |
| 108 | 228 | 0.172905 | 1344 | 0.152698 | 0.113991 |
| 107 | 228 | 0.164331 | 1344 | 0.115811 | 0.125324 |
| 106 | 229 | 0.166436 | 1345 | 0.1441 | 0.115629 |
| 105 | 229 | 0.160692 | 1346 | 0.134828 | 0.105687 |
| 104 | 230 | 0.16764 | 1346 | 0.019168 | 0.143456 |
| 103 | 231 | 0.164345 | 1347 | -0.03607 | 0.148412 |
| 102 | 231 | 0.165241 | 1347 | 0.024211 | 0.116055 |
| 101 | 232 | 0.178225 | 1348 | -0.01175 | 0.124304 |
| 100 | 232 | 0.187165 | 1349 | -0.02476 | 0.126784 |
| 99 | 233 | 0.190479 | 1349 | -0.027 | 0.132102 |
| 98 | 234 | 0.200235 | 1350 | -0.03894 | 0.141992 |
| 97 | 234 | 0.203275 | 1350 | 0.036962 | 0.115677 |
| 96 | 235 | 0.19896 | 1351 | -0.03289 | 0.136252 |
| 95 | 235 | 0.200759 | 1352 | -0.00399 | 0.125966 |
| 94 | 236 | 0.203814 | 1352 | -0.00717 | 0.134604 |
| 93 | 237 | 0.214399 | 1353 | -0.04216 | 0.13885 |
| 92 | 237 | 0.219305 | 1353 | 0.002207 | 0.12746 |
| 91 | 238 | 0.234544 | 1354 | -0.04585 | 0.145441 |
| 90 | 238 | 0.242499 | 1355 | 0.021249 | 0.122564 |

| Elevation cm | Time min | Soltrol Content | Time min | Water Content | Soltrol Content |
|---|---|---|---|---|---|
| 89 | 239 | 0.260508 | 1355 | -0.05216 | 0.15331 |
| 88 | 240 | 0.269769 | 1356 | 0.011215 | 0.130933 |
| 87 | 240 | 0.274374 | 1356 | 0.040745 | 0.118616 |
| 86 | 241 | 0.294818 | 1357 | 0.041364 | 0.120189 |
| 85 | 242 | 0.30007 | 1358 | 0.066012 | 0.115927 |
| 84 | 242 | 0.305125 | 1358 | -0.04305 | 0.156652 |
| 83 | 243 | 0.294226 | 1359 | -0.01823 | 0.153011 |
| 82 | 243 | 0.291864 | 1359 | 0.018016 | 0.145269 |
| 81 | 244 | 0.283499 | 1360 | -0.05205 | 0.170474 |
| 80 | 245 | 0.288854 | 1361 | -0.00805 | 0.157846 |
| 79 | 245 | 0.274299 | 1361 | -0.0184 | 0.16242 |
| 78 | 246 | 0.279486 | 1362 | 0.013879 | 0.148417 |
| 77 | 246 | 0.279621 | 1363 | 0.074105 | 0.13355 |
| 76 | 247 | 0.270216 | 1363 | -0.02664 | 0.175079 |
| 75 | 248 | 0.287927 | 1364 | 0.005915 | 0.16989 |
| 74 | 248 | 0.277774 | 1364 | 0.013661 | 0.17147 |
| 73 | 249 | 0.282282 | 1365 | 0.006543 | 0.177525 |
| 72 | 249 | 0.270404 | 1366 | -0.02705 | 0.193801 |
| 71 | 250 | 0.260624 | 1366 | -0.01723 | 0.181935 |
| 70 | 251 | 0.272595 | 1367 | 0.007295 | 0.179006 |

| Elevation cm | Time min | Soltrol Content |
|---|---|---|
| 69 | 251 | 0.268172 |
| 68 | 252 | 0.269798 |
| 67 | 252 | 0.264001 |
| 66 | 253 | 0.247496 |
| 65 | 254 | 0.247172 |
| 64 | 254 | 0.249213 |
| 63 | 255 | 0.227322 |
| 62 | 255 | 0.201217 |
| 61 | 256 | 0.207671 |
| 60 | 257 | 0.209191 |
| 59 | 257 | 0.199154 |
| 58 | 258 | 0.191679 |
| 57 | 258 | 0.190148 |
| 56 | 259 | 0.166872 |
| 55 | 260 | 0.136943 |
| 54 | 260 | 0.101618 |
| 53 | 261 | 0.04978 |
| 52 | 261 | 0.018463 |
| 51 | 262 | 0.005528 |
| 50 | 263 | 0.003289 |
| 49 | 263 | 0.007262 |
| 48 | 264 | -0.00237 |
| 47 | 265 | 0.001498 |
| 46 | 265 | 0.001117 |
| 45 | 266 | -0.00372 |
| 44 | 266 | -0.00225 |
| 43 | 267 | -0.00205 |
| 42 | 268 | -0.00104 |
| 41 | 268 | -0.005 |
| 40 | 269 | 0.00714 |
| 39 | 269 | 0.00117 |
| 38 | 270 | 0.00524 |
| 37 | 271 | 0.002832 |
| 36 | 271 | 0.002303 |
| 35 | 272 | 0.001559 |
| 34 | 273 | -0.007 |
| 33 | 273 | 0.004645 |
| 32 | 274 | -0.00011 |
| 31 | 274 | 0.00577 |
| 30 | 275 | 0.001388 |
| 29 | 276 | 0.003264 |
| 28 | 276 | 0.001559 |
| 27 | 277 | 0.002086 |
| 26 | 277 | -0.00667 |
| 25 | 278 | -0.00111 |
| 24 | 279 | -0.00169 |
| 23 | 279 | 0.000234 |
| 22 | 280 | 0.003263 |
| 21 | 280 | 0.003813 |
| 20 | 281 | 0.008445 |

| Elevation cm | Time min | Water Content | Soltrol Content | Time min | Water Content | Soltrol Content |
|---|---|---|---|---|---|---|
| 118 | 1370 | 0.189657 | 0.074102 | 1421 | 0.212848 | 0.059755 |
| 117 | 1370 | 0.146245 | 0.082651 | 1421 | 0.123033 | 0.092178 |
| 116 | 1371 | 0.134889 | 0.087135 | 1422 | 0.133262 | 0.081021 |
| 115 | 1372 | 0.16821 | 0.0727 | 1423 | 0.115881 | 0.090367 |
| 114 | 1372 | 0.116747 | 0.097788 | 1423 | 0.154487 | 0.084018 |
| 113 | 1373 | 0.197937 | 0.084007 | 1424 | 0.146357 | 0.096124 |
| 112 | 1373 | 0.199128 | 0.09246 | 1424 | 0.193332 | 0.095055 |
| 111 | 1374 | 0.155115 | 0.116601 | 1425 | 0.12922 | 0.121463 |
| 110 | 1375 | 0.220114 | 0.099398 | 1426 | 0.218619 | 0.093449 |
| 109 | 1375 | 0.205702 | 0.096529 | 1426 | 0.228079 | 0.091134 |
| 108 | 1376 | 0.233603 | 0.084963 | 1427 | 0.230086 | 0.090058 |
| 107 | 1376 | 0.17787 | 0.110805 | 1427 | 0.136259 | 0.122137 |
| 106 | 1377 | 0.215108 | 0.101051 | 1428 | 0.194052 | 0.10054 |
| 105 | 1378 | 0.183121 | 0.10746 | 1429 | 0.196762 | 0.103846 |
| 104 | 1378 | 0.164539 | 0.113864 | 1429 | 0.203374 | 0.100511 |
| 103 | 1379 | 0.164385 | 0.118774 | 1430 | 0.220207 | 0.093676 |
| 102 | 1379 | 0.17439 | 0.112528 | 1430 | 0.170265 | 0.111053 |
| 101 | 1380 | 0.198703 | 0.101959 | 1431 | 0.19997 | 0.10651 |
| 100 | 1381 | 0.196052 | 0.102152 | 1432 | 0.198103 | 0.109272 |
| 99 | 1381 | 0.159228 | 0.120629 | 1432 | 0.206597 | 0.104014 |
| 98 | 1382 | 0.186667 | 0.117361 | 1433 | 0.22515 | 0.096471 |
| 97 | 1382 | 0.157373 | 0.125338 | 1433 | 0.193686 | 0.109942 |
| 96 | 1383 | 0.169935 | 0.121097 | 1434 | 0.223513 | 0.096971 |
| 95 | 1384 | 0.192451 | 0.117019 | 1435 | 0.225039 | 0.103036 |
| 94 | 1384 | 0.251293 | 0.098934 | 1435 | 0.172337 | 0.124004 |
| 93 | 1385 | 0.146025 | 0.130904 | 1436 | 0.232413 | 0.098981 |
| 92 | 1385 | 0.207926 | 0.115224 | 1436 | 0.173501 | 0.121781 |
| 91 | 1386 | 0.237593 | 0.104099 | 1437 | 0.216766 | 0.10973 |
| 90 | 1387 | 0.144546 | 0.142185 | 1438 | 0.161671 | 0.131259 |
| 89 | 1387 | 0.187412 | 0.121261 | 1438 | 0.181872 | 0.123189 |
| 88 | 1388 | 0.157863 | 0.136476 | 1439 | 0.112287 | 0.151414 |
| 87 | 1388 | 0.204124 | 0.117088 | 1439 | 0.169721 | 0.129767 |
| 86 | 1389 | 0.201097 | 0.121375 | 1440 | 0.236576 | 0.109869 |
| 85 | 1390 | 0.138762 | 0.141005 | 1441 | 0.241702 | 0.110118 |
| 84 | 1390 | 0.190477 | 0.122302 | 1441 | 0.232258 | 0.115202 |
| 83 | 1391 | 0.110413 | 0.14457 | 1442 | 0.18195 | 0.133562 |
| 82 | 1391 | 0.089402 | 0.157571 | 1442 | 0.227379 | 0.121473 |
| 81 | 1392 | 0.075945 | 0.161106 | 1443 | 0.179764 | 0.138468 |
| 80 | 1393 | 0.053337 | 0.174399 | 1444 | 0.258818 | 0.115333 |
| 79 | 1393 | 0.078503 | 0.165744 | 1444 | 0.234533 | 0.120144 |
| 78 | 1394 | 0.04114 | 0.166164 | 1445 | 0.24548 | 0.12846 |
| 77 | 1394 | -0.0061 | 0.174165 | 1445 | 0.314115 | 0.101009 |
| 76 | 1395 | 0.010551 | 0.167865 | 1446 | 0.32578 | 0.104585 |
| 75 | 1396 | -0.01496 | 0.175652 | 1447 | 0.266255 | 0 12523 |
| 74 | 1396 | 0.038017 | 0.1689 | 1447 | 0.307685 | 0.113659 |
| 73 | 1397 | 0.01927 | 0.170207 | 1448 | 0.271483 | 0.123688 |
| 72 | 1397 | 0.080263 | 0.149756 | 1448 | 0.219466 | 0.137853 |
| 71 | 1398 | -0.02305 | 0.179057 | 1449 | 0.269451 | 0.124603 |
| 70 | 1399 | 0.083366 | 0.158691 | 1450 | 0.258704 | 0.132316 |
| 69 | 1399 | 0.016731 | 0.179565 | 1450 | 0.230429 | 0.137672 |
| 68 | 1400 | -0.01165 | 0.181961 | 1451 | 0.215273 | 0.146575 |
| 67 | 1401 | 0.01997 | 0.160554 | 1451 | 0.181957 | 0.162188 |
| 66 | 1401 | 0.055544 | 0.152028 | 1452 | 0.263721 | 0.135284 |
| 65 | 1402 | 0.008081 | 0.159582 | 1453 | 0.16172 | 0.167395 |
| 64 | 1402 | 0.068431 | 0.134269 | 1453 | 0.186802 | 0.155454 |
| 63 | 1403 | 0.059402 | 0.131527 | 1454 | 0.177893 | 0.15598 |
| 62 | 1404 | 0.000244 | 0.133785 | 1454 | 0.219496 | 0.132148 |
| 61 | 1404 | 0.021465 | 0.131075 | 1455 | 0.159442 | 0.160555 |
| 60 | 1405 | 0.023348 | 0.135525 | 1456 | 0.139538 | 0.170692 |

| Elevation cm | Time min | Water Content | Soltrol Content | Time min | Water Content | Soltrol Content |
|---|---|---|---|---|---|---|
| 59 | 1405 | -0.0006 | 0.148847 | 1456 | 0.122175 | 0.179691 |
| 58 | 1406 | -0.04689 | 0.16538 | 1457 | 0.14633 | 0.172853 |
| 57 | 1407 | 0.02447 | 0.148865 | 1457 | 0.205754 | 0.151969 |
| 56 | 1407 | -0.00473 | 0.161537 | 1458 | 0.205078 | 0.157801 |
| 55 | 1408 | 0.010884 | 0.167168 | 1459 | 0.159125 | 0.170924 |
| 54 | 1408 | 0.084457 | 0.167571 | 1459 | 0.187102 | 0.169052 |
| 53 | 1409 | -0.00687 | 0.208782 | 1460 | 0.162255 | 0.185849 |
| 52 | 1410 | -0.04028 | 0.215462 | 1460 | 0.147996 | 0.193578 |
| 51 | 1410 | 0.006018 | 0.199385 | 1461 | 0.136272 | 0.204128 |
| 50 | 1411 | 0.013007 | 0.183799 | 1462 | 0.068797 | 0.219681 |
| 49 | 1411 | 0.019332 | 0.168031 | 1462 | 0.022058 | 0.225937 |
| 48 | 1412 | 0.033616 | 0.157454 | 1463 | -0.01704 | 0.231223 |
| 47 | 1413 | -0.0191 | 0.17212 | 1463 | -0.04864 | 0.222632 |
| 46 | 1413 | 0.023031 | 0.149938 | 1464 | -0.05013 | 0.208662 |
| 45 | 1414 | -0.00636 | 0.161386 | 1465 | -0.0463 | 0.195959 |
| 44 | 1414 | -0.0008 | 0.159746 | 1465 | 0.009199 | 0.174433 |
| 43 | 1415 | -0.02643 | 0.172443 | 1466 | -0.0198 | 0.174243 |
| 42 | 1416 | 0.033023 | 0.150608 | 1466 | 0.002291 | 0.169585 |
| 41 | 1416 | 0.006973 | 0.165142 | 1467 | -0.03322 | 0.17926 |
| 40 | 1417 | 0.004372 | 0.172147 | 1468 | -0.01984 | 0.180829 |
| 39 | | | | 1468 | -0.03142 | 0.194223 |
| 38 | | | | 1469 | -0.0283 | 0.18433 |
| 37 | | | | 1469 | 0.029261 | 0.158068 |
| 36 | | | | 1470 | -0.00162 | 0.165354 |
| 35 | | | | 1471 | -0.02767 | 0.172547 |
| 34 | | | | 1471 | -0.10046 | 0.210637 |
| 33 | | | | 1472 | -0.06853 | 0.217613 |
| 32 | | | | 1472 | -0.10423 | 0.226376 |
| 31 | | | | 1473 | -0.08295 | 0.206278 |
| 30 | | | | 1474 | -0.08867 | 0.217552 |
| 29 | | | | 1474 | -0.0519 | 0.210588 |
| 28 | | | | 1475 | -0.05169 | 0.205241 |
| 27 | | | | 1475 | -0.09289 | 0.193792 |
| 26 | | | | 1476 | -0.03094 | 0.176691 |
| 25 | | | | 1477 | -0.09616 | 0.206175 |
| 24 | | | | 1477 | -0.11323 | 0.2206 |
| 23 | | | | 1478 | -0.07694 | 0.225417 |
| 22 | | | | 1478 | -0.0668 | 0.223501 |
| 21 | | | | 1479 | -0.11033 | 0.235993 |
| 20 | | | | 1480 | -0.11824 | 0.229901 |

| Elevation cm | Time min | Water Content | Soltrol Content |
|---|---|---|---|
| 118 | 1484 | 0.061236 | 0.08141 |
| 117 | 1485 | 0.044601 | 0.080946 |
| 116 | 1485 | 0.006856 | 0.093891 |
| 115 | 1486 | 0.032048 | 0.092214 |
| 114 | 1486 | 0.08351 | 0.079274 |
| 113 | 1487 | 0.081976 | 0.090446 |
| 112 | 1488 | 0.090117 | 0.100017 |
| 111 | 1488 | 0.08964 | 0.107004 |
| 110 | 1489 | 0.090645 | 0.110578 |
| 109 | 1490 | 0.124996 | 0.102127 |
| 108 | 1490 | 0.161922 | 0.089849 |
| 107 | 1491 | 0.103073 | 0.102376 |
| 106 | 1491 | 0.105764 | 0.106999 |
| 105 | 1492 | 0.119324 | 0.100525 |

| Elevation cm | Time min | Water Content | Soltrol Content |
|---|---|---|---|
| 104 | 1493 | 0.115838 | 0.100936 |
| 103 | 1493 | 0.065231 | 0.119766 |
| 102 | 1494 | 0.162207 | 0.083157 |
| 101 | 1494 | 0.120098 | 0.104282 |
| 100 | 1495 | 0.115342 | 0.117123 |
| 99 | 1496 | 0.094805 | 0.125817 |
| 98 | 1496 | 0.121346 | 0.118018 |
| 97 | 1497 | 0.09438 | 0.124045 |
| 96 | 1497 | 0.138762 | 0.110468 |
| 95 | 1498 | 0.186386 | 0.097228 |
| 94 | 1499 | 0.126535 | 0.116942 |
| 93 | 1499 | 0.190156 | 0.093685 |
| 92 | 1500 | 0.183173 | 0.099742 |
| 91 | 1500 | 0.151218 | 0.115075 |
| 90 | 1501 | 0.175737 | 0.110644 |
| 89 | 1502 | 0.168375 | 0.114088 |
| 88 | 1502 | 0.133456 | 0.122018 |
| 87 | 1503 | 0.129029 | 0.122154 |
| 86 | 1503 | 0.197049 | 0.102719 |
| 85 | 1504 | 0.197929 | 0.106968 |
| 84 | 1505 | 0.217584 | 0.106734 |
| 83 | 1505 | 0.13869 | 0.132964 |
| 82 | 1506 | 0.259071 | 0.096413 |
| 81 | 1506 | 0.171773 | 0.128152 |
| 80 | 1507 | 0.272299 | 0.102031 |
| 79 | 1508 | 0.222305 | 0.116873 |
| 78 | 1508 | 0.229145 | 0.118235 |
| 77 | 1509 | 0.220628 | 0.128201 |
| 76 | 1509 | 0.190466 | 0.139519 |
| 75 | 1510 | 0.277376 | 0.114196 |
| 74 | 1511 | 0.272957 | 0.121322 |
| 73 | 1511 | 0.263115 | 0.126254 |
| 72 | 1512 | 0.256208 | 0.127574 |
| 71 | 1512 | 0.259806 | 0.120467 |
| 70 | 1513 | 0.270841 | 0.120139 |
| 69 | 1514 | 0.266627 | 0.127637 |
| 68 | 1514 | 0.280435 | 0.122583 |
| 67 | 1515 | 0.249207 | 0.135872 |
| 66 | 1515 | 0.220444 | 0.144672 |
| 65 | 1516 | 0.208149 | 0.144098 |
| 64 | 1517 | 0.250906 | 0 117634 |
| 63 | 1517 | 0.148623 | 0.151004 |
| 62 | 1518 | 0.174418 | 0.138138 |
| 61 | 1518 | 0.163573 | 0.141622 |
| 60 | 1519 | 0.173 | 0.138408 |
| 59 | 1520 | 0.139739 | 0.155967 |
| 58 | 1520 | 0.182027 | 0.144798 |
| 57 | 1521 | 0.165833 | 0.152995 |
| 56 | 1521 | 0.171598 | 0.155905 |
| 55 | 1522 | 0.160237 | 0.159549 |
| 54 | 1523 | 0.166245 | 0.17084 |
| 53 | 1523 | 0.169404 | 0.168451 |
| 52 | 1524 | 0.232623 | 0.153225 |
| 51 | 1524 | 0 254598 | 0.140716 |
| 50 | 1525 | 0.138983 | 0.177721 |
| 49 | 1526 | 0.14647 | 0.169235 |
| 48 | 1526 | 0.159429 | 0.16835 |
| 47 | 1527 | 0.158867 | 0.156214 |
| 46 | 1527 | 0.154249 | 0.153087 |

| Elevation cm | Time min | Water Content | *Soltrol* Content |
|---|---|---|---|
| 45 | 1528 | 0.101796 | 0.174772 |
| 44 | 1529 | 0.124403 | 0.166265 |
| 43 | 1529 | 0.1583 | 0.151789 |
| 42 | 1530 | 0.155863 | 0.160407 |
| 41 | 1530 | 0.117311 | 0.174846 |
| 40 | 1531 | 0.129716 | 0.16813 |
| 39 | 1532 | 0.090141 | 0.192192 |
| 38 | 1532 | 0.150839 | 0.169155 |
| 37 | 1533 | 0.118676 | 0.170757 |
| 36 | 1533 | 0.07105 | 0.176235 |
| 35 | 1534 | 0.114519 | 0.160796 |
| 34 | 1535 | 0.052259 | 0.187935 |
| 33 | 1535 | 0.121778 | 0.17587 |
| 32 | 1536 | -0.00313 | 0.222959 |
| 31 | 1536 | 0.052774 | 0.205294 |
| 30 | 1537 | -0.04636 | 0.252437 |
| 29 | 1538 | -0.0588 | 0.266917 |
| 28 | 1538 | -0.04835 | 0.253028 |
| 27 | 1539 | -0.08856 | 0.234422 |
| 26 | 1539 | -0.02005 | 0.205467 |
| 25 | 1540 | -0.04287 | 0.209988 |
| 24 | 1541 | -0.06391 | 0.228482 |
| 23 | 1541 | -0.14335 | 0.268172 |
| 22 | 1542 | -0.1131 | 0.257297 |
| 21 | 1543 | -0.10331 | 0.248302 |
| 20 | 1543 | -0.11041 | 0.23797 |

Spill D
#125 Sand 1000 ml Soltrol Spill

Bulk Density grav.: 1.67g $cm^{-3}$
Porosity: 0.37

| Elevation cm | Soltrol Content after 6 hours | Soltrol Content after 27 hours |
|---|---|---|
| 114.14 | 0.082366 | 0.091152 |
| 111.6 | 0.142187 | 0.064798 |
| 109.06 | 0.091357 | 0.069389 |
| 106.52 | 0.109112 | 0.064 |
| 103.98 | 0.142605 | 0.075153 |
| 101.44 | 0.109846 | 0.092247 |
| 98.9 | 0.160281 | 0.076759 |
| 96.36 | 0.143359 | 0.051913 |
| 93.82 | 0.186652 | 0.099619 |
| 91.28 | 0.161901 | 0.108893 |
| 88.74 | 0.197024 | 0.107505 |
| 86.2 | 0.169978 | 0.089045 |
| 83.66 | 0.239673 | 0.097301 |
| 81.12 | 0.222566 | 0.092384 |
| 78.58 | 0.231926 | 0.10736 |
| 76.04 | 0.274829 | 0.139032 |
| 73.5 | 0.304318 | 0.142354 |
| 70.96 | 0.317352 | 0.123591 |
| 68.42 | 0.273139 | 0.134211 |
| 65.88 | 0.266491 | 0.121273 |
| 63.34 | 0.291925 | 0.109406 |
| 60.8 | 0.281703 | 0.101675 |
| 58.26 | 0.343395 | 0.16055 |
| 55.72 | 0.292227 | 0.10303 |
| 53.18 | 0.28433 | 0.114969 |
| 50.64 | 0.26855 | 0.146399 |
| 48.1 | 0.31173 | 0.151808 |
| 45.56 | 0.274124 | 0.176784 |
| 43.02 | 0.280544 | 0.138455 |
| 40.48 | 0.268412 | 0.178901 |
| 37.94 | 0.255917 | 0.181523 |
| 35.4 | 0.23372 | 0.250728 |
| 32.86 | 0.16046 | 0.22861 |
| 30.32 | 0.079091 | 0.25895 |
| 27.78 | 0.00193 | 0.270626 |
| 25.24 | -0.04131 | 0.268964 |
| 22.7 | -0.02677 | 0.29604 |
| 20.16 | 0.000306 | 0.38219 |
| 17.62 | 0.005551 | 0.39054 |
| 15.08 | -0.01449 | 0.316351 |
| 12.54 | -0.03344 | 0.286392 |

Spill I
#125 Sand 1000 ml Soltrol Spill

Bulk Density grav.: 1.58g $cm^{-3}$
Porosity: 0.40
Temperature Soltrol: 25°C
Residual Water Content: 0.08.

| Elevation cm | Time min | Soltrol Content | Time min | Soltrol Content | Time min | Soltrol Content |
|---|---|---|---|---|---|---|
| 120.00 | 15.00 | 0.32 | 32.00 | 0.26 | 52.00 | 0.32 |
| 119.00 | 16.00 | 0.32 | 33.00 | 0.27 | 53.00 | 0.31 |
| 118.00 | 16.00 | 0.32 | 33.00 | 0.32 | 53.00 | 0.32 |
| 117.00 | 17.00 | 0.32 | 34.00 | 0.32 | 54.00 | 0.31 |
| 116.00 | 17.00 | 0.31 | 34.00 | 0.31 | 54.00 | 0.31 |
| 115.00 | 18.00 | 0.32 | 35.00 | 0.32 | 55.00 | 0.32 |
| 114.00 | 18.00 | 0.31 | 36.00 | 0.31 | 55.00 | 0.32 |
| 113.00 | 19.00 | 0.32 | 36.00 | 0.31 | 56.00 | 0.31 |
| 112.00 | 19.00 | 0.27 | 37.00 | 0.31 | 57.00 | 0.31 |
| 111.00 | 20.00 | 0.26 | 37.00 | 0.31 | 57.00 | 0.31 |
| 110.00 | 20.00 | 0.26 | 38.00 | 0.31 | 58.00 | 0.31 |
| 109.00 | 21.00 | 0.26 | 38.00 | 0.32 | 58.00 | 0.31 |
| 108.00 | 22.00 | 0.26 | 39.00 | 0.31 | 59.00 | 0.31 |
| 107.00 | 22.00 | 0.26 | 39.00 | 0.31 | 59.00 | 0.31 |
| 106.00 | 23.00 | 0.26 | 40.00 | 0.31 | 60.00 | 0.31 |
| 105.00 | 23.00 | 0.26 | 40.00 | 0.31 | 60.00 | 0.30 |
| 104.00 | 24.00 | 0.26 | 41.00 | 0.32 | 61.00 | 0.31 |
| 103.00 | 24.00 | 0.26 | 41.00 | 0.32 | 61.00 | 0.31 |
| 102.00 | 25.00 | 0.26 | 42.00 | 0.31 | 62.00 | 0.30 |
| 101.00 | 25.00 | 0.26 | 42.00 | 0.31 | 62.00 | 0.30 |
| 100.00 | 26.00 | 0.26 | 43.00 | 0.31 | 63.00 | 0.30 |
| 99.00 | 26.00 | 0.26 | 43.00 | 0.31 | 63.00 | 0.30 |
| 98.00 | 27.00 | 0.25 | 45.00 | 0.31 | 64.00 | 0.30 |
| 97.00 | 27.00 | 0.18 | 45.00 | 0.31 | 64.00 | 0.31 |
| 96.00 | 28.00 | 0.07 | 46.00 | 0.31 | 65.00 | 0.30 |
| 95.00 | 28.00 | 0.01 | 46.00 | 0.31 | 66.00 | 0.31 |
| 94.00 | 29.00 | -0.01 | 47.00 | 0.31 | 66.00 | 0.30 |
| 93.00 | 29.00 | -0.02 | 47.00 | 0.31 | 67.00 | 0.30 |
| 92.00 | 30.00 | -0.01 | 48.00 | 0.31 | 67.00 | 0.30 |
| 91.00 | 31.00 | -0.01 | 48.00 | 0.31 | 68.00 | 0.30 |
| 90.00 | 31.00 | -0.02 | 49.00 | 0.29 | 68.00 | 0.30 |
| 89.00 | | | 49.00 | 0.25 | 69.00 | 0.30 |
| 88.00 | | | 50.00 | 0.13 | 69.00 | 0.31 |
| 87.00 | | | 50.00 | 0.05 | 70.00 | 0.31 |
| 86.00 | | | 51.00 | 0.01 | 70.00 | 0.30 |
| 85.00 | | | | | 71.00 | 0.30 |
| 84.00 | | | | | 71.00 | 0.28 |
| 83.00 | | | | | 72.00 | 0.26 |
| 82.00 | | | | | 72.00 | 0.26 |
| 81.00 | | | | | 73.00 | 0.25 |
| 80.00 | | | | | 73.00 | 0.24 |
| 79.00 | | | | | 74.00 | 0.17 |
| 78.00 | | | | | 75.00 | 0.07 |
| 77.00 | | | | | 75.00 | 0.00 |
| 76.00 | | | | | 76.00 | -0.01 |
| 75.00 | | | | | 76.00 | -0.01 |

| Elevation cm | Time min | Soltrol Content | Time min | Soltrol Content | Time min | Soltrol Content |
|---|---|---|---|---|---|---|
| 120.00 | 78.00 | 0.27 | 106.00 | 0.26 | 154.00 | 0.20 |
| 119.00 | 78.00 | 0.28 | 107.00 | 0.26 | 154.00 | 0.20 |
| 118.00 | 79.00 | 0.27 | 107.00 | 0.26 | 155.00 | 0.21 |
| 117.00 | 79.00 | 0.27 | 108.00 | 0.26 | 155.00 | 0.22 |
| 116.00 | 80.00 | 0.27 | 108.00 | 0.26 | 156.00 | 0.23 |
| 115.00 | 80.00 | 0.27 | 109.00 | 0.26 | 156.00 | 0.24 |
| 114.00 | 81.00 | 0.26 | 109.00 | 0.31 | 157.00 | 0.25 |
| 113.00 | 82.00 | 0.26 | 110.00 | 0.31 | 157.00 | 0.24 |
| 112.00 | 82.00 | 0.26 | 110.00 | 0.31 | 158.00 | 0.25 |
| 111.00 | 83.00 | 0.26 | 111.00 | 0.31 | 158.00 | 0.25 |
| 110.00 | 83.00 | 0.26 | 111.00 | 0.31 | 159.00 | 0.24 |
| 109.00 | 84.00 | 0.26 | 112.00 | 0.31 | 159.00 | 0.25 |
| 108.00 | 84.00 | 0.26 | 112.00 | 0.31 | 160.00 | 0.25 |
| 107.00 | 85.00 | 0.25 | 113.00 | 0.31 | 160.00 | 0.26 |
| 106.00 | 85.00 | 0.26 | 113.00 | 0.30 | 161.00 | 0.27 |
| 105.00 | 86.00 | 0.26 | 114.00 | 0.31 | 161.00 | 0.28 |
| 104.00 | 86.00 | 0.26 | 115.00 | 0.31 | 162.00 | 0.28 |
| 103.00 | 87.00 | 0.26 | 115.00 | 0.31 | 163.00 | 0.28 |
| 102.00 | 87.00 | 0.26 | 116.00 | 0.31 | 163.00 | 0.28 |
| 101.00 | 88.00 | 0.26 | 116.00 | 0.31 | 164.00 | 0.29 |
| 100.00 | 88.00 | 0.26 | 117.00 | 0.30 | 164.00 | 0.29 |
| 99.00 | 89.00 | 0.26 | 117.00 | 0.31 | 165.00 | 0.29 |
| 98.00 | 89.00 | 0.29 | 118.00 | 0.31 | 165.00 | 0.29 |
| 97.00 | 90.00 | 0.31 | 118.00 | 0.30 | 166.00 | 0.30 |
| 96.00 | 91.00 | 0.30 | 119.00 | 0.31 | 166.00 | 0.30 |
| 95.00 | 91.00 | 0.30 | 119.00 | 0.30 | 167.00 | 0.30 |
| 94.00 | 92.00 | 0.31 | 120.00 | 0.31 | 167.00 | 0.30 |
| 93.00 | 92.00 | 0.30 | 120.00 | 0.30 | 168.00 | 0.31 |
| 92.00 | 93.00 | 0.30 | 121.00 | 0.30 | 168.00 | 0.31 |
| 91.00 | 93.00 | 0.31 | 121.00 | 0.31 | 169.00 | 0.30 |
| 90.00 | 94.00 | 0.31 | 122.00 | 0.30 | 169.00 | 0.31 |
| 89.00 | 94.00 | 0.31 | 122.00 | 0.31 | 170.00 | 0.30 |
| 88.00 | 95.00 | 0.31 | 123.00 | 0.30 | 170.00 | 0.30 |
| 87.00 | 95.00 | 0.30 | 124.00 | 0.31 | 171.00 | 0.31 |
| 86.00 | 96.00 | 0.31 | 124.00 | 0.31 | 172.00 | 0.30 |
| 85.00 | 96.00 | 0.32 | 125.00 | 0.31 | 172.00 | 0.31 |
| 84.00 | 97.00 | 0.30 | 125.00 | 0.31 | 173.00 | 0.30 |
| 83.00 | 97.00 | 0.31 | 126.00 | 0.30 | 173.00 | 0.31 |
| 82.00 | 98.00 | 0.31 | 126.00 | 0.31 | 174.00 | 0.31 |
| 81.00 | 98.00 | 0.30 | 127.00 | 0.31 | 174.00 | 0.31 |
| 80.00 | 99.00 | 0.31 | 127.00 | 0.31 | 175.00 | 0.30 |
| 79.00 | 100.00 | 0.30 | 128.00 | 0.31 | 175.00 | 0.31 |
| 78.00 | 100.00 | 0.31 | 128.00 | 0.30 | 176.00 | 0.30 |
| 77.00 | 101.00 | 0.31 | 129.00 | 0.30 | 176.00 | 0.31 |
| 76.00 | 101.00 | 0.31 | 129.00 | 0.30 | 177.00 | 0.31 |
| 75.00 | 102.00 | 0.31 | 130.00 | 0.31 | 177.00 | 0.30 |
| 74.00 | 102.00 | 0.30 | 130.00 | 0.31 | 178.00 | 0.30 |
| 73.00 | 103.00 | 0.31 | 131 00 | 0.30 | 178.00 | 0.25 |
| 72.00 | 103 00 | 0.25 | 131.00 | 0.30 | 179.00 | 0.25 |
| 71.00 | 104.00 | 0.25 | 132.00 | 0.30 | 179.00 | 0.26 |
| 70.00 | 104 00 | 0.21 | 133.00 | 0 30 | 180.00 | 0.25 |
| 69.00 | | | 133.00 | 0.30 | 181.00 | 0.25 |
| 68.00 | | | 134.00 | 0.30 | 181.00 | 0.26 |
| 67.00 | | | 134.00 | 0.30 | 182.00 | 0.25 |
| 66.00 | | | 135.00 | 0.30 | 182.00 | 0.25 |
| 65.00 | | | 135 00 | 0.30 | 183.00 | 0.25 |
| 64 00 | | | 136.00 | 0.30 | 183.00 | 0.25 |
| 63.00 | | | 136.00 | 0.24 | 184.00 | 0.27 |

| Elevation cm | Time min | Soltrol Content | Time min | Soltrol Content | Time min | Soltrol Content |
|---|---|---|---|---|---|---|
| 62.00 | | | 137.00 | 0.22 | 184.00 | 0.25 |
| 61.00 | | | 137.00 | 0.18 | 185.00 | 0.24 |
| 60.00 | | | 143.00 | 0.10 | 185.00 | 0.24 |
| 59.00 | | | 144.00 | 0.03 | 186.00 | 0.25 |
| 58.00 | | | 144.00 | -0.01 | 186.00 | 0.23 |
| 57.00 | | | 145.00 | -0.02 | 187.00 | 0.23 |
| 56.00 | | | 145.00 | -0.02 | 187.00 | 0.22 |
| 55.00 | | | 146.00 | -0.02 | 188.00 | 0.21 |
| 54.00 | | | 146.00 | -0.02 | 188.00 | 0.19 |
| 53.00 | | | 147.00 | -0.01 | 189.00 | 0.15 |
| 52.00 | | | 147.00 | -0.02 | 190.00 | 0.08 |
| 51.00 | | | 148.00 | -0.01 | 190.00 | 0.03 |
| 50.00 | | | 148.00 | -0.01 | 191.00 | 0.00 |
| 49.00 | | | 149.00 | -0.02 | 191.00 | -0.01 |
| 48.00 | | | 149.00 | -0.01 | 192.00 | -0.02 |
| 47.00 | | | 150.00 | -0.02 | 192.00 | -0.02 |
| 46.00 | | | 151.00 | -0.02 | 193.00 | -0.03 |
| 45.00 | | | 151.00 | -0.02 | 193.00 | -0.03 |
| 44.00 | | | | | 194.00 | -0.03 |
| 43.00 | | | | | 194.00 | -0.03 |
| 42.00 | | | | | 195.00 | -0.03 |
| 41.00 | | | | | 195.00 | -0.03 |
| 40.00 | | | | | 196.00 | -0.03 |
| 39.00 | | | | | 197.00 | -0.04 |
| 38.00 | | | | | 197.00 | -0.03 |
| 37.00 | | | | | 198.00 | -0.04 |
| 36.00 | | | | | 198.00 | -0.03 |
| 35.00 | | | | | 199.00 | -0.03 |
| 34.00 | | | | | 199.00 | -0.03 |
| 33.00 | | | | | 200.00 | -0.03 |

| Elevation cm | Time min | Soltrol Content | Time min | Soltrol Content | Time min | Soltrol Content |
|---|---|---|---|---|---|---|
| 120.00 | 207.00 | 0.13 | 261.00 | 0.10 | 314.00 | 0.10 |
| 119.00 | 208.00 | 0.12 | 261.00 | 0.10 | 315.00 | 0.10 |
| 118.00 | 208.00 | 0.13 | 262.00 | 0.10 | 315.00 | 0.10 |
| 117.00 | 209.00 | 0.15 | 262.00 | 0.11 | 316.00 | 0.11 |
| 116.00 | 209.00 | 0.15 | 263.00 | 0.12 | 316.00 | 0.12 |
| 115.00 | 210.00 | 0.17 | 263.00 | 0.14 | 317.00 | 0.14 |
| 114.00 | 210.00 | 0.18 | 264.00 | 0.15 | 317.00 | 0.15 |
| 113.00 | 211.00 | 0.18 | 264.00 | 0.16 | 318.00 | 0.16 |
| 112.00 | 211.00 | 0.17 | 265.00 | 0.16 | 318.00 | 0.16 |
| 111.00 | 212.00 | 0.18 | 265.00 | 0.16 | 319.00 | 0.16 |
| 110.00 | 212.00 | 0.17 | 266.00 | 0.14 | 319.00 | 0.15 |
| 109.00 | 213.00 | 0.17 | 266.00 | 0.15 | 320.00 | 0.14 |
| 108.00 | 213.00 | 0.18 | 267.00 | 0.15 | 320.00 | 0.13 |
| 107.00 | 214.00 | 0.17 | 267.00 | 0.15 | 321.00 | 0.14 |
| 106.00 | 214.00 | 0.17 | 268.00 | 0.15 | 321.00 | 0.13 |
| 105.00 | 215.00 | 0.18 | 268.00 | 0.15 | 322.00 | 0.14 |
| 104.00 | 216.00 | 0.17 | 269.00 | 0.15 | 323.00 | 0.14 |
| 103.00 | 216.00 | 0.17 | 270.00 | 0.14 | 323.00 | 0.13 |
| 102.00 | 217.00 | 0.17 | 270.00 | 0.15 | 324.00 | 0.13 |
| 101.00 | 217.00 | 0.18 | 271.00 | 0.15 | 324.00 | 0.13 |
| 100.00 | 218.00 | 0.18 | 271.00 | 0.15 | 325.00 | 0.14 |
| 99.00 | 218.00 | 0.19 | 272.00 | 0.16 | 325.00 | 0.14 |
| 98.00 | 219.00 | 0.18 | 272.00 | 0.16 | 326.00 | 0.14 |
| 97.00 | 219.00 | 0.19 | 273.00 | 0.16 | 326.00 | 0.14 |
| 96.00 | 220.00 | 0.19 | 273.00 | 0.15 | 327.00 | 0.14 |
| 95.00 | 220.00 | 0.19 | 274.00 | 0.16 | 327.00 | 0.14 |
| 94.00 | 221.00 | 0.20 | 274.00 | 0.16 | 328.00 | 0.14 |
| 93.00 | 221.00 | 0.20 | 275.00 | 0.16 | 328.00 | 0.14 |
| 92.00 | 222.00 | 0.21 | 275.00 | 0.16 | 329.00 | 0.14 |
| 91.00 | 222.00 | 0.21 | 276.00 | 0.17 | 329.00 | 0.14 |
| 90.00 | 223.00 | 0.21 | 276.00 | 0.16 | 330.00 | 0.14 |
| 89.00 | 224.00 | 0.21 | 277.00 | 0.17 | 331.00 | 0.15 |
| 88.00 | 224.00 | 0.22 | 278.00 | 0.17 | 331.00 | 0.15 |
| 87.00 | 225.00 | 0.22 | 278.00 | 0.17 | 332.00 | 0.14 |
| 86.00 | 225.00 | 0.23 | 279.00 | 0.17 | 332.00 | 0.17 |
| 85.00 | 226.00 | 0.24 | 279.00 | 0.18 | 333.00 | 0.15 |
| 84.00 | 226.00 | 0.25 | 280.00 | 0.18 | 333.00 | 0.16 |
| 83.00 | 227.00 | 0.25 | 280.00 | 0.19 | 334.00 | 0.16 |
| 82.00 | 227.00 | 0.26 | 281.00 | 0.19 | 334.00 | 0.17 |
| 81.00 | 228.00 | 0.27 | 281.00 | 0.21 | 335.00 | 0.17 |
| 80.00 | 228.00 | 0.26 | 282.00 | 0.22 | 335.00 | 0.17 |
| 79.00 | 229.00 | 0.25 | 282.00 | 0.22 | 336.00 | 0.19 |
| 78.00 | 229.00 | 0.26 | 283.00 | 0.24 | 336.00 | 0.18 |
| 77.00 | 230.00 | 0.25 | 283.00 | 0.24 | 337.00 | 0.20 |
| 76.00 | 230.00 | 0.25 | 284.00 | 0.25 | 337.00 | 0.23 |
| 75.00 | 231.00 | 0.26 | 284.00 | 0.25 | 338.00 | 0.22 |
| 74.00 | 231.00 | 0.25 | 285.00 | 0.26 | 338.00 | 0.20 |
| 73.00 | 232.00 | 0.25 | 285.00 | 0.26 | 339.00 | 0.22 |
| 72.00 | 233.00 | 0.25 | 286.00 | 0.25 | 340.00 | 0.23 |
| 71.00 | 233.00 | 0.25 | 287.00 | 0.25 | 340.00 | 0 25 |
| 70.00 | 234.00 | 0.25 | 287.00 | 0.25 | 341.00 | 0.25 |
| 69.00 | 234.00 | 0.26 | 288.00 | 0.25 | 341.00 | 0.25 |
| 68.00 | 235.00 | 0.26 | 288.00 | 0.25 | 342.00 | 0.25 |
| 67.00 | 235.00 | 0.25 | 289.00 | 0.25 | 342.00 | 0.25 |
| 66.00 | 236.00 | 0.25 | 289.00 | 0.25 | 343.00 | 0.26 |
| 65.00 | 236.00 | 0.25 | 290.00 | 0.25 | 343.00 | 0.25 |
| 64.00 | 237.00 | 0.25 | 290.00 | 0.25 | 344.00 | 0.26 |
| 63.00 | 237.00 | 0.25 | 291.00 | 0.24 | 344.00 | 0.26 |
| 62.00 | 238.00 | 0.24 | 291.00 | 0.24 | 345.00 | 0.26 |

| Elevation cm | Time min | Soltrol Content | Time min | Soltrol Content | Time min | Soltrol Content |
|---|---|---|---|---|---|---|
| 61.00 | 238.00 | 0.24 | 292.00 | 0.24 | 345.00 | 0.25 |
| 60.00 | 239.00 | 0.24 | 292.00 | 0.24 | 346.00 | 0.24 |
| 59.00 | 239.00 | 0.24 | 293.00 | 0.24 | 346.00 | 0.25 |
| 58.00 | 240.00 | 0.24 | 293.00 | 0.23 | 347.00 | 0.24 |
| 57.00 | 240.00 | 0.24 | 294.00 | 0.24 | 347.00 | 0.23 |
| 56.00 | 241.00 | 0.24 | 294.00 | 0.23 | 348.00 | 0.23 |
| 55.00 | 242.00 | 0.24 | 295.00 | 0.24 | 349.00 | 0.23 |
| 54.00 | 242.00 | 0.24 | 296.00 | 0.24 | 349.00 | 0.23 |
| 53.00 | 243.00 | 0.23 | 296.00 | 0.23 | 350.00 | 0.27 |
| 52.00 | 243.00 | 0.22 | 297.00 | 0.22 | 350.00 | 0.24 |
| 51.00 | 244.00 | 0.21 | 297.00 | 0.22 | 351.00 | 0.22 |
| 50.00 | 244.00 | 0.21 | 298.00 | 0.22 | 351.00 | 0.22 |
| 49.00 | 245.00 | 0.21 | 298.00 | 0.22 | 352.00 | 0.22 |
| 48.00 | 245.00 | 0.20 | 299.00 | 0.21 | 352.00 | 0.23 |
| 47.00 | 246.00 | 0.20 | 299.00 | 0.21 | 353.00 | 0.21 |
| 46.00 | 246.00 | 0.18 | 300.00 | 0.21 | 353.00 | 0.23 |
| 45.00 | 247.00 | 0.16 | 300.00 | 0.21 | 354.00 | 0.21 |
| 44.00 | 247.00 | 0.10 | 301.00 | 0.20 | 354.00 | 0.22 |
| 43.00 | 248.00 | 0.02 | 301.00 | 0.20 | 355.00 | 0.22 |
| 42.00 | 248.00 | -0.02 | 302.00 | 0.19 | 355.00 | 0.21 |
| 41.00 | 249.00 | -0.03 | 302.00 | 0.19 | 356.00 | 0.22 |
| 40.00 | 249.00 | -0.03 | 303.00 | 0.17 | 356.00 | 0.19 |
| 39.00 | 250.00 | -0.03 | 304.00 | 0.15 | 357.00 | 0.18 |
| 38.00 | 251.00 | -0.03 | 304.00 | 0.13 | 358.00 | 0.18 |
| 37.00 | 251.00 | -0.04 | 305.00 | 0.10 | 358.00 | 0.17 |
| 36.00 | 252.00 | -0.03 | 305.00 | 0.05 | 359.00 | 0.18 |
| 35.00 | 252.00 | -0.03 | 306.00 | 0.01 | 359.00 | 0.18 |
| 34.00 | 253.00 | -0.03 | 306.00 | -0.01 | 360.00 | 0.17 |
| 33.00 | 253.00 | -0.03 | 307.00 | -0.02 | 360.00 | 0.15 |
| 32.00 | 254.00 | -0.03 | 307.00 | -0.03 | 361.00 | 0.12 |
| 31.00 | 254.00 | -0.03 | 308.00 | -0.03 | 361.00 | 0.11 |
| 30.00 | 255.00 | -0.03 | 308.00 | -0.03 | 362.00 | 0.08 |
| 29.00 | 255.00 | -0.03 | 309.00 | -0.03 | 362.00 | 0.04 |
| 28.00 | 256.00 | -0.03 | 309.00 | -0.03 | 363.00 | 0.01 |
| 27.00 | 256.00 | -0.03 | 310.00 | -0.03 | 363.00 | -0.01 |
| 26.00 | 257.00 | -0.03 | 310.00 | -0.03 | 364.00 | -0.02 |
| 25.00 | 258.00 | -0.02 | 311.00 | -0.02 | 364.00 | -0.02 |

| Elevation cm | Time min | Soltrol Content |
|---|---|---|
| 120.00 | 367.00 | 0.09 |
| 119.00 | 368.00 | 0.09 |
| 118.00 | 369.00 | 0.09 |
| 117.00 | 369.00 | 0.10 |
| 116.00 | 370.00 | 0.12 |
| 115.00 | 370.00 | 0.13 |
| 114.00 | 371.00 | 0.14 |
| 113.00 | 371.00 | 0.15 |
| 112.00 | 372.00 | 0.15 |
| 111.00 | 372.00 | 0.15 |
| 110.00 | 373.00 | 0.15 |
| 109.00 | 373.00 | 0.14 |
| 108.00 | 374.00 | 0.15 |
| 107.00 | 374.00 | 0.13 |
| 106.00 | 375.00 | 0.13 |
| 105.00 | 376.00 | 0.13 |
| 104.00 | 376.00 | 0.13 |
| 103.00 | 377.00 | 0.13 |
| 102.00 | 377.00 | 0.12 |
| 101.00 | 378.00 | 0.13 |
| 100.00 | 378.00 | 0.13 |
| 99.00 | 379.00 | 0.13 |
| 98.00 | 379.00 | 0.14 |
| 97.00 | 380.00 | 0.13 |
| 96.00 | 380.00 | 0.13 |
| 95.00 | 381.00 | 0.13 |
| 94.00 | 381.00 | 0.13 |
| 93.00 | 382.00 | 0.13 |
| 92.00 | 382.00 | 0.13 |
| 91.00 | 383.00 | 0.14 |
| 90.00 | 384.00 | 0.13 |
| 89.00 | 384.00 | 0.13 |
| 88.00 | 385.00 | 0.13 |
| 87.00 | 385.00 | 0.13 |
| 86.00 | 386.00 | 0.14 |
| 85.00 | 386.00 | 0.16 |
| 84.00 | 387.00 | 0.16 |
| 83.00 | 387.00 | 0.16 |
| 82.00 | 388.00 | 0.16 |
| 81.00 | 388.00 | 0.15 |
| 80.00 | 389.00 | 0.15 |
| 79.00 | 389.00 | 0.15 |
| 78.00 | 390.00 | 0.14 |
| 77.00 | 390.00 | 0.16 |
| 76.00 | 391.00 | 0.15 |
| 75.00 | 391.00 | 0.17 |
| 74.00 | 392.00 | 0.17 |
| 73.00 | 393.00 | 0.16 |
| 72.00 | 393.00 | 0.18 |
| 71.00 | 394.00 | 0.19 |
| 70.00 | 394.00 | 0.21 |
| 69.00 | 395.00 | 0.22 |
| 68.00 | 395.00 | 0.22 |
| 67.00 | 396.00 | 0.23 |
| 66.00 | 396.00 | 0.23 |
| 65.00 | 397.00 | 0.23 |
| 64.00 | 397.00 | 0.24 |
| 63.00 | 398.00 | 0.24 |
| 62.00 | 398.00 | 0.24 |

| Elevation cm | Time min | Soltrol Content |
|---|---|---|
| 61.00 | 399.00 | 0.24 |
| 60.00 | 399.00 | 0.23 |
| 59.00 | 400.00 | 0.23 |
| 58.00 | 401.00 | 0.23 |
| 57.00 | 401.00 | 0.22 |
| 56.00 | 402.00 | 0.23 |
| 55.00 | 402.00 | 0.22 |
| 54.00 | 403.00 | 0.23 |
| 53.00 | 403.00 | 0.23 |
| 52.00 | 404.00 | 0.24 |
| 51.00 | 404.00 | 0.23 |
| 50.00 | 405.00 | 0.23 |
| 49.00 | 405.00 | 0.24 |
| 48.00 | 406.00 | 0.23 |
| 47.00 | 406.00 | 0.23 |
| 46.00 | 407.00 | 0.24 |
| 45.00 | 407.00 | 0.23 |
| 44.00 | 408.00 | 0.23 |
| 43.00 | 409.00 | 0.24 |
| 42.00 | 409.00 | 0.22 |
| 41.00 | 410.00 | 0.23 |
| 40.00 | 410.00 | 0.23 |
| 39.00 | 411.00 | 0.20 |
| 38.00 | 411.00 | 0.20 |
| 37.00 | 412.00 | 0.18 |
| 36.00 | 412.00 | 0.18 |
| 35.00 | 413.00 | 0.19 |
| 34.00 | 413.00 | 0.18 |
| 33.00 | 414.00 | 0.18 |
| 32.00 | 414.00 | 0.17 |
| 31.00 | 415.00 | 0.17 |
| 30.00 | 415.00 | 0.18 |
| 29.00 | 416.00 | 0.17 |
| 28.00 | 416.00 | 0.15 |
| 27.00 | 417.00 | 0.13 |
| 26.00 | 418.00 | 0.12 |
| 25.00 | 418.00 | 0.10 |

Spill J
#70 Sand 500 ml Soltrol Spill Porosity: 0.47

Bulk Density grav.: 1.40g $cm^{-3}$

Temperature Soltrol: 22°C

| Elevation cm | Time min | Soltrol Content | Time min | Soltrol Content | Time min | Soltrol Content |
|---|---|---|---|---|---|---|
| 120.00 | 3.00 | 0.32 | 16.00 | 0.30 | 32.00 | 0.31 |
| 118.00 | 3.00 | 0.31 | 16.00 | 0.31 | 33.00 | 0.31 |
| 116.00 | 4.00 | 0.32 | 17.00 | 0.31 | 33.00 | 0.31 |
| 114.00 | 4.00 | 0.31 | 17.00 | 0.32 | 34.00 | 0.31 |
| 112.00 | 5.00 | 0.17 | 18.00 | 0.30 | 34.00 | 0.31 |
| 110.00 | 6.00 | 0.02 | 18.00 | 0.31 | 35.00 | 0.30 |
| 108.00 | 6.00 | 0.00 | 19.00 | 0.31 | 35.00 | 0.30 |
| 106.00 | 7.00 | -0.01 | 19.00 | 0.31 | 36.00 | 0.31 |
| 104.00 | 7.00 | -0.01 | 20.00 | 0.30 | 37.00 | 0.30 |
| 102.00 | 8.00 | -0.01 | 21.00 | 0.27 | 37.00 | 0.31 |
| 100.00 | 8.00 | -0.01 | 21.00 | 0.02 | 38.00 | 0.31 |
| 98.00 | 9.00 | -0.01 | 22.00 | 0.00 | 38.00 | 0.30 |
| 96.00 | 9.00 | 0.00 | 22.00 | 0.00 | 39.00 | 0.23 |
| 94.00 | 10.00 | -0.01 | 23.00 | 0.00 | 39.00 | 0.01 |
| 92.00 | 11.00 | 0.00 | 23.00 | 0.00 | 40.00 | -0.01 |
| 90.00 | 11.00 | 0.00 | 24.00 | 0.00 | 40.00 | 0.00 |
| 88.00 | 12.00 | 0.00 | 25.00 | 0.00 | 41.00 | 0.00 |
| 86.00 | 12.00 | 0.01 | 25.00 | 0.00 | 42.00 | 0.01 |
| 84.00 | 13.00 | 0.01 | 26.00 | 0.01 | 42.00 | 0.01 |
| 82.00 | 13.00 | 0.00 | 26.00 | 0.00 | 43.00 | 0.00 |
| 80.00 | 14.00 | 0.00 | 27.00 | 0.01 | 43.00 | 0.00 |
| 78.00 | | | 27.00 | 0.01 | 44.00 | 0.00 |
| 76.00 | | | 28.00 | 0.00 | 44.00 | 0.00 |
| 74.00 | | | 29.00 | 0.00 | 45.00 | 0.00 |
| 72.00 | | | 29.00 | 0.01 | 46.00 | 0.00 |
| 70.00 | | | 30.00 | 0.00 | 46.00 | 0.01 |
| 68.00 | | | | | 47.00 | 0.01 |
| 66.00 | | | | | 47.00 | 0.00 |
| 64.00 | | | | | 48.00 | 0.00 |
| 62.00 | | | | | 48.00 | 0.00 |

| Elevation cm | Time min | Soltrol Content | Time min | Soltrol Content | Time min | Soltrol Content |
|---|---|---|---|---|---|---|
| 120.00 | 52.00 | 0.25 | 74.00 | 0.21 | 99.00 | 0.14 |
| 118.00 | 52.00 | 0.23 | 74.00 | 0.18 | 100.00 | 0.17 |
| 116.00 | 53.00 | 0.23 | 75.00 | 0.18 | 100.00 | 0.14 |
| 114.00 | 53.00 | 0.25 | 76.00 | 0.19 | 101.00 | 0.16 |
| 112.00 | 54.00 | 0.29 | 76.00 | 0.22 | 101.00 | 0.18 |
| 110.00 | 54.00 | 0.30 | 77.00 | 0.26 | 102.00 | 0.22 |
| 108.00 | 55.00 | 0.30 | 77.00 | 0.27 | 103.00 | 0.24 |
| 106.00 | 56.00 | 0.31 | 78.00 | 0.28 | 103.00 | 0.24 |
| 104.00 | 56.00 | 0.30 | 78.00 | 0.30 | 104.00 | 0.26 |
| 102.00 | 57.00 | 0.30 | 79.00 | 0.31 | 104.00 | 0.27 |
| 100.00 | 57.00 | 0.31 | 79.00 | 0.31 | 105.00 | 0.30 |
| 98.00 | 58.00 | 0.30 | 80.00 | 0.30 | 105.00 | 0.31 |
| 96.00 | 58.00 | 0.29 | 81.00 | 0.28 | 106.00 | 0.29 |
| 94.00 | 59.00 | 0.25 | 81.00 | 0.28 | 106.00 | 0.28 |
| 92.00 | 59.00 | 0.05 | 82.00 | 0.27 | 107.00 | 0.28 |
| 90.00 | 60.00 | 0.00 | 82.00 | 0.26 | 108.00 | 0.28 |
| 88.00 | 61.00 | 0.01 | 83.00 | 0.07 | 108.00 | 0.29 |
| 86.00 | 61.00 | 0.00 | 83.00 | 0.01 | 109.00 | 0.27 |
| 84.00 | 62.00 | 0.00 | 84.00 | 0.00 | 109.00 | 0.06 |
| 82.00 | 62.00 | 0.00 | 84.00 | 0.00 | 110.00 | 0.00 |

| Elevation cm | Time min | Soltrol Content | Time min | Soltrol Content | Time min | Soltrol Content |
|---|---|---|---|---|---|---|
| 80.00 | 63.00 | 0.01 | 85.00 | 0.01 | 110.00 | 0.00 |
| 78.00 | 63.00 | 0.00 | 86.00 | 0.00 | 111.00 | 0.00 |
| 76.00 | 64.00 | 0.00 | 86.00 | 0.00 | 111.00 | 0.01 |
| 74.00 | 65.00 | 0.00 | 87.00 | 0.00 | 112.00 | 0.00 |
| 72.00 | 65.00 | 0.00 | 87.00 | 0.00 | 113.00 | 0.00 |
| 70.00 | 66.00 | 0.01 | 88.00 | 0.01 | 113.00 | 0.00 |
| 68.00 | 66.00 | 0.00 | 88.00 | 0.01 | 114.00 | 0.01 |
| 66.00 | 67.00 | 0.00 | 89.00 | -0.01 | 114.00 | 0.00 |
| 64.00 | 67.00 | 0.00 | 90.00 | 0.00 | 115.00 | 0.00 |
| 62.00 | 68.00 | 0.00 | 90.00 | 0.00 | 115.00 | 0.00 |
| 60.00 | 69.00 | 0.00 | 91.00 | -0.01 | 116.00 | 0.00 |
| 58.00 | 69.00 | 0.00 | 91.00 | 0.00 | 117.00 | -0.01 |
| 56.00 | 70.00 | 0.00 | 92.00 | 0.00 | 117.00 | 0.00 |
| 54.00 | 70.00 | -0.01 | 92.00 | 0.00 | 118.00 | 0.00 |
| 52.00 | | | 93.00 | 0.00 | 118.00 | 0.00 |
| 50.00 | | | 94.00 | 0.00 | 119.00 | 0.00 |
| 48.00 | | | 94.00 | 0.00 | 119.00 | 0.00 |
| 46.00 | | | 95.00 | -0.01 | 120.00 | 0.00 |
| 44.00 | | | 95.00 | -0.01 | 121.00 | -0.01 |
| 42.00 | | | | | 121.00 | -0.01 |
| 40.00 | | | | | 122.00 | 0.00 |
| 38.00 | | | | | 122.00 | -0.01 |
| 36.00 | | | | | 123.00 | -0.01 |
| 34.00 | | | | | 123.00 | 0.00 |

| Elevation cm | Time min | Soltrol Content | Time min | Soltrol Content | Time min | Soltrol Content |
|---|---|---|---|---|---|---|
| 120.00 | 128.00 | 0.17 | 157.00 | 0.15 | 186.00 | 0.15 |
| 118.00 | 129.00 | 0.14 | 158.00 | 0.12 | 186.00 | 0.13 |
| 116.00 | 129.00 | 0.13 | 158.00 | 0.13 | 187.00 | 0.12 |
| 114.00 | 130.00 | 0.15 | 159.00 | 0.15 | 187.00 | 0.13 |
| 112.00 | 130.00 | 0.17 | 159.00 | 0.17 | 188.00 | 0.14 |
| 110.00 | 131.00 | 0.22 | 160.00 | 0.20 | 189.00 | 0.18 |
| 108.00 | 132.00 | 0.21 | 161.00 | 0.19 | 189.00 | 0.19 |
| 106.00 | 132.00 | 0.22 | 161.00 | 0.20 | 190.00 | 0.19 |
| 104.00 | 133.00 | 0.23 | 162.00 | 0.19 | 190.00 | 0.19 |
| 102.00 | 133.00 | 0.25 | 162.00 | 0.22 | 191.00 | 0.19 |
| 100.00 | 134.00 | 0.28 | 163.00 | 0.28 | 191.00 | 0.22 |
| 98.00 | 134.00 | 0.28 | 163.00 | 0.27 | 192.00 | 0.25 |
| 96.00 | 135.00 | 0.28 | 164.00 | 0.26 | 192.00 | 0.25 |
| 94.00 | 135.00 | 0.28 | 164.00 | 0.26 | 193.00 | 0.25 |
| 92.00 | 136.00 | 0.27 | 165.00 | 0.27 | 194.00 | 0.26 |
| 90.00 | 137.00 | 0.28 | 166.00 | 0.28 | 194.00 | 0.27 |
| 88.00 | 137.00 | 0.29 | 166.00 | 0.29 | 195.00 | 0.29 |
| 86.00 | 138.00 | 0.29 | 167.00 | 0.28 | 195.00 | 0.29 |
| 84.00 | 138.00 | 0.23 | 167.00 | 0.28 | 196.00 | 0.27 |
| 82.00 | 139.00 | 0.03 | 168.00 | 0.17 | 196.00 | 0.27 |
| 80.00 | 139.00 | 0.01 | 168.00 | 0.02 | 197.00 | 0.24 |
| 78.00 | 140.00 | 0.01 | 169.00 | 0.01 | 197.00 | 0.05 |
| 76.00 | 140.00 | 0.00 | 169.00 | 0.00 | 198.00 | 0.01 |
| 74.00 | 141.00 | 0.00 | 170.00 | 0.01 | 199.00 | 0.01 |
| 72.00 | 142.00 | 0.00 | 171.00 | 0.00 | 199.00 | 0.00 |
| 70.00 | 142.00 | 0.01 | 171.00 | 0.01 | 200.00 | 0.01 |
| 68.00 | 143.00 | 0.00 | 172.00 | 0.00 | 200.00 | 0.00 |
| 66.00 | 143.00 | 0.00 | 172.00 | -0.01 | 201.00 | 0.00 |
| 64.00 | 144.00 | 0.00 | 173.00 | 0.01 | 201.00 | 0.00 |
| 62.00 | 144.00 | -0.01 | 173.00 | 0.00 | 202.00 | 0.00 |
| 60.00 | 145.00 | 0.00 | 174.00 | 0.00 | 203.00 | -0.01 |

| Elevation cm | Time min | Soltrol Content | Time min | Soltrol Content | Time min | Soltrol Content |
|---|---|---|---|---|---|---|
| 58.00 | 146.00 | 0.00 | 175.00 | 0.00 | 203.00 | 0.00 |
| 56.00 | 146.00 | 0.00 | 175.00 | 0.00 | 204.00 | 0.00 |
| 54.00 | 147.00 | -0.01 | 176.00 | -0.01 | 204.00 | 0.00 |
| 52.00 | 147.00 | 0.00 | 176.00 | -0.01 | 205.00 | 0.00 |
| 50.00 | 148.00 | -0.01 | 177.00 | -0.01 | 205.00 | 0.00 |
| 48.00 | 148.00 | -0.01 | 177.00 | 0.00 | 206.00 | 0.00 |
| 46.00 | 149.00 | 0.00 | 178.00 | -0.01 | 206.00 | 0.00 |
| 44.00 | 149.00 | -0.01 | 179.00 | -0.01 | 207.00 | -0.01 |
| 42.00 | 150.00 | 0.00 | 179.00 | 0.01 | 208.00 | -0.01 |
| 40.00 | 151.00 | 0.00 | 180.00 | 0.00 | 208.00 | 0.00 |
| 38.00 | 151.00 | 0.00 | 180.00 | -0.01 | 209.00 | -0.01 |
| 36.00 | 152.00 | -0.01 | | | | |

| Elevation cm | Time min | Soltrol Content | Time min | Soltrol Content |
|---|---|---|---|---|
| 120.00 | 215.00 | 0.13 | 1035.00 | 0.09 |
| 118.00 | 215.00 | 0.11 | 1036.00 | 0.07 |
| 116.00 | 216.00 | 0.12 | 1036.00 | 0.07 |
| 114.00 | 217.00 | 0.14 | 1037.00 | 0.08 |
| 112.00 | 217.00 | 0.16 | 1038.00 | 0.10 |
| 110.00 | 218.00 | 0.18 | 1038.00 | 0.12 |
| 108.00 | 218.00 | 0.17 | 1039.00 | 0.11 |
| 106.00 | 219.00 | 0.18 | 1039.00 | 0.12 |
| 104.00 | 219.00 | 0.17 | 1040.00 | 0.11 |
| 102.00 | 220.00 | 0.18 | 1040.00 | 0.11 |
| 100.00 | 220.00 | 0.21 | 1041.00 | 0.13 |
| 98.00 | 221.00 | 0.23 | 1041.00 | 0.14 |
| 96.00 | 222.00 | 0.24 | 1042.00 | 0.14 |
| 94.00 | 222.00 | 0.25 | 1043.00 | 0.15 |
| 92.00 | 223.00 | 0.25 | 1043.00 | 0.15 |
| 90.00 | 223.00 | 0.28 | 1044.00 | 0.16 |
| 88.00 | 224.00 | 0.28 | 1044.00 | 0.19 |
| 86.00 | 224.00 | 0.27 | 1045.00 | 0.19 |
| 84.00 | 225.00 | 0.27 | 1045.00 | 0.19 |
| 82.00 | 225.00 | 0.27 | 1046.00 | 0.19 |
| 80.00 | 226.00 | 0.27 | 1046.00 | 0.22 |
| 78.00 | 227.00 | 0.10 | 1047.00 | 0.21 |
| 76.00 | 227.00 | 0.01 | 1048.00 | 0.21 |
| 74.00 | 228.00 | 0.01 | 1048.00 | 0.22 |
| 72.00 | 228.00 | 0.00 | 1049.00 | 0.23 |
| 70.00 | 229.00 | 0.01 | 1049.00 | 0.24 |
| 68.00 | 229.00 | 0.00 | 1050.00 | 0.22 |
| 66.00 | 230.00 | 0.00 | 1050.00 | 0.22 |
| 64.00 | 231.00 | 0.00 | 1051.00 | 0.22 |
| 62.00 | 231.00 | 0.00 | 1051.00 | 0.18 |
| 60.00 | 232.00 | -0.01 | 1052.00 | 0.06 |
| 58.00 | 232.00 | 0.00 | 1053.00 | 0.01 |
| 56.00 | 233.00 | 0.00 | 1053.00 | 0.00 |
| 54.00 | 233.00 | 0.00 | 1054.00 | 0.00 |
| 52.00 | 234.00 | -0.01 | 1054.00 | 0.00 |
| 50.00 | 235.00 | -0.01 | 1055.00 | 0.00 |
| 48.00 | 235.00 | -0.01 | 1055.00 | 0.01 |
| 46.00 | 236.00 | -0.01 | 1056.00 | 0.00 |
| 44.00 | 236.00 | -0.01 | 1057.00 | 0.00 |
| 42.00 | 237.00 | 0.00 | 1057.00 | 0.01 |
| 40.00 | 237.00 | -0.01 | 1058.00 | 0.00 |
| 38.00 | | | 1058.00 | 0.00 |
| 36.00 | | | 1059.00 | 0.00 |

| Elevation cm | Time min | Soltrol Content | Time min | Soltrol Content |
|---|---|---|---|---|
| 34.00 | | | 1059.00 | 0.00 |
| 32.00 | | | 1060.00 | 0.00 |

Spill N
#70 Sand 750 ml Soltrol Spill Porosity: 0.48
Rain 500ml/hour after 86 minutes.

Bulk Density grav.: 1.39g $cm^{-3}$

Temperature Soltrol: 21°C
Temperature Water: 24°C
Residual water content: 0.06.

| Elevation cm | Time min | Water Content | Soltrol Content | Time min | Water Content | Soltrol Content |
|---|---|---|---|---|---|---|
| 115 | 3 | -0.0021 | 0.436065 | 32 | 0.020082 | 0.415094 |
| 114 | 4 | 0.021777 | 0.413878 | 32 | 0.005478 | 0.419199 |
| 113 | 4 | 0.024549 | 0.399624 | 33 | -0.01243 | 0.41538 |
| 112 | 5 | -0.0135 | 0.417071 | 33 | -0.00579 | 0.413683 |
| 111 | 5 | 0.009536 | 0.400511 | 34 | 0.004664 | 0.401148 |
| 110 | 6 | -0.01279 | 0.407971 | 35 | -0.0171 | 0.413873 |
| 109 | 6 | -0.0234 | 0.417602 | 35 | -0.01399 | 0.404229 |
| 108 | 7 | -0.00719 | 0.409034 | 36 | -0.0336 | 0.411386 |
| 107 | 7 | -0.02569 | 0.410186 | 36 | -0.05216 | 0.417362 |
| 106 | 8 | -0.00513 | 0.404954 | 37 | -0.0156 | 0.409714 |
| 105 | 8 | -0.01745 | 0.406887 | 37 | 0.013324 | 0.39179 |
| 104 | 9 | -0.03513 | 0.410969 | 38 | -0.01365 | 0.408329 |
| 103 | 9 | -0.01843 | 0.406296 | 38 | 0.007238 | 0.393551 |
| 102 | 10 | -0.01576 | 0.405126 | 39 | -0.00883 | 0.399143 |
| 101 | 10 | -0.00637 | 0.400578 | 39 | 0.017353 | 0.392564 |
| 100 | 11 | -0.0066 | 0.398688 | 40 | -0.01226 | 0.409243 |
| 99 | 11 | 0.014298 | 0.385375 | 40 | -0.02152 | 0.402164 |
| 98 | 12 | -0.00681 | 0.390456 | 41 | -0.03101 | 0.412982 |
| 97 | 13 | -0.00504 | 0.384054 | 41 | -0.01643 | 0.414145 |
| 96 | 13 | 0.045165 | 0.291223 | 42 | -0.00428 | 0.405086 |
| 95 | 14 | 0.024269 | 0.185312 | 42 | 0.002645 | 0.397021 |
| 94 | 14 | 0.063355 | 0.081416 | 43 | -0.01593 | 0.403012 |
| 93 | 15 | 0.034546 | 0.041725 | 43 | -0.00675 | 0.403795 |
| 92 | 15 | 0.039022 | 0.015172 | 44 | -0.0173 | 0.408682 |
| 91 | 16 | 0.034515 | 0.007598 | 44 | -0.0305 | 0.410149 |
| 90 | 16 | 0.070401 | -0.00017 | 45 | 0.008034 | 0.394425 |
| 89 | 17 | 0.048104 | 0.008655 | 45 | -0.03066 | 0.416712 |
| 88 | 17 | 0.041587 | 0.007629 | 46 | -0.0298 | 0.413679 |
| 87 | 18 | 0.056925 | 0.003662 | 46 | -0.01833 | 0.409451 |
| 86 | 18 | 0.076364 | -0.00215 | 47 | -0.01634 | 0.409847 |
| 85 | 19 | 0.063285 | 0.00202 | 47 | 0.006168 | 0.396108 |
| 84 | 19 | 0.038303 | 0.007975 | 48 | -0.01412 | 0.40303 |
| 83 | 20 | 0.077923 | -0.00362 | 48 | -0.00205 | 0.39128 |
| 82 | 20 | 0.059252 | 0.003331 | 49 | -0.01823 | 0.395289 |
| 81 | 21 | 0.06711 | 0.013714 | 49 | 0.042915 | 0.382415 |
| 80 | 21 | 0.086986 | 0.015609 | 50 | -0.02025 | 0.405123 |
| 79 | 22 | 0.087412 | 0.008011 | 50 | 0.025825 | 0.383095 |
| 78 | 22 | 0.087937 | 0.012111 | 51 | 0.045757 | 0.372582 |
| 77 | 23 | 0.095409 | -0.00328 | 51 | 0.029589 | 0.380606 |
| 76 | 23 | 0.012663 | 0.017714 | 52 | -0.00193 | 0.388573 |
| 75 | 24 | 0.062379 | -0.00524 | 52 | -0.01929 | 0.378288 |
| 74 | 24 | 0.045206 | -0.00276 | 53 | -0.01017 | 0.362655 |
| 73 | 25 | 0.047899 | 0.003382 | 53 | -0.00161 | 0.291322 |
| 72 | 25 | 0.05624 | -0.00632 | 54 | 0.067099 | 0.115503 |
| 71 | 26 | 0.041488 | 0.003214 | 54 | 0.062777 | 0.022412 |
| 70 | 26 | 0.045979 | -0.0012 | 55 | 0.060637 | -0.00191 |
| 69 | 27 | 0.036653 | 0.006206 | 55 | 0.064453 | -0.00182 |
| 68 | 27 | 0.073485 | -0.01006 | 56 | 0.055944 | -0.00412 |
| 67 | 28 | 0.042619 | 0.000257 | 56 | 0.076373 | -0.00702 |
| 66 | 29 | 0.027008 | 0.010582 | 57 | 0.056413 | 0.000667 |
| 65 | 29 | 0.045546 | 0.003159 | 57 | 0.068445 | -0.00859 |
| 64 | | | | 58 | 0.041902 | 0.002838 |
| 63 | | | | 58 | 0.049095 | 0.000235 |

| Elevation cm | Time min | Water Content | Soltrol Content | Time min | Water Content | Soltrol Content |
|---|---|---|---|---|---|---|
| 62 | | | | 59 | 0.064315 | -0.00019 |
| 61 | | | | 59 | 0.027563 | 0.008226 |
| 60 | | | | 60 | 0.095963 | -0.00927 |
| 59 | | | | 60 | 0.05727 | 0.006669 |
| 58 | | | | 61 | 0.084154 | -0.0025 |
| 57 | | | | 62 | 0.085811 | -0.00216 |
| 56 | | | | 62 | 0.090741 | 0.000776 |
| 55 | | | | 63 | 0.077892 | 0.010098 |
| 54 | | | | 63 | 0.071837 | 0.012652 |
| 53 | | | | 64 | 0.083629 | 0.012699 |
| 52 | | | | 64 | 0.116087 | -0.0019 |
| 51 | | | | 65 | 0.073912 | 0.013418 |
| 50 | | | | 65 | 0.099507 | 0.006069 |
| 49 | | | | 66 | 0.075754 | 0.014068 |
| 48 | | | | 66 | 0.075725 | 0.011621 |
| 47 | | | | 67 | 0.06341 | 0.003127 |
| 46 | | | | 67 | 0.068737 | 0.000941 |
| 45 | | | | 68 | 0.064166 | -0.00178 |
| 44 | | | | 68 | 0.078085 | -0.00678 |
| 43 | | | | 69 | 0.050592 | 0.004157 |
| 42 | | | | 69 | 0.061946 | -0.00149 |
| 41 | | | | 70 | 0.048876 | 0.008604 |
| 40 | | | | 70 | 0.071824 | -0.00188 |
| 39 | | | | 71 | 0.057461 | 0.008032 |
| 38 | | | | 71 | 0.09276 | -0.00013 |
| 37 | | | | 72 | 0.084912 | 0.00101 |
| 36 | | | | 72 | 0.072391 | 0.003344 |
| 35 | | | | 73 | 0.053982 | 0.006252 |
| 34 | | | | 73 | 0.071546 | 0.008956 |
| 33 | | | | 74 | 0.066908 | 0.008329 |
| 32 | | | | 74 | 0.06512 | 0.018392 |
| 31 | | | | 75 | 0.085681 | 0.006983 |
| 30 | | | | 75 | 0.101994 | -0.00194 |
| 29 | | | | 76 | 0.045738 | 0.015103 |
| 28 | | | | 77 | 0.130186 | -0.00171 |
| 27 | | | | 77 | 0.094898 | 0.008647 |
| 26 | | | | 78 | 0.09689 | 0.008789 |
| 25 | | | | 78 | 0.101672 | -0.00088 |
| 24 | | | | 79 | 0.069094 | 0.004156 |
| 23 | | | | 79 | 0.048835 | 0.011686 |
| 22 | | | | 80 | 0.0494 | 0.005208 |
| 21 | | | | 80 | 0.061252 | -0.00338 |
| 20 | | | | 81 | 0.040356 | 0.003319 |
| 19 | | | | 81 | 0.032076 | 0.003279 |
| 18 | | | | 82 | 0.052453 | -0.00062 |
| 17 | | | | 82 | 0.064478 | -0.00571 |
| 16 | | | | 83 | 0.041998 | 0.002677 |
| 15 | | | | 83 | 0.056759 | -0.00037 |

| Elevation cm | Time min | Water Content | Soltrol Content | Time min | Water Content | Soltrol Content |
|---|---|---|---|---|---|---|
| 115 | 88 | 0.022644 | 0.156551 | 143 | 0.072491 | 0.149466 |
| 114 | 88 | 0.055459 | 0.182696 | 144 | 0.107793 | 0.174561 |
| 113 | 89 | 0.06938 | 0.162365 | 144 | 0.180822 | 0.105462 |
| 112 | 89 | 0.078093 | 0.167817 | 145 | 0.213918 | 0.090573 |
| 111 | 90 | 0.041314 | 0.193194 | 145 | 0.217118 | 0.095836 |
| 110 | 90 | 0.02089 | 0.207253 | 146 | 0.190631 | 0.100615 |

| Elevation cm | Time min | Water Content | Soltrol Content | Time min | Water Content | Soltrol Content |
|---|---|---|---|---|---|---|
| 109 | 91 | -0.00605 | 0.228421 | 146 | 0.206981 | 0.090989 |
| 108 | 91 | 0.011992 | 0.218539 | 147 | 0.171666 | 0.109689 |
| 107 | 92 | -0.02121 | 0.232044 | 147 | 0.201489 | 0.097334 |
| 106 | 92 | -0.03051 | 0.237543 | 148 | 0.15615 | 0.121053 |
| 105 | 93 | -0.00343 | 0.220387 | 148 | 0.189729 | 0.116199 |
| 104 | 93 | -0.00778 | 0.227932 | 149 | 0.160903 | 0.130014 |
| 103 | 94 | -0.02422 | 0.245168 | 149 | 0.189334 | 0.130138 |
| 102 | 94 | -0.01186 | 0.257878 | 150 | 0.195649 | 0.142742 |
| 101 | 95 | -0.03223 | 0.275399 | 150 | 0.177031 | 0.154491 |
| 100 | 95 | 0.002654 | 0.271863 | 151 | 0.237925 | 0.138043 |
| 99 | 96 | 0.018802 | 0.259855 | 151 | 0.221911 | 0.153349 |
| 98 | 96 | -0.0087 | 0.270393 | 152 | 0.185897 | 0.172979 |
| 97 | 97 | -0.0132 | 0.292161 | 152 | 0.205324 | 0.169737 |
| 96 | 97 | 0.006032 | 0.300987 | 153 | 0.192156 | 0.186786 |
| 95 | 98 | 0.011961 | 0.296928 | 153 | 0.214664 | 0.171516 |
| 94 | 98 | -0.0207 | 0.299525 | 154 | 0.148386 | 0.197688 |
| 93 | 99 | -0.02953 | 0.30899 | 154 | 0.189197 | 0.18497 |
| 92 | 99 | 0.003333 | 0.298718 | 155 | 0.165128 | 0.202099 |
| 91 | 100 | 0.015468 | 0.298666 | 155 | 0.189162 | 0.193066 |
| 90 | 100 | -0.02006 | 0.308923 | 156 | 0.173717 | 0.202995 |
| 89 | 101 | -0.04854 | 0.313236 | 156 | 0.172978 | 0.202177 |
| 88 | 101 | -0.00489 | 0.302811 | 157 | 0.183894 | 0.19959 |
| 87 | 102 | 0.022442 | 0.299859 | 157 | 0.166785 | 0.208403 |
| 86 | 102 | -0.01772 | 0.327471 | 158 | 0.174723 | 0.207461 |
| 85 | 103 | 0.005251 | 0.330999 | 158 | 0.162955 | 0.202781 |
| 84 | 103 | -0.03341 | 0.363687 | 159 | 0.170111 | 0.210764 |
| 83 | 104 | -0.01059 | 0.359557 | 159 | 0.161521 | 0.210105 |
| 82 | 104 | -0.02473 | 0.373286 | 160 | 0.177936 | 0.207978 |
| 81 | 105 | -0.01093 | 0.377271 | 160 | 0.144711 | 0.226641 |
| 80 | 105 | 0.023235 | 0.374419 | 161 | 0.151869 | 0.225546 |
| 79 | 106 | 0.021165 | 0.373624 | 161 | 0.203353 | 0.201965 |
| 78 | 106 | 0.006692 | 0.387854 | 162 | 0.176867 | 0.213113 |
| 77 | 107 | -0.00614 | 0.390446 | 162 | 0.195188 | 0.200659 |
| 76 | 107 | 0.023209 | 0.371627 | 163 | 0.154749 | 0.21482 |
| 75 | 108 | -0.01695 | 0.372594 | 163 | 0.135938 | 0.228269 |
| 74 | 108 | 0.023749 | 0.35892 | 164 | 0.165928 | 0.218631 |
| 73 | 109 | -0.02788 | 0.380152 | 164 | 0.142003 | 0.228474 |
| 72 | 109 | -0.00811 | 0.363572 | 165 | 0.15949 | 0.225929 |
| 71 | 110 | -0.04779 | 0.372731 | 165 | 0.139761 | 0.22603 |
| 70 | 110 | -0.01543 | 0.368509 | 166 | 0.169607 | 0.219998 |
| 69 | 111 | -0.04573 | 0.383671 | 166 | 0.167785 | 0.219563 |
| 68 | 111 | -0.01424 | 0.371026 | 167 | 0.162655 | 0.22039 |
| 67 | 112 | 0.003839 | 0.360974 | 167 | 0.159116 | 0.218361 |
| 66 | 112 | -0.01382 | 0.37202 | 168 | 0.158203 | 0.219687 |
| 65 | 113 | -0.0109 | 0.367767 | 168 | 0.166471 | 0.216898 |
| 64 | 113 | -0.01944 | 0.372904 | 169 | 0.158695 | 0.212992 |
| 63 | 114 | -0.01347 | 0.363123 | 169 | 0.167614 | 0.217657 |
| 62 | 114 | -0.0028 | 0.36403 | 170 | 0.152086 | 0.221567 |
| 61 | 115 | -0.00738 | 0.360622 | 170 | 0.185208 | 0.211461 |
| 60 | 115 | -0.00752 | 0.360684 | 171 | 0.176736 | 0.212884 |
| 59 | 116 | -0.00692 | 0.355766 | 171 | 0.162644 | 0.217736 |
| 58 | 117 | 0.002361 | 0.323213 | 172 | 0.156262 | 0.225235 |
| 57 | 117 | 0.029263 | 0.205877 | 172 | 0.140765 | 0.230212 |
| 56 | 118 | 0.072158 | 0.068899 | 173 | 0.17926 | 0.219342 |
| 55 | 118 | 0.100058 | 0.013461 | 173 | 0.158846 | 0.229055 |
| 54 | 119 | 0.079208 | 0.017385 | 174 | 0.170585 | 0.225101 |
| 53 | 119 | 0.118315 | 0.004975 | 174 | 0.16892 | 0.227589 |
| 52 | 120 | 0.072457 | 0.018005 | 175 | 0.184322 | 0.222699 |
| 51 | 120 | 0.079455 | 0.013836 | 175 | 0.160628 | 0.236005 |

| Elevation cm | Time min | Water Content | Soltrol Content | Time min | Water Content | Soltrol Content |
|---|---|---|---|---|---|---|
| 50 | 121 | 0.060267 | 0.021747 | 176 | 0.156299 | 0.240446 |
| 49 | 121 | 0.075933 | 0.020877 | 177 | 0.162142 | 0.248383 |
| 48 | 122 | 0.085141 | 0.0052 | 177 | 0.099237 | 0.283836 |
| 47 | 122 | 0.05814 | 0.005564 | 178 | 0.109774 | 0.286074 |
| 46 | 123 | 0.061648 | 0.00492 | 178 | 0.089905 | 0.317966 |
| 45 | 123 | 0.063874 | -0.00139 | 179 | -0.00825 | 0.376745 |
| 44 | 124 | 0.08412 | -0.0066 | 179 | 0.028591 | 0.374102 |
| 43 | 124 | 0.042494 | 0.006602 | 180 | -0.00782 | 0.391797 |
| 42 | 125 | 0.068497 | -0.00218 | 180 | 0.011563 | 0.386313 |
| 41 | 125 | 0.066523 | 0.001345 | 181 | -0.01597 | 0.408361 |
| 40 | 126 | 0.072138 | 0.003327 | 181 | 0.01514 | 0.388966 |
| 39 | 126 | 0.098947 | -0.00193 | 182 | -0.01935 | 0.401654 |
| 38 | 127 | 0.071426 | 0.003283 | 182 | 0.004017 | 0.398619 |
| 37 | 127 | 0.070858 | 0.006232 | 183 | -0.01617 | 0.402514 |
| 36 | 128 | 0.077555 | 0.002881 | 183 | -0.02289 | 0.401456 |
| 35 | 128 | 0.08199 | -0.00324 | 184 | 0.023933 | 0.377691 |
| 34 | 129 | 0.089298 | 0.002095 | 184 | 0.015658 | 0.385259 |
| 33 | 129 | 0.061944 | 0.014541 | 185 | 0.04831 | 0.368877 |
| 32 | 130 | 0.096124 | 0.004179 | 185 | 0.069403 | 0.366537 |
| 31 | 130 | 0.108651 | -0.00072 | 186 | 0.033693 | 0.376103 |
| 30 | 131 | 0.089279 | 0.007056 | 186 | 0.066177 | 0.366537 |
| 29 | 131 | 0.087401 | 0.007195 | 187 | 0.042906 | 0.374579 |
| 28 | 132 | 0.09958 | 0.006608 | 187 | 0.071789 | 0.361509 |
| 27 | 133 | 0.115403 | 0.006201 | 188 | 0.024662 | 0.369361 |
| 26 | 133 | 0.102845 | 0.009456 | 188 | 0.117155 | 0.224971 |
| 25 | 134 | 0.094817 | 0.004839 | 189 | 0.092692 | 0.114325 |
| 24 | 134 | 0.094007 | -0.00393 | 189 | 0.05557 | 0.044422 |
| 23 | 135 | 0.09646 | -0.00755 | 190 | 0.072773 | 0.0089 |
| 22 | 135 | 0.093639 | -0.01065 | 190 | 0.053973 | 0.005443 |
| 21 | 136 | 0.050796 | 0.003306 | 191 | 0.068047 | 0.000132 |
| 20 | 136 | 0.06146 | -0.00309 | 191 | 0.046103 | 0.002342 |
| 19 | 137 | 0.055359 | -0.00484 | 192 | 0.06032 | -0.00442 |
| 18 | 137 | 0.067513 | -0.00699 | 192 | 0.058187 | -0.0009 |
| 17 | 138 | 0.059252 | -0.00413 | 193 | 0.029373 | 0.007116 |
| 16 | 138 | 0.056705 | -0.001 | 193 | 0.057959 | -0.00279 |
| 15 | 139 | 0.033281 | 0.008964 | 194 | 0.038233 | 0.007165 |

| Elevation cm | Time min | Water Content | Soltrol Content |
|---|---|---|---|
| 115 | 198 | 0.158447 | 0.041455 |
| 114 | 199 | 0.088609 | 0.172532 |
| 113 | 199 | 0.169189 | 0.111806 |
| 112 | 200 | 0.208869 | 0.084312 |
| 111 | 200 | 0.208635 | 0.087846 |
| 110 | 201 | 0.180898 | 0.094052 |
| 109 | 201 | 0.184568 | 0.085904 |
| 108 | 202 | 0.188848 | 0.084934 |
| 107 | 202 | 0.157865 | 0.097205 |
| 106 | 203 | 0.172016 | 0.093064 |
| 105 | 203 | 0.147474 | 0.10888 |
| 104 | 204 | 0.141321 | 0.106529 |
| 103 | 204 | 0.189481 | 0.092579 |
| 102 | 205 | 0.171868 | 0.105292 |
| 101 | 205 | 0.15171 | 0.121853 |
| 100 | 206 | 0.192056 | 0.112672 |
| 99 | 206 | 0.193703 | 0.119625 |
| 98 | 207 | 0.177577 | 0.124196 |

| Elevation cm | Time min | Water Content | Soltrol Content |
|---|---|---|---|
| 97 | 207 | 0.192774 | 0.12986 |
| 96 | 208 | 0.195179 | 0.137563 |
| 95 | 208 | 0.159506 | 0.150583 |
| 94 | 209 | 0.176238 | 0.13632 |
| 93 | 209 | 0.18202 | 0.140489 |
| 92 | 210 | 0.181726 | 0.143658 |
| 91 | 210 | 0.175744 | 0.145356 |
| 90 | 211 | 0.15007 | 0.152555 |
| 89 | 211 | 0.154756 | 0.156087 |
| 88 | 212 | 0.165962 | 0.149461 |
| 87 | 212 | 0.147759 | 0.15195 |
| 86 | 213 | 0.180137 | 0.148418 |
| 85 | 213 | 0.153657 | 0.152612 |
| 84 | 214 | 0.190578 | 0.14649 |
| 83 | 214 | 0.161468 | 0.155877 |
| 82 | 215 | 0.16807 | 0.160164 |
| 81 | 215 | 0.159354 | 0.163551 |
| 80 | 216 | 0.219149 | 0.158842 |
| 79 | 216 | 0.178564 | 0.18348 |
| 78 | 217 | 0.166979 | 0.187385 |
| 77 | 217 | 0.205682 | 0.182357 |
| 76 | 218 | 0.168699 | 0.18734 |
| 75 | 219 | 0.186284 | 0.175737 |
| 74 | 219 | 0.143084 | 0.190746 |
| 73 | 220 | 0.130015 | 0.200492 |
| 72 | 220 | 0.153211 | 0.188861 |
| 71 | 221 | 0.12715 | 0.192942 |
| 70 | 221 | 0.120798 | 0.197469 |
| 69 | 222 | 0.137465 | 0.193048 |
| 68 | 222 | 0.163926 | 0.186154 |
| 67 | 223 | 0.151861 | 0.188678 |
| 66 | 223 | 0.180475 | 0.185053 |
| 65 | 224 | 0.157808 | 0.19453 |
| 64 | 224 | 0.144398 | 0.198124 |
| 63 | 225 | 0.153256 | 0.196483 |
| 62 | 225 | 0.156112 | 0.197965 |
| 61 | 226 | 0.17701 | 0.192433 |
| 60 | 226 | 0.20781 | 0.191214 |
| 59 | 227 | 0.168711 | 0.200335 |
| 58 | 227 | 0.166432 | 0.20097 |
| 57 | 228 | 0.146123 | 0.214465 |
| 56 | 228 | 0.181502 | 0.199311 |
| 55 | 229 | 0.13288 | 0.219292 |
| 54 | 229 | 0.215018 | 0.193142 |
| 53 | 230 | 0.183802 | 0.211836 |
| 52 | 230 | 0.168196 | 0.213815 |
| 51 | 231 | 0.180275 | 0.210876 |
| 50 | 231 | 0.188921 | 0.20561 |
| 49 | 232 | 0.182757 | 0.206011 |
| 48 | 232 | 0.197966 | 0.202048 |
| 47 | 233 | 0.163351 | 0.216811 |
| 46 | 233 | 0.179693 | 0.207118 |
| 45 | 234 | 0.165376 | 0.207331 |
| 44 | 234 | 0.193399 | 0.20517 |
| 43 | 235 | 0.134813 | 0.228695 |
| 42 | 235 | 0.127916 | 0.231759 |
| 41 | 236 | 0.161476 | 0.215973 |
| 40 | 236 | 0.189092 | 0.20322 |
| 39 | 237 | 0.173606 | 0.210795 |

| Elevation cm | Time min | Water Content | Soltrol Content |
|---|---|---|---|
| 38 | 237 | 0.160175 | 0.214959 |
| 37 | 238 | 0.157986 | 0.219362 |
| 36 | 238 | 0.17089 | 0.210099 |
| 35 | 239 | 0.153454 | 0.22209 |
| 34 | 239 | 0.15006 | 0.217396 |
| 33 | 240 | 0.173378 | 0.213209 |
| 32 | 240 | 0.17079 | 0.22051 |
| 31 | 241 | 0.165479 | 0.216855 |
| 30 | 241 | 0.189581 | 0.208458 |
| 29 | 242 | 0.183579 | 0.211463 |
| 28 | 242 | 0.196487 | 0.209028 |
| 27 | 243 | 0.227302 | 0.193052 |
| 26 | 243 | 0.18677 | 0.212231 |
| 25 | 244 | 0.177735 | 0.207444 |
| 24 | 244 | 0.206018 | 0.198866 |
| 23 | 245 | 0.183987 | 0.20882 |
| 22 | 245 | 0.166645 | 0.214743 |
| 21 | 246 | 0.135436 | 0.229005 |
| 20 | 246 | 0.125499 | 0.230917 |
| 19 | 247 | 0.147409 | 0.215785 |
| 18 | 247 | 0.144637 | 0.209865 |
| 17 | 248 | 0.147388 | 0.214136 |
| 16 | 248 | 0.121985 | 0.217448 |
| 15 | 249 | 0.126341 | 0.221398 |

Spill M
#70 Sand 1000 ml Soltrol Spill
Rain 500ml/hour after 197 minutes.

Bulk Density grav.: 1.54g $cm^{-3}$
Porosity: 0.42
Temperature Soltrol: 21°C
Temperature : 24°C
Residual water content: 0.09.

| Elevation cm | Time min | Soltrol Content | Time min | Soltrol Content | Time min | Soltrol Content |
|---|---|---|---|---|---|---|
| 120 | 4 | 0.38078 | 21 | 0.382045 | 66 | 0.172758 |
| 119 | 5 | 0.375924 | 22 | 0.378838 | 66 | 0.218248 |
| 118 | 5 | 0.37668 | 22 | 0.380073 | 67 | 0.236879 |
| 117 | 6 | 0.378568 | 23 | 0.376006 | 67 | 0.238478 |
| 116 | 6 | 0.375065 | 23 | 0.376569 | 68 | 0.246606 |
| 115 | 7 | 0.37321 | 24 | 0.37063 | 68 | 0.245382 |
| 114 | 7 | 0.371031 | 24 | 0.368886 | 69 | 0.263249 |
| 113 | 8 | 0.373713 | 25 | 0.373408 | 69 | 0.272684 |
| 112 | 8 | 0.365993 | 25 | 0.368896 | 70 | 0.269281 |
| 111 | 9 | 0.368771 | 26 | 0.369257 | 70 | 0.266618 |
| 110 | 9 | 0.366413 | 26 | 0.365636 | 71 | 0.277642 |
| 109 | 10 | 0.372206 | 27 | 0.369567 | 71 | 0.275143 |
| 108 | 11 | 0.371737 | 27 | 0.368245 | 72 | 0.279838 |
| 107 | 11 | 0.363836 | 28 | 0.368642 | 72 | 0.280328 |
| 106 | 12 | 0.368107 | 28 | 0.370051 | 73 | 0.284853 |
| 105 | 12 | 0.375115 | 29 | 0.374197 | 73 | 0.28706 |
| 104 | 13 | 0.371829 | 30 | 0.369012 | 74 | 0.298654 |
| 103 | 13 | 0.360849 | 30 | 0.368216 | 74 | 0.305934 |
| 102 | 14 | 0.370519 | 31 | 0.369471 | 75 | 0.317301 |
| 101 | 14 | 0.36304 | 31 | 0.361226 | 75 | 0.328764 |
| 100 | 15 | 0.36725 | 32 | 0.366363 | 76 | 0.328229 |
| 99 | 15 | 0.362401 | 32 | 0.364112 | 76 | 0.333405 |
| 98 | 16 | 0.359936 | 33 | 0.367113 | 77 | 0.338522 |
| 97 | 16 | 0.331833 | 33 | 0.364345 | 77 | 0.347776 |
| 96 | 17 | 0.247436 | 34 | 0.370771 | 78 | 0.347226 |
| 95 | 17 | 0.145503 | 34 | 0.360914 | 79 | 0.34394 |
| 94 | 18 | 0.064516 | 35 | 0.359397 | 79 | 0.340401 |
| 93 | 18 | 0.02844 | 35 | 0.369124 | 80 | 0.349505 |
| 92 | | | 36 | 0.360417 | 80 | 0.346429 |
| 91 | | | 36 | 0.362968 | 81 | 0.34239 |
| 90 | | | 37 | 0.362053 | 81 | 0.339208 |
| 89 | | | 37 | 0.354929 | 82 | 0.346113 |
| 88 | | | 38 | 0.368426 | 82 | 0.347363 |
| 87 | | | 38 | 0.361734 | 83 | 0.34175 |
| 86 | | | 39 | 0.368548 | 83 | 0.339961 |
| 85 | | | 39 | 0.359956 | 84 | 0.345558 |
| 84 | | | 40 | 0.36311 | 84 | 0.346061 |
| 83 | | | 40 | 0.363388 | 85 | 0.339826 |
| 82 | | | 46 | 0.363703 | 85 | 0.339924 |
| 81 | | | 46 | 0.364781 | 86 | 0.337306 |
| 80 | | | 47 | 0.357003 | 86 | 0.344133 |
| 79 | | | 47 | 0.363778 | 87 | 0.347123 |
| 78 | | | 48 | 0.36157 | 87 | 0.338315 |
| 77 | | | 48 | 0.358426 | 88 | 0.335977 |
| 76 | | | 49 | 0.350583 | 88 | 0.335429 |
| 75 | | | 49 | 0.347682 | 89 | 0.334882 |
| 74 | | | 50 | 0.316525 | 89 | 0.337923 |
| 73 | | | 50 | 0.180121 | 90 | 0.340998 |
| 72 | | | 51 | 0.081155 | 90 | 0.33737 |
| 71 | | | 51 | 0.014973 | 91 | 0.337792 |
| 70 | | | 52 | -0.00157 | 92 | 0.332524 |
| 69 | | | 52 | 0.000109 | 92 | 0.3364 |
| 68 | | | 53 | -0.00339 | 93 | 0.338311 |

| Elevation cm | Time min | Soltrol Content | Time min | Soltrol Content | Time min | Soltrol Content |
|---|---|---|---|---|---|---|
| 67 | | | 53 | 0.001381 | 93 | 0.333674 |
| 66 | | | 54 | -0.00537 | 94 | 0.332245 |
| 65 | | | 55 | 0.000853 | 94 | 0.329068 |
| 64 | | | 55 | 0.004277 | 95 | 0.330891 |
| 63 | | | 56 | -0.00352 | 95 | 0.33203 |
| 62 | | | 56 | -0.00212 | 96 | 0.328328 |
| 61 | | | 57 | -0.00478 | 96 | 0.330552 |
| 60 | | | 57 | -0.00112 | 97 | 0.327372 |
| 59 | | | 58 | -0.00186 | 97 | 0.325339 |
| 58 | | | 58 | -0.00537 | 98 | 0.313994 |
| 57 | | | 59 | -0.0107 | 98 | 0.288732 |
| 56 | | | 59 | -0.00997 | 99 | 0.175899 |
| 55 | | | 60 | -0.00901 | 99 | 0.05306 |
| 54 | | | 60 | -0.00769 | 100 | 0.001652 |
| 53 | | | 61 | -0.00838 | 100 | -0.00243 |
| 52 | | | 61 | -0.00655 | 101 | -0.00584 |
| 51 | | | | | 101 | -0.00685 |
| 50 | | | | | 102 | -0.00594 |
| 49 | | | | | 102 | 0.001275 |
| 48 | | | | | 103 | 0.003101 |
| 47 | | | | | 104 | 0.003255 |
| 46 | | | | | 104 | 0.000215 |
| 45 | | | | | 105 | -0.0005 |
| 44 | | | | | 105 | 0.001131 |
| 43 | | | | | 106 | -0.00045 |
| 42 | | | | | 106 | 0.002684 |
| 41 | | | | | 107 | 0.009521 |
| 40 | | | | | 107 | 0.003812 |
| 39 | | | | | 108 | 0.00385 |
| 38 | | | | | 108 | 0.002506 |
| 37 | | | | | 109 | 0.001023 |
| 36 | | | | | 109 | -0.00113 |
| 35 | | | | | 110 | 0.004774 |
| 34 | | | | | 110 | -0.0014 |
| 33 | | | | | 111 | 0.002491 |

| Elevation cm | Time min | Soltrol Content | Elevation cm | Time min | Water Content | Soltrol Content |
|---|---|---|---|---|---|---|
| 120 | 120 | 0.109185 | 119 | 174 | 0.022596 | 0.132895 |
| 119 | 120 | 0.13508 | 117 | 175 | 0.049853 | 0.129024 |
| 118 | 121 | 0.139412 | 115 | 175 | 0.034437 | 0.147994 |
| 117 | 121 | 0.1388 | 113 | 176 | -0.01122 | 0.156578 |
| 116 | 122 | 0.146128 | 111 | 176 | 0.027283 | 0.16413 |
| 115 | 122 | 0.145665 | 109 | 177 | 0.033178 | 0.164993 |
| 114 | 123 | 0.155995 | 107 | 177 | -0.02291 | 0.192861 |
| 113 | 123 | 0.162719 | 105 | 178 | 0.014256 | 0.185089 |
| 112 | 124 | 0.155592 | 103 | 179 | 0.03526 | 0.183976 |
| 111 | 124 | 0.154525 | 101 | 179 | 0.004643 | 0.203913 |
| 110 | 125 | 0.161459 | 99 | 180 | -0.01465 | 0.221793 |
| 109 | 125 | 0.172154 | 97 | 180 | 0.023935 | 0.21545 |
| 108 | 126 | 0.16468 | 95 | 181 | 0.03122 | 0.229573 |
| 107 | 126 | 0.174349 | 93 | 181 | 0.03694 | 0.235493 |
| 106 | 127 | 0.176445 | 91 | 182 | 0.085124 | 0.231261 |
| 105 | 127 | 0.181949 | 89 | 182 | 0.039559 | 0.280542 |
| 104 | 128 | 0.192551 | 87 | 183 | 0.057081 | 0.243386 |
| 103 | 128 | 0.184965 | 85 | 184 | 0.102681 | 0.239705 |
| 102 | 129 | 0.196635 | 83 | 184 | 0.069012 | 0.238562 |
| 101 | 130 | 0.195548 | 81 | 185 | 0.035836 | 0.267795 |

| Elevation cm | Time min | Soltrol Content | Elevation cm | Time min | Water Content | Soltrol Content |
|---|---|---|---|---|---|---|
| 100 | 130 | 0.201461 | 79 | 185 | 0.068783 | 0.271208 |
| 99 | 131 | 0.202318 | 77 | 186 | 0.055828 | 0.270481 |
| 98 | 131 | 0.203005 | 75 | 186 | 0.04292 | 0.278495 |
| 97 | 132 | 0.218628 | 73 | 187 | 0.069708 | 0.274293 |
| 96 | 132 | 0.22772 | 71 | 187 | 0.060701 | 0.28319 |
| 95 | 133 | 0.226875 | 69 | 188 | 0.069072 | 0.286798 |
| 94 | 133 | 0.229624 | 67 | 188 | 0.102566 | 0.282693 |
| 93 | 134 | 0.241596 | 65 | 189 | 0.073502 | 0.315018 |
| 92 | 134 | 0.248672 | 63 | 190 | 0.07688 | 0.310709 |
| 91 | 135 | 0.245526 | 61 | 190 | 0.083597 | 0.330754 |
| 90 | 135 | 0.252386 | 59 | 191 | 0.026087 | 0.35338 |
| 89 | 136 | 0.272771 | 57 | 191 | 0.059297 | 0.344513 |
| 88 | 136 | 0.301661 | 55 | 192 | 0.082529 | 0.337559 |
| 87 | 137 | 0.280627 | 53 | 192 | 0.044919 | 0.357007 |
| 86 | 137 | 0.264297 | 51 | 193 | 0.092513 | 0.337607 |
| 85 | 138 | 0.262558 | 49 | 193 | 0.109599 | 0.33774 |
| 84 | 138 | 0.277086 | 47 | 194 | 0.104569 | 0.349641 |
| 83 | 139 | 0.276444 | 45 | 194 | 0.063194 | 0.362871 |
| 82 | 139 | 0.267789 | 43 | 195 | 0.076791 | 0.352688 |
| 81 | 140 | 0.275319 | 41 | 196 | 0.091378 | 0.349946 |
| 80 | 140 | 0.282532 | 39 | 196 | 0.046074 | 0.363852 |
| 79 | 141 | 0.296788 | 37 | 197 | 0.062484 | 0.327034 |
| 78 | 142 | 0.315689 | 35 | 197 | 0.099056 | 0.061648 |
| 77 | 142 | 0.305748 | 33 | | | |
| 76 | 143 | 0.307222 | | | | |
| 75 | 143 | 0.313109 | | | | |
| 74 | 144 | 0.320344 | | | | |
| 73 | 144 | 0.31875 | | | | |
| 72 | 145 | 0.325898 | | | | |
| 71 | 145 | 0.338214 | | | | |
| 70 | 146 | 0.329491 | | | | |
| 69 | 146 | 0.337143 | | | | |
| 68 | 147 | 0.338994 | | | | |
| 67 | 147 | 0.343167 | | | | |
| 66 | 148 | 0.350017 | | | | |
| 65 | 148 | 0.346027 | | | | |
| 64 | 149 | 0.344354 | | | | |
| 63 | 149 | 0.346087 | | | | |
| 62 | 150 | 0.336756 | | | | |
| 61 | 150 | 0.338081 | | | | |
| 60 | 151 | 0.344609 | | | | |
| 59 | 151 | 0.334673 | | | | |
| 58 | 152 | 0.335217 | | | | |
| 57 | 152 | 0.338111 | | | | |
| 56 | 153 | 0.339635 | | | | |
| 55 | 153 | 0.332614 | | | | |
| 54 | 154 | 0.334614 | | | | |
| 53 | 155 | 0.339048 | | | | |
| 52 | 155 | 0.336308 | | | | |
| 51 | 156 | 0.333189 | | | | |
| 50 | 156 | 0.339338 | | | | |
| 49 | 157 | 0.335224 | | | | |
| 48 | 157 | 0.340667 | | | | |
| 47 | 158 | 0.34266 | | | | |
| 46 | 158 | 0.341741 | | | | |
| 45 | 159 | 0.336567 | | | | |
| 44 | 159 | 0.327185 | | | | |
| 43 | 160 | 0.305856 | | | | |
| 42 | 160 | 0.273611 | | | | |

| Elevation cm | Time min | Soltrol Content | Elevation cm | Time min | Water Content | Soltrol Content |
|---|---|---|---|---|---|---|
| 41 | 161 | 0.151574 | | | | |
| 40 | 161 | 0.047519 | | | | |
| 39 | 162 | 0.010692 | | | | |
| 38 | 162 | 0.000492 | | | | |
| 37 | 163 | -0.00059 | | | | |
| 36 | 163 | -0.00182 | | | | |
| 35 | 164 | -0.0014 | | | | |
| 34 | 165 | -0.00166 | | | | |
| 33 | 165 | -0.00365 | | | | |

| Elevation cm | Time min | Water Content | Soltrol Content | Time min | Water Content | Soltrol Content |
|---|---|---|---|---|---|---|
| 119 | 201 | 0.239309 | 0.072972 | 230 | 0.264158 | 0.069247 |
| 117 | 202 | 0.257014 | 0.086041 | 230 | 0.213852 | 0.090368 |
| 115 | 202 | 0.25558 | 0.088396 | 231 | 0.242138 | 0.088358 |
| 113 | 203 | 0.261764 | 0.097207 | 231 | 0.231937 | 0.097169 |
| 111 | 204 | 0.238647 | 0.111259 | 232 | 0.205524 | 0.108806 |
| 109 | 204 | 0.271055 | 0.105498 | 232 | 0.216627 | 0.112457 |
| 107 | 205 | 0.257131 | 0.11721 | 233 | 0.247397 | 0.096923 |
| 105 | 205 | 0.225081 | 0.128984 | 233 | 0.225929 | 0.107072 |
| 103 | 206 | 0.247826 | 0.129007 | 234 | 0.244003 | 0.112685 |
| 101 | 206 | 0.260028 | 0.134835 | 235 | 0.270293 | 0.111939 |
| 99 | 207 | 0.195924 | 0.173374 | 235 | 0.244638 | 0.125769 |
| 97 | 207 | 0.177262 | 0.192864 | 236 | 0.202503 | 0.155727 |
| 95 | 208 | 0.183549 | 0.205545 | 236 | 0.259148 | 0.142019 |
| 93 | 208 | 0.091556 | 0.258207 | 237 | 0.248581 | 0.154967 |
| 91 | 209 | 0.075163 | 0.276195 | 237 | 0.238882 | 0.163657 |
| 89 | 210 | 0.05993 | 0.256753 | 238 | 0.261449 | 0.163081 |
| 87 | 210 | 0.050638 | 0.272592 | 238 | 0.302674 | 0.158145 |
| 85 | 211 | 0.047858 | 0.255742 | 239 | 0.26048 | 0.170112 |
| 83 | 211 | 0.056674 | 0.23904 | 239 | 0.286256 | 0.166893 |
| 81 | 212 | 0.035375 | 0.241361 | 240 | 0.251627 | 0.186039 |
| 79 | 212 | 0.048282 | 0.241561 | 241 | 0.250592 | 0.189527 |
| 77 | 213 | 0.078261 | 0.252176 | 241 | 0.263255 | 0.185158 |
| 75 | 213 | 0.075063 | 0.249853 | 242 | 0.23406 | 0.208158 |
| 73 | 214 | 0.050809 | 0.262873 | 242 | 0.232628 | 0.216524 |
| 71 | 214 | 0.038783 | 0.262018 | 243 | 0.171168 | 0.264934 |
| 69 | 215 | 0.028314 | 0.277179 | 243 | 0.13149 | 0.318537 |
| 67 | 216 | 0.091452 | 0.255687 | 244 | 0.077367 | 0.366255 |
| 65 | 216 | 0.042391 | 0.277617 | 244 | 0.111522 | 0.358893 |
| 63 | 217 | 0.050134 | 0.279428 | 245 | 0.07708 | 0.370646 |
| 61 | 217 | 0.069004 | 0.275723 | 245 | 0.071849 | 0.359889 |
| 59 | 218 | 0.081507 | 0.274692 | 246 | 0.091689 | 0.338395 |
| 57 | 218 | 0.045036 | 0.30608 | 247 | 0.038945 | 0.337643 |
| 55 | 219 | 0.033726 | 0.309254 | 247 | 0.044974 | 0.324756 |
| 53 | 219 | 0.048818 | 0.320688 | 248 | 0.035743 | 0.322487 |
| 51 | 220 | 0.045707 | 0.343354 | 248 | 0.069342 | 0.318906 |
| 49 | 221 | 0.034196 | 0.344799 | 249 | 0.072242 | 0.325357 |
| 47 | 221 | 0.068016 | 0.343669 | 249 | 0.07532 | 0.337503 |
| 45 | 222 | 0.10154 | 0.341012 | 250 | 0.065596 | 0.355909 |
| 43 | 222 | 0.108332 | 0.346361 | 250 | 0.103279 | 0.332727 |
| 41 | 223 | 0.059817 | 0.349368 | 251 | 0.050104 | 0.360161 |
| 39 | 223 | 0.103307 | 0.34935 | 252 | 0.055066 | 0.361036 |
| 37 | 224 | 0.071794 | 0.349391 | 252 | 0.045147 | 0.359836 |
| 35 | | | | 253 | 0.059356 | 0.350412 |

| Elevation cm | Time min | Water Content | Soltrol Content | Time min | Water Content | Soltrol Content |
|---|---|---|---|---|---|---|
| 119 | 257 | 0.236304 | 0.060133 | 286 | 0.290339 | 0.052462 |
| 117 | 258 | 0.239956 | 0.077781 | 286 | 0.244356 | 0.066779 |
| 115 | 259 | 0.216507 | 0.081337 | 287 | 0.255862 | 0.069245 |
| 113 | 259 | 0.213728 | 0.087926 | 287 | 0.217388 | 0.088693 |
| 111 | 260 | 0.234525 | 0.087599 | 288 | 0.194816 | 0.091504 |
| 109 | 260 | 0.203073 | 0.097679 | 289 | 0.247605 | 0.085901 |
| 107 | 261 | 0.249328 | 0.087763 | 289 | 0.262235 | 0.077606 |
| 105 | 261 | 0.236474 | 0.086281 | 290 | 0.253059 | 0.082573 |
| 103 | 262 | 0.202755 | 0.108536 | 290 | 0.268187 | 0.080298 |
| 101 | 262 | 0.202582 | 0.117352 | 291 | 0.244845 | 0.098575 |
| 99 | 263 | 0.221312 | 0.115818 | 291 | 0.253744 | 0.102754 |
| 97 | 263 | 0.234767 | 0.117641 | 292 | 0.282258 | 0.103684 |
| 95 | 264 | 0.251781 | 0.123358 | 292 | 0.293098 | 0.104344 |
| 93 | 265 | 0.219186 | 0.140182 | 293 | 0.278322 | 0.125301 |
| 91 | 265 | 0.306258 | 0.119054 | 294 | 0.293429 | 0.129956 |
| 89 | 266 | 0.293141 | 0.128174 | 294 | 0.330107 | 0.118657 |
| 87 | 266 | 0.29926 | 0.141492 | 295 | 0.313999 | 0.129884 |
| 85 | 267 | 0.279315 | 0.145057 | 295 | 0.283878 | 0.148978 |
| 83 | 267 | 0.262188 | 0.15557 | 296 | 0.315134 | 0.143008 |
| 81 | 268 | 0.299975 | 0.153649 | 296 | 0.270039 | 0.164807 |
| 79 | 268 | 0.293739 | 0.161926 | 297 | 0.318291 | 0.149236 |
| 77 | 269 | 0.312737 | 0.162069 | 297 | 0.333206 | 0.136037 |
| 75 | 269 | 0.267543 | 0.171436 | 298 | 0.282293 | 0.159372 |
| 73 | 270 | 0.255471 | 0.180474 | 298 | 0.293712 | 0.158408 |
| 71 | 271 | 0.268374 | 0.179908 | 299 | 0.241943 | 0.185006 |
| 69 | 271 | 0.233942 | 0.196161 | 300 | 0.225005 | 0.196234 |
| 67 | 272 | 0.256176 | 0.188821 | 300 | 0.295491 | 0.168389 |
| 65 | 272 | 0.250755 | 0.192989 | 301 | 0.279028 | 0.173439 |
| 63 | 273 | 0.219511 | 0.210159 | 301 | 0.301968 | 0.170135 |
| 61 | 273 | 0.26 | 0.197421 | 302 | 0.242073 | 0.193253 |
| 59 | 274 | 0.23021 | 0.209667 | 302 | 0.246361 | 0.191141 |
| 57 | 274 | 0.256778 | 0.20123 | 303 | 0.249593 | 0.193854 |
| 55 | 275 | 0.21519 | 0.221577 | 303 | 0.242212 | 0.195181 |
| 53 | 275 | 0.263777 | 0.202243 | 304 | 0.208726 | 0.209672 |
| 51 | 276 | 0.190807 | 0.24485 | 304 | 0.245528 | 0.201359 |
| 49 | 277 | 0.160426 | 0.272479 | 305 | 0.265931 | 0.197708 |
| 47 | 277 | 0.109634 | 0.326434 | 306 | 0.301205 | 0.188368 |
| 45 | 278 | 0.075805 | 0.369031 | 306 | 0.255559 | 0.210886 |
| 43 | 278 | 0.11384 | 0.364382 | 307 | 0.253478 | 0.203375 |
| 41 | 279 | 0.069354 | 0.378734 | 307 | 0.264056 | 0.206668 |
| 39 | 279 | 0.096327 | 0.370862 | 308 | 0.232859 | 0.218233 |
| 37 | 280 | 0.057551 | 0.390308 | 308 | 0.236952 | 0.23008 |
| 35 | 280 | 0.100549 | 0.371543 | | | |

Tank A
#70 Sand 9.5cm Soltrol Ponding Depth
Temperature Soltrol: 23°C

| Elevation cm | Time min | Soltrol Content | Time min | Soltrol Content | Time min | Soltrol Content |
|---|---|---|---|---|---|---|
| 120 | 15 | 0.335185 | 68 | 0.145101 | 121 | 0.14083 |
| 119 | 16 | 0.350383 | 69 | 0.151197 | 122 | 0.144964 |
| 118 | 16 | 0.360118 | 69 | 0.166528 | 122 | 0.140674 |
| 117 | 17 | 0.362661 | 70 | 0.185728 | 123 | 0.14324 |
| 116 | 18 | 0.353848 | 71 | 0.18599 | 124 | 0.133752 |
| 115 | 18 | 0.337875 | 71 | 0.175085 | 124 | 0.113024 |
| 114 | 19 | 0.350075 | 72 | 0.174667 | 125 | 0.118653 |
| 113 | 19 | 0.355796 | 72 | 0.174366 | 126 | 0.141232 |
| 112 | 20 | 0.3607 | 73 | 0.178328 | 126 | 0.156462 |
| 111 | 21 | 0.34467 | 74 | 0.15549 | 127 | 0.142047 |
| 110 | 21 | 0.343592 | 74 | 0.138024 | 127 | 0.147203 |
| 109 | 22 | 0.391261 | 75 | 0.159517 | 132 | 0.20316 |
| 108 | 23 | 0.414393 | 76 | 0.187042 | 133 | 0.217242 |
| 107 | 23 | 0.396858 | 76 | 0.193214 | 134 | 0.219895 |
| 106 | 24 | 0.363273 | 77 | 0.179339 | 134 | 0.227894 |
| 105 | 24 | 0.361114 | 77 | 0.206203 | 135 | 0.229355 |
| 104 | 25 | 0.35 | 78 | 0.23 | 135 | 0.215374 |
| 96 | 30 | 0.160614 | 83 | 0.262985 | 136 | 0.207881 |
| 95 | 30 | 0.054263 | 84 | 0.268566 | 137 | 0.203004 |
| 94 | 31 | 0.005208 | 84 | 0.271967 | 137 | 0.215822 |
| 93 | 32 | -0.00838 | 85 | 0.26277 | 138 | 0.233348 |
| 92 | 32 | -0.01059 | 85 | 0.25282 | 139 | 0.245742 |
| 91 | 33 | -0.02013 | 86 | 0.234971 | 139 | 0.24828 |
| 90 | 34 | -0.01364 | 87 | 0.236328 | 140 | 0.240389 |
| 89 | 34 | -0.01121 | 87 | 0.256615 | 140 | 0.242788 |
| 88 | 35 | -0.00222 | 88 | 0.270824 | 141 | 0.247158 |
| 87 | 36 | -0.00455 | 89 | 0.27964 | 142 | 0.243009 |
| 86 | 36 | -0.01385 | 89 | 0.267809 | 142 | 0.247298 |
| 85 | 37 | -0.00707 | 90 | 0.231042 | 143 | 0.26311 |
| 84 | 37 | -0.0037 | 90 | 0.128614 | 144 | 0.251949 |
| 83 | 38 | -0.00541 | 91 | 0.038376 | 144 | 0.240123 |
| 82 | 39 | -0.00375 | 92 | 0.002689 | 145 | 0.231562 |
| 81 | 39 | -0.00421 | 92 | 0.003575 | 145 | 0.251949 |
| 80 | 40 | 0.010074 | 93 | 0.009323 | 146 | 0.124374 |
| 79 | 41 | 0.002807 | 94 | 0.005136 | 147 | 0.027653 |
| 78 | 41 | -0.00158 | 94 | 0.000364 | 147 | -0.00241 |
| 77 | 42 | -0.00719 | 95 | -0.0067 | 148 | 0.001611 |
| 76 | 43 | -0.00608 | 96 | -0.0042 | 149 | 0.000841 |
| 75 | 43 | -0.00353 | 96 | -0.00139 | 149 | -0.00308 |
| 74 | 44 | -0.01113 | 97 | -0.00624 | 150 | 0.000781 |
| 73 | 44 | -0.00297 | 97 | -0.00523 | 151 | -0.00364 |
| 72 | 45 | -0.00657 | 98 | -0.00188 | 151 | -0.0016 |
| 71 | 46 | -0.00169 | 99 | -0.00382 | 152 | 0.000125 |
| 70 | 46 | -0.00305 | 99 | -0.00403 | 152 | -0.0047 |
| 69 | 47 | -0.00298 | 100 | -0.00349 | 153 | -0.0019 |
| 68 | 48 | -0.00133 | 101 | -0.00271 | 154 | -0.00593 |
| 67 | 48 | -0.00412 | 101 | -0.00635 | 154 | -0.00099 |
| 66 | 49 | -0.00685 | 102 | -0.00866 | 155 | -0.00863 |
| 65 | 50 | -0.00655 | 103 | -0.00529 | 156 | -0.00435 |
| 64 | 50 | -0.00707 | 103 | -0.00372 | | |
| 63 | 51 | -0.00104 | 104 | -0.00819 | | |
| 62 | 52 | -0.00964 | 104 | -0.00707 | | |
| 61 | 52 | -0.00713 | 105 | -0.00134 | | |
| 60 | 53 | -0.0041 | 106 | -0.0104 | | |
| 59 | 53 | 0.001775 | 106 | -0.00277 | | |

| Elevation cm | Time min | Soltrol Content | Time min | Soltrol Content | Time min | Soltrol Content |
|---|---|---|---|---|---|---|
| 58 | 54 | -0.00237 | 107 | -0.00117 | | |
| 57 | 55 | 0.000953 | 108 | -0.00123 | | |
| 56 | 55 | -0.00139 | 108 | -0.00372 | | |
| 55 | 56 | 0.001473 | 109 | -0.00035 | | |
| 54 | 57 | 0.001255 | 110 | 0.003253 | | |
| 53 | 57 | -0.00158 | 110 | -0.00086 | | |
| 52 | 58 | -0.00245 | 111 | 0.001656 | | |
| 51 | 59 | -0.00245 | 111 | 0.003835 | | |
| 50 | 59 | 0.010421 | 112 | 0.007419 | | |
| 49 | 60 | 0.002574 | 113 | 0.005267 | | |
| 48 | 60 | 0.000394 | 113 | -0.00438 | | |
| 47 | 61 | 0.001256 | 114 | 0.003093 | | |
| 46 | 62 | -0.00041 | 115 | -0.00178 | | |
| 45 | 62 | 0.001243 | 115 | -0.00127 | | |
| 44 | 63 | 0.004851 | 116 | 0.003285 | | |
| 43 | 64 | 0.001872 | 117 | 0.002311 | | |

| Elevation cm | Time min | Soltrol Content |
|---|---|---|
| 120 | 171 | 0.113639 |
| 119 | 171 | 0.119516 |
| 118 | 172 | 0.122855 |
| 117 | 173 | 0.133055 |
| 116 | 173 | 0.13609 |
| 115 | 174 | 0.123831 |
| 114 | 174 | 0.124824 |
| 113 | 175 | 0.126251 |
| 112 | 176 | 0.125343 |
| 111 | 176 | 0.111306 |
| 110 | 177 | 0.091076 |
| 109 | 178 | 0.107388 |
| 108 | 178 | 0.127332 |
| 107 | 179 | 0.133719 |
| 106 | 179 | 0.125217 |
| 105 | 180 | 0.131232 |
| 104 | 185 | 0.171888 |
| 96 | 186 | 0.177524 |
| 95 | 186 | 0.185131 |
| 94 | 187 | 0.191158 |
| 93 | 187 | 0.188585 |
| 92 | 188 | 0.176972 |
| 91 | 189 | 0.171484 |
| 90 | 189 | 0.173469 |
| 89 | 190 | 0.19082 |
| 88 | 191 | 0.212616 |
| 87 | 191 | 0.225083 |
| 86 | 192 | 0.218606 |
| 85 | 192 | 0.215071 |
| 84 | 193 | 0.223459 |
| 83 | 194 | 0.22426 |
| 82 | 194 | 0.226133 |
| 81 | 195 | 0.227559 |
| 80 | 196 | 0.24931 |
| 79 | 196 | 0.266689 |
| 78 | 197 | 0.256118 |
| 77 | 197 | 0.2405 |
| 76 | 198 | 0.230234 |
| 75 | 199 | 0.209973 |

| Elevation cm | Time min | Soltrol Content |
|---|---|---|
| 74 | 199 | 0.108384 |
| 73 | 200 | 0.02375 |
| 72 | 201 | 0.004511 |
| 71 | 201 | 0.001703 |
| 70 | 202 | 0.003089 |
| 69 | 202 | -0.00327 |

Tank B
#70 Sand 9.5cm Soltrol Ponding Depth
Rain 12000ml/h after 22 hours
Rain end after 24 hours
Residual water content assumed constant at 0.06.

| Elevation cm | Time min | Water Content | Soltrol Content | Time min | Water Content | Soltrol Content |
|---|---|---|---|---|---|---|
| 120 | 7 | 0.06239 | 0.380415 | 32 | 0.051818 | 0.177212 |
| 119 | 7 | 0.064171 | 0.369694 | 33 | 0.016052 | 0.219551 |
| 118 | 8 | 0.018889 | 0.373156 | 34 | 0.052969 | 0.173085 |
| 117 | 9 | 0.081584 | 0.34694 | 34 | 0.049894 | 0.167317 |
| 116 | 9 | 0.091061 | 0.34845 | 35 | -0.01144 | 0.196705 |
| 115 | 10 | 0.123558 | 0.336452 | 35 | 0.046766 | 0.194484 |
| 114 | 10 | 0.116566 | 0.339065 | 36 | 0.090354 | 0.191042 |
| 113 | 11 | 0.088546 | 0.360088 | 37 | 0.104996 | 0.201764 |
| 112 | 12 | 0.138062 | 0.342297 | 37 | 0.002361 | 0.261831 |
| 111 | 12 | 0.105408 | 0.338063 | 38 | 0.112462 | 0.241555 |
| 110 | 13 | 0.11099 | 0.337725 | 38 | 0.135694 | 0.256734 |
| 109 | 13 | 0.101597 | 0.349861 | 39 | 0.087892 | 0.29352 |
| 108 | 14 | 0.147845 | 0.334453 | 40 | 0.111108 | 0.314377 |
| 107 | 14 | 0.157013 | 0.332685 | 40 | 0.117092 | 0.3297 |
| 106 | 19 | 0.061979 | 0.022284 | 45 | 0.122808 | 0.279154 |
| 98 | 20 | 0.060853 | -0.00721 | 46 | 0.088845 | 0.279213 |
| 97 | 20 | 0.051959 | -0.01241 | 46 | 0.05419 | 0.284217 |
| 96 | 21 | 0.049788 | -0.0154 | 47 | 0.111406 | 0.255271 |
| 95 | 22 | 0.023055 | -0.0047 | 47 | 0.074253 | 0.24899 |
| 94 | 22 | 0.070986 | -0.01429 | 48 | 0.040554 | 0.231928 |
| 93 | 23 | 0.080244 | -0.0125 | 49 | 0.075849 | 0.174763 |
| 92 | 23 | 0.059032 | -0.00628 | 49 | 0.107507 | 0.077763 |
| 91 | 24 | 0.034132 | 0.018775 | 50 | 0.103747 | 0.017674 |
| 90 | 25 | 0.079058 | -0.00586 | 50 | 0.00511 | 0.018305 |
| 89 | 25 | 0.030363 | 0.001083 | 51 | 0.046281 | -0.00719 |
| 88 | 26 | 0.000945 | -0.00147 | 52 | -0.0013 | 0.004376 |
| 87 | 26 | 0.058244 | -0.01405 | 52 | 0.10958 | -0.04072 |
| 86 | 27 | 0.055242 | -0.00764 | 53 | 0.084242 | -0.01592 |
| 85 | 28 | 0.069321 | -0.00861 | 53 | 0.079702 | -0.01304 |
| 84 | 28 | 0.053829 | -0.00675 | 54 | 0.011301 | 0.016097 |
| 83 | 29 | 0.045889 | -0.00604 | 55 | 0.096011 | -0.01511 |
| 82 | 30 | 0.114024 | -0.03315 | 55 | 0.056034 | -0.01411 |
| 81 | | | | 56 | 0.091905 | -0.03 |
| 80 | | | | 56 | -0.02254 | 0.011075 |
| 79 | | | | 57 | -0.01057 | 0.007369 |
| 78 | | | | 58 | 0.020959 | -0.0025 |
| 77 | | | | 58 | 0.022164 | -0.00589 |
| 76 | | | | 59 | 0.055111 | -0.01909 |
| 75 | | | | 59 | -0.01289 | 0.009454 |
| 74 | | | | 60 | 0.055679 | -0.01407 |
| 73 | | | | 61 | 0.039006 | 0.000006 |
| 72 | | | | 61 | 0.07637 | -0.01091 |
| 71 | | | | 62 | 0.092931 | -0.01888 |
| 70 | | | | 62 | 0.070676 | -0.01785 |
| 69 | | | | 63 | 0.11497 | -0.03699 |
| 68 | | | | 64 | 0.015448 | -0.00046 |
| 67 | | | | 64 | 0.075492 | -0.02616 |
| 66 | | | | 65 | 0.061327 | -0.01598 |
| 65 | | | | 65 | 0.074612 | -0.01992 |
| 64 | | | | 66 | 0.040309 | -0.00888 |
| 63 | | | | 67 | 0.16001 | -0.0462 |
| 62 | | | | 67 | 0.123636 | -0.02491 |

| Elevation cm | Time min | Water Content | Soltrol Content | Time min | Water Content | Soltrol Content |
|---|---|---|---|---|---|---|
| 120 | 71 | 0.06304 | 0.103591 | 121 | 0.020878 | 0.082231 |
| 119 | 71 | -0.00051 | 0.159539 | 122 | 0.008307 | 0.128111 |
| 118 | 72 | 0.04831 | 0.113125 | 123 | -0.04982 | 0.125537 |
| 117 | 72 | 0.063109 | 0.105738 | 123 | 0.033241 | 0.096678 |
| 116 | 73 | 0.020461 | 0.140301 | 124 | 0.016525 | 0.103042 |
| 115 | 74 | 0.05107 | 0.136033 | 124 | 0.060802 | 0.102015 |
| 114 | 74 | 0.007961 | 0.16343 | 125 | 0.049795 | 0.119406 |
| 113 | 75 | 0.056531 | 0.149604 | 126 | 0.072495 | 0.105232 |
| 112 | 75 | 0.068307 | 0.149985 | 126 | 0.014301 | 0.136346 |
| 111 | 76 | 0.043392 | 0.16961 | 127 | 0.079443 | 0.122078 |
| 110 | 77 | 0.021388 | 0.184017 | 127 | 0.09504 | 0.115977 |
| 109 | 77 | 0.070542 | 0.17769 | 128 | 0.077831 | 0.132534 |
| 108 | 78 | 0.124284 | 0.186548 | 129 | 0.089806 | 0.134665 |
| 107 | 78 | 0.098089 | 0.23377 | 129 | 0.025054 | 0.182857 |
| 106 | 83 | 0.034825 | 0.293614 | 134 | 0.081933 | 0.250379 |
| 98 | 84 | 0.103537 | 0.251334 | 135 | 0.074515 | 0.222408 |
| 97 | 84 | 0.040309 | 0.278249 | 135 | 0.065986 | 0.231579 |
| 96 | 85 | 0.073002 | 0.245978 | 136 | 0.034469 | 0.238025 |
| 95 | 86 | 0.127658 | 0.224697 | 136 | 0.029531 | 0.237577 |
| 94 | 86 | 0.194962 | 0.206828 | 137 | 0.092313 | 0.213862 |
| 93 | 87 | 0.102187 | 0.241174 | 138 | 0.02471 | 0.25015 |
| 92 | 87 | 0.126211 | 0.248295 | 138 | 0.116506 | 0.228601 |
| 91 | 88 | 0.147292 | 0.260559 | 139 | 0.173677 | 0.240552 |
| 90 | 89 | 0.117993 | 0.276845 | 139 | 0.139867 | 0.250609 |
| 89 | 89 | 0.091245 | 0.250434 | 140 | 0.070315 | 0.264513 |
| 88 | 90 | 0.035697 | 0.241383 | 141 | 0.136546 | 0.215304 |
| 87 | 90 | 0.07336 | 0.156725 | 141 | 0.080838 | 0.245786 |
| 86 | 91 | 0.046362 | 0.070324 | 142 | 0.058556 | 0.257572 |
| 85 | 92 | 0.049721 | 0.017088 | 142 | 0.14331 | 0.233878 |
| 84 | 92 | 0.050697 | -0.00288 | 143 | 0.120687 | 0.234752 |
| 83 | 93 | 0.066847 | -0.01217 | 144 | 0.043572 | 0.227313 |
| 82 | 93 | 0.047436 | -0.01241 | 144 | 0.048251 | 0.113123 |
| 81 | 94 | 0.04072 | -0.01165 | 145 | 0.004174 | 0.036761 |
| 80 | 95 | 0.076525 | -0.02626 | 145 | 0.056081 | -0.01368 |
| 79 | 95 | 0.072024 | -0.01669 | 146 | 0.003983 | 0.002256 |
| 78 | 96 | 0.083231 | -0.0301 | 147 | 0.070559 | -0.02605 |
| 77 | 96 | 0.115089 | -0.04043 | 147 | 0.010544 | 0.001978 |
| 76 | 97 | 0.119113 | -0.04369 | 148 | -0.04346 | 0.014748 |
| 75 | 98 | 0.084432 | -0.02904 | 148 | 0.085139 | -0.02502 |
| 74 | 98 | 0.054914 | -0.00424 | 149 | 0.020909 | 0.005849 |
| 73 | 99 | 0.101987 | -0.01557 | 150 | 0.095654 | -0.01682 |
| 72 | 99 | 0.078151 | -0.00455 | 150 | 0.049965 | 0.005506 |
| 71 | 100 | 0.080859 | -0.01488 | 151 | 0.052975 | 0.002653 |
| 70 | 101 | 0.077882 | -0.01273 | 152 | 0.044588 | -0.00571 |
| 69 | 101 | 0.011603 | -0.00028 | 152 | 0.150569 | -0.04915 |
| 68 | 102 | 0.047944 | -0.00919 | 153 | 0.044848 | -0.00488 |
| 67 | 102 | 0.03383 | 0.002316 | 153 | -0.019 | 0.007031 |
| 66 | 103 | 0.018084 | -0.00288 | 154 | 0.063714 | -0.01961 |
| 65 | 104 | 0.041562 | -0.00488 | 155 | 0.04021 | -0.00469 |
| 64 | 104 | 0.072307 | -0.02005 | 155 | 0.051499 | -0.01177 |
| 63 | 105 | 0.027178 | 0.000315 | 156 | 0.149511 | -0.03995 |
| 62 | 105 | 0.119163 | -0.02432 | 156 | 0.003151 | 0.006106 |
| 61 | 106 | 0.096294 | -0.0154 | 157 | 0.092654 | -0.01572 |
| 60 | 107 | 0.081111 | -0.00431 | 158 | 0.065792 | 0.00577 |
| 59 | 107 | 0.11991 | -0.01067 | 158 | 0.073981 | 0.009159 |
| 58 | 108 | 0.116474 | -0.00949 | 159 | 0.153732 | -0.02421 |
| 57 | 109 | 0.046988 | 0.007862 | 159 | 0.039614 | 0.013817 |

| Elevation cm | Time min | Water Content | Soltrol Content | Time min | Water Content | Soltrol Content |
|---|---|---|---|---|---|---|
| 56 | 109 | 0.049074 | 0.003027 | 160 | 0.091239 | -0.00682 |
| 55 | 110 | 0.043412 | 0.008223 | 161 | 0.095945 | -0.00277 |
| 54 | 110 | 0.153542 | -0.02176 | 161 | 0.067757 | -0.00582 |
| 53 | 111 | 0.150973 | -0.01907 | 162 | 0.099333 | -0.00669 |
| 52 | 112 | 0.046848 | 0.00691 | 162 | 0.102863 | -0.01192 |
| 51 | 112 | 0.126721 | -0.01329 | 163 | 0.056211 | 0.004683 |
| 50 | 113 | 0.063305 | -0.00172 | 164 | 0.085473 | -0.00934 |
| 49 | 113 | 0.058329 | -0.01178 | 164 | 0.066734 | -0.00508 |
| 48 | 114 | 0.034526 | -0.00333 | 165 | -0.01412 | 0.009975 |
| 47 | 115 | 0.023134 | -0.00822 | 165 | 0.137599 | -0.03535 |
| 46 | 115 | 0.042207 | -0.01424 | 166 | 0.01705 | 0.004333 |
| 45 | 116 | -0.04709 | 0.027945 | 167 | 0.060079 | -0.01286 |
| 44 | 116 | -0.01048 | 0.025293 | 167 | 0.091521 | -0.01684 |
| 120 | 172 | 0.001371 | 0.072323 | 223 | 0.050346 | 0.046257 |
| 119 | 173 | 0.039336 | 0.099751 | 224 | 0.051439 | 0.080425 |
| 118 | 174 | 0.014275 | 0.091799 | 224 | 0.003084 | 0.084552 |
| 117 | 174 | 0.031769 | 0.081291 | 225 | 0.038798 | 0.068961 |
| 116 | 175 | 0.004804 | 0.097076 | 226 | -0.00306 | 0.095195 |
| 115 | 175 | 0.056856 | 0.088281 | 226 | 0.058709 | 0.079487 |
| 114 | 176 | 0.023833 | 0.115389 | 227 | 0.019412 | 0.105965 |
| 113 | 177 | 0.004239 | 0.131317 | 227 | 0.063083 | 0.086636 |
| 112 | 177 | 0.044059 | 0.121062 | 228 | 0.035113 | 0.107674 |
| 111 | 178 | 0.091984 | 0.101434 | 229 | 0.055456 | 0.104245 |
| 110 | 178 | 0.061844 | 0.116314 | 229 | 0.0528 | 0.108858 |
| 109 | 179 | 0.040491 | 0.130626 | 230 | 0.035441 | 0.123088 |
| 108 | 180 | 0.03982 | 0.140506 | 230 | 0.056993 | 0.119735 |
| 107 | 180 | 0.073496 | 0.140322 | 231 | 0.04433 | 0.140363 |
| 106 | 185 | 0.018644 | 0.226593 | 236 | 0.054956 | 0.188828 |
| 98 | 186 | 0.10056 | 0.187849 | 236 | 0.043834 | 0.17887 |
| 97 | 186 | 0.076629 | 0.198936 | 237 | -0.0308 | 0.20167 |
| 96 | 187 | 0.120584 | 0.177334 | 238 | 0.151635 | 0.139383 |
| 95 | 187 | 0.00514 | 0.218495 | 238 | 0.033177 | 0.180793 |
| 94 | 188 | 0.098119 | 0.189425 | 239 | 0.091142 | 0.173322 |
| 93 | 189 | 0.055873 | 0.218545 | 239 | 0.041862 | 0.205556 |
| 92 | 189 | 0.115753 | 0.216521 | 240 | 0.102707 | 0.202114 |
| 91 | 190 | 0.108956 | 0.248787 | 241 | 0.182012 | 0.211981 |
| 90 | 190 | 0.042962 | 0.278782 | 241 | 0.139889 | 0.218448 |
| 89 | 191 | 0.098682 | 0.227986 | 242 | 0.119859 | 0.206367 |
| 88 | 192 | 0.004156 | 0.257825 | 242 | 0.041539 | 0.230724 |
| 87 | 192 | 0.0851 | 0.23175 | 243 | 0.089311 | 0.218558 |
| 86 | 193 | 0.100481 | 0.236072 | 244 | 0.083117 | 0.223075 |
| 85 | 193 | 0.113349 | 0.240667 | 244 | 0.064025 | 0.251456 |
| 84 | 194 | 0.10784 | 0.2487 | 245 | 0.106715 | 0.248232 |
| 83 | 195 | 0.188303 | 0.206529 | 245 | 0.042896 | 0.262097 |
| 82 | 195 | 0.078859 | 0.244043 | 246 | 0.071397 | 0.235311 |
| 81 | 196 | 0.035891 | 0.235064 | 247 | 0.031108 | 0.249845 |
| 80 | 196 | 0.068935 | 0.198469 | 247 | 0.02831 | 0.253589 |
| 79 | 197 | 0.062215 | 0.093804 | 248 | 0.131387 | 0.202461 |
| 78 | 198 | 0.053684 | 0.011078 | 248 | 0.038204 | 0.19935 |
| 77 | 198 | 0.050216 | -0.00489 | 249 | 0.053143 | 0.110735 |
| 76 | 199 | 0.059099 | -0.0205 | 250 | 0.137887 | -0.01626 |
| 75 | 199 | 0.048239 | -0.01192 | 250 | 0.135458 | -0.03503 |
| 74 | 200 | 0.086785 | -0.01809 | 251 | 0.07991 | -0.01364 |
| 73 | 201 | 0.04755 | 0.001841 | 251 | 0.024185 | 0.000966 |
| 72 | 201 | 0.109883 | -0.01592 | 252 | 0.108426 | -0.00986 |
| 71 | 202 | 0.105132 | -0.0243 | 253 | 0.013208 | 0.012928 |
| 70 | 202 | 0.040983 | -0.00327 | 253 | 0.114873 | -0.03171 |
| 69 | 203 | 0.010541 | 0.007763 | 254 | -0.01383 | 0.013029 |

| Elevation cm | Time min | Water Content | Soltrol Content | Time min | Water Content | Soltrol Content |
|---|---|---|---|---|---|---|
| 68 | 204 | 0.049027 | -0.01757 | 254 | 0.048683 | -0.01602 |
| 67 | 204 | 0.032258 | -0.00482 | 255 | 0.079431 | -0.02347 |
| 66 | 205 | 0.093953 | -0.02826 | 256 | 0.041314 | -0.01196 |
| 65 | 205 | 0.057846 | -0.01206 | 256 | 0.020381 | 0.001515 |
| 64 | 206 | -0.00731 | 0.005621 | 257 | 0.03174 | -0.00727 |
| 63 | 207 | 0.094133 | -0.02187 | 257 | 0.030242 | -0.00505 |
| 62 | 207 | 0.012585 | 0.00917 | 258 | 0.021972 | 0.005342 |
| 61 | 208 | 0.091366 | -0.01119 | 259 | 0.072438 | -0.01227 |
| 60 | 208 | 0.067975 | 0.00716 | 259 | 0.125094 | -0.01389 |
| 59 | 209 | 0.147115 | -0.01454 | 260 | 0.094205 | 0.003436 |
| 58 | 210 | 0.096795 | -0.01076 | 260 | 0.161875 | -0.02097 |
| 57 | 210 | 0.014242 | 0.0193 | 261 | 0.062796 | 0.0004 |
| 56 | 211 | 0.104995 | -0.01306 | 262 | 0.042648 | 0.013224 |
| 55 | 211 | 0.037091 | 0.010273 | 262 | 0.060832 | 0.005819 |
| 54 | 212 | 0.136409 | -0.0228 | 263 | 0.113 | -0.0149 |
| 53 | 213 | 0.039244 | 0.013291 | 264 | 0.027359 | 0.013644 |
| 52 | 213 | 0.05097 | 0.015203 | 264 | 0.119477 | -0.01712 |
| 51 | 214 | 0.037171 | 0.016244 | 265 | 0.109016 | -0.00718 |
| 50 | 214 | 0.078995 | -0.00499 | 265 | 0.058646 | -0.0032 |
| 49 | 215 | 0.098603 | -0.01629 | 266 | 0.040834 | 0.002267 |
| 48 | 216 | 0.003281 | 0.007773 | 267 | 0.04937 | -0.0059 |
| 47 | 216 | 0.118572 | -0.03376 | 267 | 0.075749 | -0.01939 |
| 46 | 217 | 0.057905 | -0.01273 | 268 | 0.06724 | -0.01961 |
| 45 | 217 | 0.029507 | -0.00866 | 268 | -0.00797 | 0.016575 |
| 44 | 218 | 0.077562 | -0.01226 | 269 | 0.086693 | -0.00961 |

| Elevation cm | Time min | Water Content | Soltrol Content | Time min | Water Content | Soltrol Content |
|---|---|---|---|---|---|---|
| 120 | 1226 | -0.02332 | 0.037382 | 1366 | 0.348018 | 0.001628 |
| 119 | 1227 | 0.03017 | 0.055837 | 1367 | 0.313075 | 0.036929 |
| 118 | 1228 | -0.00779 | 0.058641 | 1367 | 0.28648 | 0.03427 |
| 117 | 1228 | -0.03034 | 0.060362 | 1368 | 0.24598 | 0.043673 |
| 116 | 1229 | 0.002413 | 0.057691 | 1369 | 0.292191 | 0.033524 |
| 115 | 1229 | -0.00825 | 0.068463 | 1369 | 0.334267 | 0.020225 |
| 114 | 1230 | 0.026991 | 0.062563 | 1370 | 0.337171 | 0.02745 |
| 113 | 1231 | 0.015507 | 0.061348 | 1370 | 0.305849 | 0.040872 |
| 112 | 1231 | 0.047997 | 0.056271 | 1371 | 0.307626 | 0.048635 |
| 111 | 1232 | 0.055527 | 0.055438 | 1372 | 0.319626 | 0.044778 |
| 110 | 1232 | 0.055224 | 0.060521 | 1372 | 0.322862 | 0.04098 |
| 109 | 1233 | 0.062351 | 0.06196 | 1373 | 0.328212 | 0.040562 |
| 108 | 1234 | -0.0088 | 0.095897 | 1373 | 0.339784 | 0.046287 |
| 107 | 1234 | 0.047135 | 0.083827 | 1374 | 0.342437 | 0.057573 |
| 106 | 1239 | 0.050996 | 0.105359 | 1379 | 0.274335 | 0.099505 |
| 98 | 1240 | 0.031119 | 0.105919 | 1379 | 0.342551 | 0.053176 |
| 97 | 1240 | 0.021728 | 0.096087 | 1380 | 0.344141 | 0.0574 |
| 96 | 1241 | 0.020452 | 0.098398 | 1381 | 0.356734 | 0.047866 |
| 95 | 1241 | 0.052854 | 0.080594 | 1381 | 0.358073 | 0.044207 |
| 94 | 1242 | 0.041061 | 0.083615 | 1382 | 0.325879 | 0.065058 |
| 93 | 1243 | 0.025922 | 0.109952 | 1382 | 0.303862 | 0.070697 |
| 92 | 1243 | 0.113544 | 0.092294 | 1383 | 0.30723 | 0.083691 |
| 91 | 1244 | 0.100192 | 0.122851 | 1384 | 0.44837 | 0.042531 |
| 90 | 1244 | 0.032008 | 0.144407 | 1384 | 0.395905 | 0.059132 |
| 89 | 1245 | 0.025945 | 0.121785 | 1385 | 0.360926 | 0.066131 |
| 88 | 1246 | 0.049708 | 0.104739 | 1385 | 0.391729 | 0.051406 |
| 87 | 1246 | 0.00416 | 0.133281 | 1386 | 0.289643 | 0.092478 |
| 86 | 1247 | 0.0781 | 0.117669 | 1387 | 0.345085 | 0.080709 |
| 85 | 1247 | 0.090382 | 0.136476 | 1387 | 0.339724 | 0.095237 |
| 84 | 1248 | 0.077282 | 0.148831 | 1388 | 0.415638 | 0.07362 |

| Elevation cm | Time min | Water Content | Soltrol Content | Time min | Water Content | Soltrol Content |
|---|---|---|---|---|---|---|
| 83 | 1249 | 0.077735 | 0.14502 | 1388 | 0.363334 | 0.098357 |
| 82 | 1249 | 0.094697 | 0.136693 | 1389 | 0.255176 | 0.127433 |
| 81 | 1250 | 0.049286 | 0.150148 | 1390 | 0.288842 | 0.123204 |
| 80 | 1250 | 0.01101 | 0.166063 | 1390 | 0.324796 | 0.113955 |
| 79 | 1251 | 0.023659 | 0.172334 | 1391 | 0.323171 | 0.115085 |
| 78 | 1252 | 0.066486 | 0.152912 | 1391 | 0.292324 | 0.128546 |
| 77 | 1252 | 0.046878 | 0.156467 | 1392 | 0.318004 | 0.113833 |
| 76 | 1253 | 0.023156 | 0.170615 | 1393 | 0.347007 | 0.108627 |
| 75 | 1253 | 0.060458 | 0.155228 | 1393 | 0.255328 | 0.155616 |
| 74 | 1254 | 0.03812 | 0.180875 | 1394 | 0.390817 | 0.124135 |
| 73 | 1255 | 0.050764 | 0.189875 | 1394 | 0.28437 | 0.155787 |
| 72 | 1255 | 0.036535 | 0.202349 | 1395 | 0.404945 | 0.113331 |
| 71 | 1256 | 0.013385 | 0.208023 | 1396 | 0.362385 | 0.137089 |
| 70 | 1256 | 0.039373 | 0.177336 | 1396 | 0.397175 | 0.127407 |
| 69 | 1257 | 0.068717 | 0.163614 | 1397 | 0.392436 | 0.121525 |
| 68 | 1258 | 0.039945 | 0.180036 | 1397 | 0.313786 | 0.158915 |
| 67 | 1258 | 0.047844 | 0.164875 | 1398 | 0.269912 | 0.191577 |
| 66 | 1259 | -0.00843 | 0.171898 | 1399 | 0.257062 | 0.20697 |
| 65 | 1259 | 0.053083 | 0.151373 | 1399 | 0.291328 | 0.206691 |
| 64 | 1260 | 0.048417 | 0.137047 | 1400 | 0.138643 | 0.269448 |
| 63 | 1261 | 0.033969 | 0.100832 | 1400 | 0.208714 | 0.22217 |
| 62 | 1261 | 0.100541 | 0.01536 | 1401 | 0.107473 | 0.19062 |
| 61 | 1262 | 0.047587 | 0.004238 | 1402 | 0.023096 | 0.13632 |
| 60 | 1263 | 0.089722 | 0.002282 | 1402 | 0.114893 | 0.035009 |
| 59 | 1263 | 0.112153 | -0.00846 | 1403 | 0.051437 | 0.036119 |
| 58 | 1264 | 0.082801 | 0.00298 | 1403 | 0.084547 | 0.012322 |
| 57 | 1264 | 0.050501 | 0.004803 | 1404 | 0.069573 | 0.001111 |
| 56 | 1265 | 0.049626 | 0.010695 | 1405 | 0.01695 | 0.020761 |
| 55 | 1266 | 0.184415 | -0.03786 | 1405 | 0.144497 | -0.0207 |
| 54 | 1266 | 0.066327 | 0.001468 | 1406 | 0.052768 | 0.004799 |
| 53 | 1267 | 0.131352 | -0.019 | 1406 | 0.115168 | -0.01379 |
| 52 | 1267 | 0.096103 | -0.012 | 1407 | 0.050554 | 0.013187 |
| 51 | 1268 | 0.074364 | 0.003419 | 1408 | 0.067412 | 0.010181 |
| 50 | 1269 | 0.046109 | 0.008607 | 1408 | 0.04026 | 0.010171 |
| 49 | 1269 | 0.006254 | 0.016362 | 1409 | 0.021432 | 0.00837 |
| 48 | 1270 | 0.091823 | -0.01634 | 1409 | 0.049697 | -0.00584 |
| 47 | 1270 | 0.018015 | -0.00119 | 1410 | 0.002754 | 0.007612 |
| 46 | 1271 | 0.005031 | 0.002088 | 1411 | 0.070656 | -0.00834 |
| 45 | 1272 | 0.095541 | -0.02121 | 1411 | 0.006093 | 0.006813 |
| 44 | 1272 | 0.043731 | 0.008592 | 1412 | 0.053601 | 0.000927 |

| Elevation cm | Time min | Water Content | Soltrol Content | Time min | Water Content | Soltrol Content |
|---|---|---|---|---|---|---|
| 120 | 1417 | 0.368587 | -0.01598 | 1518 | 0.151874 | 0.011343 |
| 119 | 1418 | 0.259888 | 0.038901 | 1519 | 0.144045 | 0.034503 |
| 118 | 1418 | 0.213705 | 0.035303 | 1519 | 0.099395 | 0.034845 |
| 117 | 1419 | 0.255747 | 0.016989 | 1520 | 0.078074 | 0.05089 |
| 116 | 1419 | 0.235806 | 0.035807 | 1521 | 0.150682 | 0.026869 |
| 115 | 1420 | 0.216977 | 0.055252 | 1521 | 0.155736 | 0.030551 |
| 114 | 1421 | 0.307343 | 0.019061 | 1522 | 0.145331 | 0.050912 |
| 113 | 1421 | 0.226397 | 0.053054 | 1522 | 0.157919 | 0.042162 |
| 112 | 1422 | 0.265674 | 0.043824 | 1523 | 0.186251 | 0.032063 |
| 111 | 1422 | 0.257841 | 0.0488 | 1524 | 0.156269 | 0.050653 |
| 110 | 1423 | 0.259977 | 0.046029 | 1524 | 0.154379 | 0.057661 |
| 109 | 1424 | 0.26701 | 0.04799 | 1525 | 0.129385 | 0.066557 |
| 108 | 1424 | 0.288946 | 0.047493 | 1525 | 0.163284 | 0.058252 |
| 107 | 1425 | 0.254451 | 0.062805 | 1526 | 0.242275 | 0.038 |
| 106 | 1430 | 0.242645 | 0.072009 | 1531 | 0.116878 | 0.09421 |

| Elevation cm | Time min | Water Content | Soltrol Content | Time min | Water Content | Soltrol Content |
|---|---|---|---|---|---|---|
| 98 | 1430 | 0.29057 | 0.050668 | 1531 | 0.176401 | 0.061053 |
| 97 | 1431 | 0.287298 | 0.046145 | 1532 | 0.170125 | 0.059504 |
| 96 | 1431 | 0.26068 | 0.051689 | 1533 | 0.165808 | 0.049301 |
| 95 | 1432 | 0.283807 | 0.04307 | 1533 | 0.162368 | 0.049015 |
| 94 | 1433 | 0.276167 | 0.045633 | 1534 | 0.242623 | 0.035419 |
| 93 | 1433 | 0.309292 | 0.044902 | 1534 | 0.211326 | 0.052446 |
| 92 | 1434 | 0.227712 | 0.089483 | 1535 | 0.161224 | 0.080127 |
| 91 | 1434 | 0.370408 | 0.045192 | 1536 | 0.246984 | 0.07114 |
| 90 | 1435 | 0.299906 | 0.067954 | 1536 | 0.21238 | 0.075006 |
| 89 | 1436 | 0.231711 | 0.076214 | 1537 | 0.15908 | 0.073262 |
| 88 | 1436 | 0.315814 | 0.030642 | 1537 | 0.217598 | 0.040701 |
| 87 | 1437 | 0.194199 | 0.080837 | 1538 | 0.160322 | 0.067983 |
| 86 | 1437 | 0.325086 | 0.037184 | 1539 | 0.264746 | 0.041053 |
| 85 | 1438 | 0.288764 | 0.064254 | 1539 | 0.183187 | 0.080305 |
| 84 | 1439 | 0.36143 | 0.042797 | 1540 | 0.262525 | 0.048805 |
| 83 | 1439 | 0.341279 | 0.048673 | 1540 | 0.238141 | 0.046352 |
| 82 | 1440 | 0.282841 | 0.066755 | 1541 | 0.177443 | 0.075968 |
| 81 | 1440 | 0.283161 | 0.069261 | 1542 | 0.161341 | 0.078385 |
| 80 | 1441 | 0.279097 | 0.065775 | 1542 | 0.230765 | 0.050933 |
| 79 | 1442 | 0.304016 | 0.05405 | 1543 | 0.205736 | 0.06407 |
| 78 | 1442 | 0.211042 | 0.092654 | 1543 | 0.120027 | 0.093676 |
| 77 | 1443 | 0.259886 | 0.082576 | 1544 | 0.183639 | 0.069701 |
| 76 | 1443 | 0.245979 | 0.080958 | 1545 | 0.2145 | 0.065893 |
| 75 | 1444 | 0.268496 | 0.077729 | 1545 | 0.256107 | 0.039977 |
| 74 | 1445 | 0.317788 | 0.068233 | 1546 | 0.208945 | 0.070336 |
| 73 | 1445 | 0.329733 | 0.069375 | 1546 | 0.250291 | 0.075802 |
| 72 | 1446 | 0.353927 | 0.075663 | 1547 | 0.297049 | 0.057576 |
| 71 | 1446 | 0.24364 | 0.118347 | 1548 | 0.270093 | 0.070153 |
| 70 | 1447 | 0.309804 | 0.091961 | 1548 | 0.23152 | 0.079991 |
| 69 | 1448 | 0.310654 | 0.0865 | 1549 | 0.193834 | 0.078305 |
| 68 | 1448 | 0.346445 | 0.072318 | 1549 | 0.178007 | 0.086096 |
| 67 | 1449 | 0.35818 | 0.075738 | 1550 | 0.218807 | 0.070771 |
| 66 | 1449 | 0.292448 | 0.109846 | 1551 | 0.139574 | 0.093953 |
| 65 | 1450 | 0.294617 | 0.132708 | 1551 | 0.255396 | 0.049995 |
| 64 | 1451 | 0.317714 | 0.123567 | 1552 | 0.243774 | 0.064055 |
| 63 | 1451 | 0.31714 | 0.134098 | 1552 | 0.159496 | 0.093016 |
| 62 | 1452 | 0.321702 | 0.116491 | 1553 | 0.21075 | 0.083457 |
| 61 | 1452 | 0.314409 | 0.12493 | 1554 | 0.257605 | 0.084269 |
| 60 | 1453 | 0.338841 | 0.124129 | 1554 | 0.313137 | 0.098916 |
| 59 | 1454 | 0.316347 | 0.132426 | 1555 | 0.281543 | 0.142427 |
| 58 | 1454 | 0.367118 | 0.120528 | 1555 | 0.31886 | 0.142484 |
| 57 | 1455 | 0.326676 | 0.127204 | 1556 | 0.2477 | 0.181318 |
| 56 | 1455 | 0.335393 | 0.128116 | 1557 | 0.267296 | 0.149283 |
| 55 | 1456 | 0.23145 | 0.150114 | 1557 | 0.30417 | 0.127259 |
| 54 | 1457 | 0.275174 | 0.124975 | 1558 | 0.282376 | 0.130498 |
| 53 | 1457 | 0.308645 | 0.062583 | 1558 | 0.228082 | 0.141792 |
| 52 | 1458 | 0.231476 | 0.032215 | 1559 | 0.200328 | 0.144014 |
| 51 | 1458 | 0.277801 | -0.00762 | 1560 | 0.232239 | 0.113402 |
| 50 | 1459 | 0.306735 | -0.01604 | 1560 | 0.176993 | 0.107952 |
| 49 | 1460 | 0.240395 | -0.00836 | 1561 | 0.168685 | 0.048875 |
| 48 | 1460 | 0.247856 | -0.01789 | 1561 | 0.164603 | 0.00131 |
| 47 | 1461 | 0.201419 | 0.004632 | 1562 | 0.150843 | -0.00789 |
| 46 | 1461 | 0.294729 | -0.02922 | 1563 | 0.200403 | -0.02396 |
| 45 | 1462 | 0.272732 | -0.02382 | 1563 | 0.123615 | -0.00157 |
| 44 | 1463 | 0.209996 | -0.0031 | 1564 | 0.159382 | -0.00887 |

| Elevation cm | Time min | Water Content | Soltrol Content |
|---|---|---|---|
| 120 | 1614 | 0.099299 | 0.02202 |
| 119 | 1615 | 0.083579 | 0.048354 |
| 118 | 1615 | 0.072562 | 0.042834 |
| 117 | 1616 | 0.059697 | 0.041956 |
| 116 | 1616 | 0.051822 | 0.056324 |
| 115 | 1617 | 0.093766 | 0.055203 |
| 114 | 1618 | 0.091534 | 0.053666 |
| 113 | 1618 | 0.110886 | 0.040651 |
| 112 | 1619 | 0.143819 | 0.034404 |
| 111 | 1619 | 0.123151 | 0.053359 |
| 110 | 1620 | 0.165009 | 0.041218 |
| 109 | 1621 | 0.129995 | 0.051944 |
| 108 | 1621 | 0.135897 | 0.057053 |
| 107 | 1622 | 0.149208 | 0.057743 |
| 106 | 1627 | 0.091378 | 0.089324 |
| 98 | 1627 | 0.144688 | 0.058669 |
| 97 | 1628 | 0.175418 | 0.045101 |
| 96 | 1628 | 0.181729 | 0.037301 |
| 95 | 1629 | 0.127456 | 0.061107 |
| 94 | 1630 | 0.16576 | 0.046309 |
| 93 | 1630 | 0.158323 | 0.060312 |
| 92 | 1631 | 0.151458 | 0.076068 |
| 91 | 1631 | 0.231703 | 0.063182 |
| 90 | 1632 | 0.198277 | 0.063709 |
| 89 | 1633 | 0.20321 | 0.047485 |
| 88 | 1633 | 0.187102 | 0.037537 |
| 87 | 1634 | 0.152129 | 0.060156 |
| 86 | 1634 | 0.156417 | 0.068696 |
| 85 | 1635 | 0.197846 | 0.058619 |
| 84 | 1636 | 0.210148 | 0.060002 |
| 83 | 1636 | 0.178734 | 0.06356 |
| 82 | 1637 | 0.113472 | 0.085417 |
| 81 | 1637 | 0.184015 | 0.0562 |
| 80 | 1638 | 0.137339 | 0.081122 |
| 79 | 1639 | 0.189683 | 0.060616 |
| 78 | 1639 | 0.185799 | 0.061229 |
| 77 | 1640 | 0.146014 | 0.073604 |
| 76 | 1640 | 0.201541 | 0.05847 |
| 75 | 1641 | 0.138815 | 0.075818 |
| 74 | 1642 | 0.18777 | 0.073524 |
| 73 | 1642 | 0.122137 | 0.104369 |
| 72 | 1643 | 0.172322 | 0.096589 |
| 71 | 1643 | 0.195035 | 0.07849 |
| 70 | 1644 | 0.160347 | 0.091739 |
| 69 | 1645 | 0.154111 | 0.091089 |
| 68 | 1645 | 0.197118 | 0.060282 |
| 67 | 1646 | 0.148312 | 0.086098 |
| 66 | 1646 | 0.164346 | 0.070255 |
| 65 | 1647 | 0.179721 | 0.069543 |
| 64 | 1648 | 0.162082 | 0.066642 |
| 63 | 1648 | 0.137765 | 0.082798 |
| 62 | 1649 | 0.175702 | 0.072233 |
| 61 | 1649 | 0.102128 | 0.106718 |
| 60 | 1650 | 0.234009 | 0.106609 |
| 59 | 1651 | 0.190371 | 0.149036 |
| 58 | 1651 | 0.255789 | 0.140009 |
| 57 | 1652 | 0.228852 | 0.153947 |
| 56 | 1652 | 0.282847 | 0.138625 |

| Elevation cm | Time min | Water Content | Soltrol Content |
|---|---|---|---|
| 55 | 1653 | 0.203331 | 0.15988 |
| 54 | 1654 | 0.266334 | 0.13949 |
| 53 | 1654 | 0.223111 | 0.144302 |
| 52 | 1655 | 0.148463 | 0.160737 |
| 51 | 1655 | 0.169797 | 0.148268 |
| 50 | 1656 | 0.122262 | 0.149697 |
| 49 | 1657 | 0.025402 | 0.131732 |
| 48 | 1657 | 0.092049 | 0.038992 |
| 47 | 1658 | 0.055426 | 0.016816 |
| 46 | 1658 | 0.158824 | -0.02134 |
| 45 | 1659 | 0.086434 | 0.000933 |
| 44 | 1660 | 0.102159 | 0.003652 |


U.S. GOVERNMENT PRINTING OFFICE: 1994 - 650-006/00216